

Progress and perspectives on the electron-doped cuprates*

N.P. Armitage

The Institute of Quantum Matter, Department of Physics and Astronomy, The Johns Hopkins University, Baltimore, MD 21218, USA.

P. Fournier

*Regroupement québécois sur les matériaux de pointe and
Département de Physique, Université de Sherbrooke, Sherbrooke, Québec, CANADA, J1K 2R1.*

R.L. Greene

Center for Nanophysics and Advanced Materials, Department of Physics, University of Maryland, College Park, MD 20742, USA.

(Dated: June 16, 2022)

Although the vast majority of high- T_c cuprate superconductors are hole-doped, a small family of electron-doped compounds exists. Under investigated until recently, there has been tremendous recent progress in their characterization. A consistent view is being reached on a number of formerly contentious issues, such as their order parameter symmetry, phase diagram, and normal state electronic structure. Many other aspects have been revealed exhibiting both their similarities and differences with the hole-doped compounds. This review summarizes the current experimental status of these materials, with a goal to providing a snapshot of our current understanding of electron-doped cuprates. When possible we put our results in the context of the hole-doped compounds. We attempt to synthesize this information into a consistent view on a number of topics important to both this material class as well as the overall cuprate phenomenology including the phase diagram, the superconducting order parameter symmetry, phase separation, pseudogap effects, the role of competing orders, the spin-density wave mean-field description of the normal state, and electron-phonon coupling.

Contents

I. Introduction	1	IV. Discussion	44
II. Overview	4	A. Symmetry of the superconducting order parameter	44
A. Short review of high- T_c superconductors	4	1. Penetration depth	45
B. General aspects of the phase diagram	9	2. Tunnelling spectroscopy	46
C. Specific considerations of the cuprate electronic structure upon electron doping	10	3. Low-energy spectroscopy using Raman scattering	47
D. Crystal structure and solid-state chemistry	12	4. ARPES	49
E. Materials growth	15	5. Specific Heat	50
1. Single crystals	16	6. Thermal conductivity	51
2. Role of the reduction process and effects of oxygen stoichiometry	17	7. Nuclear Magnetic Resonance	52
3. Thin films	19	8. Phase sensitive measurements	52
F. Unique aspects of the copper and rare earth magnetism	21	9. Order parameter of the infinite layer compounds	54
1. Cu spin order	21	B. Position of the chemical potential and midgap states	55
2. Effects of rare earth ions on magnetism	22	C. How do we even know for sure it is n -type?	56
III. Experimental survey	24	D. Electron-phonon interaction	58
A. Transport	24	E. Inhomogeneous charge distributions	59
1. Resistivity and Hall effect	24	F. Nature of normal state near optimal doping	60
2. Nernst effect, thermopower and magnetoresistance	26	G. Extent of antiferromagnetism and existence of a quantum critical point	62
3. c -axis transport	28	H. Spin-density wave description of the normal state	64
4. Effects of disorder on transport	28	I. Existence of a pseudogap in the electron-doped cuprates?	66
5. Normal State Thermal conductivity	29	V. Concluding remarks	68
B. Tunneling	30	Acknowledgments	68
C. ARPES	31	References	69
D. Optics	35	I. INTRODUCTION	
E. Raman spectroscopy	37	It has now been over 20 years since the discovery of high temperature superconductivity in the layered copper-oxide perovskites by Bednorz and Müller (1986).	
F. Neutron scattering	38		
1. Commensurate magnetism and doping dependence	38		
2. The magnetic ‘resonance’	41		
3. Magnetic field dependence	41		
G. Local magnetic probes: μ SR and NMR	43		

Despite an almost unprecedented material science effort, the origin of the superconductivity or indeed even much consensus on their dominate physics remains elusive (Campuzano *et al.*, 2004; Damascelli *et al.*, 2003; Kastner *et al.*, 1998; Lee *et al.*, 2006b; Orenstein and Millis, 2000; Scalapino, 1995; Timusk and Statt, 1999). This review describes recent progress in one route towards understanding the cuprate superconductors, that of a synthesized description and comparison of both electron and hole-doped sides of the phase diagram.

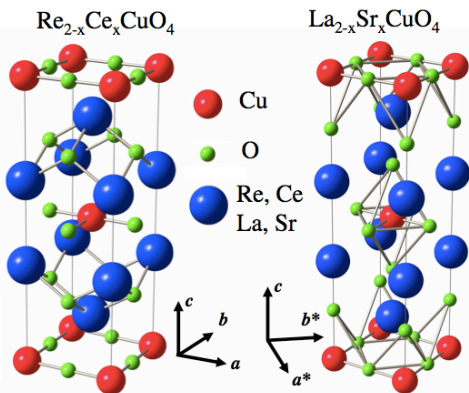


FIG. 1 A comparison of the crystal structures of the electron-doped cuprates of general formula $RE_{2-x}Ce_xCuO_4$ on the left and of its closest hole-doped counterpart $La_{2-x}Sr_xCuO_4$. Here RE is one of a number of rare earth ions, including Nd, Pr, Sm, and PR. One should note the different directions for the in-plane lattice parameters with respect to the Cu-O bonds.

The undoped parent compounds of high-temperature cuprate superconductors are known to be antiferromagnetic (AFM) Mott insulators. As the CuO_2 planes are doped with charge carriers, the antiferromagnetic phase subsides and superconductivity emerges. The symmetry, or the lack thereof, between doping with electrons (n -type) or holes (p -type) has important theoretical implications as most models implicitly assume symmetry. One possible route towards understanding the cuprate superconductors may come through a detailed comparison of these two sides of the phase diagram. However, most of what we know about these superconductors comes from experiments performed on p -type materials. The much fewer number of measurements from n -type compounds suggest that there may be both commonalities and differences between these two classes of compounds. This issue of electron/hole symmetry has not been seriously discussed, perhaps, because until recently, the experimental database of n -type results was very limited. The case of electron doping provides an important additional example of the result of introducing charge into the CuO_2 planes. The hope is that a detailed such study will give insight into what aspects of these compounds are universal, what aspects are important for the existence of

superconductivity and the anomalous and perhaps non-Fermi liquid normal state, what aspects are not universal, and how various phenomena depend on the microscopies of the states involved.

The high-temperature cuprate superconductors are all based on a certain class of ceramic perovskites. They share the common feature of square planar copper-oxygen layers separated by charge reservoir layers. These block layers serve to donate charge carriers to the CuO_2 planes, as well as stabilize the in-plane properties. Shown on the right of Fig. 1 is the crystal structures for the canonical single layer parent materials La_2CuO_4 (LCO). The undoped materials are antiferromagnetic insulators. With the substitution of Sr for La in La_2CuO_4 , holes are introduced into the CuO_2 planes. The Néel temperature precipitously drops and the material at some higher hole doping level becomes a superconductor (Fig. 2). As will be discussed below, the effects of electron doping on the antiferromagnetism is not nearly so dramatic.

Although the majority of known high- T_c superconductors are hole doped compounds there are a small number of other cuprate superconductors that can be doped with electrons (Takagi *et al.*, 1989; Tokura *et al.*, 1989b). Along with the mostly commonly investigated compound $Nd_{2-x}Ce_xCuO_4$ (NCCO), most members of this material class have the chemical formula $RE_{2-x}M_xCuO_4$ where the lanthanide rare earth (RE) substitution is Pr, Nd, Sm or Eu and M is Ce or Th (Dalichaouch *et al.*, 1993; Maple, 1990). These are single-layer compounds which, unlike their other brethren 214 hole-doped systems (for instance the T' crystal structured $La_{2-x}Sr_xCuO_{4\pm\delta}$ discussed above), have a T' crystal structure that is characterized by a lack of oxygen in the apical position (see Fig. 1 left).

The most dramatic and immediate difference between electron- and hole-doped materials is in their phase diagrams. Only an approximate symmetry exists about zero doping between p - and n -type, as the antiferromagnetic phase is much more robust in the electron-doped material and persists to much higher doping levels (Fig. 2). Superconductivity occurs in a doping range that is almost five times narrower. In addition, these two ground states occur in much closer proximity to each other and may even coincide unlike the hole-doped materials. Additionally, in contrast to many p -type cuprates, it is found that in doped compounds spin fluctuations remains commensurate where they can be resolved (Thurston *et al.*, 1990; Yamada *et al.*, 1999). Various other differences are found including a resistivity that goes like $\approx T^2$ near optimal and lower superconducting T_c 's. Moreover, a convenient aspect for the investigation of their low temperature properties is that their critical magnetic field is much smaller ($\approx 10T$) than the p -type materials ($> 60T$), allowing their normal state properties to be accessed in many laboratory based magnets. One of the other remarkable aspects of the n -type cuprates, is that a mean-field spin-density wave treatment of the normal metallic state near optimal doping describes many ma-

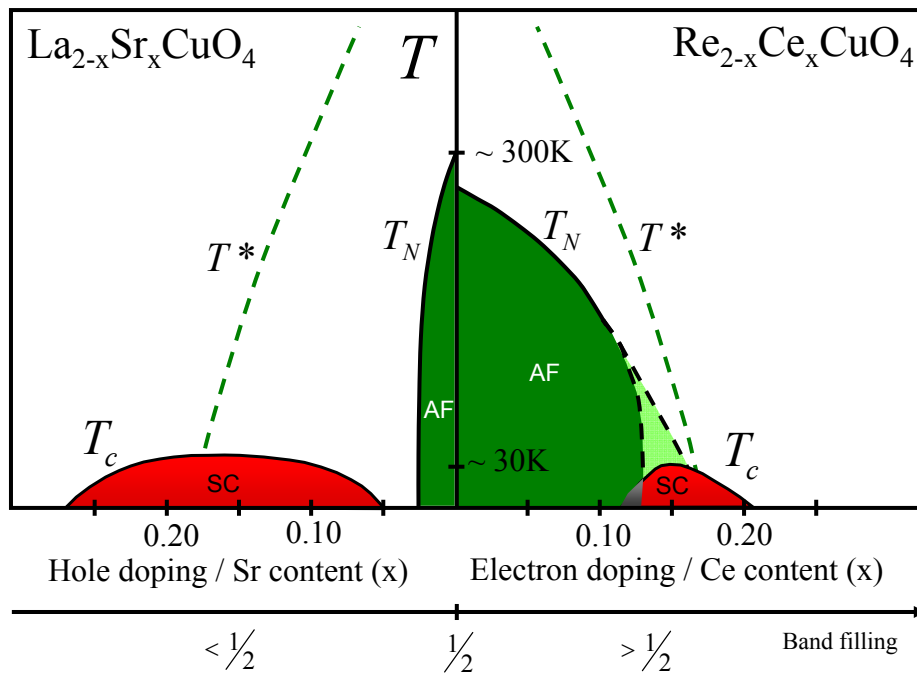


FIG. 2 Joint phase diagram of the LCCO/NCCO material systems. The uncertainty in the extent of AF on the electron-doped side and its coexistence with superconductivity is shown by the white/green dotted area. Maximum Néel temperatures have been reported as 270 K on the electron-doped side in NCO (Mang *et al.*, 2004b), 284 K in PCO (Sumarlin *et al.*, 1995) and 320 K on the hole-doped side in LCO (Keimer *et al.*, 1992). T^* indicates the approximate extent of the pseudogap phase.

terial properties quite well. Such a description is not possible in the hole-doped compounds. Whether this is a consequence of the close proximity of antiferromagnetism and superconductivity in the phase diagram, smaller correlation effects than the p -type, or the absence of other competing effects (stripes etc.) is unknown. This issue will be addressed more completely in Sec. IV.H.

This review focuses on the most widely studied class of n -doped cuprates, the (RE)CCO 214 system. This is the class of n -type materials that has had the most work performed and the most is known. We should mention however that there is at least one more class of electron-doped HTSC cuprates, the so-called infinite layer compounds. The electron-doped infinite-layer superconductor $\text{Sr}_{0.9}\text{La}_{0.1}\text{CuO}_2$ (SLCO) has been known for almost as long as the (RE)CCO material class (Siegrist *et al.*, 1988). It has the highest T_c ($\approx 42\text{K}$) of any n -doped cuprate. However, there has been comparatively little research performed on the SLCO system due to difficulties in sample preparation. This system will be touched only briefly here.

In the last few years incredible progress has been made both in regards to material quality as well as in the experimental understanding of these compounds. In this review we seek to summarize the current experimental

situation on the n -type cuprate compounds as well as provide an overview and perspective of how these materials fit into the overall phenomenology of the cuprate high- T_c superconductors. We concentrate primarily on experimental results from high quality single crystals and thin films with an emphasis on the most recent results. Early work has been discussed in a prior review (Fontcuberta and Fabrega, 1996). Theoretical treatments are covered where they have specific insight to the compounds being considered. A number of aspects will be emphasized. We pay particular description to issues such as the evolution of the magnetism with doping, the precise boundaries of the ordered states in the phase diagram, the superconducting order parameter symmetry, evidence for a pseudogap, quantum criticality, and the spin-density wave description of the electronic structure.

Unfortunately even in the comparatively under-investigated and well-defined scope of the n -type cuprates, the experimental literature is vast and we cannot hope to cover all the excellent work. Important omissions are regrettable, but inevitable.

II. OVERVIEW

A. Short review of high- T_c superconductors

In this section, we give a brief overview of the current experimental situation in the high- T_c superconductors, centered primarily on the hole-doped compounds. The field is overwhelmingly large and it is impossible to review it *in toto* here. We give only the most precursory overview. Interested readers are referred to specialized reviews (Campuzano *et al.*, 2004; Damascelli *et al.*, 2003; Kastner *et al.*, 1998; Lee *et al.*, 2006b; Orenstein and Millis, 2000; Scalapino, 1995; Timusk and Statt, 1999).

As emphasized early on (Anderson, 1987), the central defining feature of all these materials is their ubiquitous CuO_2 layers and the resulting strong hybridization between Cu and O orbitals, which is the primary contribution to their magnetic and electronic properties. The CuO_2 planes are separated by intervening charge reservoir layers that are believed to primarily donate charge to the planes and provide structural stability. The exception to this is the YBCO family, where the intermediate layers also contain metallic Cu-O chains. The majority of the cuprate compounds have the archetypical perovskite structure where the in-plane Cu atoms are coordinated by O atoms in an octahedral arrangement. Again the notable exceptions are the YBCO compounds, which have only one apical oxygen and form instead a pyramidal structure, and the main subject of this review, the T' structure electron-doped materials, which have no apical oxygens. It is believed that the states relevant for superconductivity are formed out of primarily in-plane Cu $d_{x^2-y^2}$ and O $p_{x,y}$ orbitals¹.

The formal valences in the CuO_2 planes of the undoped parent compounds are Cu^{+2} and O^{-2} . With one hole per unit cell, band theory predicts the undoped parent compounds (for instance La_2CuO_4 and Nd_2CuO_4) of these materials to be metallic. In fact they are insulators, which is believed to be driven by a strong local Coulomb interaction that suppresses charge fluctuations. Mott insulators, where insulation is caused by a strong on-site correlation energy that discourages double occupation, are frequently described by the single-band Hubbard Hamiltonian $H = \sum_{ij} t_{ij} c_j^\dagger c_i + \sum_i U n_{i\uparrow} n_{i\downarrow}$. If $U \gg t_{ij}$ the single band is split into two, the so-called upper and lower Hubbard bands (see Fig. 3 (top)) that are respectively empty and completely full at half-filling. The Hubbard Hamiltonian is the minimal model that includes the strong local interactions that are believed to be so central to these compounds. Although frequently referred to as Mott insulators, the cuprates are more properly referred to as charge-transfer band insulators

within the Zaanen-Sawatsky-Allen scheme (Zaanen *et al.*, 1985). Here the energy to overcome for charge motion is not the strong on-site Coulomb interaction on say the Cu site, but instead the energy associated with the local potential difference between Cu $d_{x^2-y^2}$ and O $p_{x,y}$ orbitals Δ_{pd} (Fig. 3 (middle)). The optical gap in the undoped cuprates is found to be 1.5 – 2 eV (Basov and Timusk, 2005), which is close to the expected value of Δ_{pd} . This means that doped holes preferentially reside in the so-called ‘charge transfer band’ composed primarily of oxygen orbitals (with a local configuration primarily $3d^9\bar{\underline{L}}$ where $\bar{\underline{L}}$ is the oxygen ‘ligand’ hole), whereas doped electron preferentially reside on the Cu sites (Fig. 3 (bottom)) (with a local configuration mostly $3d^{10}$). In the half-filled cuprates, with a single electron on the Cu $d_{x^2-y^2}$ orbital and filled O $p_{x,y}$ orbitals these compounds can be then described by a three band Hubbard model, which generally takes into account hopping, the onsite Coulomb interactions U_d , the energy difference between oxygen and copper orbitals Δ_{pd} , and intersite interactions V_{pd} (Varma *et al.*, 1987).

A number of simplifications of the three band model may be possible. Zhang and Rice (1988) argued that the maximum gain in hybridization energy is gained by placing doped holes in a linear combination of the O $p_{x,y}$ orbitals with the same symmetry as the existing hole in the Cu $d_{x^2-y^2}$ orbital that they surround. This requires an antisymmetry of the wave function in their spin coordinates, so that the two holes must form a singlet. Zhang and Rice argued that this split-off state retained its integrity even when intercell hopping is taken into account. Evidence for the singlet character of the nearest- E_F orbitals in CuO and the hole-doped cuprates may have been seen directly *via* spin-resolved photoemission (Brookes *et al.*, 2001; Tjeng *et al.*, 1997) and perhaps *via* NMR (Walstedt and Warren, 1990). With this simplification, the separate degrees of freedom of the Cu and O orbitals are removed and the CuO_2 plaquette is real space renormalized to an effective site centered on Cu. In this case, it may be possible to reduce the three band model to an effective single band one, where the role of the lower Hubbard band is played by the primarily oxygen based charge transfer band (of possibly singlet character) and an effective Hubbard gap given primarily by the charge transfer energy Δ_{pd} . Even though the local structure of the states is different upon hole or electron doping (Fig. 3 (bottom)), both would be of singlet character ($3d^9\bar{\underline{L}}$ and $3d^{10}$ respectively).

In general, it may be possible to reduce the one band Hubbard model even further by taking the limit of large effective U (the charge transfer energy Δ_{pd} in the cuprates). One can find an effective Hamiltonian in the subspace of only singly occupied sites. The effect of U becomes virtual. Localized electrons with oppositely aligned spins on adjacent sites can still reduce their kinetic energy by undergoing virtual hops to neighboring sites. As such, hops are only allowed with neighboring electrons being anti-aligned, this gives an effective

¹ Small admixtures of other orbitals like Cu $d_{z^2-r^2}$ are also typically present, but these make usually less than a 10 % contribution (Nücker *et al.*, 1989; Pellegrin *et al.*, 1993).

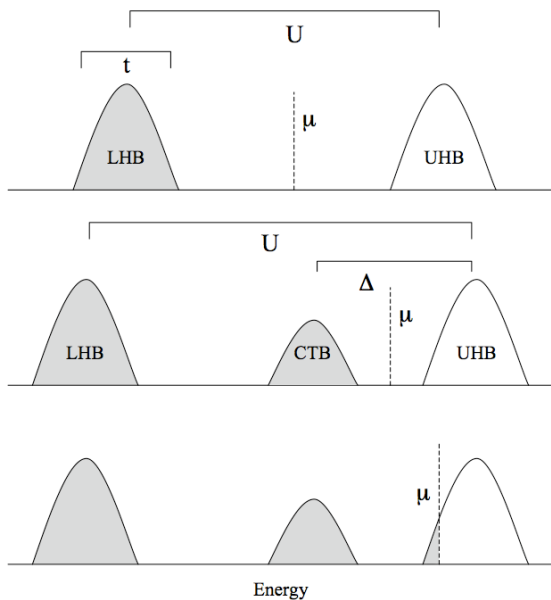


FIG. 3 (top) Schematic of the one band Hubbard model with $U \gg t$. At half-filling the chemical potential μ lies in the middle of the Mott gap. (middle) Schematic for a charge-transfer band insulator. Δ_{pd} may play the role of an effective Hubbard U with the charge transfer band (CTB) standing in for the lower Hubbard band. (bottom) Upon doping the CTB insulator with electrons, the chemical potential μ presumably moves into the UHB.

tive spin-spin exchange interaction which favors antiferromagnetism. The effect of the upper Hubbard band comes in only through these virtual hops. Second order perturbation theory gives an energy lowering for oppositely directed spins of $4t^2/U$. By neglecting correlated hopping terms, the one band Hubbard model can then be replaced by the so-called ' $t-J$ ' model which is a possible minimal model for the cuprates. The $t-J$ model can be refined by the inclusion of next-nearest t' and next-next-nearest t'' hopping terms.

Despite the successes of motivating these models from first principles calculations (Dagotto, 1994; Hybertsen *et al.*, 1990) and the successful modeling of other aspects of the differences between hole- and electron-doped materials within a $t-J$ context, we should note that the reduction of the three band model to models of the $t-J$ or $t-U$ variety is still very controversial. Emery and Reiter (1988) argued that in fact the quasiparticles of the three band model have both charge and a spin of $1/2$, in contrast to the singlets of Zhang and Rice and that the $t-J$ model was incomplete. Similarly, Varma has proposed that one must consider the full three band Hubbard model (Varma, 1997, 1999) as non-trivial phase factors between the bands become possible at low energies, which leads to a state with orbital currents on the O-Cu-O triangular plaquettes. The order associated with these currents has been proposed to be a candidate for the pseudogap phase. Moreover, questions regarding

even the validity of the parameter J remain. It is derived for the insulating case of localized electrons. Is it still a valid parameter when many holes or electrons have been introduced? Although throughout this review we will frequently appeal to the insight given by these simpler models (single band Hubbard or $t-J$), we caution that it is far from clear whether or not these models are missing some very important physics. However, as at least some of the debate revolves around the local-spin character (singlet or doublet) of the split-off oxygen derived state that holes principally occupy, we avoid this particular issue altogether and refer to this low energy state of primarily oxygen character as the charge transfer band (CTB) (and not as a Zhang-Rice singlet).

The undoped parent compounds of the cuprate superconductors are textbook antiferromagnetic correlated insulators with a moment reduced by $1/3$ from the free ion value due to quantum fluctuations (Vaknin *et al.*, 1987). As discussed above, upon hole doping, the transition temperature of the antiferromagnetism is quickly suppressed. At these low dopings a spin-glass phase is found, whose stability appears to be related to the amount of disorder in the system (Rullier-Albenque *et al.*, 2008). As charge is added to the CuO_2 planes, superconductivity eventually emerges with a T_c that typically becomes maximal around $\delta \approx 0.16$ charges per unit cell, before eventually becoming non superconducting at high enough doping levels. At and below optimal doping, the normal state has a number of anomalous characteristics, which are challenging to understand within the conventional theory of metals. In addition to spin-glass behavior, the underdoped regime is characterized by a suppression at low energies of various excitation spectra. This is a manifestation of the famous 'pseudogap' (PG) phenomenon. Whether this is indicative of the onset of an actual ordered state of matter, or is instead a crossover phenomenon will be discussed below.

The superconducting state is believed to have a dominant order parameter of a higher $d_{x^2-y^2}$ wave $L=2$ angular momentum variety than conventional $L=0$ superconductors (Scalapino, 1995; Tsuei and Kirtley, 2000a). Such a symmetry was first theoretically postulated as being the one most likely for a material with dominant repulsive and antiferromagnetic interactions (Beal-Monod *et al.*, 1986; Lee and Read, 1987; Miyake *et al.*, 1986; Scalapino *et al.*, 1986). It was later confirmed by a variety of techniques. In a relatively messy material-based field like the high- T_c superconductors, it is a remarkable convergence of experimental data. It is interesting to note however that, aside from its symmetry and a low superfluid density (to be discussed below), the superconducting state properties are much more 'normal' than the anomalous normal state properties. At low temperatures it can be described by a d -wave BCS-type charge $2e$ order parameter in the extreme type II limit ($\xi_{ab} \approx 20\text{\AA}$ and $\xi_c \approx 2\text{\AA}$ with 2000 - 4000 \AA penetration depth for optimal doping (Uemura *et al.*, 1988)). Its conventional properties include apparently good quasiparticles

as evidenced by both their direct observation in photoemission (Kaminski *et al.*, 2000) and scanning tunneling microscopy (STM) impurity scattering (Hoffman *et al.*, 2002b)² as well as a collapse in the scattering rate as inferred from microwave (Bonn *et al.*, 1992), THz spectroscopy (Corson *et al.*, 1999) and thermal conductivity (Chiao *et al.*, 2000; Krishana *et al.*, 1995).

The underdoped ‘pseudogap’ regime of the hole-doped cuprates has been the focus of most of the attention. As mentioned, below a temperature scale T^* (the precise boundary of which depends on the experimental probe) these materials are dominated by a low-energy suppression in various excitation spectra (Randeria, 2007; Timusk and Statt, 1999). There has been a long standing debate whether this pseudogap is a manifestation of precursor superconductivity at temperatures well above T_c , or rather is indicative of some competing ordered phase. Early experimental evidence for pseudogap formation was in terms of a *spin-gap via* NMR measurements where it was found that the spin lattice relaxation rate dropped strongly well before the onset of superconductivity (Martindale *et al.*, 1993; Warren *et al.*, 1989). It was also found that the spin susceptibility (*via* the Knight shift) also falls below the Heisenberg model prediction at temperatures well above the onset of superconductivity (Alloul *et al.*, 1989; Curro *et al.*, 1997). Such data has been taken as evidence for singlet formation at high temperatures. Additional evidence for a pseudogap due to singlet formation comes from the strong decrease in the linear coefficient of the specific heat below T^* and its decreasing jump magnitude with underdoping (Loram *et al.*, 1993) which shows that a loss of entropy begins to occur at temperatures much higher than T_c .

The in-plane optical conductivity shows an interesting midinfrared absorption (Cooper *et al.*, 1989; Rotter *et al.*, 1991). This can be seen in an inversion of the optical conductivity as a sharp upturn in the scattering rate (Basov *et al.*, 1996). As discussed below this phenomenon has also been explained somewhat inconsistently as coupling to a bosonic mode. More dramatically, the c-axis conductivity itself shows a large gap developing below T^* (Takigawa *et al.*, 1989). The temperature dependence of the subgap conductivity (Homes *et al.*, 1993) tracks the suppression in the spin susceptibility.

Despite the considerable interest in this phenomena, arguably it was angle resolved photoemission measurements that made the field take the pseudogap seriously. In underdoped samples, Ding *et al.* (1996); Loeser *et al.* (1996) found an above T_c ‘leading edge’ gap that had the same order of magnitude and a similar functional form as the d-wave superconducting gap, which lead to speculation that the pseudogap was a precursor to the

pairing gap. Later experiments claimed that the pseudogap’s minimum gap locus coincided with the normal state Fermi surface giving evidence that the pseudogap should be associated with a $q = 0$ Fermi surface instability (like superconductivity) (Ding *et al.*, 1997). More recent ARPES experiments using higher momentum resolution have refined this picture however and claim that there are two distinct gaps that show different momentum and temperature dependencies (Lee *et al.*, 2007), although aspects of this was implied in earlier work (Norman *et al.*, 1998). The claim is that there is a gap exhibited near the zone diagonal, which opens up at T_c , whereas the zone face gap doesn’t close until much higher temperatures. These results are consistent with Andreev tunneling spectra (Deutscher, 1999) and some quasiparticle tunneling that claimed a second gap opened up actually at T_c itself. More recent STM data also claims the existence of two gaps in underdoped cuprates (Boyer *et al.*, 2007; Gomes *et al.*, 2007). Whether or not both gaps show a minimum gap locus that coincides with the normal state Fermi surface is an open issue and one that deserves further investigation.

If in fact the pseudogap originates in a pairing gap that persists far above T_c , the implication is that the superconducting transition is non-mean field like and instead characterized by the ordering of the phase of the superconducting order parameter while its amplitude is already well formed. Early on Uemura *et al.* (1989) showed that the T_c of the underdoped compounds scaled with their superfluid density (stiffness)³, implying that the transition was a phase-ordering one. It can be motivated on quite general grounds that this is the expectation for superconductors with small superfluid density (Emery and Kivelson, 1995) like the cuprates⁴. Strong evidence for phase fluctuations at temperature well above T_c has been found in the recent work on the Nernst effect (Wang *et al.*, 2006b, 2001; Xu *et al.*, 2000)⁵, torque magnetometry (Wang *et al.*, 2005a), and THz conductivity (Corson *et al.*, 1999). Although there is a remarkable amount of evidence that the pseudogap regime has strong superconducting correlations, there is also a large amount of experimental evidence that the primary

² Although some aspects of the q space pattern derived from STM are straightforwardly consistent with quasiparticle scattering, it is disputed that all features can be described in this fashion (Kivelson *et al.*, 2003).

³ We note that there is recent evidence that the celebrated ‘Uemura’ scaling (Uemura *et al.*, 1989) is disrupted for the lowest doped samples (Broun *et al.*, 2007). This does not change the implication that the transition is still essentially a phase-ordering one.

⁴ The electron-doped cuprates appear to have a significantly larger relative superfluid stiffness (4-15 times) as compared to hole-doped compounds of similar T_c (Emery and Kivelson, 1995; Shengelaya *et al.*, 2005; Wu *et al.*, 1993). This gives evidence for a significantly smaller role played by phase fluctuations and indicates that the superconducting transition may be more mean field-like in these compounds.

⁵ Recently it has been claimed that the majority of the Nernst signal far above T_c comes from the appearance of multiple bands from density wave formation (Cyr-Choiniere *et al.*, 2009)

driver of the pseudogap is a competing order that dominates the underdoped region. A major question with regards to competing order scenarios, is whether or not T^* represents a true phase transition or a crossover where fluctuations of the order become strong. Possibilities for this competing order include the remnants of antiferromagnetism at higher dopings, ‘stripes’ and other inhomogeneous states (Carlson *et al.*, 2003; Emery and Kivelson, 1993; Zaanen and Gunnarsson, 1989), d-density wave (DDW) (Chakravarty *et al.*, 2001), various other orbital current states (Lee *et al.*, 2006b; Varma, 1999), and charge ordering scenarios including ‘checkerboards’ (Seo *et al.*, 2007) and localized Cooper pair insulators (Chen *et al.*, 2004; Granath *et al.*, 2001; Podolsky *et al.*, 2003; Tešanović, 2004) (which are related to the precursor pairing scenarios discussed above). Clearly, the literature on this subject is vast and we cannot cover all important scenarios.

A pseudogap state originating in some manner from antiferromagnetism has always been a natural scenario, considering the strong antiferromagnetic fluctuations that persist up to reasonably high dopings (Kastner *et al.*, 1998). There have been many proposals which emphasize a coupling of charge carriers to the bosonic antiferromagnetic spectrum within a generalized strong coupling Eliashberg scenario (Abanov *et al.*, 2001; Carbotte *et al.*, 1999; Schachinger *et al.*, 2003).

Doping a Mott insulator does not automatically result in a spatially homogeneous state (Emery and Kivelson, 1993; Lee and Kivelson, 2003). The magnetic energy loss that comes from breaking magnetic bonds by doping charge can be minimized by forming segregated charge rich regions. This tendency towards phase separation is opposed by the charge’s long range Coulomb interaction. STM has given evidence for such an intrinsic inhomogeneity (Howald *et al.*, 2001; Lang *et al.*, 2002), although other STM work claims that it is related to chemical inhomogeneities (Renner and Fischer, 1995) and possibly correlated with oxygen dopant atom position (McElroy *et al.*, 2005; Renner and Fischer, 1995). A number of different inhomogeneous charge structures are possible that may be sources for pseudogap physics. One of the most considered has been the formation of one dimensional structures - so-called ‘stripes’ - in an effort to minimize this competition (Carlson *et al.*, 2003; Emery and Kivelson, 1993; Kivelson *et al.*, 2003; Zaanen and Gunnarsson, 1989). There has been evidence for stripes in a number of underdoped compounds. Tranquada *et al.* (1995) found static 1D ordering in the LTT phase of Nd-doped LSCO. Evidence for fluctuations of this order has been found in Nd free materials (Fujita *et al.*, 2002; Wakimoto *et al.*, 1999; Yamada *et al.*, 1998) via neutron and x-ray scattering. Resonant soft x-ray scattering has found charge modulation consistent with stripe formation (Abamonte *et al.*, 2005). However, there is a question of how generic this phenomenon is, although strong incommensurate scatterings have been found via inelastic neutron scattering in LSCO (Cheong *et al.*, 1991) and Y123

(Mook *et al.*, 1998, 2002) that have been interpreted as dynamic stripe fluctuations given their strong resemblance to that pattern found by Tranquada *et al.* (1995). These stripe correlations appear to be strongest at “ $\frac{1}{8}$ doping” ($x=0.125$ in LSCO) where the charge and magnetic periodicity is commensurate with the lattice and presumably has an enhanced tendency for pinning. Evidence for spin/charge order has also been reported for the vortex state of $\text{La}_{2-x}\text{Sr}_x\text{CuO}_4$ via neutron scattering (Lake *et al.*, 2001), NMR (Mitrovic *et al.*, 2001), and STM (Hoffman *et al.*, 2002a; Howald *et al.*, 2003a,b). The state observed is consistent with stripe order, although other possibilities exist. Fluctuations of stripe order or charge order are one plausible candidate for the pseudogap.

There has also been a great deal of recent interest in competing ordered states that break time reversal symmetry (TRS) as the origin of the pseudogap. For instance as mentioned above Varma has proposed a state with bond currents that exist on O-Cu-O triangular plaquettes (Varma, 1999). This state breaks time-reversal and inversion, although the symmetry that is a product of the two is preserved. Using an asymmetry in the ARPES circular dichroism Kaminski *et al.* (2002) claimed to find such a state. However, later work has claimed that this result can be explained by the parity breaking of the Bi2212 superstructure (Armitage and Hu, 2004; Borisenko *et al.*, 2004). Recently, via neutron scattering, Fauqué *et al.* (2006) have claimed to find a pattern consistent with that proposed by Varma. The observed magnetic moment however has a significant projection in-plane, which is superficially at odds with the notion of an in-plane orbital current although proposals exist to rationalize these views (Weber *et al.*, 2009)⁶. Even more recently Xia *et al.* (2008) have found evidence for a phase transition at a temperature $T_s(p)$, below which their Sagnac loop interferometer detects a nonzero Kerr angle, indicating the existence of a phase with a ferromagnetic moment and hence broken TRS. Although the signal found by Xia *et al.* (2008) is naively inconsistent with the current loops, impurities may induce a small ferromagnetic component in the state proposed by Varma.

We should mention that different experimental probes disagree on the exact phase diagram boundaries of the pseudogap regime (Lee *et al.*, 2006b; Timusk and Statt, 1999). Discrepancies exist with how high the T^* per-

⁶ Weber *et al.* (2009) have found through variational Monte Carlo that the inclusion of apical oxygen orbitals into the multi-band Hubbard model serves to stabilize the bond current state by allowing out-of-plane orbital current, which effectively reverses the sign of t_{pd} . This also provides a natural explanation for Fauqué *et al.* (2006)’s observation of in-plane moments. It is also consistent with the out-of-plane moments found in $\text{HgBa}_2\text{CuO}_{4+\delta}$ by Li *et al.* (2008b). This is particularly interesting in light of the lack of apical oxygen in the electron-doped cuprates and the very different phenomenology of their pseudogap and underdoped regime.

sists and where exactly it intersects the superconducting dome (i.e. does it skim the overdoped side (Shibauchi *et al.*, 2001) or does it intersect it at more or less optimal doping (Tallon *et al.*, 1999)?). Discrepancies also exist as to its magnitude. Some refer to a lower energy scale on the order of the superconducting gap (at optimal doping) while others refer to it more as an energy scale on the order of 50 - 150 meV ($\approx J$) where spectral suppression is observed over a larger energy region in, for instance, the angle resolved photoemission spectra and optical scattering rate. In this regard, it is possible and even likely that there are multiple sources for ‘pseudogap’ phenomena, with phonons, various kinds of magnetic and charge order, and superconducting fluctuations all playing a role.

There are also anomalous normal state properties which are not explicitly related to the pseudogap, although they may be related. The most famous of these is the linear in T dependence of the resistivity in many compounds near optimal doping. We should note that linear temperature dependence of the resistivity is not in itself anomalous, as within conventional transport theory, one will almost invariably have a phonon contribution that in certain temperature limits will give a linear dependence. Remarkably however this linearity extends to *both* low temperatures and unprecedentedly high temperatures. This behavior is particularly dramatic in the case of LSCO near optimal doping where the linearity persists from a T_c of ≈ 40 K to 1100 K (Gurvitch and Fiory, 1987) and Bi2201 where the linearity persists from T_c of 7 K to 700 K (Martin *et al.*, 1990). There is no sign of the “resistivity saturation” that is found in most metals when the electronic mean free path l decreases to be on the order of a the lattice constant. As these materials then are in strong violation on the Ioffe-Regel criterion (Ioffe and Regel, 1960), the implication is that the charge carriers are not electron-like quasiparticle objects and hence the normal state is a non-Fermi liquid. The linear dependence of the resistivity has been interpreted in a few specific ways, including as evidence for a hidden quantum critical point (QCP) and a *marginal* Fermi liquid state (Varma *et al.*, 1989). However, the implication that at a QCP the loss of any energy scale but the temperature itself, implies a resistivity linear in T has recently been disputed on general scaling grounds (Phillips and Chamon, 2005).

Last but by no means least there is the question of the mechanism for superconductivity itself. A number of distinct views exist. One class of views holds that the superconductivity can be understood within some generalization of the strong coupling BCS-Eliashberg theory to the proper correlated degrees of freedom. In this prescription, one identifies the pairing boson exchanged between electrons, which along with the rapid screening of the repulsive interaction of other electrons gives a residual attractive interaction near the Fermi surface and leads to pairing. Such theories posit that in correspondence with the phonon mechanism of conventional

superconductivity that there is a boson which can be taken as the pairing “glue” between electrons. This boson could be the phonon, although more frequently it is taken to be a magnon. This is the situation for instance in superfluid He3, where in the absence of a lattice, pairing is mediated by paramagnon exchange resulting in a non-conventional *p*-wave order parameter symmetry (in its ‘*B*’ phase). Insofar as a similar scenario might be appropriate for the cuprates, the debate here has revolved around the character of the boson involved. Can phonons in a low carrier density system with concomitantly low ionic screening, along with strong local Coulomb repulsion, give *d*-wave superconductivity and high T_c (Chakraverty, 1981; Micnas *et al.*, 1990)? Or is superconductivity mediated by antiferromagnetic magnon exchange? Certainly it was pointed out early on, that *d*-wave was a natural scenario for an antiferromagnetic interaction (Kampf and Schrieffer, 1990), but questions have been raised to the internal consistency of such a mechanism for superconductivity (Anderson, 1997). As mentioned earlier, there have been many proposals which emphasize a coupling of charge carriers to the bosonic antiferromagnetic spectrum within a generalized strong coupling Eliashberg scenario (Abanov *et al.*, 2001; Carbotte *et al.*, 1999; Schachinger *et al.*, 2003).

Much recent debate concerning ARPES, optics, and tunneling data concerns whether or not various features in these charge excitation spectra can be regarded as being indicative of strong electron-phonon or electron-magnon coupling. Implicit in these discussions, is that the strongly coupled boson may be implicated in pairing. It has been observed for instance that a mass renormalization, or “kink”, in the dispersion is found ubiquitously in the low-energy ARPES spectra of a number of high-temperature hole-doped cuprate superconductors in the *p*-type materials (at ≈ 70 meV)(Bogdanov *et al.*, 2000; Lanzara *et al.*, 2001). Its origin is a matter of much current debate. Some groups have pointed to a many-body electronic source(Gromko *et al.*, 2003; Johnson *et al.*, 2001; Kaminski *et al.*, 2001) related to the ‘41 meV’ magnetic resonance mode discovered via neutron scattering (Mook *et al.*, 1993; Rossat-Mignod *et al.*, 1991). Others have argued that the kink’s presence above T_c , the relative doping independence of its energy scale, and its universality among material classes demonstrate a phononic origin and indicates the strong role that lattice effects have on the low-energy physics(Lanzara *et al.*, 2001). We note that whatever the origin of this effect, it is almost certainly the same as that which causes the upturn in the optical scattering rate (Basov and Timusk, 2005). We should also mention that much of the discussion regarding “kinks” and the like has implicitly assumed that the only possibility of understanding such features are a consequence of some sort of electron-boson coupling, but this is not necessarily the case. There are proposals that purely electronic interactions and proximity to a Mott insulator can give such features (Byczuk *et al.*, 2007; Shiladitya Chakraborty, 2007).

In contrast to this line of reasoning about the mechanism, there have been a number of theoretical proposals that are distinctly different from the generalized BCS-Eliashberg paradigm of a boson exchange. Most of these proposals emphasize the enhanced effect of interactions in the cuprates and or non-Fermi liquid states as an essential part of the mechanism. For instance in the original resonating valence bond (RVB) theory of Anderson (Anderson, 1987), pairing is inherited from the resonating singlet bonds of the parent Mott insulating state. These pairs are bound by the essentially instantaneous superexchange interaction J that is not describable in terms of boson exchange (See discussion and references in Anderson (2006); B. Kyung (2009); Maier *et al.* (2008)). Superconductivity then results from the Bose condensation of the holons in the spin-charge separated RVB state giving a charge superfluid.

There have been a number of other novel routes to understanding the superconductivity. For instance, Zhang (1997) proposed that there exists an approximate symmetry between antiferromagnetism and superconductivity in the cuprates that could be understood within a generalized SO(5) order parameter. To investigate novel kinetic energy lowering based mechanisms, there has also been a great deal of work in investigating spectral weight transfer in the optical conductivity (Molegraaf *et al.*, 2002). There are many other proposed novel routes to superconductivity; too many to detail here. The interested reader is referred to the literature for scenarios based on for instance, quantum criticality (Sachdev, 2003), bipolarons (Alexandrov and Mott, 1996), and SU(2) theories of gauge antiferromagnetism (Lee *et al.*, 2006b) to give a stupendously incomplete list. One should also note that there has been tremendous progress with numerical methods that allow one to take into account Mott physics within the Hubbard model. These methods are cluster generalizations (Maier *et al.*, 2005a) of Dynamical Mean Field Theory (Georges *et al.*, 1996). Phase diagrams that are in quite close to the experimentally observed ones are obtained for both hole- and electron-doped compounds (Kancharla *et al.*, 2008; Senechal *et al.*, 2005; Tremblay *et al.*, 2006) when realistic band parameters and intermediate values of U are used. Many physical properties are also accounted for by these methods (Haule and Kotliar, 2007; Maier *et al.*, 2005b).

B. General aspects of the phase diagram

Like many great discoveries in material science the discovery of superconductivity in the $\text{Nd}_{2-x}\text{RE}_x\text{CuO}_4$ material class came from a blend of systematic investigation and serendipity (Khurana, 1989). Along with the intense activity on the hole-doped compounds in the late 1980's, a number of groups had investigated n -type substitutions. These efforts were given up as there were no signs of superconductivity and with the pace of research and discovery being what it was they could not afford to

pursue non-fruitful directions for long. The work on the $\text{Nd}_{2-x}\text{RE}_x\text{CuO}_4$ system was motivated after the discovery of 28K superconductivity in $\text{Nd}_{2-x-y}\text{Sr}_x\text{Ce}_y\text{CuO}_4$, by Akimitsu *et al.* (1988). There it was found that higher cerium concentrations actually reduced and eventually killed the superconducting T_c (Tokura *et al.*, 1989a).

As no one had found a superconducting electron-doped cuprate, the original work on NCCO at the University of Tokyo was done with the likely result in mind that the material when doped with electrons may become an n -type metal, but it would not become a *superconductor*. This would indicate the special role played by superconducting holes. Initial work seemed to back up this prejudice. The group found that indeed the conductivity seemed to rise when increasing cerium concentration and that for well-doped samples the behavior was metallic ($d\rho/dT > 0$) for much of the temperature range. Hall effect measurements confirmed the presence of mobile electrons. This underscored the suspicion that cerium was substituting tetravalently (+4) for trivalent neodymium (+3) and was donating electrons for conduction.

At the lowest temperatures the materials were not good metals and showed residual semiconducting tendencies with $d\rho/dT < 0$. In an attempt to create a true metallic state at low temperature, various growth conditions and sample compositions were tried. A breakthrough occurred when a student, H. Matsubara, accidentally quenched a sample in air from 900°C to room temperature. This sample, presumed to be destroyed by such a violent process, actually showed superconductivity at 10K. Further work showed that in samples with $x=0.15$ cerium concentration superconductivity could be induced at 20K, by oxygen *reducing* them in a flowing argon (or similar) environment. Later it was found that by optimizing the conditions T_c could be pushed as high as 24K (Takagi *et al.*, 1989; Tokura *et al.*, 1989b). n -type superconductivity was subsequently discovered in a number of related compounds based on rare-earths (Dalichaouch *et al.*, 1993; Maple, 1990). It should be mentioned here that the crucial reduction process has been found thus far to be always required to obtain superconductivity. Naively, one expects removing oxygen to increase the electron concentration, but one can not compensate for excess oxygen with excess cerium. As we will show below, although this oxygen reduction certainly modifies the carrier concentration, this cannot be its only role.

The first reports of superconductivity in $\text{Nd}_{2-x}\text{Ce}_x\text{CuO}_4$ and $\text{Pr}_{2-x}\text{Ce}_x\text{CuO}_4$ by Takagi *et al.* (1989) also presented the first phase diagram of this family (see Fig. 4). In comparison to $\text{La}_{2-x}\text{Sr}_x\text{CuO}_4$, the doping dependence of the critical temperature (T_c) of these materials was sharply peaked around $x_{opt} = 0.15$ (optimal doping) corresponding to the maximum value of $T_{c,opt}$ ($\sim 24\text{K}$). As mentioned above, a striking and as of yet unexplained difference between the $(\text{RE,Ce})_2\text{CuO}_4$ and $(\text{La,Sr})_2\text{CuO}_4$ $T_c(x)$ dependence is the very narrow range of doping for which superconductivity is observed for the electron-doped cuprates.

In fact, at first glance, the $T_c(x)$ relation showed no underdoped regime ($x < x_{opt}$) with T_c rising from zero to its maximum value within a Δx of ~ 0.01 (from $x = 0.13$ to 0.14). Even the overdoped regime ($x > x_{opt}$) presents a sharp variation of T_c ($\frac{dT_c}{dx} \sim 80K/unit$). As discussed below, such steep dependence of $T_c(x)$ makes the exploration of the phase diagram very difficult.

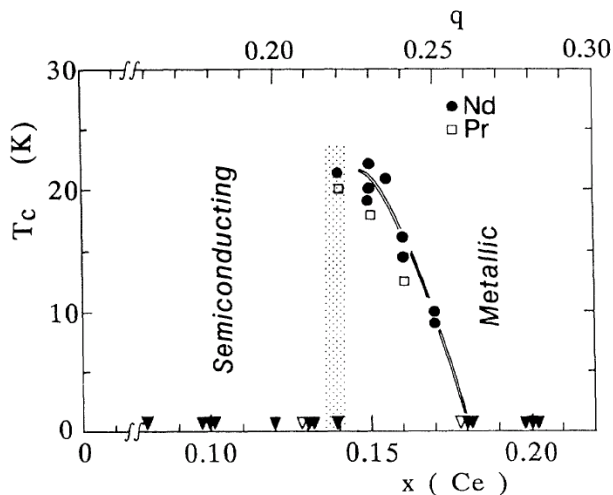


FIG. 4 Transition temperature T_c as a function of the Ce concentration in reduced NCCO (circles) and PCCO (squares). The closed and open triangles indicate that bulk superconductivity was not observed above 5 K for the Nd or Pr systems respectively. From the original paper of Takagi *et al.* (1989).

Another important difference in the phase diagram of electron-doped cuprates with respect to their hole-doped cousins is the close proximity of the antiferromagnetic phase to the superconducting phase. Using muon spin resonance and rotation on polycrystalline samples, Luke *et al.* (1990) first found that the Mott insulating parent compound Nd_2CuO_4 has a Néel temperature (T_N) of approximately 250K⁷. Upon substitution of Nd by Ce, T_N of $\text{Nd}_{2-x}\text{Ce}_x\text{CuO}_4$ decreases gradually to reach zero close to optimal doping ($x \sim 0.15$)⁸. As noted previously, this should be contrasted with the case of $\text{La}_{2-x}\text{Sr}_x\text{CuO}_4$ in which antiferromagnetism collapses completely with dopings as small as $x = 0.02$ (Kastner *et al.*, 1998; Luke *et al.*, 1990). In the case of NCCO, the antiferromagnetic phase extends over a much wider range of cerium doping. This difference gives us a first hint that electron doping and

hole doping are not affecting the electronic properties in the same exact manner in the cuprates. Luke *et al.* mentioned that a possible interpretation of this marked difference is that while hole doping in the CuO_2 planes frustrates the AF order, electron doping leads instead to spin *dilution* (Luke *et al.*, 1990). This issue is discussed in more detail below. The proximity of the AF phase to the superconducting one is reminiscent of the situation in strongly correlated electronic systems like the organic superconductors (Lefebvre *et al.*, 2000; McKenzie, 1997) and some heavy fermion compounds (Coleman, 2007; Joynt and Taillefer, 2002). However, it still remains unclear up to now whether or not AF actually coexists with superconductivity. This will also be discussed in detail below.

C. Specific considerations of the cuprate electronic structure upon electron doping

As mentioned, doped electrons are believed to reside primarily on Cu sites. This nominal $3d^{10}$ atomic configuration of an added electron has been confirmed via a number of resonant photoemission studies which show a dominant Cu $3d$ character at the Fermi level (Allen *et al.*, 1990; Sakisaka *et al.*, 1990) in electron doped compounds. As discussed above, within the context of the single band Hubbard or $t - J$ models, the effective orbital of a hole-doped into the CuO_2 plane $3d^9 \underline{L}$ may be approximated as a singlet formed between the local Cu^{+2} spin and the hole on the oxygen atoms. This is viewed as equivalent to the state of a spinless hole $3d^8$ on the copper atom (albeit with different effective parameters). Although their actual local character is different, such an approximation makes the effective model describing holes and electrons doped into $3d^9$ virtually identical between the p - and n -type cuprates leading to the prediction of an electron-hole symmetry. The noted *asymmetry* between the two sides of the phase diagram means that there are specific extra considerations that must go into the two different cases.

There are a number of considerations regarding the cuprate electronic structure that apply specifically to the case of electron doping. As mentioned repeatedly, the phase diagrams of the hole and electron-doped compounds differ considerably, with the antiferromagnetic phase being much more robust on the electron-doped side. One approach to understanding this difference has been to consider *spin-dilution models*. It was shown via neutron scattering that Zn doping into La_2CuO_4 reduces the Néel temperature at a similar rate as Ce doping in $\text{Pr}_{2-x}\text{Ce}_x\text{CuO}_{4\pm\delta}$ (Keimer *et al.*, 1992). Since Zn substitutes in a configuration that is nominally a localized d^{10} filled shell, it can be regarded as a spinless impurity. In this regard Zn substitution can be seen as simple dilution of the spin system. The similarity with the case of Ce doping into $\text{Pr}_{2-x}\text{Ce}_x\text{CuO}_{4\pm\delta}$ implies that one of the effects of electron doping is to dilute the spin system

⁷ T_N is very sensitive function of oxygen concentration. Subsequent work has shown that the Néel temperature of ideally reduced NCO is probably closer to 270 K (Mang *et al.*, 2004b)

⁸ The precise extent of the AF state and its coexistence or not with SC is a matter of much debate. See Sec. IV.G for further details.

by neutralizing the spin on a d^9 Cu site. It subsequently was shown that the reduction of the Néel temperature in $\text{Nd}_{2-x}\text{Ce}_x\text{CuO}_{4\pm\delta}$ comes through a continuous reduction of the spin stiffness ρ_s which is consistent with this model (Matsuda *et al.*, 1992). In contrast, in the hole-doped case Aharony *et al.* (1988) have proposed that only a small number of *holes* is required to suppress antiferromagnetism because they primarily exist on the in-plane oxygen atoms and result in not spin-*dilution* but instead spin-*frustration*. The oxygen-hole/copper-hole interaction, whether ferromagnetic or antiferromagnetic, causes the spins of adjoining Cu-holes to align. This interaction competes with the antiferromagnetic superexchange and frustrates the Néel order and so a small density of doped holes has a catastrophic effect on the long-range order. This additional frustration does not occur with electron doping as electrons are primarily introduced onto Cu sites.

This comparison of Ce with Zn doping is compelling, but cannot be exact as Zn does not add itinerant charge carriers like Ce does, as its d^{10} electrons are tightly bound and can more efficiently frustrate the spin order. Models or analysis which takes into account electron itinerancy must be used to describe the phase diagrams. But this simple model gives some indication how the operative physics can be very different between electron and hole-doping.

Alternatively, it has been argued that the observed *asymmetry* between hole and electron doping (say for instance in their phase diagrams) can be understood within single band models ($t - J$ or single band Hubbard), by considering the difference in the manner that the next nearest t' and next-next nearest neighbor t'' hopping terms are introduced (Tohyama and Maekawa, 1994, 2001). The same models developed to handle hole doping can be applied to electron doping with the transformation

$$c_{i\sigma}^\dagger \rightarrow (-1)^i c_{i\sigma} \quad (1)$$

where c and c^\dagger are particle creation and annihilation operators and i is a site index. This means that the hopping terms, which have values $t > 0$, $t' < 0$, and $t'' > 0$ for hole doping assume values $t < 0$, $t' > 0$, and $t'' < 0$ for electron doping⁹.

Since the next nearest t' and next-next nearest neighbor t'' terms facilitate hopping on the same sub-lattice of the Néel state, the energy and stability of antiferromagnetic order is very sensitive to their values. For instance, it has been argued that the greater stability of antiferromagnetism in the electron-doped compounds is primarily a consequence of $t' > 0$. This scenario is supported by

a number of numerical calculations and analytical treatments (Gooding *et al.*, 1994; Pathak *et al.*, 2009; Singh and Ghosh, 2002; Tohyama and Maekawa, 1994, 2001).

Models that account for the effective sign change of the hopping parameter, also appear to successfully account for the fact that the lowest energy hole addition (electron removal) states are near $(\pi/2, \pi/2)$ (Wells *et al.*, 1995), while the lowest energy electron addition states (hole removal) are near $(\pi, 0)$ (Armitage *et al.*, 2002). This manifests as a small hole-like Fermi arc (or perhaps pocket (Doiron-Leyraud *et al.*, 2007; LeBoeuf *et al.*, 2007)) for low hole dopings near the $(\pi/2, \pi/2)$ point and a small electron-pocket near the $(\pi, 0)$ point for low electron dopings (Armitage *et al.*, 2002). Such considerations also mean that the insulating gap of the parent compounds is indirect. Aspects of $t - J$ type models applied to both sign of charge carriers have been reviewed by Tohyama (2004).

Although it may be that such a mapping can be applied so that the same model (for instance $t - J$) captures aspects of the physics for both hole and electron doping, the intrinsic object that is undergoing hopping in each case has very different spatial structure and local character ($3d^{10}$ vs. a $3d^9\bar{L}$ ZR singlet). It is reasonable to expect that the values for their effective hopping parameters could be very different. It is also reasonable to expect that their interaction with degrees of freedom not explicitly considered in these electronic models, such as the strength of their lattice coupling, could also be very different (unique aspects related to lattice coupling in the electron-doped cuprates are discussed in Sec. IV.D below.). It is surprising then, that the magnitudes of t and t' extracted from Cu-O cluster calculations has been found to be reasonably similar for electron and hole doping. Hybertsen *et al.* (1990) used *ab initio* local-density-functional theory to generate input parameters for the three-band Hubbard model. They then computed spectral functions exactly on finite clusters using the three band Hubbard model and compared the results with the spectra of the one band Hubbard and the $t - t' - J$ models. Interestingly the extracted effective nearest neighbor and next nearest neighbor hopping parameters were found to be almost identical at $t = 0.41$ and $|t'| = 0.07$ eV for electron doping and $t = 0.44$ and $|t'| = 0.06$ eV for hole doping. J was found in this study to be 128 ± 5 meV which is in reasonable agreement with neutron (Mang *et al.*, 2004b) and two-magnon Raman scattering (Blumberg *et al.*, 1996; Lyons *et al.*, 1988; Singh *et al.*, 1989; Sulewski *et al.*, 1990). Somewhat similar results for the hole-doped case were obtained by Bacci *et al.* (1991). However these results conflicted with those of Eskes *et al.* (1989) who found slightly different values between hole ($t = -0.44$, $t' = 0.18$ eV) and electron doping ($t = 0.40$, $t' = -0.10$ eV) in their numerical diagonalization study of Cu_2O_7 and Cu_2O_8 clusters. In a similar calculation but with slightly different parameters and also taking into account the apical oxygen for the hole-doped case Tohyama and Maekawa (1990) found the even more dif-

⁹ Note that the final results in either doping case are invariant with respect to the sign of t .

ferent $t = -0.224$ and $t' = 0.124$ eV for the p -type and $t = 0.3$ and $t' = -0.06$ eV for the n -type cases. This shows the strong sensitivity that these effective parameters likely have on the local energies and the presence of apical oxygen. Despite differences in the estimates for these parameters it is still remarkable that the values for holes and electrons are so close to each other considering the large differences in these states' local character. We should also point out that it is interesting that the values of $|t'/t| \approx 0.3 - 0.4$ found by most *ab initio* studies coincides with the range with the largest pairing correlations in $t - J$ type models (Lee *et al.*, 2006b).

It is also interesting to note that although very different behavior of the electronic structure is expected and indeed found at low dopings, at higher dopings it appears that in both systems the sets of small Fermi pockets go away and a large Fermi surface centered around the (π, π) point emerges (Anderson *et al.*, 1993; Armitage *et al.*, 2002; King *et al.*, 1993). In the electron-doped materials, aside from the 'hot-spot' effect discussed in detail below, the Fermi surface resembles the one calculated *via* LDA band structure calculations.

A number of workers (Kusko *et al.*, 2002; Kyung *et al.*, 2004, 2003; Tremblay *et al.*, 2006) have pointed out that due to the different size of the effective onsite repulsion U and the electronic bandwidth W in the n -type systems, the expansion parameter W/U is less than unity, which puts the electron-doped cuprates in a weaker correlated regime than the p -type compounds. Among other things, this may make Hubbard model-like calculations more amenable¹⁰. Smaller values of U/W physically derive from better screening and the Madelung potential differences noted above, as well as a larger occupied bandwidth. This somewhat weaker coupling may allow for more realistic comparisons between theoretical models and experiment and serve as a check on what models are most appropriate for the more correlated hole-doped materials. The fact that we may be able to regard the n -type systems as weaker correlated is manifest in a number of ways, including the remarkable fact that a mean-field spin-density wave (SDW) like treatment can capture many of the gross features of transport, optics, and photoemission quite well. It also makes the issue of AF fluctuations easier to incorporate. For instance, the Two-Particle Self-Consistent (Kyung *et al.*, 2004) approach to the Hubbard model allows one to predict the momentum dependence of the PG in the ARPES spectra, the onset temperature of the pseudogap T^* , and the temperature and doping dependence of the AF correlation length. A similar treatment fails in hole-doped compounds with their corresponding values of U/W . The n -type com-

pounds appear to be the first cuprate superconductors whose normal state lends itself to such a detailed theoretical treatment. These issues are dealt with in more detail below.

D. Crystal structure and solid-state chemistry

RE_2CuO_4 with RE = Nd, Pr, Sm, Eu, Gd crystallizes in the so-called T' crystal structure. These compounds are tetragonal with typical lattice parameters of $a = b \sim 3.95$ Å and $c \sim 12.15$ Å. This close cousin of T structure La_2CuO_4 (LCO) is represented by the D_{4h}^{17} point group (I4/mmm). It has a body-centered unit cell where the copper ions of adjacent copper-oxygen CuO_2 layers are displaced by $(a/2, a/2)$ with respect to each other (Kastner *et al.*, 1998). In Fig. 1, we compare the crystal structure of these parent compounds. Similar to other HTSC, the building blocks of the electron-doped cuprates are the CuO_2 planes with strong covalent bonding (hybridization of Cu 3d and O 2p atomic levels) sandwiched between rare earth-oxygen layers with strong ionic character, which are the so-called reservoir layers.

Although aspects of the LCO and NCO crystal structures are similar closer inspection (Kwei *et al.*, 1989; Marin *et al.*, 1993) reveals notable differences. First, the coordination number of the in-plane copper is different. The T' structure has no apical oxygen above the in-plane Cu and hence only four oxygen ions O(1) surround each copper. The T structure has 6 surrounding O atoms, one of which is in the apical position.

The different relative positions of the reservoir oxygens O(2) with respect to the T -structure results in an expanded in-plane unit cell with respect to La_2CuO_4 that allows a further decrease of the unit cell volume with decreasing rare earth ionic radius (see Table I). While La_2CuO_4 with the T -structure has typical lattice parameters on the order of $a = b \sim 3.81$ Å and $c \sim 13.2$ Å (Kastner *et al.*, 1998)¹¹ and a unit cell volume of 191.6 Å³, the largest undoped T' phase cuprate, Pr_2CuO_4 , has $a = b \sim 3.96$ Å and $c \sim 12.20$ Å and similar unit cell volume of 191.3 Å³. The smallest, Eu_2CuO_4 , has $a = b \sim 3.90$ Å and $c \sim 11.9$ Å (Fontcuberta and Fabrega, 1996; Nedil'ko, 1982; Uzunaki *et al.*, 1991; Vigoureux, 1995)¹². The second notable difference arising from the expanded in-plane lattice parameters is that the rare-earth and oxygen ions in the reservoirs are not positioned in the same plane (parallel to the CuO_2 planes).

Until recently it was believed that only T' crystal structures without apical oxygen are electron doped. This

¹⁰ In a reanalysis of optical and ARPES data Xiang *et al.* (2008) in fact have argued that the charge transfer gap Δ , which is the effective onsite Hubbard repulsion is much smaller than usually assumed in the electron-doped compounds. They claim $\Delta \approx 0.5$ eV.

¹¹ The real in-plane lattice parameters of LCO are actually $a^* b^* = \sqrt{2}a$ as shown in Fig. 1. In this case, a^* and b^* are at 45° with respect to the Cu-O bonds.

¹² Here we neglect the other (RE)CCO compound in this series Gd_2CuO_4 , since it does not become superconducting upon Ce doping

was understood within a Madelung potential analysis, where the local ionic potential on the Cu site is influenced strongly by the presence of an O^{-2} ion in the apical site immediately above it (Torrance and Metzger, 1989). As doped electrons are expected to primarily occupy the Cu site, while doped holes primarily occupy in-plane O sites the local ionic potentials play a strong role in determining which sites mobile charges can occupy. Recent developments may not be entirely consistent with this scenario as there has been a report of superconductivity in T phase $La_{2-x}Ce_xCuO_4$ (Oka *et al.*, 2003). However this report contrasts with various thin film studies, which claim that although T phase $La_{2-x}Ce_xCuO_4$ can be electron-doped (i.e with Ce in valence state +4) it does not become a superconductor (Tsukada *et al.*, 2005, 2007).

As observed originally by Takagi *et al.* (1989) and expanded upon by Fontcuberta and Fabrega (1996), the actual phase diagram of the electron-doped family is sensitive to the rare-earth ion size. The smaller the ionic radius of the rare-earth the smaller the optimal $T_{c,max}$ (see Table I, Fig. 5, and Fontcuberta and Fabrega (1996); Vigoureux (1995) and references therein). The most obvious effect of the decreasing ionic size (Table I) is a decrease of roughly 2.6% of the c -axis and 1.5% of the a -axis across the series. One should note also that the lattice expands with Ce substitution for Pr or Nd in PCCO and NCCO (Fontcuberta and Fabrega, 1996; Tarascon *et al.*, 1989; Vigoureux, 1995) as shown in Figure 6 for NCCO.

	La^{3+}	Pr^{3+}	Nd^{3+}	Sm^{3+}	Eu^{3+}	Gd^{3+}	Ce^{4+}
Ionic radius (Å)	1.032	0.99	0.983	0.958	0.947	0.938	0.87
a (Å)	-	3.9615	3.942	3.915	3.901	3.894	-
c (Å)	-	12.214	12.16	11.97	11.90	11.88	-
t	-	0.856	0.851	0.841	0.837	0.832	-
$T_{c,max}(K)$	-*	22	24	20	13	0	-

TABLE I Dependence on ionic radius of unit cell parameters of the parent compound, the tolerance factor t (Cox *et al.*, 1989; Muller-Buschbaum and Wollschlager, 1975; Nedil'ko, 1982; Uzumaki *et al.*, 1991), and the maximum transition temperature $T_{c,max}$ obtained by cerium doping for $x \sim 0.15$ (Fontcuberta and Fabrega, 1996; Maple, 1990). It should be noted that the T' (La,Ce) $_2CuO_4$ can only be stabilized in thin films, giving $T_{c,max} \sim 25K$ for unusual x values (Naito *et al.*, 2002). See Sec. II.E.

As the RE-O distance gradually decreases with decreasing ionic radius, the crystal structure is subjected to increasing internal stress indicated by a decreasing tolerance factor $t \equiv \frac{r_{RE}+r_O}{\sqrt{2}(r_{Cu}+r_O)}$ where r_{RE} , r_O and r_{Cu} are respectively the ionic sizes of the rare earth, the oxygen and the copper ions (see Table I). Several neutron and high-resolution x-ray scattering studies report structural distortions when the Cu-O bond length becomes too large with respect to the shrinking RE-O ionic distance

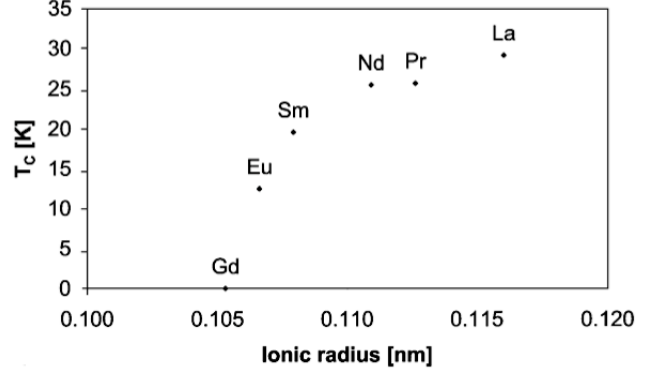


FIG. 5 The highest superconducting onset temperature versus rare earth ionic radius in $RE_{2-x}Ce_xCuO_{4+\delta}$. The data for RE=La,Pr, Nd, and Sm are for MBE grown films, and those for RE=Eu and Gd are bulk values. Note that T' phase $La_{2-x}Ce_xCuO_{4+\delta}$ can only be stabilized in thin film form as discussed in the text. From Naito and Hepp (2000).

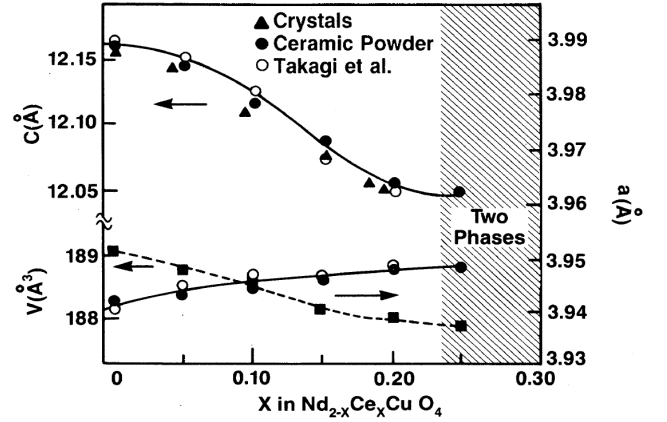


FIG. 6 The lattice parameters of NCCO single crystals and ceramic powders as a function of cerium content x showing the decreasing unit cell volume with increasing x . Solid circles and triangles refer to powder samples and single crystals respectively. Open circles are the results from (Takagi *et al.*, 1989). From Tarascon *et al.* (1989).

which promotes bond angles that deviate from 90° . The most striking result is the distorted structure of (non-superconducting) Gd_2CuO_4 with its commensurate distortion corresponding to the rigid rotation of the four planar oxygen atoms around each copper sites (Braden *et al.*, 1994; Vigoureux *et al.*, 1997). This distortion leads to antisymmetric exchange term of *Dzyaloshinski-Moriya* type that may account for the weak ferromagnetism of Gd_2CuO_4 (Oseroff *et al.*, 1990; Stepanov *et al.*, 1993).

At the other extreme, for large ionic radius, the crystal structure approaches the T' to T structural transition, which is expected for an ionic radius between those of

Pr and La (Fontcuberta and Fabrega, 1996). PCO is at the limit of the bulk T' phase: the next compound in the RE series with a larger atomic radius is LCO which crystallizes not in the T' phase, but instead in the more compressed T -phase form where the out-of plane oxygens are in apical positions as mentioned previously. It does seem to be possible to stabilize a doped T' phase of $\text{La}_{2-x}\text{Ce}_x\text{CuO}_{4+\delta}$ by substitution of La by the smaller Ce ion, although bulk crystals are not of that high quality due to the low growth temperatures required (Yamada *et al.*, 1994). However as discussed below it has been shown by Naito and Hepp (2000); Naito *et al.* (2002) that the T' phase of $\text{La}_{2-x}\text{Ce}_x\text{CuO}_{4+\delta}$ (LCCO) can be strain stabilized in *thin film* form leading to high quality superconducting materials with T_c as high as 27K. One can also drive the T' structure even closer to the structural instability by only partial substitution of Pr by La (Fontcuberta and Fabrega, 1996; Koike *et al.*, 1992) as $\text{Pr}_{1-y-x}\text{La}_y\text{Ce}_x\text{CuO}_{4\delta}$. This substitution provokes a significant modification to the phase diagram, with an optimal $T_{c,opt} \sim 25\text{K}$ for $\text{Pr}_{1-x}\text{LaCe}_x\text{CuO}_{4\delta}$ at $x \sim 0.11$ and superconductivity extending as low as $x = 0.09$ and as high as $x = 0.20$ (Fujita *et al.*, 2003) (See Fig. 7). The mechanism leading to a different phase diagram remains a mystery, but it has been suggested that it corresponds to the ability to remove a larger amount of oxygen during the necessary reduction process compared to PCCO and NCCO, which leads to larger electron concentrations (Kuroshima *et al.*, 2003). In recent years, there have been several reports of large $\text{Pr}_{1-x}\text{LaCe}_x\text{CuO}_4$ single crystals grown by the traveling-solvent floating zone (TSFZ) method (see Ref. (Kuroshima *et al.*, 2003; Wilson *et al.*, 2006c) and references therein).

There is another intriguing path to doping in the RECCO electron-doped family using fluorine substitution for oxygen (James *et al.*, 1989). $\text{Nd}_2\text{CuO}_{4-y}\text{F}_y$ (see Ref. (Sugiyama *et al.*, 1992) and references therein) which was shown to become superconducting without cerium doping. The threshold fluorine content to obtain superconductivity is roughly $y \sim 0.14 - 0.18$ with the maximum T_c reaching roughly 22K (with an onset starting as high as 27K in some instances (Sugiyama *et al.*, 1992)). Essentially, each substituted fluorine atom provides an additional electron to the crystal structure in a similar fashion as cerium doping. The systematic dependence of the physical properties with fluorine doping is quite similar to cerium as shown by a combination of both dopings (Asaf *et al.*, 1993). As the fluorine doping y is gradually increased, the resistivity and the Hall coefficient of the materials decrease (Sugiyama *et al.*, 1992). In order to dope effectively the materials with electrons, fluorine must substitute for oxygen¹³. XAFS studies have shown that fluorine substitutes for both planar O(1) and

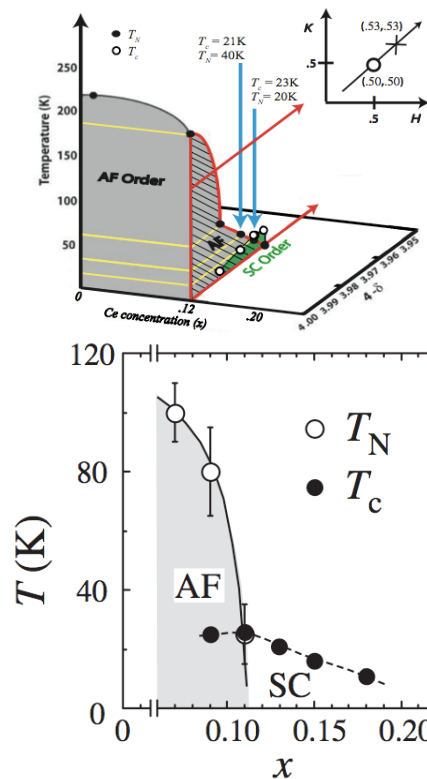


FIG. 7 (top) $\delta - x$ phase diagram of PLCCO (Wilson *et al.*, 2006b). (bottom) Phase diagram for PLCCO as a function of Ce content x (Fujita *et al.*, 2008a). As determined by neutron scattering and SQUID measurements.

out-of-plane O(2) oxygen atoms (Krol *et al.*, 1992) with proportions of 1/3 and 2/3 respectively. We note that these fluorine-doped materials must also be subjected to the enigmatic reduction process (see Section II.E.2 below) to induce superconductivity.

As mentioned above, there have been many fewer studies of the infinite layer class of electron-doped cuprate superconductors $\text{Sr}_{1-x}\text{Nd}_x\text{CuO}_2$ (SNCO) (Smith *et al.*, 1991) and $\text{Sr}_{1-x}\text{La}_x\text{CuO}_2$ (SLCO) (Kikkawa *et al.*, 1992). To date no single crystals have been produced and the data up to now relies on ceramic samples (Ikeda *et al.*, 1993; Jorgensen *et al.*, 1993; Khasanov *et al.*, 2008; Kim *et al.*, 2002) and thin films (Ichi Karimoto and Naito, 2004; Leca *et al.*, 2006; Li *et al.*, 2008c; Naito *et al.*, 2002; Nie *et al.*, 2003). Its simple structure (Fig. 8) is based on alternating of CuO_2 planes with Sr (La) layers with lattice parameters $a = b \sim 3.94 \text{ \AA}$ and $c \sim 3.40 \text{ \AA}$. Electron doping is suggested because the La (Nd) nominal valence is +3 as compared to Sr's +2 valence. n -type doping is supported by a negative thermopower (Kikkawa *et al.*, 1992) and XANES results (Liu *et al.*, 2001) confirming the presence of Cu^{1+} ions. However, a systematic study of the Hall effect with doping is still lacking, which makes difficult any comparison with the well-established behavior of transport for T' electron-doped RECCO (see

¹³ If fluorine was introduced as an interstitial it would result in hole doping

Section III.A).

The most complete phase diagram for the $\text{Sr}_{1-x}\text{La}_x\text{CuO}_2$ system has been established from the MBE film studies (ichi Karimoto and Naito, 2004). In this exploration, which was limited to the existence or not of superconductivity, the ab-plane resistivity shows that superconductivity exists in the doping range $0.08 < x < 0.15$ with the maximum $T_c \sim 40\text{K}$ for $x \sim 0.1$ as shown in Fig. 9. Because of the limited sample size, very little is known about the possible existence of an antiferromagnetic phase in the lightly doped materials and a complete phase diagram showing antiferromagnetic and superconducting phase boundaries has not been produced. However, muon spin rotation (uSR) measurements (Shengelaya *et al.*, 2005) on ceramic samples have claimed that magnetism and SC do not coexist at the $\text{La}=0.1$ doping and that the superfluid density is four times larger than in p -type cuprates with comparable T_c (i.e. off the Uemura line (Uemura *et al.*, 1991, 1989)). A similar doping dependence of T_c with substitution of Pr (Smith *et al.*, 1991), Sm and Gd (Ikeda *et al.*, 1993) rules out the possibility that superconductivity in SLCO arises due to the intercalation of the $(\text{La},\text{Sr})_2\text{CuO}_4$ phase. Early neutron scattering studies on bulk materials have shown that superconducting SLCO is perfectly stoichiometric and presents no excess (interstitial) oxygen in the Sr(La) layers (Jorgensen *et al.*, 1993). Thus, neither oxygen vacancies nor interstitial oxygen seem to play a role in the doping of this compound. Interestingly, divalent Ca can also be substituted for divalent Sr. In this case, $\text{Sr}_{0.6}\text{Ca}_{0.4}\text{CuO}_{2-\delta}$ thin films must be grown in low partial pressures of oxygen to be superconducting (Nie *et al.*, 2003), which suggests the need for oxygen vacancies. Very recently, a similar post-annealing reduction was used to induce superconductivity in $\text{Sr}_{1-x}\text{La}_x\text{CuO}_2$ thin films grown by RF sputtering (Li *et al.*, 2008c). Obviously, these contradicting reports on the need or not for reducing the infinite-layer thin films emphasize the demanding growth conditions required by these infinite-layer cuprates, and a thorough systematic study of their physical properties is definitely warranted before comparing them to the T' electron-doped cuprates.

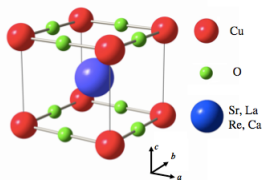


FIG. 8 Crystal structure of electron-doped infinite layer superconductor $\text{Sr}_{0.9}\text{La}_{0.1}\text{CuO}_2$. Red: Cu; Blue: Sr or La; Green: oxygen.

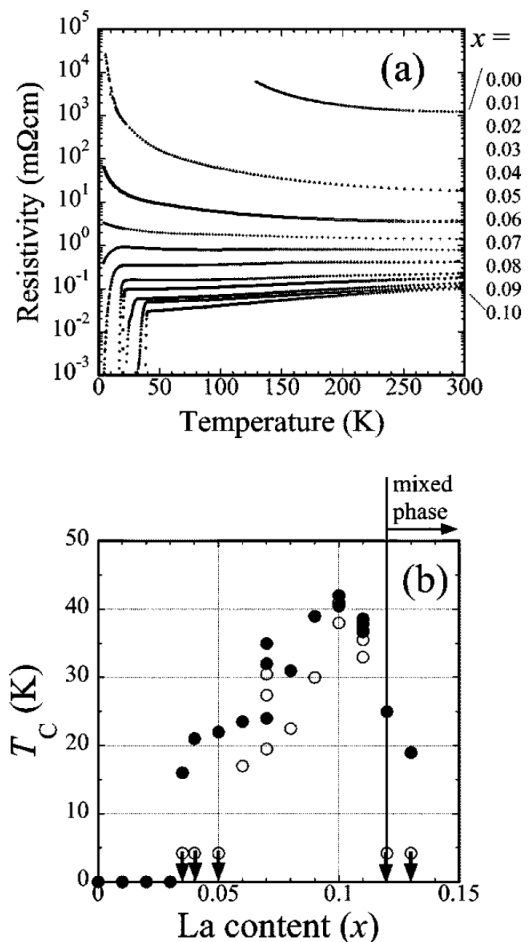


FIG. 9 (a) Resistivity as a function of temperature for $\text{Sr}_{1-x}\text{La}_x\text{CuO}_2$ thin films made by MBE. (b) Extracted values of T_c as a function of doping. Solid and open circles are for the onset and zero resistivity respectively. From ichi Karimoto and Naito (2004).

E. Materials growth

The growth of electron-doped cuprate materials has been a challenge since their discovery. Because their are in principle two doping degrees of freedom (cerium and oxygen)¹⁴. It, the optimisation of their growth and annealing parameters is tedious and has been the source of great variability in their physical properties. For instance, it took almost 10 years after the discovery of the n -type compounds until superconducting crystals of sufficient size and quality could be prepared to perform inelastic neutron scattering (Yamada *et al.*, 1999). Although great advances were initially made with poly-

¹⁴ As discussed below the role of oxygen is very complicated in the n -type compounds. Oxygen reduction clearly has other effects than changing carrier concentration

crystalline samples, it was obvious that many properties, for example the temperature dependence of the resistivity, were strongly affected by grain boundaries. Due to these difficulties and because the growth and properties of such polycrystalline samples have been described in a previous review (Fontcuberta and Fabrega, 1996), we focus our attention here on the growth of single crystals and epitaxial thin films.

1. Single crystals

Two main techniques have been used to grow single crystals of the n -type family: in-flux solidification and traveling-solvent floating zone (TSFZ). The first single crystals of $\text{Nd}_{2-x}\text{Ce}_x\text{CuO}_4$ were grown using the directional solidification flux technique taking advantage of the stability of the NCCO T' phase in a flux of CuO close to an eutectic point (Tarascon *et al.*, 1989). As shown in Fig. 10, the $T-x$ phase diagram of the NdCeO-CuO mixture presents a large region between 1030 and 1250°C for which the growth of NCCO crystals is possible within a liquid phase (Maljuk *et al.*, 1996; Oka and Unoki, 1990; Pinol *et al.*, 1990). Typical crucibles used for the flux growth of the electron-doped cuprates are high purity alumina (Brinkmann *et al.*, 1996a; Dalichaouch *et al.*, 1993; Peng *et al.*, 1991; Sadowski *et al.*, 1990), magnesia, zirconia (Kaneko *et al.*, 1999) and platinum (Kaneko *et al.*, 1999; Matsuda *et al.*, 1991; Tarascon *et al.*, 1989). After reaching temperatures high enough for melting the whole content of a crucible (above 1250°C following the phase diagram in Fig. 10), the temperature is slowly ramped down with typical rates of 1 to 6°C/h while imposing a temperature gradient at the crucible position promoting the growth of the CuO_2 planes along its direction. As the crucible is further cooled down, the flux solidifies leaving the NCCO single crystals usually embedded in a solid matrix. Platelet crystals can reach sizes on the order of several millimeters in the $a-b$ direction, with the c axis limited to a few tens to several hundred microns.

When their growth and annealing processes are under control, flux grown single crystals present very high crystalline quality with little defects. They also have well-defined faces which necessitate little cutting and polishing to prepare for most experiments. Flux grown crystals can however contain a fair amount of 'flux spots' and their cerium content can vary substantially even within the same batch (Dalichaouch *et al.*, 1993). Moreover, the thickest crystals have been shown to have an inhomogeneous cerium distribution along their thickness (Skelton *et al.*, 1994). Finally, since the flux properties change considerably with composition, it remains quite difficult to vary the cerium content substantially around optimal doping and preserve narrow transitions. A variant of this directional flux technique, a top seeded solution method has also been developed (Cassanho *et al.*, 1989; Maljuk *et al.*, 2000) which leads to large single crystals with apparently more uniform cerium content (Maljuk *et al.*,

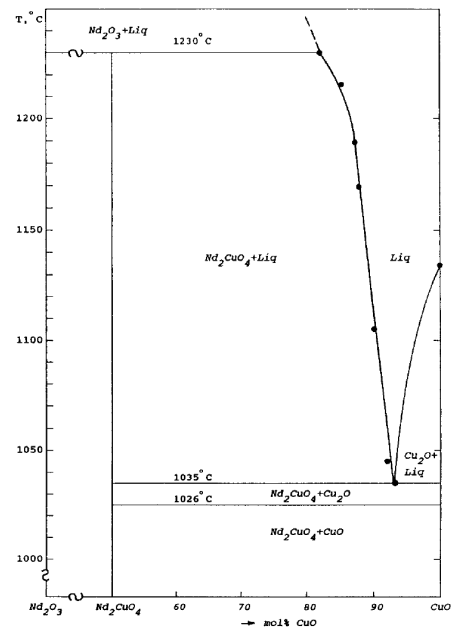


FIG. 10 Phase diagram of the Nd_2O_3 -CuO binary system. Without Ce, the eutectic point corresponds to approximately 90% CuO content in the flux. From Maljuk *et al.* (1996).

2000).

These millimeter-size crystals are large enough for most experiments, however, their limited volume is a drawback for others like neutron scattering. As is also the case for the p -type cuprates, larger single crystals can be grown by the TSFZ technique using image furnaces (Gamayunov *et al.*, 1994; Kurahashi *et al.*, 2002; Tanaka *et al.*, 1991). Light sources from halogen lamps are focused using confocal mirrors onto the tips of two counter-rotating polycrystalline rods. The melted zone at their meeting point is slowly moved upward leaving a large highly-ordered cylindrical boule of materials with sizes reaching several centimeters in length and half a centimeter in diameter (Tanaka *et al.*, 1991). During the growth by the TSFZ method, heat evacuation along the rod's axis favors the growth of electron-doped materials with their CuO_2 planes oriented dominantly parallel to the rod axis. Large boules of electron-doped cuprates can be produced with close to stoichiometric flux in various atmospheres and pressures. Using such conditions, crystals with x as large as 0.18, the solubility limit, could be grown and studied by neutron scattering (Mang *et al.*, 2004b; Motoyama *et al.*, 2007).

Large TSFZ single crystals of $\text{Pr}_{1-y-x}\text{La}_y\text{Ce}_x\text{CuO}_{4\delta}$ have also been grown successfully in recent years. Interestingly, it appears that the presence of La stabilizes their growth (Fujita *et al.*, 2003; Lavrov *et al.*, 2004). As mentioned above, PLCCO presents an extended phase diagram (Fig. 7) with superconductivity appearing for $x > 0.08$ (Fontcuberta and Fabrega, 1996) which may repre-

sent a great advantage in exploring the actual relationship between antiferromagnetism and superconductivity in the underdoped regime ($x < 0.15$).

2. Role of the reduction process and effects of oxygen stoichiometry

As mentioned elsewhere, superconductivity in the electron-doped cuprates can *only* be achieved after reducing the as-grown materials (Takagi *et al.*, 1989; Tokura *et al.*, 1989b). Unannealed crystals are never superconducting. This reduction process removes only a small fraction of the oxygen atoms as measured by many techniques (Klamut *et al.*, 1997; Moran *et al.*, 1989; Navarro *et al.*, 2001; Radaelli *et al.*, 1994; Schultz *et al.*, 1996; Tarascon *et al.*, 1989), but has dramatic consequences for its conducting and magnetic properties. The oxygen removed in general ranges between 0.1 and 2% and decreases with increasing cerium content (Kim and Gaskell, 1993; Schultz *et al.*, 1996; Suzuki *et al.*, 1990; Takayama-Muromachi *et al.*, 1989). The exact effect of oxygen reduction is unknown. Although reduction in principle should contribute electrons, it clearly has an additional effects as it is not possible to compensate for a lack of reduction by the addition of extra Ce.

There are many different procedures mentioned in the literature for the reduction process. In general, the single crystals are annealed at high temperature (850 to 1080°C in flowing inert gas or vacuum) for tens of hours to several days. In some of these annealing procedures, the single crystals are also covered by polycrystalline materials, powder and pellets, in order to protect them against decomposition (Brinkmann *et al.*, 1996a). As revealed by a recent thermogravimetric study (Navarro *et al.*, 2001) of polycrystalline $\text{Nd}_{1.85}\text{Ce}_{0.15}\text{CuO}_{4+\delta}$, the annealing process in small oxygen partial pressures at a fixed temperature (900°) consists of two distinct regimes as shown in Fig. 11: a first one at high pressure leading to non-superconducting materials and a second one at low pressure inducing superconductivity. Interestingly, the separation of these two regimes coincides with the phase stability line between CuO and Cu_2O with their respective Cu^{2+} and Cu^{1+} oxidation states (Navarro *et al.*, 2001). A similar conclusion has been reported by Kim and Gaskell (1993) in a very detailed phase stability diagram shown in Fig. 12. The coincidence of the $\text{Cu}^{2+}/\text{Cu}^{1+}$ ($\text{CuO}/\text{Cu}_2\text{O}$) transition and the onset of superconductivity may be interpreted as a sign that oxygen reduction removes oxygen atoms in the CuO_2 planes leaving behind localized electrons on the Cu sites in proximity to the oxygen vacancies (these Cu ions then have oxidation state +1). Fig. 12 also shows that annealing electron-doped cuprates in lower pressures and/or higher temperatures leads eventually to the decomposition of the materials into a mixture of Nd_2O_3 , $\text{NdCeO}_{3.5}$ and Cu_2O . As emphasized by Kim and Gaskell (1993) and more recently by Mang *et al.* (2004a) it is interesting that the highest

T_c samples are found when the reduction conditions push the crystal almost to the limit of decomposition (Fig. 12). Obviously, this underlines the difficulty of achieving high quality reduction when it requires exploring annealing conditions on the verge of decomposition.

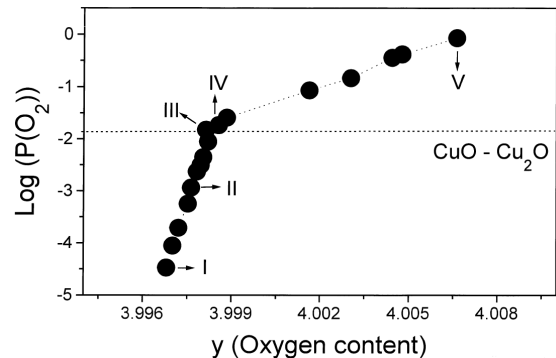


FIG. 11 Equilibrium oxygen partial pressure $p(\text{O}_2)$ as a function of oxygen content y for $\text{Nd}_{1.85}\text{Ce}_{0.15}\text{CuO}_y$ at 900°C. The dashed line indicates the $\text{Cu}^{2+}/\text{Cu}^{1+}$ transition. Samples below this line are superconducting, while those above are not. From Navarro *et al.* (2001).

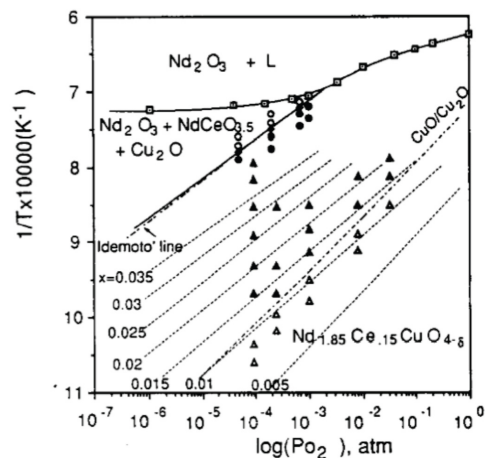


FIG. 12 The phase stability diagram for $x=0.15$ NCCO. The filled diamond symbols are obtained by thermogravimetric analysis and the filled and open circles are compounds which lie within and outside the field of stability respectively. The filled triangles represent superconducting samples and the open triangles represent nonsuperconducting oxides. The dash-dot-dash line is for the $\text{Cu}_2\text{O} - \text{CuO}$ transition and the dotted lines are isocompositions. From Kim and Gaskell (1993).

The small changes in oxygen content have a dramatic impact on the physical properties. The as-grown materials is antiferromagnetic with a Néel temperature T_N above 100K for $x = 0.15$ (Mang *et al.*, 2004b; Uefuji *et al.*,

2001). It shows fairly large resistivity with a low temperature upturn (see section III.A). After reduction, antiferromagnetism is suppressed with the emergence of superconductivity. As mentioned, there is still no consensus on the exact mechanism for this striking sensitivity to oxygen stoichiometry and the annealing process. There are three main (not necessarily exclusive) proposals to explain how a 0.1% change in oxygen content can have such an important effect, which is similar to the impact of changing the cerium doping by $\Delta x \sim 0.05 - 0.10$.

The first proposal and historically the mostly widely assumed, proposes that apical oxygen atoms, an interstitial defect observed in the T' structure by neutron scattering in Nd_2CuO_4 (Radaelli *et al.*, 1994), acts as a strong scattering center (increasing resistivity) and as a source of pair breaking (Xu *et al.*, 1996). By Madelung potential consideration, one expects that apical oxygen may strongly perturb the local ionic potential on the Cu site immediately below it (Torrance and Metzger, 1989). Radaelli *et al.* (1994) showed that reduction leads to a decrease in apical occupancy to approximately 0.04 from 0.1 for the *undoped compounds* (Radaelli *et al.*, 1994). In doped compounds, the oxygen loss is less and almost at the detection limit of the diffraction experiments, however Schultz *et al.* (1996) showed that their results in $\text{Nd}_{1.85}\text{Ce}_{0.15}\text{CuO}_{4+\delta}$ were consistent with a loss of a small amount of oxygen at the apical position.

However, there are several recent reports that favor a 2nd scenario in which only oxygen ions on the intrinsic sites [O(1) in-plane and O(2) out-of-plane in Fig. 1] are removed. It was found that a local Raman mode which is associated with the presence of apical oxygen is not affected at all by reduction in cerium-doped crystals (Richard *et al.*, 2004; Riou *et al.*, 2001, 2004). This appears to indicate that reduction does not change the apical site's oxygen occupation as originally believed. In the same reports, crystal-field spectroscopy of the Nd or Pr ions on their low symmetry site show also that the excitations associated with the interstitial oxygen ions are not changed by reduction while new sets of excitations appear (Richard *et al.*, 2004; Riou *et al.*, 2001, 2004). These new excitations were naturally related to the creation of O(1) and O(2) vacancies; in-plane O(1) vacancies appear to be favored at large cerium doping. Such a surprising conclusion was first formulated by Brinkmann *et al.* (1996b) from the results of a wide exploration of the cerium and oxygen doping dependence of transport properties in single crystals. In order to explain the appearance of a minimum in resistivity as a function of oxygen content (for a fixed cerium content), these authors proposed that the increasing scattering rate (increasing ρ_{xx}) with decreasing oxygen content for extreme annealing conditions could only be due to an increasing density of defects (vacancies) into or in close proximity to the CuO_2 planes. In this important work, they targeted principally the reservoir O(2) as the likely site for vacancies.

Finally, a third scenario has been suggested by

a recent detailed study of the microstructure of $\text{Nd}_{1.85}\text{Ce}_{0.15}\text{CuO}_{4+\delta}$ single crystals grown by TSFZ, which showed the appearance of an intercalated epitaxial $(\text{Nd,Ce})_2\text{O}_3$ impurity phase after reduction (Mang *et al.*, 2004a). This observation has an important repercussion on the interpretation of neutron scattering experiments, but it also suggests a scenario for the role of reduction in this family. In Fig. 13, high resolution transmission electron microscopy (HRTEM) images reveal the presence of narrow bands of this parasitic phase about 60\AA thick on average extending well over $1\mu\text{m}$ along the CuO_2 planes. This phase represents approximately 1% of the entire volume. Since this phase is claimed to appear with reduction and to disappear surprisingly with oxygenation, it was recently proposed that these zones act as copper reservoirs to cure intrinsic Cu vacancies in the as-grown CuO_2 planes (Kang *et al.*, 2007). Within this scenario, during the reduction process Cu atoms migrate from these layers to the NCCO structure to “repair” defects present in the as-grown materials resulting in Cu deficient regions with the epitaxial $(\text{Nd,Ce})_2\text{O}_3$ intercalation. Thus, the decreasing density of Cu vacancies in the CuO_2 planes removes pair-breaking sites favoring superconductivity.

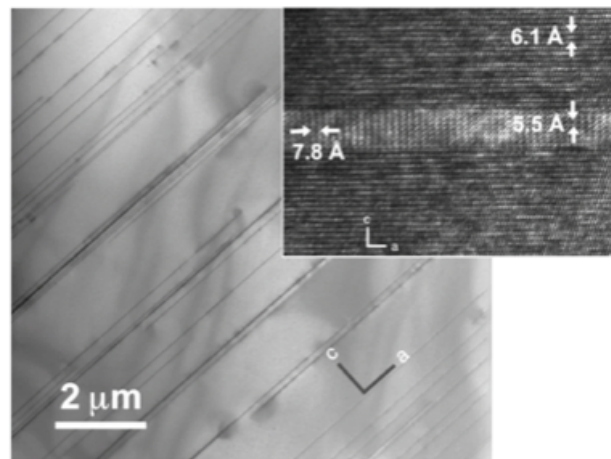


FIG. 13 HRTEM images of a reduced $\text{Nd}_{1.84}\text{Ce}_{0.16}\text{CuO}_{4+\delta}$ single crystal showing the intercalated layers. The $(\text{Nd,Ce})_2\text{O}_3$ layers are found to be parallel to the CuO_2 planes. From Mang *et al.* (2004a).

In addition to whatever role it plays in enabling superconductivity, the oxygen reduction process may also add charge carriers. Using neutron scattering on TSFZ single crystals with various values of x and annealing conditions to tune the presence of superconductivity, Mang *et al.* (2004b) confirmed Luke *et al.* (1990)'s results for reduced samples, with the $T_N(x)$ line plunging to zero at $x \sim 0.17$ as shown in Fig. 14(a). They found that for unreduced samples $T_N(x)$ extrapolated somewhere around $x = 0.21$. For a fixed x value below 0.17, reduction lowers T_N and the corresponding staggered in-plane magnetization (Fig. 14(b)), while promoting superconductivity. This report is consistent with a previous report by Uefuji *et al.* (Ue-

fuji *et al.*, 2001). However, the AF magnetic order persists even for the reduced superconducting compositions. The change in $T_N(x)$ with oxygen content was interpreted as a direct consequence of carrier doping i.e. that removal of oxygen acts exactly like cerium substitution (Mang *et al.*, 2004b), because one could simply rigidly shift the as-grown $T_N(x)$ line by $\Delta x \approx 0.03$ to overlay the reduced one¹⁵. Similarly, Arima *et al.* (1993) found that reduced and unreduced infrared spectra which differed by $\Delta x \approx 0.05$ could be overlaid on top of each other. If one considers the reduction of oxygen content corresponds to an addition of electron carriers to the CuO_2 plane this implies a oxygen reduction of 0.02-0.03, which is consistent with thermogravimetric studies.

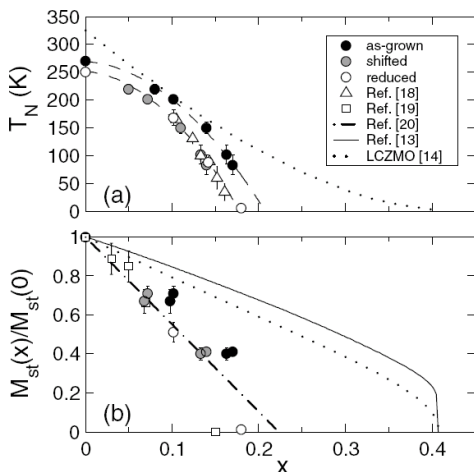


FIG. 14 (a) Phase diagram for $\text{Nd}_{2-x}\text{Ce}_x\text{CuO}_{4+\delta}$ single crystals as determined by neutron scattering. It shows the Néel temperature as a function of cerium content (x). Full circles: as-grown (oxygenated) samples. Open symbols: reduced samples. Grey circles is the data for the as-grown crystals shifted to simulate the carrier density change with reduction; (b) Corresponding staggered magnetization for both types of samples. From Mang *et al.* (2004b).

One of the main issues with the growth of high quality single crystals is control of their stoichiometry. Since the major features in the phase diagram of electron-doped cuprates are evolving sharply with doping (for example the variation of T_c with x), a detailed exploration of their properties using large crystals (and boules) with clear signs of inhomogeneity should be treated with great care. For example, the confirmation of the coexistence of antiferromagnetism and superconductivity at underdoping

where $dT_c/dx > 1000\text{K}$ should rely on samples as homogeneous as possible in order to test that such coexistence is really an intrinsic electronic property not driven by phase segregation or disorder. Such quality seems difficult to achieve taking into account the above mentioned microstructural defects that are modified during the annealing process (Kang *et al.*, 2007).

3. Thin films

Thin film growth offers additional control on the stoichiometry of the electron-doped system, for both cerium and oxygen content. Thin films have been grown using most of the usual techniques for the deposition of other cuprates and oxides, including pulsed-laser deposition (PLD) (Gauthier *et al.*, 2007; Gupta *et al.*, 1989; Maiser *et al.*, 1998; Mao *et al.*, 1992) and molecular beam epitaxy (MBE) (Naito *et al.*, 2002, 1997). Both techniques lead to a single crystalline phase with the cerium content accuracies better than 3%. Since film thicknesses are in the range of 10 to 500 nm and the flux and proportion of each constituent can be accurately controlled during deposition, their cerium content is more homogeneous in contrast to single crystals. Moreover, since oxygen diffusion along the c -axis is easier they can be reduced much more uniformly and efficiently with post-annealing periods on the order of one to several tens of minutes (Maiser *et al.*, 1998; Mao *et al.*, 1992). As a consequence of the greater stoichiometry control, superconducting transition widths as small as $\Delta T_c \sim 0.3\text{K}$ (from AC susceptibility) have been regularly reported (Maiser *et al.*, 1998). For PLD films, growth in a nitrous oxide (N_2O) atmosphere (Maiser *et al.*, 1998; Mao *et al.*, 1992) instead of molecular oxygen (Gupta *et al.*, 1989) has also been used in an effort to decrease the time needed for reduction. Unlike single crystals, it is possible to finely control the oxygen content using in-situ post-annealing in low pressure of O_2 . Within a narrow range of increasing pressure, the resulting films show a gradual decrease of T_c and related changes in transport properties (Gauthier *et al.*, 2007) (see sections III.A.4 and Fig. 30).

Since they are grown on single crystalline substrates with closely matching lattice parameters (LaAlO_3 , SrTiO_3 , etc.), films are generally epitaxial with a highly ordered (001) structure with their c axis oriented normal to the substrate and providing the needed template for the exploration of in-plane transport and optical properties. Unlike other high T_c cuprates like $\text{YBa}_2\text{Cu}_3\text{O}_7$ (Covington *et al.*, 1996), there have been very few reports on films with other orientations. There is evidence that films with (110) and (103) orientations can be grown on selected substrates as confirmed by x-ray diffraction and anisotropic resistivity (Ponomarev *et al.*, 2004; Wu *et al.*, 2006), but the width of their superconducting transition ($\Delta T_c \sim 1\text{K}$) shows that there is room for further optimisation as compared to c -axis films. These particular film orientations could be of interest for directional tunneling

¹⁵ The conclusions of Mang *et al.* (2004b) may be called into question by later work of Motoyama *et al.* (2007), who claim that the AF state terminates at x approximately 0.134. It may be then that this picture of shifting the $T_N(x)$ line by an amount corresponding to the added electron contribution from reduction is only valid at low dopings. Different physics may come into play near superconducting compositions.

experiments(Covington *et al.*, 1996).

A number of drawbacks to thin films do exist. There has been reports of parasitic phases detected by x-ray diffraction in PLD films(Gupta *et al.*, 1989; Lanfredi *et al.*, 2006; Maiser *et al.*, 1998; Mao *et al.*, 1992) as shown in Fig. 15 and HRTEM(Beesabathina *et al.*, 1993; Roberge *et al.*, 2009). These phases have been indexed to other crystalline orientations(Maiser *et al.*, 1998; Prijamboedi and Kashiwaya, 2006) or Cu-poor intercalated phases(Beesabathina *et al.*, 1993; Lanfredi *et al.*, 2006; Mao *et al.*, 1992; Roberge *et al.*, 2009), which have also been observed in single crystals(Mang *et al.*, 2004a). These parasitic phases are mostly absent in MBE films(Naito *et al.*, 2002) except for extreme cases when the substrate/film lattice mismatch becomes important. This microstructural difference between MBE and PLD films may be at the origin of the difference in the magnitude of their in-plane resistivity(Naito *et al.*, 2002) as was confirmed recently by Roberge *et al.* (2009). Moreover, a significant effect of a strain-induced shift of T_c shown in Fig. 16 has been observed as it decreases with decreasing thickness(Mao *et al.*, 1994).

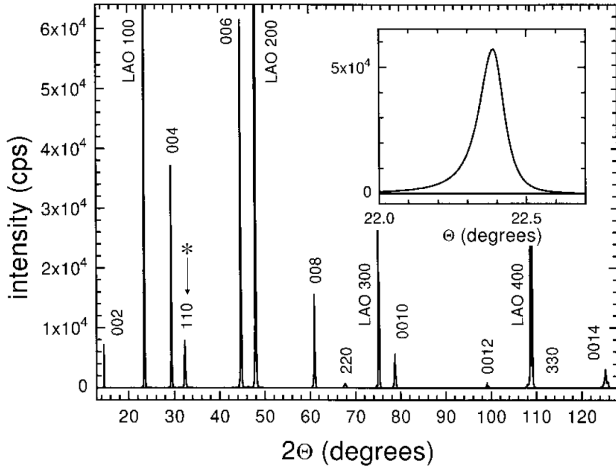


FIG. 15 Typical x-ray diffraction pattern of a (001)-oriented PCCO thin film grown by PLD. The asterisk marks one of the signatures of the parasitic phase identified here as (110) phase of PCCO. However, HRTEM images and further analysis confirms instead that this peak should be indexed to a $(\text{Pr,Ce})\text{O}_x$ phase(Beesabathina *et al.*, 1993; Lanfredi *et al.*, 2006; Mao *et al.*, 1992; Roberge *et al.*, 2009). From Maiser *et al.* (1998).

Strain from the substrate however can also play a crucial role to help stabilizing the T' structure. As mentioned previously, usual bulk LCO is found in the T phase. It was shown by Naito *et al.* that $\text{La}_{2-x}\text{Ce}_x\text{CuO}_{4+\delta}$ (LCCO) can actually be grown successfully in the T' by MBE on a selection of substrates leading to superconducting materials with T_c as high as 27K(Naito and Hepp, 2000; Naito *et al.*, 2002). These electron-doped films also exhibit a modified phase diagram with superconductivity extending to x values below

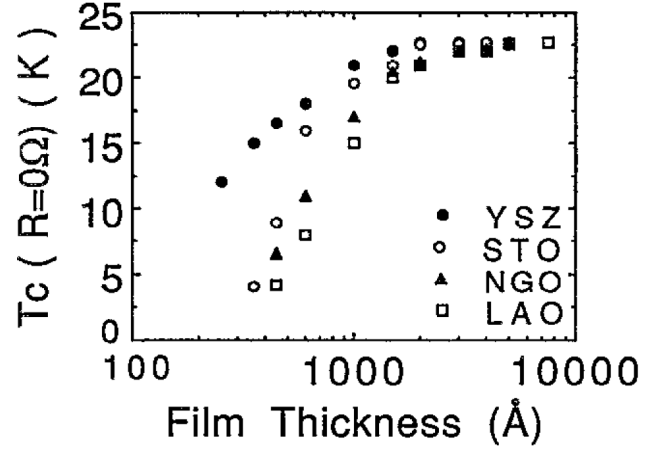


FIG. 16 Variation of the transition temperature with the thickness of the PLD films on various substrates. From Mao *et al.* (1994).

0.10 as shown in Fig. 17, which is fairly similar to that of the $(\text{Pr,La})_{2-x}\text{Ce}_x\text{CuO}_{4+\delta}$ compounds(Fontcuberta and Fabrega, 1996; Fujita *et al.*, 2003, 2008a). The LCCO T' phase has also been successfully grown by DC magnetron sputtering(Zhao *et al.*, 2004) and PLD (Sawa *et al.*, 2002).

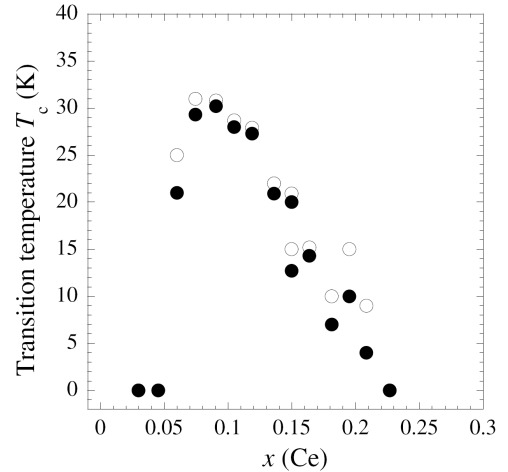


FIG. 17 The transition temperature as a function of cerium doping for $\text{La}_{2-x}\text{Ce}_x\text{CuO}_{4+\delta}$ T' thin films grown by MBE. Open and solid circles correspond to the resistive $T_{c,onset}$ and $T_{c,\rho=0}$ respectively. From Naito *et al.* (2002).

Recently, Matsumoto *et al.* (2009) have shown that it is possible to grow superconducting thin films of the undoped T' structure Re_2CuO_4 with $\text{Re} = \text{Pr, Nd, Sm, Eu, Gd}$ with T_c 's as high as 30K using metal-organic deposition (MOD). This is obviously quite a different behavior compared to the abovementioned trends, in particular the observation of superconductivity in Gd_2CuO_4 . The

authors claim that a complete removal of all the apical oxygen acting as a scatterer and a source of pair breaking during the reduction process may explain the observation of superconductivity in these undoped compound. It could also be that such films are the T' electron doped analog of superconducting $\text{La}_2\text{CuO}_{4+\delta}$ where δ is excess interstitial ‘staged’ oxygen. Obviously, such behavior is intriguing and may raise important questions on the actual mechanism of superconductivity and deserves definitely further investigation.

F. Unique aspects of the copper and rare earth magnetism

Irrespective of the exact mechanism for superconductivity, it is clear that the magnetism of the high- T_c superconductors dominates their phenomenology. The magnetic properties of the electron-doped cuprates are unusually complex and intriguing and demand special consideration. On top of the usual AF order of the in-plane Cu spins observed for example in Nd_2CuO_4 at $T_{N,Cu} \sim 270\text{K}$ (Mang *et al.*, 2004b), additional magnetism arises from the response of the rare-earth ions to the local crystal field. The rare-earth ions sit on a low-symmetry site (point group C_{4v}) where they experience a local electric field leading to a splitting of their 4f atomic levels (Nekvasil and Divis, 2001; Sachidanandam *et al.*, 1997). Since each rare earth possesses a different number of electrons in their 4f shells, they acquire different magnetic moments following Hund’s rule. In Table II, we present the estimated magnetic moment of the most common RE ions used in the n -type. Since some of these magnetic moments are large, interactions between the RE ions and localized Cu spins give rise to a rich set of properties and signatures of magnetic order. As an emblematic example, Nd magnetic moments are known to grow as the temperature is decreased since it is a Kramers doublet (Kramers, 1930), implying a complex temperature-dependent interaction with the Cu sub-lattice and other Nd ions. Among other things, these growing Nd moments at low temperature have an impact on several low temperature properties that are used to characterize the pairing symmetry (see Section IV.A.1). Here we summarize the different magnetic states observed in the electron-doped cuprates. We first focus on the Néel order of the Cu spins, and then follow with a quick overview of its interaction with the RE moments.

1. Cu spin order

The antiferromagnetic order of the Cu spins observed for the parent compounds of the electron-doped family is quite different from that of La_2CuO_4 , despite close values of $T_{N,Cu} \sim 300\text{K}$ and similar crystal structures

	PCO	NCO	SCO	ECO	GCO	PLCO
J	4	9/2	5/2	0	7/2	
effective moment Curie-Weiss	$3.65\mu_B$	$3.56\mu_B$	$0.5\mu_B$	$0\mu_B$	$7.8\mu_B$	
ordered moment measured	$0.08\mu_B$	$1.23\mu_B$	$0.37\mu_B$	$0\mu_B$	$6.5\mu_B$	$0.08\mu_B$
RE Néel Temp. (K)	–	1.7	5.95	–	6.7	–

TABLE II Table summarizing the magnetic properties arising from RE moments. The RE effective moment is from a fit of the high-temperature susceptibility to the Curie-Weiss law while the ordered moment is estimated at low temperature from 0.4 to 10K mostly from neutron scattering experiments. The Néel temperature corresponding to the magnetic ordering of the RE moments was determined using specific heat. From Ghamaty *et al.* (1989); Matsuda *et al.* (1990); Vigoureux (1995) and references therein.

and Cu-O bond lengths¹⁶. In Fig. 18, we compare the magnetic orders deduced from elastic neutron scattering for both families. Although the magnetic moments lie in the CuO_2 planes for both systems with fairly strong intraplane AF exchange interaction, the in-plane alignment differs as the spins lie along the Cu-O bonds in the case of electron-doped cuprates (Skanthakumar *et al.*, 1993) while they point at 45° to the Cu-O bond directions for LCO (Kastner *et al.*, 1998). Since the resulting isotropic exchange between planes cancels out due to this in-plane alignment and crystal symmetry, the 3D magnetic order in the case of the electron-doped cuprates is governed by weak pseudo-dipolar interactions (Petitgrand *et al.*, 1999; Sachidanandam *et al.*, 1997) which derive from Cu-RE exchange. They lead to a spin configuration where the in-plane magnetization alternates in directions between adjacent layers (Lynn and Skanthakumar, 2001; Sachidanandam *et al.*, 1997; Sumarlin *et al.*, 1995) in a non-collinear structure as shown in Fig. 18. For LCO, the spin structure is collinear along the c -axis (Kastner *et al.*, 1998). Experimentally, the non-collinear structure of the Cu spins has been confirmed for NCO, SCO, PCO and PLCCO using elastic neutron scattering (Lavrov *et al.*, 2004; Skanthakumar *et al.*, 1991, 1993; Sumarlin *et al.*, 1995). Their spin wave spectrum

¹⁶ Note that the maximum Néel temperature of NCO is reported different in different studies. For instance, Matsuda *et al.* (1990) report 255 K, Bourges *et al.* (1997) report 243 K, whereas Mang *et al.* (2004b) report ≈ 270 K. This is likely due to the strong dependency on oxygen content. The maximum reported T_N for PCO appears to be 284 K (Sumarlin *et al.*, 1995). In contrast, the maximum reported T_N for LCO is 320 K (Keimer *et al.*, 1992).

is gapped due to anisotropy by about 5 meV in PCO (Sumarlin *et al.*, 1995) and (Bourges *et al.*, 1992), which compares with the anisotropy gap of 2.5 meV in LCO (Peters *et al.*, 1988). Magnetic exchange constants are of the same order as the hole-doped compound. See for instance the two magnon Raman data of Sulewski *et al.* (1990), who find exchange constants of 128, 108 and 110 meV for LCO, NCO and SCO respectively. These values are similar to those found by fits to spin-wave theory (Sumarlin *et al.*, 1995).

For small cerium doping ($x \sim 0.01 - 0.03$), non-collinear magnetic structure persists and has a detectable impact on the electronic properties, in particular electrical transport in large magnetic fields, indicate the coupling of the free charge carriers to the underlying antiferromagnetism (Lavrov *et al.*, 2004). The carriers couple strongly to the AF structure leading to large angular magnetoresistance (MR) oscillations for both in-plane and out-of-plane resistivity when a large magnetic field is applied along the CuO_2 planes (Chen *et al.*, 2005; Lavrov *et al.*, 2004; Li *et al.*, 2005a; Wu *et al.*, 2008; Yu *et al.*, 2007a). Although originally thought to be related to magnetic domains (Fournier *et al.*, 2004), these oscillations are now agreed to be related to the first-order spin-flop transition at a magnetic field of the order of 5T observed in magnetization and elastic neutron scattering measurements (Cherny *et al.*, 1992; Plakhty *et al.*, 2003). At that field applied along the Cu-O bonds, the in-plane and c -axis MR changes dramatically as the magnetic structure changes from the non-collinear order to a collinear one (Cherny *et al.*, 1992; Lavrov *et al.*, 2004) as shown in Fig. 19. Similar signatures but with smaller amplitudes were also observed at higher doping (Fournier *et al.*, 2004; Yu *et al.*, 2007b) for as-grown non-superconducting PCCO crystals with $x = 0.15$ indicating that AF correlations are preserved over a wide range of doping in these as-grown materials and that it continues to interact with the carriers even if their concentration becomes large. This observation is in agreement with the above mentioned phase diagrams (Fig. 14) showing the persistence of the AF phase up to optimal doping. The effect of doping on the Cu spin structure is dealt with in more detail below.

2. Effects of rare earth ions on magnetism

Additional magnetism arises from the large magnetic moments that can exist at the RE sites. Because of the differing magnitudes for various RE compositions and thus varying couplings with the Cu spin sublattice, different RE ions lead to very different magnetic structures, some of which with well-defined order. For this reason, we will discuss the various cases separately.¹⁷

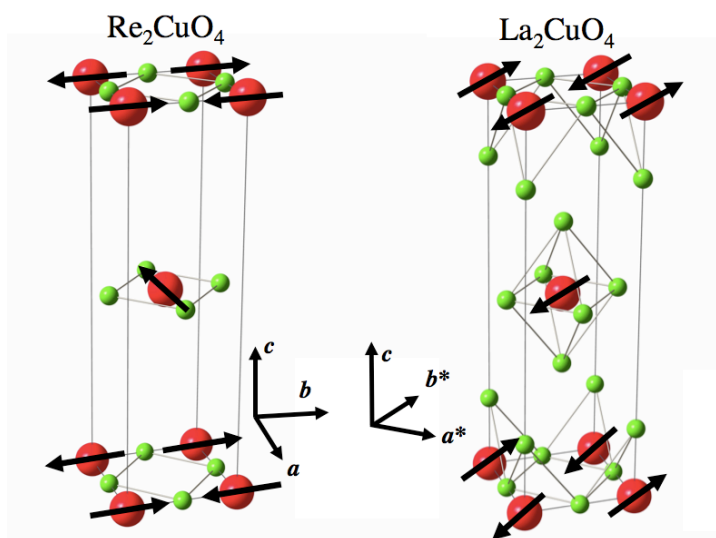


FIG. 18 Cu spins magnetic structures for the non-collinear structure of RE_2CuO_4 (left) and the collinear structure of La_2CuO_4 (right). The moments (arrows) are aligned toward the nearest neighbor Cu along the Cu-O bonds [(100) and (010)] for RE_2CuO_4 while they point toward the next-nearest neighbor Cu at 45° with respect to the Cu-O bonds [along (110)] for La_2CuO_4 .

In the case of $\text{RE} = \text{Nd}$, the fairly strong magnetic moment of the Nd ion was found rather early on to couple to the Cu spins sub-lattice (Cherny *et al.*, 1992; Lynn *et al.*, 1990). A number of successive Cu spin transitions can be observed in Nd_2CuO_4 with decreasing temperature using neutron scattering (Endoh *et al.*, 1989; Matsuda *et al.*, 1990; Matsuura *et al.*, 2003; Skanthakumar *et al.*, 1993). These transitions seen as sharp changes of intensity for specific magnetic Bragg reflections (see Fig. 20) reveal a clear growing interaction between the Cu and Nd spins as the temperature decreases. First, Cu spins order below $T_{N1} \approx 276$ K in a structure defined as phase I, which is the non-collinear spin structure presented previously in Fig. 18. At still lower temperatures there are two successive spin reorientations transitions at $T_{N2} = 75$ K and again at $T_{N3} = 30$ K. At T_{N2} the Cu spins rotate by 90 degree about the c axis (phase II). The rotation direction is opposite for two successive Cu planes. At T_{N3} they realign back to their initial direction (phase III). Phases I and III are identical with the exception that the Nd magnetic moment is larger at low temperature since it is a Kramers doublet. Finally, as shown in the inset of Fig. 20, additional Bragg intensity is detected below 1K arising from the AF ordering of the Nd moments. This feature is a clear indication that substantial Nd-Nd interaction is present on top of the Nd-Cu ones which lead to the transitions at T_{N2} and T_{N3} .

These reorientations are the result of the competition between three energy scales : 1) the Cu-Cu ; 2) the Nd-Nd ; and 3) the Nd-Cu interactions. Since the Nd mo-

¹⁷ For more details on the magnetism of the rare earths than given here, see the excellent review by Lynn and Skanthakumar (2001).

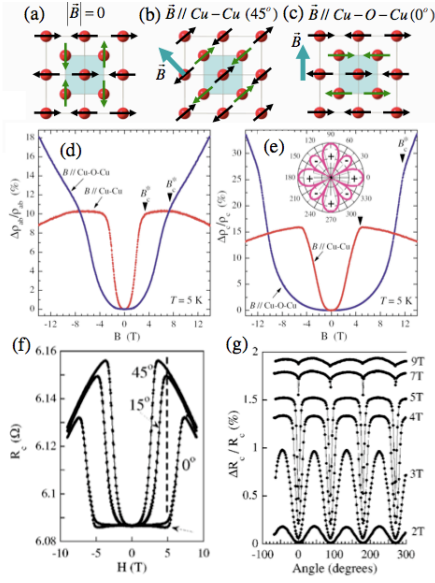


FIG. 19 In-plane Cu spin structures for (a) zero applied magnetic field and a large magnetic field beyond the spin-flop field applied at (b) 45° and (c) 0° with respect to the Cu-O-Cu bonds. (d) in-plane and (e) c-axis magnetoresistance of lightly doped $\text{Pr}_{1.3}\text{La}_{0.7}\text{Ce}_x\text{CuO}_4$ ($x = 0.01$) single crystals at 5K for a magnetic field applied along the (100) or (010) Cu-O bonds and along the (110) Cu-Cu direction (from Lavrov *et al.* (2004)). c-axis magnetoresistance at 5K for non-superconducting as-grown $\text{Pr}_{1.85}\text{Ce}_{0.15}\text{CuO}_4$. (f) as a function of field for three selected in-plane orientations (0° , 15° and 45°) and (g) as a function of angle at selected magnetic fields below and above the spin-flop field of 5T (from Ref. Fournier *et al.* (2004)).

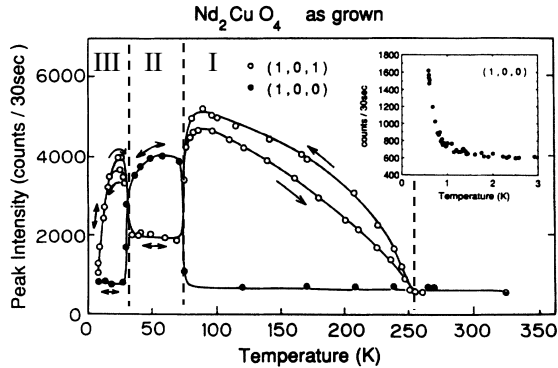


FIG. 20 Elastic neutron scattering intensity as a function of temperature at two different positions in reciprocal space for as-grown Nd_2CuO_4 . The sudden changes in intensity occur at the transition from Type-I to Type-II, then Type-II to Type-III Nd-Cu moment configurations with decreasing temperature. From Matsuda *et al.* (1990).

ment grows with decreasing temperature, the contributions from 2) and 3) grow accordingly.

The reordering and the low temperature interaction of Nd with Cu can be observed in various ways. The reorientations were first observed by muon spin resonance and rotation experiments (Luke *et al.*, 1990) and were confirmed later on by crystal-field spectroscopy (Jandl *et al.*, 1999), and more recently by ultrasound propagation experiments (Richard *et al.*, 2005b) (see Fig. 21). The growing competition between the three energy scales leads also to a wide variety of anomalies at low temperature. For example, one can observe signatures of the non-collinear to collinear (spin-flop) transition in the magnetization (Cherny *et al.*, 1992), manifestations of magnetic domains in ultrasound attenuation experiments (Richard *et al.*, 2005b) and anomalous Zeeman crystal-field effect observed by infrared transmission spectroscopy (Richard *et al.*, 2005a), irreversibility in the above mentioned angular magnetoresistance oscillations (Li *et al.*, 2005a; Wu *et al.*, 2008), and the enhancement of magnon thermal conductivity of NCO in a large in-plane magnetic field beyond the spin-flop transition (Li *et al.*, 2005b).

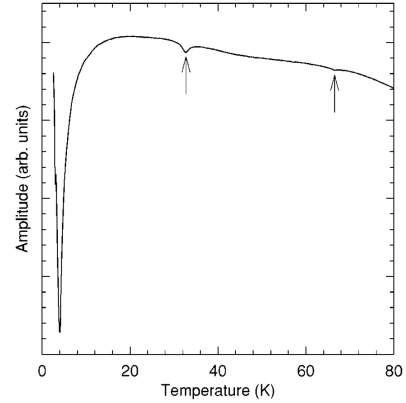


FIG. 21 Signatures of the magnetic reordering of the Cu at T_{N2} and T_{N3} moments as observed by ultrasound attenuation. The data show the amplitude of the first transmitted pulse at 208 MHz. The strong absorption at low temperature is interpreted as resulting from the growth and frustration of local magnetic domains caused by the competition between the $\text{Nd}^{3+}\text{-Cu}^{2+}$ and the $\text{Nd}^{3+}\text{-Nd}^{3+}$ interactions. This low temperature feature is very sensitive to frequency and magnetic field. From Richard *et al.* (2005b).

The larger magnetic moments at the Sm sites in SCCO order quite differently than in NCCO. In fact, Sm_2CuO_4 shows a well-defined antiferromagnetic order below $T_{N,Sm} = 6\text{K}$ with a transition easily observed by specific heat (Cho *et al.*, 2001; Dalichaouch *et al.*, 1993; Hundley *et al.*, 1989), magnetization (Dalichaouch *et al.*, 1993) and elastic neutron scattering (Sumarlin *et al.*, 1992). The corresponding structure of this magnetic order is shown in Fig. 22. Interestingly, the Sm moments present an in-plane ferromagnetic order. However, these ferromagnetic planes align antiferromagnetically along

the c -axis (Sumarlin *et al.*, 1992). This special arrangement leads to no observable coupling between the Sm and the Cu moments.

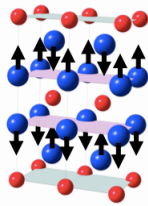


FIG. 22 Orientation of the Sm spins below $T = 6\text{K}$ for Sm_2CuO_4 . Cu : red. Sm : blue. For clarity, we have removed the oxygen atoms and did not show the magnetic moments at the Cu sites.

For $\text{Pr}_{2-x}\text{Ce}_x\text{CuO}_4$ and $\text{Pr}_{1-y-x}\text{La}_y\text{Ce}_x\text{CuO}_{4\delta}$ at low doping, the magnetic moments at the Pr site have been shown to be small, but non-zero with a value of roughly $0.08\mu_B/\text{Pr}$ (Lavrov *et al.*, 2004; Sumarlin *et al.*, 1995). These materials do exhibit the non-collinear c -axis spin order, which is a consequence of these RE moments. However due to their small magnitude the magnetic transitions associated with RE-Cu and RE-RE interaction in NCO do not appear to take place in PCO (Matsuda *et al.*, 1990). Nevertheless, there is evidence for Pr-Pr interactions in both the in-plane and out-of-plane directions (Sumarlin *et al.*, 1995) mediated by Cu spins. This is supported by the onset of a weak polarization of the Pr moments at the Néel temperature for Cu spin ordering ($T_N \sim 270\text{K}$ for Pr_2CuO_4 and $T_N \sim 236\text{K}$ for $\text{Pr}_{1.29}\text{La}_{0.7}\text{Ce}_{0.01}\text{CuO}_{4\delta}$). Despite this “induced” magnetic moments at the Pr sites, PCO and PLCCO have a very small uniform magnetic susceptibility on the order of 1 % that of NCCO (Fujita *et al.*, 2003). This represents a great advantage in the study and the understanding of their magnetic and superconducting properties without the potential perturbation from the RE moments. For instance, the small DC susceptibility of PCCO with respect to NCCO allows precision measurements of the symmetry of the order parameter (see Section IV.A.5).

Finally, there has been less effort directed towards Eu_2CuO_4 (ECO) and Gd_2CuO_4 (GCO), but both systems present evidence of weak ferromagnetism with indications that the small size of the rare earth ions and the induced lattice distortions are playing a crucial role (Alvarenga *et al.*, 1996; Mira *et al.*, 1995; Thompson *et al.*, 1989). For GCO, specific heat and magnetization anomalies at 9K demonstrates the antiferromagnetic order of the Gd sublattice with signatures very similar to SCO, while a large anisotropy of the DC susceptibility with its onset at the Cu spin order temperature ($\sim 260\text{K}$) indicates the contribution of a Dzyaloshinskii-Moriya (DM) interaction between the Cu spins leading to the weak ferromagnetism. Even for ECO, there has been reports of weak ferromagnetism correlations (Alvarenga *et al.*, 1996), but no Eu ordering (since $\mu = 0$).

III. EXPERIMENTAL SURVEY

A. Transport

1. Resistivity and Hall effect

The ab-plane electrical resistivity (ρ_{ab}) and Hall Effect for the n -type cuprates has been studied by many groups. The earliest work found, at optimal doping, $\rho_{ab} = \rho_o + AT^2$ over the temperature range from T_c to approximately 250K (Tsuei *et al.*, 1989) and a temperature dependent Hall number in the same temperature range (Wang *et al.*, 1991). The T^2 behavior is in contrast to the linear in T behavior found for the optimal hole-doped cuprates. Although $\rho \sim T^2$ is a behavior consistent with electron-electron scattering in a normal (i.e., Fermi liquid) metal, it is quite unusual to find such behavior at temperatures above 20K. This suggested that there is some anomalous scattering in the n -type cuprates and that phonons do not make a major contribution to the resistivity up to 250K.

The general doping and temperature evolution of the ab-plane resistivity is illustrated in some recent ρ_{ab} data on NCCO crystals as shown in Fig. 23 (Onose *et al.*, 2004). These data shows that even at rather low doping (i.e., in the AFM state) a “metallic”-like resistivity is observed at higher temperatures which becomes “insulator-like” at lower temperatures. The temperature of the minimum resistivity decreases as the doping increases and it extrapolates to less than T_c near optimal doping. The development of “metallic” resistivity at low doping is consistent with the ARPES data, which shows electron states near the Fermi level around $(\pi, 0)$ for $x \geq 0.04$ (Armitage *et al.*, 2002) and an increased Fermi energy density of states in other regions of the BZ as doping increases (see ARPES discussion below). Recent work (Dagan *et al.*, 2007) showed a scaling of the T^2 resistivity above 100K for dopings $x=0.11$ to 0.19. Sun *et al.* (2004) emphasizes that despite the upturns in the ab-plane resistivity, the mobility over much of the temperature range is still quite high in even lightly doped AFM samples ($5 \text{ cm}^2/\text{V} \cdot \text{sec}$). They interpreted this as consistent with the formation of metallic stripe domains.

The dependence of the high field “insulator to metal” crossover on Ce doping at low temperature ($T \ll T_c$, $H \gg H_c2$) has been studied in detail by Fournier *et al.* (1998a) and Dagan *et al.* (2004). Important aspects of their data to note are: 1) the linear in T resistivity from 35mK to 10K at one particular doping (Ce = 0.17 in (Fournier *et al.*, 1998a)), 2) the crossover from insulator to metal occurs at a $k_F l$ value of order 20, 3) the resistivity follows a T^2 dependence for all Ce doping at temperatures above the minimum or above 40K, and 4) the resistivity follows T^β with $\beta < 2$ in the temperature range less than 40K for samples in which there is no resistivity minimum.

The doping dependent “insulator to metal” crossover in the resistivity data appears very similar to behavior found in the hole-doped cuprates (Boebinger *et al.*, 1996).

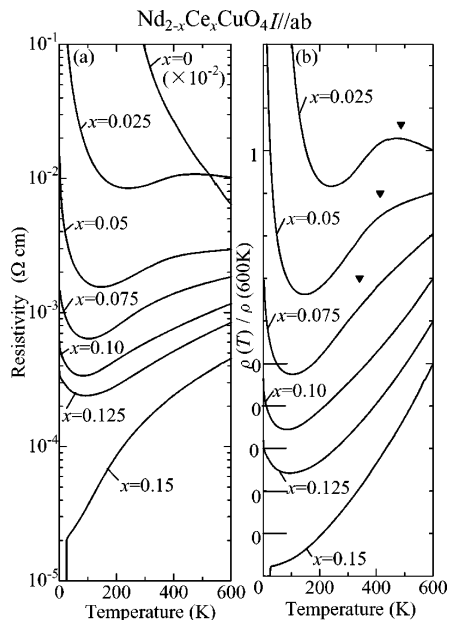


FIG. 23 a) Temperature dependence of the in-plane resistivity of NCCO crystals at various doping levels x . (b) In-plane resistivity of NCCO crystals at various doping levels x normalized by its 600 K value. From Onose *et al.* (2004).

However, electron-doped cuprates are much more convenient to investigate such physics as much larger magnetic fields are needed to suppress the superconductivity in p -type compounds to reveal the low-temperature normal state. In the few cases that sufficient fields have been used in the hole-doped compounds the low temperature upturn in resistivity occurs in samples near optimal doping with similar $k_F l$ values of order 20. The behavior of the resistivity at low T below is very similar in hole and electron-doped materials ($\rho \sim \log 1/T$) but the exact cause of the upturn is not known at present. Work by Dagan *et al.* (2005b) shows that it is related to the onset of AFM in the n -doped cuprates. Disorder may also play a role in the appearance of the resistivity upturn (and metal-insulator crossover) as recently suggested for hole-doped cuprates (Rullier-Albenque *et al.*, 2008).

An insulator-metal crossover can also be obtained at a fixed Ce concentration by varying the oxygen reduction conditions (Fournier *et al.*, 1997; Gantmakher *et al.*, 2003; Gauthier *et al.*, 2007; Gollnik and Naito, 1998; Jiang *et al.*, 1994; Tanda *et al.*, 1992). Under these conditions the crossover occurs at a $k_F l$ value of order unity and near a 2D sheet resistance (treating a single copper-oxide plane as the 2D conductor) appropriate for a superconductor to insulator transition (SIT) (Goldman and Markovic, 1998). Some authors have interpreted their data as giving convincing evidence for a SIT (Tanda *et al.*, 1992) while others have argued against this view (Gantmakher *et al.*, 2003). More detailed study will be needed to resolve this issue.

The doping and temperature dependence of the nor-

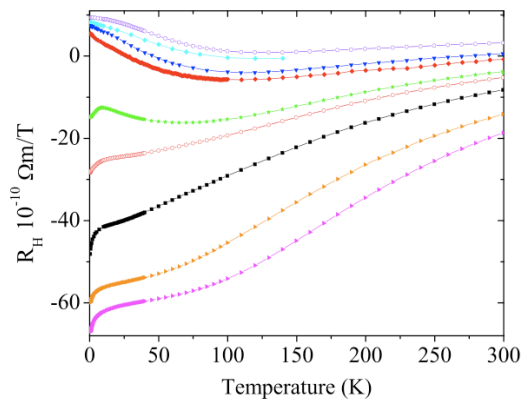


FIG. 24 The Hall coefficient R_H in $\text{Pr}_{2-x}\text{Ce}_x\text{CuO}_4$ films as function of temperature for the various doping levels (top to bottom): $x = 0.19$, $x = 0.18$, $x = 0.17$, $x = 0.16$, $x = 0.15$, $x = 0.14$, $x = 0.13$, $x = 0.12$, and $x = 0.11$ (Dagan and Greene, 2004).

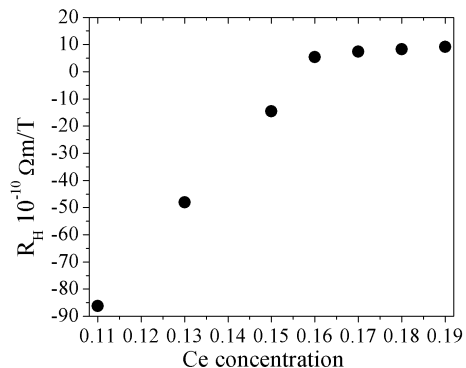


FIG. 25 The Hall coefficient at 0.35K (using the data from Fig. 24). A distinct kink in the Hall coefficient is seen between $x = 0.16$ and $x = 0.17$. The error on the concentration is approximately 0.003. The error in R_H comes primarily from the error in the film thickness; it is approximately of the size of the data points (Dagan *et al.*, 2004).

mal state ($H > H_{c2}$) ab-plane Hall coefficient (R_H) are shown in Fig 24 (Dagan *et al.*, 2004) for PCCO films. These recent results agree with previous work (Fournier *et al.*, 1997; Gollnik and Naito, 1998; Wang *et al.*, 1991) but cover a wider temperature and doping range. Notable features of these data are the significant temperature dependence for all but the most overdoped samples and the change in sign from negative to positive near optimal doping at low temperature. This latter behavior is most dramatically seen by plotting R_H versus Ce doping at 350mK (the lowest temperature measured) as shown in Fig 25 (Dagan *et al.*, 2004). At this low temperature one expects that only elastic scattering will contribute to ρ_{xy} (and hence R_H) and thus the behavior seen in Fig. 25 suggests some significant change in the Fermi surface near optimal doping. Qualitatively, the behavior of R_H is consistent with the Fermi surface evolution as shown via

ARPES in Fig. 33. At low doping an electron-like region is found and at high doping a large hole-like pocket appears to evolve (Armitage *et al.*, 2002). At intermediate doping both electron- and hole-like contributions exist. In fact, at $x = 0.15$ Ce doping, the combination of measurements of the Nernst effect, Hall effect, thermoelectric power, and transverse magnetoresistance were originally explained qualitatively in terms of a two-band model (electron and hole carriers) by several authors (Fournier *et al.*, 1997; Gollnik and Naito, 1998; Jiang *et al.*, 1994). At the time there was no clear picture of how two carrier types could emerge from a single hole-like band as predicted from LDA band structure calculations (Massidda *et al.*, 1989) and observed in the original ARPES work (Anderson *et al.*, 1993; King *et al.*, 1993). However, recent ARPES and optics measurements strongly suggest that a SDW-like band structure rearrangement occurs, which breaks up the Fermi surface into electron and hole regions (Armitage, 2001; Armitage *et al.*, 2001b; Matsui *et al.*, 2007; Zimmers *et al.*, 2005). A mean field calculation of the $T \rightarrow 0$ limit of the Hall conductance showed that the data are qualitatively consistent with the reconstruction of the Fermi surface expected upon density wave ordering (Lin and Millis, 2005). We will discuss this and the two-band transport in more detail below.

The Hall angle (θ_H) follows a behavior different than the well-known T^2 dependence found in the p-doped cuprates. Several groups (Dagan *et al.*, 2007; Fournier *et al.*, 1997; Wang *et al.*, 2005b; Woods *et al.*, 2002) have found an approximately T^4 behavior for $\cot \theta_H$ in optimal n -type cuprates. Dagan *et al.* (2007), but not Wang *et al.* (2005b), find the power law dependence on temperature of $\cot \theta_H$ becomes less than 4 for underdoped materials but cannot be fit to any power law for overdoped. This change may be related to the purported QCP which occurs near $x=0.16$, but more detailed studies will be needed to verify this. The unusual power law dependence for the Hall angle agrees with the theoretical model of Abrahams and Varma (2003) at optimal doping. These authors showed that the Hall angle is proportional to the square of the scattering rate if this rate is measured by the T dependence of the ab -plane resistivity. Since a resistivity proportional to T^2 is found at all dopings for T above 100K (Dagan *et al.*, 2007) the theoretical model is not valid at most dopings and the origin of the temperature dependence of the Hall angle needs to be reevaluated.

2. Nernst effect, thermopower and magnetoresistance

The Nernst effect has given important information about the normal and superconducting states in the cuprates. It is the thermal analog of the Hall Effect, whereby a thermal gradient in the \hat{x} direction and a magnetic field in the \hat{z} direction, induces an electric field in the \hat{y} direction. The induced field comes from the thermal drift of carriers and their deflection by the magnetic

field or by the Josephson mechanism if moving vortices exist (for details see Wang *et al.* (2006b) and references therein). In conventional superconductors one finds a large Nernst signal in the superconducting state from vortex motion and a very small signal in the normal state from the carriers. In fact, Boltzmann theory predicts a zero Nernst signal from a single band of carriers with energy independent scattering (Sondheimer, 1948; Wang *et al.*, 2001). Surprisingly, a large Nernst signal is found in the normal state of both electron and hole-doped cuprates. However, the origin of this signal appears to be quite different in the two cases. For p -type cuprates the large normal state Nernst effect has been attributed to superconducting fluctuations in a large temperature region above T_c , especially in the range of doping where the pseudogap exists (Wang *et al.*, 2001). For n -type cuprates the large Nernst signal was attributed to two types of carriers in the normal state (Balci *et al.*, 2003; Fournier *et al.*, 1997; Gollnik and Naito, 1998; Jiang *et al.*, 1994; Li *et al.*, 2007a). The evidence for a difference in behavior between p - and n -type cuprates is persuasive.

The Nernst signal as a function of magnetic field at various temperatures for optimal-doped NCCO is shown in Fig. 26 (Wang *et al.*, 2006b). A vortex signal non-linear in field is seen for $H < H_{c2}$ for $T < T_c$ whereas for $T > T_c$ a linear in H normal state dependence is found. This is behavior typical of low- T_c superconductors, i.e., the non-linear superconducting vortex Nernst signal disappears for $T > T_c$ and $H > H_{c2}$. There is evidence for a modest temperature range of superconducting (SC) fluctuations just above T_c in the underdoped compositions (Balci *et al.*, 2003; Li and Greene, 2007). However, these data contrasts dramatically from the data found in most hole-doped cuprates. In those cuprates there is a very wide parameter range (in both T and H) of Nernst signal due to SC fluctuations, interpreted as primarily vortex-like phase fluctuations (Wang *et al.*, 2006b). This interpretation of the large Nernst signal above T_c in the hole-doped cuprates is supported by recent theory (see Podolsky *et al.* (2007) and references therein). Also, the inference that phase fluctuations are larger in hole-doped cuprates than the electron-doped is consistent with “phase fluctuation” models and estimates from various material parameters (Emery and Kivelson, 1995). However, the magnitude of the Nernst signal is large for $T > T_c$ for both n - and p -type cuprates for most doping levels above and below optimal doping. The temperature dependence of the Nernst signal at 9T ($H \parallel c > H_{c2}$) for several PCCO dopings is shown in Fig. 27 (Li and Greene, 2007). Since the field dependence at a fixed temperature is linear, this signal is certainly a normal state effect, i.e. comes from normal state carriers. In contrast, in the p -doped materials the field dependence is non-linear for a wide T range above T_c , which suggests a SC origin for the large Nernst signal. As mentioned earlier, the large signal in the normal state of the n -doped materials has been interpreted as arising from two car-

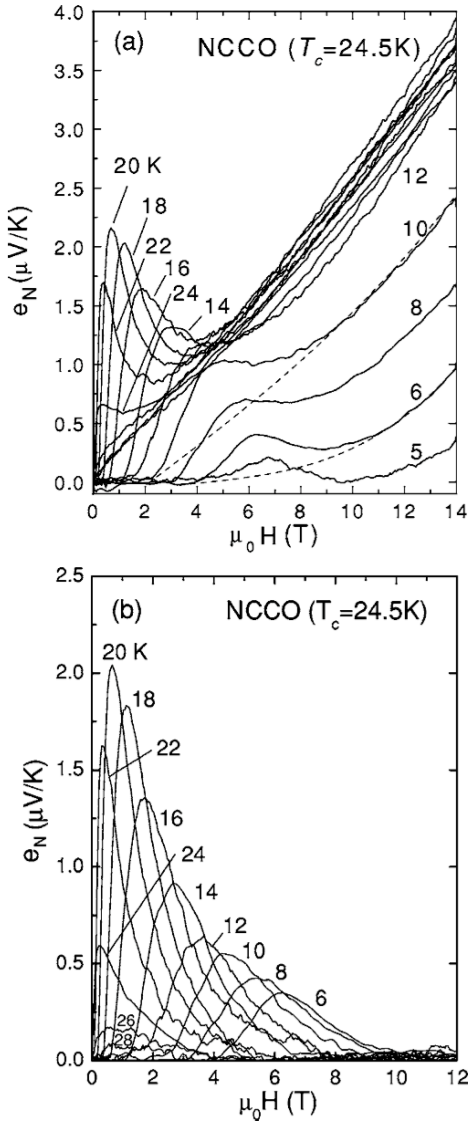


FIG. 26 (a) The experimentally measured Nernst signal e_N vs H in optimally doped $x = 0.15$ NCCO and $T_c = 24.5$ K from temperatures of 5 K to 30 K. The dashed lines are fits of the high-field segments to a quasiparticle term of the form $e_N^n(T, H) = c_1 H + c_3 H^3$ as detailed in Ref. (Wang *et al.*, 2006b). (b) The vortex contribution to the Nernst effect e_N^v as extracted from the data of panel (a) as also detailed in Ref. (Wang *et al.*, 2006b).

rier types. This is consistent with the ARPES and optics data, which shows that both electron and hole regions of the Fermi surface (FS) exist for dopings near optimal (Armitage, 2001; Armitage *et al.*, 2001b; Zimmers *et al.*, 2005). Related to the existence of two carrier types has been the recent theoretical work of Hackl and Sachdev (2009), who show that SDW order can give a magnitude and doping dependence of the enhanced Nernst signal that agrees with measurements in electron-doped cuprates. However, more quantitative interpretation of the normal state Nernst effect remains for future work.

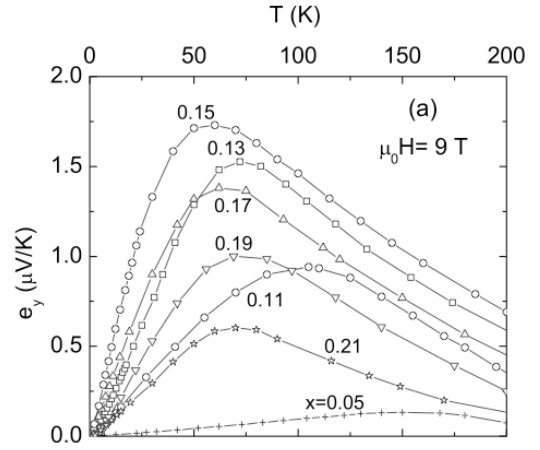


FIG. 27 Temperature dependence of normal-state Nernst signal at $\mu_0 H = 9$ T for all the doped PCCO films from Li and Greene (2007).

The ab-plane thermoelectric power (TEP) of the n-doped cuprates has been measured by many authors (Budhani *et al.*, 2002; Fournier *et al.*, 1997; Gollnik and Naito, 1998; Li *et al.*, 2007c; Li and Greene, 2007; Wang *et al.*, 2005b; Xu *et al.*, 1996) (for work prior to 1995 see Fontcuberta and Fabrega (1996)). To date, there has been no quantitative interpretation of the temperature, doping and field dependence of the TEP. However, a number of qualitative conclusions have been reached. The doping dependence of the low temperature magnitude and sign of the TEP is consistent with the evolution of the FS from electron-like at low doping to two-carrier-like near optimal doping to hole-like at the highest doping. For example, at low doping (Ce=0.03) the low-T TEP is “metallic-like” and negative (Hagen *et al.*, 1991; Wang *et al.*, 2005b) even though the resistivity has an “insulator-like” temperature dependence. This is consistent with the small pocket of electrons seen in ARPES and a possible 2D localization of these electrons at low temperature. A recent detailed study of the doping dependence of the low-temperature normal state TEP has given additional evidence for a quantum phase transition (QPT) that occurs near $x=0.16$ doping (Li *et al.*, 2007c).

The unusual and large magnetoresistance found in the n-doped cuprates has been studied by a number of authors. The most striking behavior is the large negative MR found for optimal and underdoped compositions at low temperature ($T < T_{min}$). This has been interpreted as arising from 2D weak localization (Fournier *et al.*, 2000; Hagen *et al.*, 1991), 3D Kondo scattering from Cu^{+2} spins in the CuO_2 plane (Sekitani *et al.*, 2003), or scattering from unknown magnetic entities associated with the AFM state (Dagan *et al.*, 2005b). At low doping ($x \leq 0.05$) the MR is dominated by an anisotropic effect, largest for $H \parallel c$, and can reasonably be interpreted as an orbital, 2D weak localization, effect (especially since the ab-plane resistivity is below $k_F l = 1$ and follows a log T temperature dependence). At dopings between $x=0.1$

and 0.17 the negative MR is dominated by an isotropic effect and the orbital contribution becomes weaker as the doping increases. Dagan *et al.* (2005b) have isolated the isotropic MR and shown that it disappears for $x \sim 0.16$. This suggests that this MR is associated with a QCP occurring at this doping and is caused by some heretofore unknown isotropic magnetic scattering related to the AFM state. Dagan *et al.* (2005b) also showed that the isotropic negative MR disappears above a T_{min} and this suggests that the upturn in the *ab*-plane resistivity is associated with the AFM state. Recent high-field transverse magnetoresistance measurements (i.e., H applied along the *c*-axis)(Li *et al.*, 2007b) and angular magnetoresistance measurements (H rotated in the *ab* plane)(Yu *et al.*, 2007b) support the picture of a AFM to PM quantum phase transition near $Ce=0.165$ doping. However as noted below, the existence of a QPT associated with the termination of the AF state is at odds with the work of Motoyama *et al.* (2007) who concluded *via* inelastic scattering that the spin stiffness ρ_s fell to zero at a doping level of $x \approx 0.134$ (Fig. 40a). This issue is discussed in more detail below.

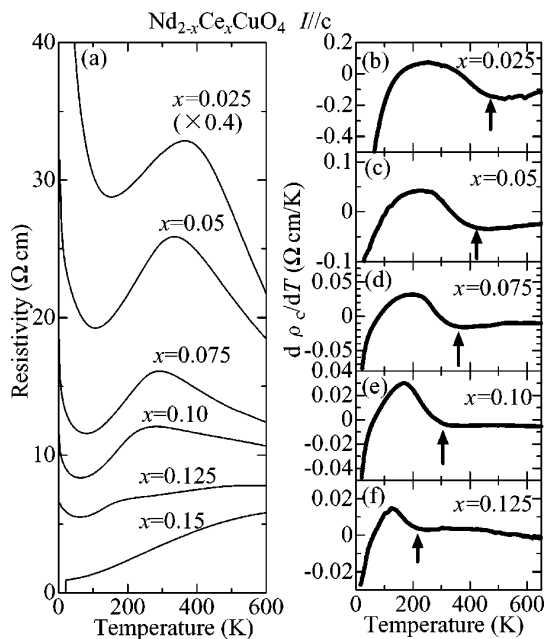


FIG. 28 The temperature dependence of the out-of-plane resistivity of NCCO at various doping. (b.) - (f.). The temperature derivative of the out-of-plane resistivity ($d\rho_c/dT$). The nominal T^* is indicated by the arrow. From Onose *et al.* (2004).

3. *c*-axis transport

The temperature and field dependence of the DC *c*-axis resistivity has been studied in single crystals by many authors [for earlier work see the review of Fontcuberta

and Fabrega (1996)]. The behavior of the *n*-doped *c*-axis resistivity is quite different than that found in *p*-type cuprates. Some recent and representative data as a function of doping and temperature is shown in Fig 28 (Onose *et al.*, 2004). This may reflect the different gapped parts of the FS in *n*- and *p*-type, since *c*-axis transport is dominated by specific FS dependent matrix elements (Andersen *et al.*, 1995; Chakravarty *et al.*, 1993) and the SDW-like state in the *n*-type as opposed to the unknown nature of the pseudogap in the *p*-type. As shown by Onose *et al.* (2004) (Fig 28) the *c*-axis resistivity has a distinct change from “insulating-like” to “metallic-like” below a temperature T^* , near the temperature at which the SDW gap is observed in optical experiments (Onose *et al.*, 2004; Zimmers *et al.*, 2005), before going insulating at the lowest temperature for the most underdoped samples. Below T^* the T dependence of the *c*-axis and *ab*-plane resistivity are similar although with an anisotropy ratio of 1000-10000. This behavior is strikingly different than that found in *p*-type cuprates. In *p*-type compounds the *c*-axis resistivity becomes “insulator-like” below the pseudogap temperature while the *ab*-plane resistivity remains “metallic” (down to T_{min} in underdoped compositions (Ando *et al.*, 2001). The interpretation of the *c*-axis resistivity upturn as a signature of the pseudogap formation in *p*-type cuprates has been reinforced by magnetic field studies, where the T^* is suppressed by field in a Zeeman-splitting-like manner (Shibauchi *et al.*, 2001). A recent field-dependent study of *n*-type SCCO near optimal doping has been interpreted as for the *p*-type cuprates (Kawakami *et al.*, 2006, 2005). However, the T^* found in this work is much lower than that found in the optical studies, casting some doubt on this interpretation. In contrast, Yu *et al.* (2006) have interpreted their field dependent *c*-axis resistivity results in terms of superconducting fluctuations. The origin of the *c*-axis resistivity upturn and its relation to the *ab*-plane upturn requires more investigation.

4. Effects of disorder on transport

Disorder has a significant impact on the *ab*-plane transport properties of the cuprates. This has been studied most extensively in the *p*-type materials [Alloul *et al.* (2009); Rullier-Albenque *et al.* (2008) and references therein]. The results obtained to date on the *n*-type cuprates seem to agree qualitatively with those found in *p*-type. Disorder in these compounds is caused by the cerium doping itself, the annealing process (where oxygen is removed from some sites), doping of Zn or Ni for Cu, and by ion or electron irradiation. The general behavior of $\rho_{ab}(T)$ as defects are introduced by irradiation is shown in Fig. 29 (Woods *et al.*, 1998) for optimally doped NCCO. The general trends are: T_c is decreased, the residual resistivity increases while the metallic T dependence at higher T remains roughly the same, and an “insulator-like” upturn appears at low temperature. As

the irradiation level increases the superconductivity is eventually completely suppressed and the upturn dominates the low temperature resistivity. The decrease of T_c is linearly proportional to the residual resistivity and extrapolates to zero at R_{\square} per unit layer of 5-10 k Ω , which is near the quantum of resistance for Cooper pairs (Woods *et al.*, 1998), similar to behavior seen in YBCO (Rullier-Albenque *et al.*, 2003). Defects introduced by irradiation do not appear to change the carrier concentration since the Hall coefficient is basically unchanged. Oxygen defects (vacancies or impurity site occupancy) can cause both changes in carrier concentration and in impurity scattering. In two recent papers, Gauthier *et al.* (2007); Higgins *et al.* (2006) have studied the effects of oxygen on the Hall effect and ρ_{ab} of slightly overdoped PCCO. As oxygen is added to an optimally prepared $x=0.17$ film the $\rho(T)$ behavior (Fig. 30) becomes quite similar to the $\rho(T)$ data under increased irradiation as shown in Fig 29. Gauthier *et al.* (2007) attribute the role of oxygen not to changing the carrier concentration significantly but to having a dramatic impact on the quasi-particle scattering rate. Higgins *et al.* (2006) compare resistivity and Hall effect for films with oxygen variation and with irradiation. They conclude that oxygen changes both the carrier concentration and the scattering rate. The exact origin of all these disorder effects on T_c and the transport properties has not yet been determined. However, the recent proposals (Alloul *et al.*, 2009; Rullier-Albenque *et al.*, 2008) for how defects influence the properties of hole-doped cuprates are most probably valid for n-doped cuprates as well.

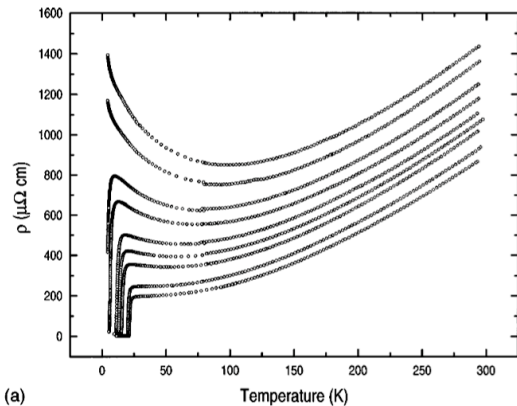


FIG. 29 Temperature dependent resistivity for NCCO $x = 0.14$ films damaged with He $^+$ ions. From bottom to top, ion fluences are 0, 0.5, 1, 1.5, 2, 2.5, 3, 4, and 4.5 $\cdot 10^{14}$ ions/cm 2 . From Woods *et al.* (1998).

5. Normal State Thermal conductivity

Thermal conductivity (κ) or heat transport measurements in the n-doped cuprates are also not as extensive as in hole-doped but there have been several important

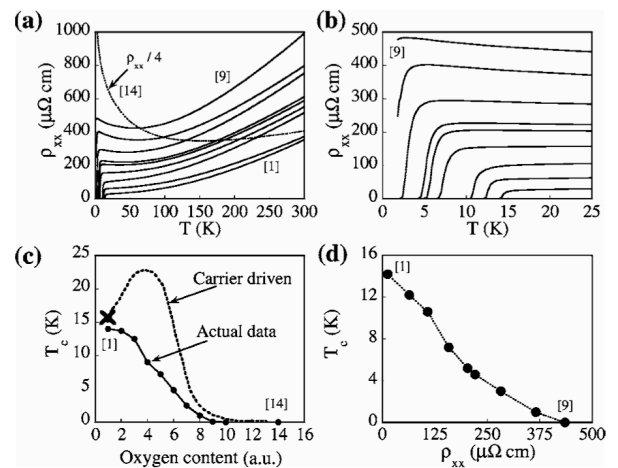


FIG. 30 (a) Resistivity as a function of temperature for $x = 0.17$ thin films with various oxygen contents. (b) Low-temperature region of the same data. (c) Critical temperature T_c as a function of oxygen content for $x = 0.17$ for films grown in oxygen full circles, solid line is a guide to the eye. Cross: highest T_c under N $_2$ O. Dashed line: schematic of the expected behavior for a carrier driven T_c (see (Gauthier *et al.*, 2007)). (d) T_c as a function of the in-plane resistivity at 30 K. From Gauthier *et al.* (2007).

results. In general their ab plane κ resembles that of the hole-doped compounds. In the best crystals an increase in κ_{ab} is found at T_c and can be attributed to a change in electron-phonon scattering as in the hole-doped cuprates (Yu *et al.*, 1992). The most significant κ data has been taken below T_c at temperatures down to 50mK for $H > H_{c2}$. A striking result was the report of a violation of the Wiedemann-Franz law below 1K in slightly underdoped PCCO (Hill *et al.*, 2001) samples, which was interpreted as a possible signature of a non-Fermi liquid in the normal state. This will be discussed in more detail in section IV.F below.

Sun *et al.* (2004) measured the ab -plane and c -axis thermal conductivity for underdoped crystals of Pr $_{1.3-x}$ La $_{0.7}$ Ce $_x$ CuO $_4$. They found that the low T phonon conductivity κ has a very anisotropic evolution upon electron doping: namely, the low-T peak of κ_c was much more rapidly suppressed with doping than the peak in κ_{ab} . Over the same doping range the ab -plane resistivity develops a “high mobility” metallic transport in the AFM state. They interpret these two peculiar transport features as evidence for stripe formation in the underdoped n -type cuprates. Essentially the same features are seen in underdoped p -type cuprates (Ando *et al.*, 2001) where the evidence for stripe formation is stronger.

In the underdoped n -type compounds phonons, magnons and electronic carriers (quasiparticles) all contribute to the thermal conductivity. Only at very low temperature it is possible to separate out the various contributions. However since phonons and magnons both have a T^3 variation, it has been necessary in undoped and AFM Nd $_2$ CuO $_4$ to use the magnetic field induced

spin-flop transition to switch on and off the acoustic Nd magnons and hence separate the magnon and phonon contributions to the heat transport (Li *et al.*, 2005b).

B. Tunneling

Tunnelling experiments on n-doped cuprates have been difficult and controversial. This is likely due to the problems associated with preparing adequate tunnel barriers and the sensitivity of the electron-doped material to preparation conditions. Some of these difficulties have been discussed by Yamamoto *et al.* (1997). Improvements have been made in recent years and we will focus on the most recent results. It is important to keep in mind that the surface layer being probed by tunnelling is very thin (of order the coherence length) and the surface may have properties different than the bulk because the oxygen reduction conditions at the barrier may not be the same as the interior. Experiments that show a bulk T_c or H_{c2} in their tunnel spectra are most likely to represent properties of the bulk. We only discuss what appear to be measurements representative of the bulk. Tunnelling experiments have been performed on films and single crystals using four methods; natural barriers with metals such as Pb, Sn, Al, In, and Au, point contact spectroscopy with Au or Pt alloy tips, bi-crystal grain boundary Josephson junctions (GBJ) on STO substrates, and Scanning Tunnelling Measurements (STM). Thus, these experiments are either in superconductor-insulator-superconductor (SIS), superconductor-insulator-normal metal (SIN), or SN configurations. Very few STM studies have been performed on the *n*-type compounds as compared to the extensive measurements on the hole-doped materials (Fischer *et al.*, 2007).

The aim of the tunnelling experiments has been to determine the SC energy gap, find evidence for bosonic coupling, the SC pairing symmetry, and evidence for normal state gap (pseudogap). We first discuss the SC state measurements. Typical quasi-particle conductance $G(V)=dI/dV$ spectra on optimal-doped NCCO using point contact spectroscopy are shown in Fig 31. Similar spectra are found for Pb/PCCO natural barrier junctions (Dagan *et al.*, 2005b) and GB junctions (Alff *et al.*, 1998a; Chesca *et al.*, 2005). The main features of the n-doped tunnel spectra are: prominent coherence peaks (which give an energy gap of order 4 meV at 1.8K), an asymmetric linear background $G(V)$ for voltage well above the energy gap, a characteristic 'V' shape, coherence peaks which disappear completely by $T \approx T_c$ at $H=0$ (and by $H \approx H_{c2}$ for $T=1.8K$), and typically the absence of a zero bias conductance peak (ZBCP) at $V=0$. The characteristic 'V' shape of $G(V)$ cannot be fit by s-wave BCS behavior and closely resembles that of d-wave hole-doped cuprates (Fischer *et al.*, 2007). Issues related to the determination of the order parameter are discussed in more detail in Sec. IV.A.2 below.

Tunneling experiments have also found evidence for a

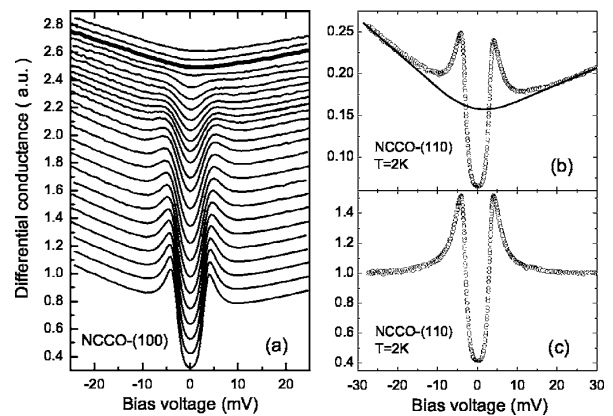


FIG. 31 Raw data of the directional tunneling measurements for optimally doped NCCO. (a) Temperature dependence of the tunnelling spectra measured along 00 direction. The curves have been shifted for clarity. The temperature increases from the bottom upwards in steps of 1 K (from 2 to 22 K) and then 2 K (from 22 to 30 K). The thick solid line denotes the data at 26 K which is approximately T_c . (b) An illustration of the constructed normal conductance background above T_c . (c) The normalized 2 K spectrum in the (110) direction. From Shan *et al.* (2005)

normal state energy gap (“pseudogap”) with energy ~ 5 meV at 2K, which is of the same order as the superconducting gap energy (Biswas *et al.*, 2001; Kleefisch *et al.*, 2001). This normal state gap (NSG) is found in SIS experiments and point contact spectroscopy experiments which probe the ab-plane by applying a c-axis magnetic field greater than H_{c2} . The low energy NSG is distinctly different than the high energy (~ 100 meV) “pseudogap” seen in ARPES and optical experiments (Armitage *et al.*, 2001b; Zimmers *et al.*, 2005) and most recently in a local tunneling spectroscopy experiment (Zimmers *et al.*, 2007a). The high energy gap is suggested to be associated with SDW-like gapping of the FS. The origin of the low energy NSG is not conclusively determined at this time. Proposed explanations include: coulomb gap from electron-electron interactions (Biswas *et al.*, 2001); hidden and competing order parameter under the SC dome which vanishes near optimal doping (Alff *et al.*, 2003); and preformed SC singlet pairs (Dagan *et al.*, 2005a). Dagan *et al.* (2005a) claim to rule out the Coulomb gap and competing order scenarios. They find that the NSG is present at all doping from 0.11 to 0.19 and the temperature at which it disappears correlates with T_c , at least on the overdoped side of the SC dome. However, the NSG also survives to surprisingly high magnetic fields and this is not obviously explained by the preformed pair (SC fluctuation) picture (Biswas *et al.*, 2001; Kleefisch *et al.*, 2001; Yu *et al.*, 2006). Additionally, Shan *et al.* (2008b) reported that the NSG and the SC gap are distinct entities at all dopings, which is consistent with the ‘two-gap’ scenario in the underdoped *p*-type cuprates.

Recently Niestemski *et al.* (2007) reported repro-

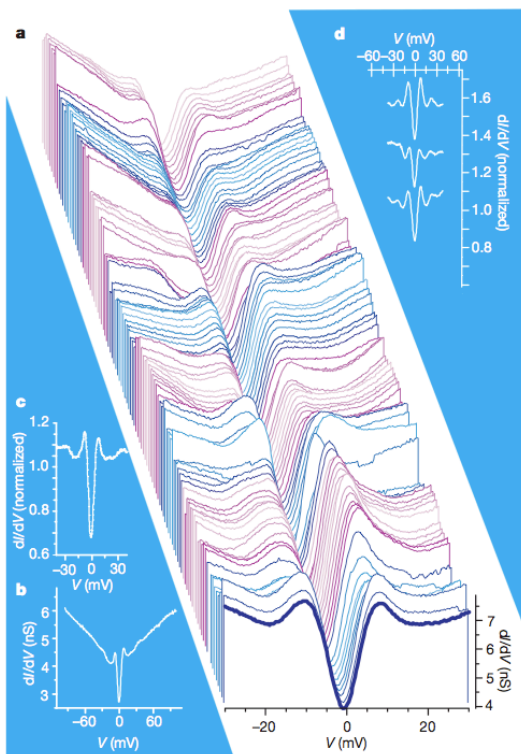


FIG. 32 (Color) (a) A 200 Å linecut that shows the variations in coherence peak heights and gap magnitude (Δ). The spectra have been offset for clarity. The gap magnitude, which is defined as half the energy separation between the coherence peaks varies from 5 meV to 8 meV in this linecut. (b) A representative ± 100 -mV range (dI/dV) spectrum that illustrates the dominate ‘V’-shaped background. (c) The spectrum in (b) after division by a linear V-shaped function. (d) Additional examples of dI/dV spectra that demonstrate the clearly resolved coherence peaks and modes resulting from a V-shaped division. From Niemetski *et al.* (2007).

ducible high resolution STM measurements of PLCCO ($T_c = 24$ K) (Fig. 32). The extremely inhomogeneous nature of doped transition metal oxides makes spatially resolved STM an essential tool for probing local energy scales. Statistics of the superconducting gap spatial variation were obtained through thousands of mappings in various regions of the sample. Previous STM measurements on NCCO gave gaps of 3.5 to 5 meV, but no obvious coherence peaks (Kashiwaya *et al.*, 1998). The linecut (Fig. 32a) shows spectra that vary from ones with sharp coherence peaks to a few with more pseudogap-like features and no coherence peaks. Although most measured samples at this doping (9 out of 13 mappings) gave gaps in the range of 6.5 - 7.0 meV, the average gap over all measured maps was 7.2 ± 1.2 meV, which gives a $2\Delta/k_B T_c$ ratio of 7.5, which is consistent with a strong

coupling scenario.¹⁸ The spectra also have a very notable ‘V’ shaped higher energy background. When this background is divided out a number of other features become visible. Similar to the hole-doped compounds (Fischer *et al.*, 2007), the claim is that features in the tunneling spectra can be related to an electron-bosonic mode coupling here at energies of 10.5 ± 2.5 meV. This energy is consistent with an inferred magnetic resonance mode energy in PLCCO (Wilson *et al.*, 2006a) as measured by inelastic neutron scattering as well as low-energy acoustic phonon modes, but differs substantially from the oxygen vibrational mode identified as coupling to charge in BSCCO *via* STM (Lee *et al.*, 2006a). Niemetski *et al.* (2007)’s analysis of the variation of the local mode energy and intensity with the local gap energy scale indicates an electronic origin of the mode consistent with spin-excitations rather than phonons.

C. ARPES

The first angle resolved photoemission (ARPES) studies of the electron-doped cuprates appeared in adjoining 1993 Physical Review Letters (Anderson *et al.*, 1993; King *et al.*, 1993). Both reported the existence of a large Fermi surface centered around the (π, π) position in $\text{Nd}_{1.85}\text{Ce}_{0.15}\text{CuO}_4$. It had a volume that scaled approximately with the number of charge carriers thereby satisfying Luttinger’s theorem and a shape similar to existing band structure calculations (Massidda *et al.*, 1989). It was pointed out by King *et al.* (1993) that the extended Van Hove states at the $(\pi, 0)$ point located at approximately 350 meV binding energy contrasted with the hole-doped case, where these states were located with tens of meV of E_F . It was speculated at that time that the lack of a large near- E_F density of states may be responsible for some of the very different hole and electron-doped compound properties.

Recently there have been a number of electron-doped ARPES studies which take advantage of recent dramatic advances in photoemission technology, including the vastly improved energy (< 10 meV) and momentum ($< 1\%$ of π/a for a typical cuprate) ARPES resolution as well as the utility provided by parallel angle scanning in *Scientia*-style detectors (Armitage *et al.*, 2001a,b, 2003, 2002; Matsui *et al.*, 2005a,b; Sato *et al.*, 2001). The contribution of ARPES to the study of the superconducting order parameter is detailed below in Sec. IV.A.4.

In studies concerning the overall electronic structure, the large Fermi surface around the (π, π) position was confirmed in the later high resolution studies by Armitage *et al.* (2001b), but it was also found that there are

¹⁸ This ratio strongly differs with point contact (Shan *et al.*, 2008a) and SIS planar tunneling results Dagan and Greene (2007) as well as Raman scattering (Qazilbash *et al.*, 2005), which have given a $2\Delta/k_B T_c$ ratio of approximately 3.5.

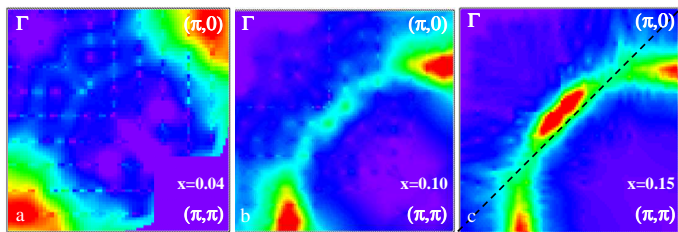


FIG. 33 (Color) Fermi surface plot: (a) $x = 0.04$, (b) $x = 0.10$, and (c) $x = 0.15$. EDCs integrated in a 60meV window (-40meV,+20meV) plotted as a function of \vec{k} . Data were typically taken in the displayed upper octant and symmetrized across the zone diagonal. Adapted from Armitage *et al.* (2003).

anomalous regions on the Fermi surface where the near E_F intensity is suppressed (Fig. 33(c)). A detailed look at the Energy Distribution Curves (EDCs) through the suppressed region of the Fermi surface reveals that the electronic peak initially approaches E_F , but then monotonically loses weight despite the fact that its maximum never comes closer than 100 meV to E_F . Such behavior with broad features and suppression of low-energy spectral weight is similar to the high-energy pseudogap seen in the extreme underdoped p -type materials (Marshall *et al.*, 1996), although in the present case it is observed near $(0.65\pi, 0.3\pi)$ and not at $(\pi, 0)$, the maximum of the d -wave functional form.

As noted by Armitage (2001); Armitage *et al.* (2001b) these regions of momentum space with the unusual low-energy behavior fall close to the intersection of the underlying FS with the AFBZ boundary, as shown by the dashed lines in Fig. 33(c). This suppression of low-energy spectral weight and the large scattering rate in certain regions on the FS resembles various theoretical predictions that emphasize a coupling of charge carriers to a low-energy collective mode or order parameter with characteristic momentum (π, π) . A simple phase space argument shows that it is those charge carriers which lie at the intersection of the FS with the AFBZ boundary that suffer the largest effect of anomalous (π, π) scattering as these are the only FS locations that can have low-energy coupling with $Q \approx (\pi, \pi)$. These regions were those later inferred by Blumberg *et al.* (2002); Matsui *et al.* (2005b) to have the largest superconducting gap as well. Although it is the natural choice, due to the close proximity of antiferromagnetism and superconductivity, this low-energy scattering channel need not be antiferromagnetic for the role played by the AFBZ boundary to hold; other possibilities such as d -density wave exist (Chakravarty *et al.*, 2001). It is only necessary that its characteristic wave vector be (π, π) . These heavily scattered regions of the FS have been referred to in the literature as “hot spots” (Hlubina and Rice, 1995). It has been suggested that the large backscattering felt by charge carriers in the hot spots is the origin of the pseudogap in the underdoped hole-type materials.

The gross features of the ARPES spectra in the optimally doped n -type compounds can be approximately described by a two band model exhibiting long range SDW order (Armitage, 2001; Matsui *et al.*, 2005a; Park *et al.*, 2007). Such a model reflects the folding of the underlying band structure across the AFBZ boundary and hybridization between bands *via* a potential $V_{\pi, \pi}$ (see Sec. IV.H below). It gives the two components (peak-dip-hump (PDH) structure) in the spectra near the $(\pi, 0)$ position (Armitage *et al.*, 2001a, 2003; Matsui *et al.*, 2005a; Sato *et al.*, 2001), the location of the hot spots, and perhaps more subtle features showing back folded sections of FS. As noted previously and will be discussed below in more detail, such a scenario does shed light on a number of other aspects of n -type compounds, including one long outstanding issue in transport where both hole and electron contributions to the Hall coefficient have been resolved (Dagan *et al.*, 2004; Fournier *et al.*, 1997; Gollnik and Naito, 1998; Wang *et al.*, 1991). Additionally as discussed below, this scenario appears to be consistent with aspects of the optical data (Zimmers *et al.*, 2005).

Matsui *et al.* (2005a) have also found that the lineshape in these “hot-spots” in NCCO $x=0.13$ have a strong temperature dependence, giving more credence to the idea that this suppression is due to spin density wave formation (Matsui *et al.*, 2005a). As shown in Fig. 34, Matsui *et al.* (2007) also demonstrate that the hotspot effect largely goes away by $x=0.17$ doping in NCCO, with the high-energy pseudogap filling in at the magnet-superconductor phase boundary. The magnitude (Δ_{PG}) and the temperature (T^*) at which the pseudogap fills in show a close relation to the effective magnetic coupling energy (J_{eff}) and the spin-correlation length (ξ_{AF}), respectively again suggesting the magnetic origin of the pseudogap and hot-spot effect. As seen in Fig. 35, it was shown that the lowest energy sharp peak had largely disappeared by the Néel temperature $T_N = 110K$ for the $x = 0.13$ sample while the near- E_F spectral weight suppression persisted until a higher temperature scale. These authors also claimed that the overall k -space dependence of their data was best understood within a spin density wave model with a non-uniform SDW gap in k -space.

In contrast, Park *et al.* (2007) in a comprehensive BZ wide study on SCCO claim that it was not that the gap was non-uniform, but that there appeared to be remnant bands reflective of the bare band structure that dispersed uninterrupted through the AFBZ. Through a simple model they showed how this might be reflective of short-range magnetic ordering. Moreover, these authors showed that the hot-spot effect in SCCO is so strong that the zone diagonal states were actually pushed below E_F raising the possibility of nodeless d -wave superconductivity in this compound. This observation may shed light on reports of nodeless superconductivity found in PCCO films grown on buffered substrates (Kim *et al.*, 2003). There have been various theoretical proposals in this regards recently (Das *et al.*, 2007; Yuan *et al.*, 2006b).

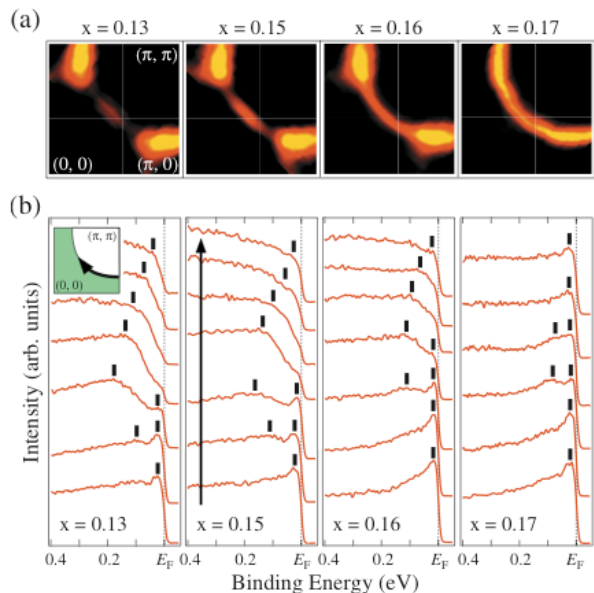


FIG. 34 (Color) (a) Doping dependence of the FS in NCCO, obtained by plotting the ARPES intensity integrated over ± 20 meV with respect to E_F as a function of momentum. The intensity is normalized to that at 400 meV binding energy and symmetrized with respect to the $(0,0) - (\pi, \pi)$ direction. (b) Doping dependence of a set of ARPES spectra measured at several k points around the FS at several dopings. From Matsui *et al.* (2007).

Richard *et al.* (2007) have made a detailed comparison of the ARPES spectra of as-grown and oxygen-reduced PCCO and PLCCO materials. They claim that to within their error bars (estimated by us to be approximately 1 %) neither the band filling nor the tight binding parameters are significantly affected by the reduction process in which a small amount of oxygen was removed ($\approx 1\%$). They demonstrated that the main observable effect of reduction was to remove an anisotropic leading edge gap around the Fermi surface. The effect of oxygen reduction is discussed in more detail below.

As mentioned above much recent discussion regarding ARPES spectra of the hole-doped cuprates has been regarding a “kink” or mass renormalization in the electronic dispersion which has been found ubiquitously in the p -type materials (at ≈ 70 meV) (Bogdanov *et al.*, 2000; Lanzara *et al.*, 2001). Its origin is a matter of much current debate (Campuzano *et al.*, 2004; Damaschelli *et al.*, 2003), with various phononic or magnetic scenarios being argued for or against. Its existence on the electron-doped side of the phase diagram has been controversial. Armitage *et al.* (2003) claimed that there was no kink feature along the zone diagonal and that the zone diagonal was best characterized by a smooth concave downward dispersion. Although apparent mass renormalizations were found along the zone face (Armitage *et al.*, 2003; Matsui *et al.*, 2005a; Sato *et al.*, 2001), it was claimed these were related to the “hot spot” effect

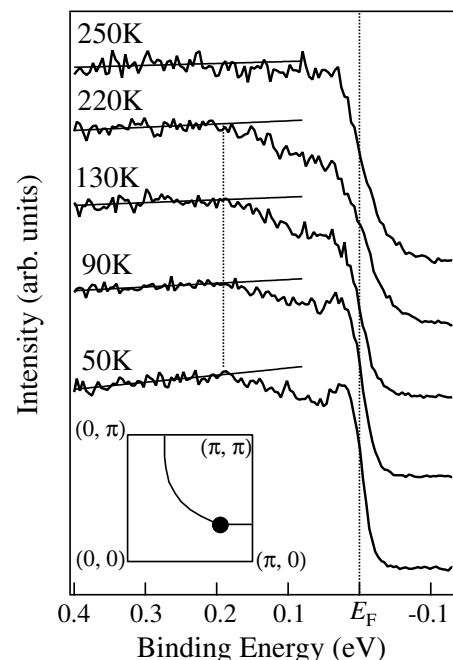


FIG. 35 Temperature dependence of the ARPES spectrum of NCCO ($x = 0.13$) measured in the “hot spot” (at the position on the Fermi surface shown by a circle in the inset) where the two component structure is observed clearly. The solid straight lines on the spectra show the linear fits to the high-energy region (0.20.5 eV) showing that it doesn’t change with temperature. From Matsui *et al.* (2005a).

and therefore of different origin. More recently, it has been claimed that a weak kink around 60 - 70 meV is in fact found along both relevant symmetry directions in NCCO with even a stronger kink found in SCCO (Liu *et al.*, 2008; Park *et al.*, 2008; Schmitt *et al.*, 2008). Liu *et al.* (2008) using laser-based photoemission report a weak kink along the zone diagonal, in which they find mass renormalization of approximately $1 + \lambda \approx 1.2$, which is less than the $1 + \lambda \approx 1.5$ for optimally doped LSCO (Lanzara *et al.*, 2001). However, Schmitt *et al.* (2008) claim a mass renormalization similar to LSCO of about $1 + \lambda \approx 1.5$. Park *et al.* (2008) estimate the coupling constant λ to be 0.8, but this value can not be directly compared to that of the hole-doped materials as it was derived in another fashion from the imaginary part of the ARPES self energy. All these groups make the point that unlike the hole-doped compounds where magnetic modes and phonons exist at similar energies, in the electron-doped cuprates the magnetic resonance mode appears to be found at much lower energies (Wilson *et al.*, 2006a; Yu *et al.*, 2008; Zhao *et al.*, 2007). A kink has also been found in recent soft x-ray angle resolved photoemission (Tsunekawa *et al.*, 2008). As phonon anomalies associated with the oxygen half-breathing mode are found in the 60 meV energy range, the mass renormalization is reasonably associated with electron-phonon interaction. As discussed below, this work gives additional evidence

that the electron-phonon interaction is not so different on the two sides of the phase diagram. Since superconductivity *is* so different on both sides of the phase diagram this may give circumstantial evidence that electron-phonon effects are not directly relevant for superconductivity.

Another item of recent interest in the photoemission spectra of cuprates is that of a universal ‘high-energy kink’ in the dispersion of the hole-doped cuprates that manifests as an almost vertical drop in the dispersion curve around 300 meV (Graf *et al.*, 2007; Meevasana *et al.*, 2007; Ronning *et al.*, 2005). Pan *et al.* (2006) found a similar anomaly in PLCCO at energies around 600 meV that they termed a quasiparticle coherence-incoherence crossover. Moritz *et al.* (2008) showed a drop in the dispersion of $x = 0.17$ NCCO around 600 meV that confirms a high energy kink in the electron-doped cuprates found at an energy approximately twice that of the hole-doped compounds. Pan *et al.* (2006) claimed that this result ruled out the super exchange interaction J as the driving interaction as the energy scales of the high energy kink were so different, yet the scale of J so similar between the two sides of the phase diagram. Through their quantum Monte Carlo calculations within the one band Hubbard model Moritz *et al.* (2008) assign the anomaly to a crossover when following the dispersion from a quasi-particle-like band at low binding energy near- E_F to an incoherent Hubbard band-like features. These features are at higher energies in the electron-doped cuprates due to the presence of the charge transfer gap on the occupied side of the spectrum. In a related fashion, Ikeda *et al.* (2009) have claimed that the difference in kink energies in these two material classes can be linked to their intrinsic chemical potential difference.

We should point out that although the general ‘‘hot-spot’’ phenomena is exhibited in all measured electron-doped cuprates close to optimal doping, the details can be considerably different. In NCCO (Matsui *et al.*, 2005a) and PLCCO (Matsui *et al.*, 2005b) there is an actual peak at E_F with greatly reduced spectral weight in the hot spot. In contrast in underdoped SCCO (Park *et al.*, 2007) and ECCO (Ikeda *et al.*, 2008, 2007) there is a clear gap at the hot spot and no sign of near- E_F quasi-particle. These differences may be directly related to changes in chemical pressure caused by different rare earth ion radii and its effect on band structure parameters like the t'/t ratio or indirectly by chemical pressure by causing the extent of antiferromagnetism (and for instance $V_{\pi,\pi}$) to be different¹⁹. Ikeda *et al.* (2008) performed a systematic ARPES study of the Nd, Sm, Eu series of rare earth substitutions, which due to decreasing ion size corresponds to increasing chemical pressure. In- and out-of-plane lat-

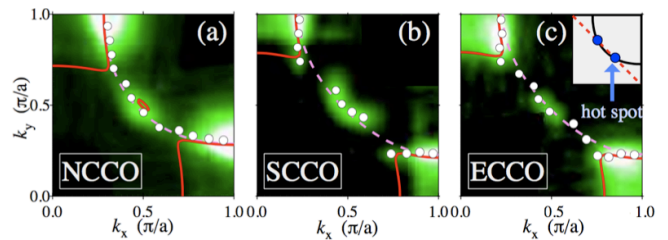


FIG. 36 (Color) ARPES intensity within ± 30 meV of E_F plotted in the BZ quadrant space for nominally $x = 0.15$ NCCO, SCCO, and ECCO. White circles show the peak positions of momentum distribution curves (MDCs) at E_F , indicating the underlying Fermi surface. Solid red curves and dashed pink curves show the Fermi surface obtained by tight-binding fit to the ARPES data assuming the paramagnetic and antiferromagnetic band structures, respectively. The FS exhibit significantly less curvature in ECCO as compared to NCCO. Inset: Schematic diagram of the hot spot. Black curve and red dashed line represent the Fermi surface and the antiferromagnetic Brillouin zone boundary, respectively. From Ikeda *et al.* (2008).

tice constants as well as T_c decreases across this series (Markert *et al.*, 1990; Uzumaki *et al.*, 1991). Ikeda *et al.* found that the underlying Fermi surface shape changes considerably (Fig. 36) and exhibits significantly less curvature when going from Nd to Eu, which is consistent with a strongly decreasing $|t'/t|$ ratio. Fitting to a tight banding band structure with nearest and next-nearest neighbors they found $|t'/t| = 0.40, 0.23,$ and 0.21 for NCCO, SCCO, and ECCO, respectively. The decreasing ratio was associated with a strong dependence on the in-plane lattice constant. The hot spot effects also change considerably within this series as seen by the increasing suppression of the near- E_F intensity in Fig. 36. Ikeda *et al.* attributed this to an increasing $V_{\pi,\pi}$, which was associated with the decreasing out-of-plane lattice constant and a strengthening of 3D antiferromagnetism. The $V_{\pi,\pi}$ undoubtedly increases across this series, however at least part of the differences in the hot-spot phenomena may be due to whether or not different $x = 0.15$ samples near the AF phase boundary exhibit long range SDW order or just strong fluctuations of it. One expects that a true gap forms at the hot spot only in the case of true long range order. This is discussed in more detail in Sec. IV.H below.

We should also mention that the observation of ‘‘hot-spots’’ has been disputed (Claesson *et al.*, 2004) in an ARPES study that used higher energy photons, thereby gaining marginally more bulk sensitivity over other measurements. It is unclear however, whether this studies’ relatively poor energy resolution (140 meV as compared to ≈ 10 meV in other studies) coupled with a large near- E_F integration window (136 meV) can realistically give any insight into this matter regarding low energy spectral suppression when the near E_F suppression is observed primarily at energies below 70 meV.

Finally, with regards to the doping dependence, Ar-

¹⁹ These differences may also be due to the differences in the optimal reduction conditions for different compounds, which are known to exist as one goes from PCCO to SCCO and ECCO.

mitage *et al.* (2002) showed the dramatic changes of the ARPES spectra as the undoped AF parent compound NCO is doped with electrons away from half filling towards the optimally doped metal as shown in Fig. 33. It was found that the spectral weight was lost from the charge transfer band (CTB) or lower Hubbard band feature observed by Ronning *et al.* (1998); Wells *et al.* (1995) and transferred to low energies as expected for a doped Mott insulator (Meinders *et al.*, 1993). One interesting feature about performing a photoemission study on an electron-doped material is that - in principle - the doping evolution of the Mott gap is observable due to it being below the chemical potential. In hole-doped compounds, such information is only available via inverse photoemission. At the lowest doping levels, $x=0.04$ it was observed the electrons reside in small ‘Fermi’ patches near the $(\pi,0)$ position, at an energy position near the bottom of the upper Hubbard band (as inferred from optics (Tokura *et al.*, 1990)). This is consistent with many models in which the lowest electron addition states to the insulator are found near $(\pi,0)$ (Tohyama, 2004). Importantly mid-gap spectral weight also develops. At higher dopings the band near $\pi,0$ becomes deeper and the midgap spectral weight becomes sharper and moves toward the chemical potential, eventually contacting the Fermi energy and forming the large Fermi surface observed in the highest- T_c compounds.

These observations showed for the very first time, at least phenomenologically, how the metallic state can develop out of the Mott insulator. Note that there was some evidence that the CT gap was renormalized to smaller energies upon electron doping as the energy from the CTB onset to the chemical potential (0.8 eV) is smaller than the energy onset of the optical gap in the undoped compound. However, these data clearly showed that the CT gap does *not* collapse or close with electron addition (Kusko *et al.*, 2002) and instead fills in. A gap that mostly fills in and does not collapse with doping is also consistent optical experiments (Arima *et al.*, 1993; Onose *et al.*, 2004). Such behavior is reproduced within slave-boson approaches (Yuan *et al.*, 2005) as well as numerical calculations within the Hubbard model (Aichhorn *et al.*, 2006; Kancharla *et al.*, 2008; Macridin *et al.*, 2006; Senechal and Tremblay, 2004; Tohyama, 2004) that show most features of the FS development can be reproduced with a doping independent CT gap.

D. Optics

As in the hole-doped cuprates, optical and infrared spectroscopy has contributed greatly to our knowledge of electronic dynamics in the n -type materials. The first detailed comparison between electron- and hole-doped insulating parent compounds was reported by Tokura *et al.* (1990). Interestingly, they found an onset in the optical conductivity around 1 eV and a peak around 1.5 eV. This is about 0.5 eV smaller than that found in analogous T

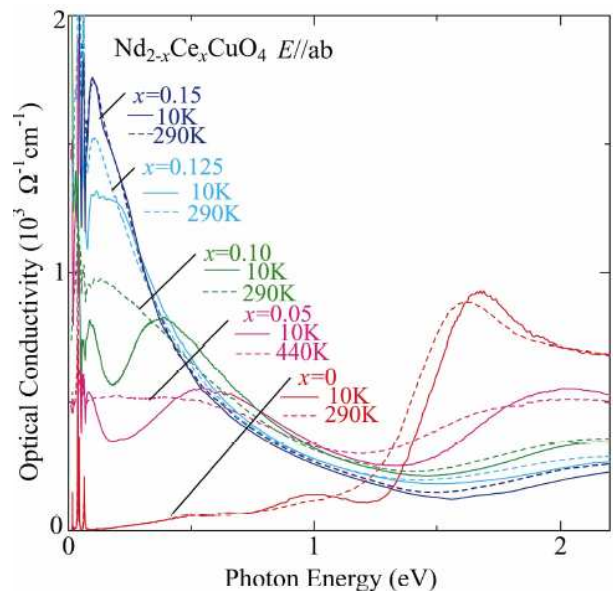


FIG. 37 (Color) Doping dependence of optical conductivity spectra for $\text{Nd}_{2-x}\text{Ce}_x\text{CuO}_4$ crystals with $x=0 - 0.15$ at 10 K and a sufficient high temperature (440 K) for the $x=0.05$ crystal and 290 K for the others. From Onose *et al.* (2004)

phase La_2CuO_4 . This optical gap was associated with a charge transfer (CT) gap of 1 - 1.5 eV in the T' structure compound Nd_2CuO_4 . In this study, the smaller charge transfer gap energy was correlated with the distance from the Cu site to the apical oxygen (essentially infinity in the apical oxygen-free T' structure compound) and its effect on the local Madelung potential.

In one of the first detailed studies of the optical spectra’s doping dependence Arima *et al.* (1993) found in $\text{Pr}_{2-x}\text{Ce}_x\text{CuO}_4$ mid-gap states that grew in intensity similar to, but at a slower rate than, the hole doped compounds. They also found a remnant of the CT band at doping levels almost as high as optimal. More recently the infrared and optical conductivity has been investigated by a number of groups (Homes *et al.*, 1997; Lupi *et al.*, 1999; Onose *et al.*, 1999, 2001, 2004; Singley *et al.*, 2001; Wang *et al.*, 2006a; Zimmers *et al.*, 2005). It is found generally, that upon rare earth substitution, a transfer of spectral weight from the CT band to lower frequencies takes place. A broad peak in the mid-infrared ($4000\text{-}5000\text{ cm}^{-1}$ or approximately 0.56 eV) is first formed at low doping levels, with a Drude component emerging at higher dopings. Fig. 37 shows typical behavior. This behavior bears a passing resemblance to the hole-doped compounds except that despite softening with Ce doping the mid-IR band can still be resolved as a distinct feature in the highest T_c samples ($x=0.15$).

Other important differences exist. For instance, Onose *et al.* (2001, 2004) found that this notable ‘pseudogapped’ mid-infrared feature ($\Delta_{pg} = 0.2 - 0.4$ eV) appeared directly in the optical conductivity spectrum for metallic but non-superconducting crystals of $\text{Nd}_{2-x}\text{Ce}_x\text{CuO}_4$

only below a characteristic temperature T^* . It was found that $\Delta_{pg} = 10k_B T^*$ and that both decrease with increasing doping. Moreover, the low temperature Δ_{pg} was comparable to the magnitude of the pseudogap measured by Armitage *et al.* (2002) via photoemission spectroscopy, which indicates that the pseudogap appearing in the optical spectra is the same as that in photoemission. Such a distinct pseudogap (PG) in the optical spectrum is not found in underdoped p -type superconductors where instead only an onset in the frequency dependent scattering-rate $1/\tau(\omega)$ derived by an extended Drude model analysis is assigned to a PG (Puchkov *et al.*, 1996). Singley *et al.* (2001) found that the frequency dependent scattering rate in the electron-doped compounds is depressed below 650 cm^{-1} , which is similar to the behavior which has been ascribed to the pseudogap state in the hole-doped materials (Puchkov *et al.*, 1996). However, whereas in the underdoped p -type compounds the energy scales associated with the pseudogap and superconducting states can be quite similar, these authors showed that in $\text{Nd}_{1.85}\text{Ce}_{0.15}\text{CuO}_4$ the two scales differ by more than an order of magnitude. In this case, the origin of pseudogap formation was ascribed to the strong T -dependent evolution of antiferromagnetic correlations in the electron-doped cuprates. It has been claimed recently that it is actually the maximum in the scattering rate and not the visible gap in the optical conductivity that correlates with the ARPES gap best (Wang *et al.*, 2006a).

Zimmers *et al.* (2005) found that the magnitude of the PG Δ_{pg} extrapolates to zero at concentration of $x = 0.17$ in $\text{Pr}_{2-x}\text{Ce}_x\text{CuO}_4$ films, implying the coexistence of magnetism and superconductivity in the highest T_c samples and the existence of a quantum critical point around this doping. Moreover, they performed a detailed analysis of their optical spectra over an extended doping range and found that a simple spin density wave model similar to the one discussed in the context of photoemission above with (π, π) commensurate order with frequency- and temperature-dependent self energies could describe many of the principal features of the data. With regards to the inference of a QCP via optics, note however, that Motoyama *et al.* (2007) gives convincing evidence the AF state terminates around $x = 0.13$ doping in NCCO. It is likely that the PG observed by Zimmers *et al.* (2005) and others corresponds to the buildup of appreciable AF correlations and not the occurrence of T_N . For instance, Wang *et al.* (2006a)'s optical data clearly show the existence of a large pseudogap in underdoped samples at temperatures well above the Néel temperature.

In an infrared Hall effect study Zimmers *et al.* (2007b) found that at the lowest temperatures their data for $x = 0.12, 0.15, 0.18$ was *qualitatively* consistent with the simple spin density wave model. However, Jenkins *et al.* (2009a) demonstrated strong *quantitative* discrepancies for underdoped materials of such a model with far infrared Hall measurements when using as input parameters the experimentally measured band structure from

ARPES. Additionally, measurements as high as 300K do not suggest a simple closing of the SDW gap (and hence formation of an unreconstructed Fermi surface around (π, π)) above T_N (Jenkins *et al.*, 2009a; Zimmers *et al.*, 2007b). There is a strong temperature dependence of the electron contribution to the Hall angle through the whole range up to and even above T_N . Jenkins *et al.* (2009a) ascribed this to the role played by AF fluctuations. Moreover, despite the success of the extended Drude model in describing σ_{xx} of overdoped $\text{Pr}_{2-x}\text{Ce}_x\text{CuO}_4$, Zimmers *et al.* (2007b) found strong deviations in its description of σ_{xy} in an $x=0.18$ sample showing, perhaps, that strong correlation effects are still playing a role even at this doping. Later work of this group using lower energy far infrared Hall data concludes that these deviations can in general be described by a model that incorporates vertex corrections due to antiferromagnetic fluctuations within the FLEX approximation (Jenkins *et al.*, 2009b; Kontani, 2008).

Onose *et al.* (1999) had found that although the temperature dependence for reduced superconducting crystals was weak, for unreduced $\text{Nd}_{1.85}\text{Ce}_{0.15}\text{CuO}_4$ the large pseudogap structure evolves around 0.3 eV, but that also activated infrared and Raman Cu-O phonon modes grew in intensity with decreasing temperature. This was interpreted as being due to a charge ordering instability promoted by a small amount of apical oxygen. Singley *et al.* (2001) also found a low energy peak in the in-plane charge response at $50\text{--}110 \text{ cm}^{-1}$ of even superconducting $\text{Nd}_{1.85}\text{Ce}_{0.15}\text{CuO}_4$ crystals, possibly indicative of residual charge localizing tendencies

Singley *et al.* (2001) also showed that in contrast to the ab -plane optical conductivity, the c -axis showed very little difference between reduced superconducting $x=0.15$ and as-grown samples. This is in contrast to the expectation for hole-doped cuprates where large changes in the c -axis response are observed below the pseudogap temperature (see Basov and Timusk (2005) and references therein). Since the matrix element for interlayer transport is believed to be largest near the $(\pi, 0)$ position and zero along the zone diagonal, interlayer transport ends up being a sensitive probe in changes of FS topology. The polarized c -axis results indicate that the biggest effects of oxygen reduction should be found along the zone diagonal. Using low frequency THz Pimenov *et al.* (2000) have shown that the out of plane low frequency conductivity closely follows the dependence of the in-plane. This is, again, likely the result of an interplane tunnelling matrix elements and the lack of a PG near $(\pi, 0)$. Using these techniques they also found that there was no apparent anomaly in the quasi-particle scattering rate at T_c , unlike in many hole-doped cuprates (Bonn and Hardy, 1996).

In the superconducting state of $\text{Nd}_{1.85}\text{Ce}_{0.15}\text{CuO}_4$ crystals Singley *et al.* (2001) found that the c -axis spectral weight which collapses into the condensate peak, was drawn from an anomalously large energy range ($E > 8\Delta$) similar to that of the hole-doped cuprates. In contrast, Zimmers *et al.* (2004) claimed that the *in-plane* Ferrell-

Glover-Tinkham spectral weight sum rule was satisfied in their $\text{Pr}_{2-x}\text{Ce}_x\text{CuO}_4$ thin films at a conventional energy scale $4\Delta_{max}$ much less than that of the hole-doped cuprates (Zimmers *et al.*, 2004). If true, the discrepancy between out-of- and in-plane sum rule ‘violation’ is unlike the p -type cuprates and is unexplained. It would be worthwhile to repeat these measurements on the same sample, perhaps with the benefit of higher accuracy far infrared ellipsometry.

Finally, Homes *et al.* (2006) has recently made the observation of a kink in the frequency dependent reflectivity of $\text{Pr}_{1.85}\text{Ce}_{0.15}\text{CuO}_4$ at T_c . This is interpreted as a signature of the superconducting gap whose presence in the optical spectra is consistent with their observation that scattering rate $1/\tau$ is bigger than 2Δ and hence that these materials are in the dirty limit. It was argued that the ability to see the gap is enhanced as consequence of its non-monotonic d-wave nature (see Sec. IV.A below). The extracted gap frequency $\Delta_0 \approx 35 \text{ cm}^{-1}$ (4.3 meV) gives a $2\Delta/k_B T_c$ ratio of approximately 5, which is in good agreement with other techniques such as tunnelling (Shan *et al.*, 2005). Schachinger *et al.* (2008) recently reanalyzed the data of Homes *et al.* (2006) as well as Zimmers *et al.* (2004, 2005) to generate a boson-electron coupling function $I^2\chi(\omega)$. They find that the optical conductivity can be modeled with a coupling function with peaks at 10 meV and 44 meV. They identified this lower peak with the magnetic resonance mode found by Wilson *et al.* (2006a) in PLCCO at 11 meV and draw attention to the correspondence of this energy scale with the 10.5 meV feature in STM (Niestemski *et al.*, 2007).

E. Raman spectroscopy

Raman spectroscopy has been extensively used for the investigation of both normal state and superconducting properties of the cuprate superconductors (Devereaux and Hackl, 2007). It is a sensitive probe of quasiparticle properties, phonon structure, superconducting order parameter symmetry, and charge order. In the electron-doped compounds, both phonons (Heyen *et al.*, 1991) and crystal-field excitations (Jandl *et al.*, 1996, 1993) were studied early on.

As mentioned above, Onose *et al.* (1999) found that activated infrared and Raman Cu-O phonon modes grew in intensity with decreasing temperature in unreduced crystals. This was interpreted in terms of a charge ordering instability induced by a minute amount of interstitial apical oxygen. Via Raman measurements, Onose *et al.* (2004) found some of the most definitive supporting evidence that antiferromagnetic correlations manifest themselves in transport anomalies and signatures in the charge spectra (ARPES, optics etc.) below a pseudogap temperature T^* . As shown in Fig. 38, the B_{1g} two-magnon peak, which is found at 2800 cm^{-1} in the $x=0$ compound (Sugai *et al.*, 1989), broadens and loses intensity with Ce doping. The peak energy itself shows

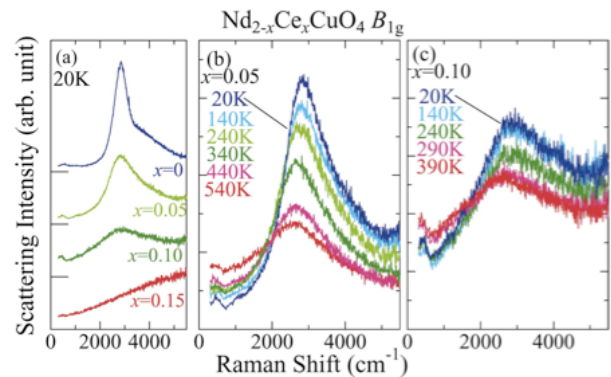


FIG. 38 (Color) (a) Doping dependence of the B_{1g} two-magnon peak Raman spectra at 20 K for crystals of $\text{Nd}_{2-x}\text{Ce}_x\text{CuO}_4$. (b),(c) Temperature variation of the B_{1g} Raman spectra for (b) $x = 0.05$ and (c) $x = 0.10$ crystals. From Onose *et al.* (2004).

little doping dependence. They found that the peak’s integrated intensity shows a sudden onset below T^* - the same temperature where the optical and ARPES pseudogaps develop and there is a crossover in the out-of-plane resistivity.

Koitzsch *et al.* (2003) studied specifically the pseudogap state of $\text{Nd}_{1.85}\text{Ce}_{0.15}\text{CuO}_4$. They observed the suppression of spectral weight below 850 cm^{-1} for the B_{2g} Raman response and identify it as an anisotropic PG in the vicinity of $(\pi/2, \pi/2)$ points of the BZ. This was consistent with a model of the pseudogap which originated in enhanced AF interactions in the hot spot region that are closer to the $(\pi/2, \pi/2)$ points in these materials than in the hole-doped compounds. They also observed a narrow Drude-like coherent peak in the B_{2g} channel in the pseudogap phase below T^* , which reveals the emergence of long-lived excitations in the vicinity of the $(\pi/2, \pi/2)$ points. Interestingly these excitations do not seem to contribute to the optical conductivity, as it is the B_{1g} response (sensitive to the $(\pi, 0)$ region) which closely tracks the optical response.

As mentioned above, although the original Raman measurements of the superconducting gap (Stadlober *et al.*, 1995) found evidence for an s-wave order parameter, more recent measurements have been interpreted in terms of an d-wave order parameter, which is non-monotonic with angle around the FS (Blumberg *et al.*, 2002; Qazilbash *et al.*, 2005). This will be discussed in more detail below. In PCCO and NCCO, Qazilbash *et al.* (2005) have also determined both an effective upper critical field $H_{c2}^*(T, x)$ at which the superfluid stiffness vanishes and an $H_{c2}^{\Delta}(T, x)$ at which the SC gap amplitude is suppressed. $H_{c2}^{\Delta}(T, x)$ is larger than $H_{c2}^*(T, x)$ for all doping concentrations. The difference between the two quantities suggests the presence of phase fluctuations that are larger for $x < 0.15$. The ability of a magnetic field to suppress the Raman gap linearly at even small fields is unlike the hole-doped compounds (Blum-

berg *et al.*, 1997) or even conventional s-wave NbSe₂ (Sooryakumar and Klein, 1980, 1981) and may be related to the non-monotonic d-wave gap where points of maximum gap amplitude are close to each other in reciprocal space. From the doping dependence of $H_{c2}^{2\Delta}(T, x)$ Qazilbash *et al.* (2005) extracted the Ginzburg-Landau coherence length $\xi_{GL} = \sqrt{\Phi_0/2\pi H_{c2}^{2\Delta}(T, x)}$. ξ_{GL} is almost an order of magnitude larger than the p-doped compounds, giving $k_F \xi_{GL}$ values between 40 and 150 (or $E_F/\Delta \approx 6 - 24$). This larger Cooper pair size requires higher order pair interactions to be taken into account and supports the existence of the nonmonotonic d-wave functional form.

F. Neutron scattering

1. Commensurate magnetism and doping dependence

Neutron scattering has been the central tool for investigating magnetic and lattice degrees of freedom in the cuprates (Bourges, 1999; Kastner *et al.*, 1998). In this section we concentrate on their contribution towards our understanding of the magnetism of the electron-doped cuprates. Their important contribution to the understanding of electron-phonon coupling in the *n*-type compounds (See for instance Braden *et al.* (2005)) will be discussed in Sec. IV.D.

The spin structure of undoped T' lattice compounds had been investigated thoroughly with neutron scattering as being, like LCO, a somewhat ideal realization of quasi-2D spin 1/2 Heisenberg antiferromagnetic (Kastner *et al.*, 1998). As discussed above (Sec. II.F), the T' cuprates have an unusual non-collinear *c*-axis spin structure, where the Cu site spins alternately point in the (100) and (010) directions in different layers along the *c*-axis Chattopadhyay *et al.* (1994); Skanthakumar *et al.* (1993). These non-collinear spin structures appear because of the presence of the magnetic exchange interaction between Cu and RE (Petitgrand *et al.*, 1999; Sachidanandam *et al.*, 1997). This structure contrasts with that found in orthorhombic LCO where at low temperatures the spins point more or less in the direction diagonal to the Cu-O bonds and are collinear along the *c*-axis (Kastner *et al.*, 1998). The spectrum is gapped due to anisotropy by about 5 meV in PCO (Sumarlin *et al.*, 1995) and NCO (Bourges *et al.*, 1992), which compares with the anisotropy gap of 2.5 meV in LCO (Peters *et al.*, 1988). Bourges *et al.* (1997) compared *p*- and *n*-type insulating parent compounds to the predictions of spin-wave theory. They found T_N 's of 320 K, 243 K, 247 K and antiferromagnetic exchange energies of 133, 155, and 121 meV in LCO, NCO, and PCO respectively, showing differences, but none systematic, between

material classes²⁰.

It was found early on (Matsuda *et al.*, 1992; Thurston *et al.*, 1990) that in doped, but not superconducting materials the spin response of the *n*-type systems remained commensurate at (π, π) unlike the hole-doped compounds, which have a large incommensurability. This commensurability is shared by all doped compounds in this material class. Doping appears to preserve the unusual non-collinear *c*-axis spin arrangement (Sumarlin *et al.*, 1995). Due primarily to the lack of large superconducting single phase crystals, it wasn't until 1999 that Yamada *et al.* (1999) showed the existence of well-defined commensurate spin fluctuations in a superconducting reduced sample. The magnetic scattering intensity was peaked at (π, π) as in the as-grown antiferromagnetic materials, but with a broader *q*-width. It was suggested by Yamada *et al.* (2003) that the commensurate dynamic (> 4 meV) short range spin correlations in the SC phase of the *n*-type cuprate reflect an inhomogeneous distribution of doped electrons in the form of droplets/bubbles in the CuO₂ planes, rather than organizing into one-dimensional stripes as the doped holes may in many *p*-type cuprates. They estimated the low temperature (8 K) in-plane and out-of-plane dynamic magnetic correlation lengths to be $\xi_{ab} = 150\text{\AA}$ and $\xi_c = 80\text{\AA}$ respectively for a $T_c = 25$ K sample. A comparison with the in-plane superconducting coherence length ($\approx 80\text{\AA}$) (Qazilbash *et al.*, 2005) gives evidence that magnetism and superconductivity compete in the electron-doped cuprate as in *p*-type compounds.

It has been emphasized recently by Krüger *et al.* (2007) that within a fermiology approach the commensurate magnetic response of the doped compounds is even more at odds with their experimentally determined FS than a commensurate response would be for hole-doped compounds (which are actually incommensurate). They demonstrated that with a momentum independent Coulomb repulsion (which derives from the dominant hard core, local repulsion inherited from the microscopic Hubbard U) the magnetic spectrum will be strongly incommensurate²¹. Indeed based on their Fermi surfaces alone (Armitage *et al.*, 2001b), one might

²⁰ As noted above, the maximum T_N of NCO is different in different studies, which is presumably due to a strong sensitivity to oxygen content. For instance, Matsuda *et al.* (1990) report 255 K, Bourges *et al.* (1997) report 243 K, whereas Mang *et al.* (2004b) report ≈ 270 K. Note that this value of Bourges *et al.* (1997) for NCO's J is also substantially larger than other studies. For instance Mang *et al.* (2004b) estimate 125 meV from their comparison of the correlation length's temperature dependence to their quantum Monte Carlo calculations. See also the two magnon Raman data of Sulewski *et al.* (1990), who find exchange constants of 128, 108 and 110 meV for LCO, NCO and SCO respectively.

²¹ In contrast, Ismer *et al.* (2007) have claimed that the magnetic spectrum can be fit well within a fermiology RPA approach. However they use a Coulomb repulsion $U(\mathbf{k})$ which is peaked strongly at (π, π) , which essentially ensures the excellent fit.

expect that their magnetic response to be even *more incommensurate* than the hole-doped. The commensurability shows the central role that strong coupling and local interactions play in these compounds.

As mentioned in Sec. II.C, one approach to understanding the relatively robust extent of the antiferromagnetic phase in the *n*-type compounds has been to consider *spin-dilution models*. Keimer *et al.* (1992) showed that Zn doping into La_2CuO_4 reduces the Néel temperature at roughly the rate as Ce doping in $\text{Pr}_{2-x}\text{Ce}_x\text{CuO}_{4\pm\delta}$. As Zn substitutes as a spinless impurity in d^{10} configuration and serves to dilute the spin system, this implies that Ce does a similar thing. Consistent with this model, Matsuda *et al.* (1992) showed that the reduction of the Néel temperature in $\text{Nd}_{2-x}\text{Ce}_x\text{CuO}_{4\pm\delta}$ comes through a continuous reduction of the spin stiffness ρ_s .

Although this comparison of Ce with Zn doping is compelling it cannot be exact as the charge carriers added by Ce doping are itinerant and cannot decrease the spin stiffness as efficiently as localized Zn. Mang *et al.* (2004b) found in as grown non-superconducting $\text{Nd}_{2-x}\text{Ce}_x\text{CuO}_{4\pm\delta}$ that by looking at the instantaneous correlation length [obtained by integrating the dynamic structure factor $S(\mathbf{q}_{2D}, \omega)$] the effects of itinerancy could apparently be mitigated. An almost quantitative agreement was found with quantum Monte Carlo calculations of the randomly site-diluted nearest-neighbor spin 1/2 square-lattice Heisenberg antiferromagnet.²²

In NCCO's superconducting state, Yamada *et al.* (2003) showed that in addition to the commensurate elastic response, a gap-like feature opens up in the inelastic signal (Fig. 39). A similar spin gap with a magnitude of 6 – 7 meV has also been reported in the *p*-type LSCO system near optimal doping. The maximum gap 2Δ behaves linearly with the SC temperature scale $Ck_B T_c$ with $C \approx 2$ irrespective of carrier type. However, Yamada *et al.* (2003) claim that whereas the spin pseudo-gap behavior in the SC state of the *p*-type cuprates has a temperature independent gap energy and slowly “fills in” upon warming, in $x = 0.15$ NCCO the gap slowly closes from 4 meV as the temperature decreases from T_c to 2 K. ‘Filling-in’ behavior has been associated with phase separation and its absence argues against such phenomena in the *n*-type cuprates. Interestingly, Motoyama *et al.* (2006) found that the superconducting magnetic gap's magnetic field dependence shows an analogous trend as the temperature dependence when comparing hole- and electron-doping. Magnetic field causes a rigid shift towards lower energies of the *n*-type compound's gap. Such behavior contrasts with the case of optimally-doped and over-doped LSCO, in which an applied field induces in-gap states and the gap slowly fills in (Gilardi *et al.*, 2004;

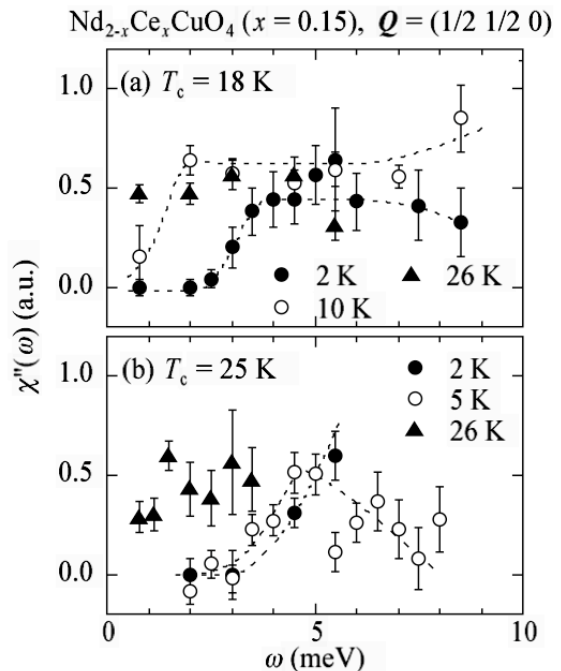


FIG. 39 Energy spectra of $\chi''(\omega)$ of NCCO obtained from the normal and SC phases (a) $x=0.15$, $T_c = 18\text{K}$ (b) $x=0.15$, $T_c = 25\text{K}$. Dotted curves are guides to the eye. From (Yamada *et al.*, 2003).

Lake *et al.*, 2001; Tranquada *et al.*, 2004a)²³.

With regards to a coexistence of antiferromagnetism and superconductivity, Motoyama *et al.* (2007) concluded *via* inelastic scattering that the spin stiffness ρ_s fell to zero at a doping level of approximately $x = 0.13$ (Fig. 40a) in NCCO which is the onset of superconductivity. They concluded that the actual antiferromagnetic phase boundary terminates at $x \approx 0.134(4)$, and that the magnetic Bragg peaks observed at higher Ce concentrations originate from rare portions of the sample which were insufficiently oxygen reduced (Fig. 40b). This issue of the precise extent of antiferromagnetism, the presence of a quantum phase transition, and coexistence regimes will be dealt with in more detail below.

Wilson *et al.* (2006b) reported inelastic neutron scattering measurements on $\text{Pr}_{1.88}\text{LaCe}_{0.12}\text{CuO}_4$ in which they tracked the response from the long-range ordered antiferromagnet into the superconducting sample via oxygen annealing. This is along the δ axis in Fig. 7 (top). As discussed above, in general oxygen annealing creates an RE_2O_3 impurity phase in these systems. An advantage of PLCCO is that its impurity phase has a

²² However other observables showed worse agreement (for instance the ordered moment), pointing to the strong role that dynamics play and that fluctuations manifest themselves differently for different observables.

²³ As discussed below (Sec. III.F.2) Yu *et al.* (2008) have disputed the claim of an approximately 4 meV spin gap and claim that the spectra is better understood as an ≈ 6.4 meV spin gap and an ≈ 4.5 meV resonance. If true, this would necessitate a reinterpretation of some of the results presented above.

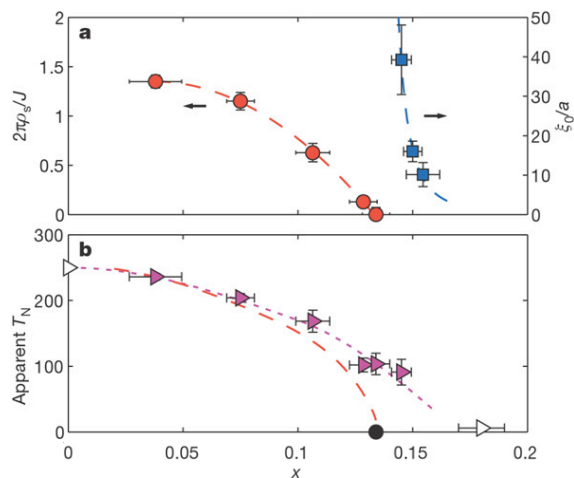


FIG. 40 (Color)(a) Doping dependence of the spin stiffness ρ_s normalized to the AF superexchange ($J = 125$ meV for the undoped Mott insulator Nd_2CuO_4) as $2\pi\rho_s/J$ as well as the low-temperature spin correlation length ξ_0 . The spin stiffness decreases smoothly with doping and reaches zero in an approximately linear fashion around $x_{AF} \approx 0.134$. The ground state for $x < x_{AF}$ has long-range AF order as indicated by the diverging ξ_0 . (b) The apparent Néel temperature T_N , as determined from elastic scattering, as a function of doping given by the dotted curve. The dashed curve is the extrapolated contour of $\xi/a = 400$. Adapted from Motoyama *et al.* (2007).

much weaker magnetic signal due to the small RE magnetic moment. They find that the spin gap of the antiferromagnet (finite in the insulator due to anisotropy) decreases rapidly with decreasing oxygen concentration, eventually resulting in a gapless low energy spectrum in this material. Note that superconducting PLCCO compounds do not exhibit the below T_c spin gap found in NCCO (Yamada *et al.*, 2003)²⁴. The linewidths of the excitations broaden dramatically with doping, and thus the spin-stiffness effectively weakens as the system is tuned toward optimal doping. The low energy response of PLCCO is characterized by two regimes. At higher temperatures and frequencies, the dynamic spin susceptibility $\chi''(\omega, T)$ can be scaled as a function of $\frac{\omega}{T}$ at AF ordering wavevectors. The low energy cut-off of the scaling regime is connected to the onset of AF order. The fact that this energy scale comes down as the antiferromagnetic phase is suppressed leads to an association of this behavior with a QCP near optimal doping.

Fujita *et al.* (2008a) performed an inelastic study on PLCCO over a wide Ce doping range that spanned the antiferromagnetic ($x = 0.07$) to superconducting regimes

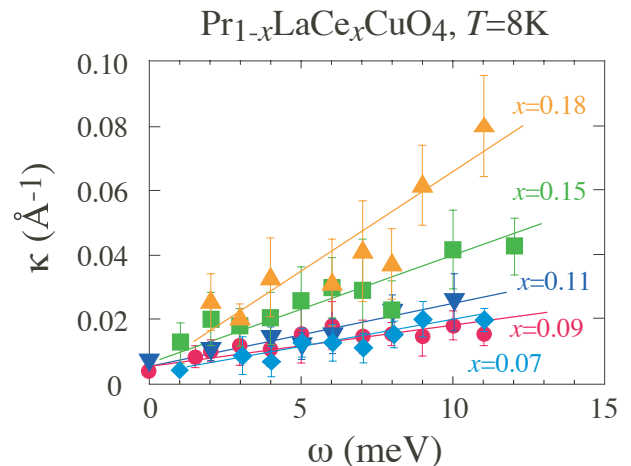


FIG. 41 (Color) ω -dependence of resolution corrected peak-width (half width at half maximum) κ of commensurate peak for $\text{Pr}_{1-x}\text{LaCe}_x\text{CuO}_4$ with $x=0.07, 0.09, 0.11, 0.15$ and 0.18 . From Fujita *et al.* (2008a).

($x = 0.18$). For all concentrations measured, the low energy spectra are commensurate and centered at (π, π) . Although they found a small coexistence regime between superconductivity and antiferromagnetism around $x = 0.11$, some characteristics, such as the relaxation rate and spin-stiffness decreases rapidly when one enters the superconducting phase. The static AF response is absent at $x > 0.13$. The spin stiffness appears to extrapolate to zero around $x = 0.21$ when superconductivity disappears²⁵. This indicates a close relation between spin fluctuations and the superconductivity in the electron-doped system. Interestingly other quantities, like the spectral weight (ω integration of $\chi''(\omega)$) do not show much doping dependence. This is unlike the p -type systems and was associated by these authors with a lack of phase separation in the n -type compounds.

In contrast to the hourglass-type dispersion observed in hole-doped cuprates, the dispersion at higher energies in optimally doped PLCCO $T_c = 21 - 25.5\text{K}$ looks like a more conventional spin wave response centered around the commensurate position, which disperses outward in a ring-like pattern at higher energy transfers (Fujita *et al.*, 2006; Wilson *et al.*, 2006b,c). It can be described in terms of three basic energy regimes (Wilson *et al.*, 2006a). At the lowest energies $\omega < 20$ meV the system shows the essentially over damped spin wave behavior discussed above with a small nearest neighbor spin coupling J_1 of approximately 29 ± 2.5 meV. At intermediate energies $50 \text{ meV} < \omega < 80$ meV the excitations are broad and only weakly dispersing. At energies above 100 meV,

²⁴ We note that a spin gap was not observed in hole-doped LSCO crystals until sample quality improved sufficiently (Yamada *et al.*, 1995). Whether the lack of spin gap in PLCCO is due to the current sample quality of single crystals or is an intrinsic effect is unknown.

²⁵ Here the spin stiffness is defined as $\omega/\Delta q$ where Δq is the momentum width of a peak at a frequency ω , and is given essentially by the slope of the lines in Fig. 41. This is a different definition than that given by Motoyama *et al.* (2007)

the fluctuations are again spin wave like with a J_1 of 162 ± 13 meV. This is substantially larger than the undoped compounds (121 meV for PCO (Bourges *et al.*, 1997) and 104 meV for LCO (Coldea *et al.*, 2001)). A similar situation with a high energy response centered around the commensurate position has also been observed in over-doped PLCCO ($T_c = 16$ K) (Fujita *et al.*, 2008b).

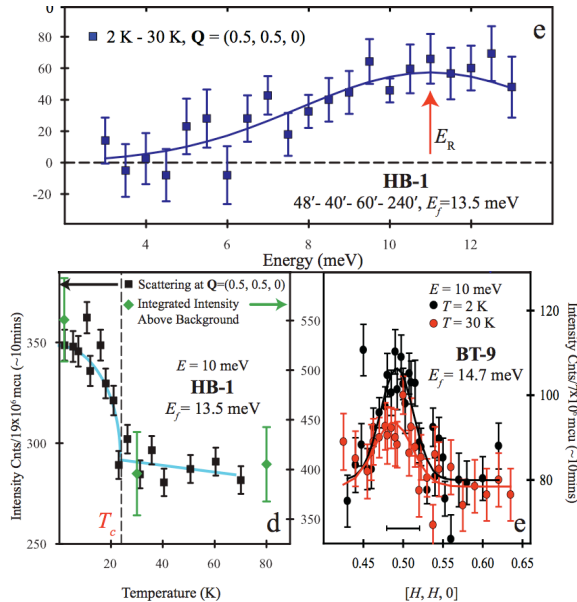


FIG. 42 (Color) (top) Temperature difference spectrum between 2 K and 30 K suggests a resonance-like enhancement at ~ 11 meV. (bottom left) Temperature dependence of the neutron intensity (~ 1 hour/point) at $(1/2, 1/2, 0)$ and 10 meV in black squares. Green diamonds are integrated intensity of the localized signal centered around $Q=(1/2, 1/2, 0)$ above backgrounds. (bottom right) Q -scans at $\omega = 10$ meV above and below the superconducting transitions. From Wilson *et al.* (2006a).

2. The magnetic ‘resonance’

In the superconducting state, Wilson *et al.* (2006a) found an enhancement of peak in the inelastic neutron scattering response of PLCCO (Fig. 42) at approximately 11 meV at $(1/2, 1/2, 0)$ (equivalent to (π, π)). This was interpreted to be the much heralded ‘resonance’ peak (Rossat-Mignod *et al.*, 1991) found in many of the hole-doped cuprates, perhaps indicating that it is an essential part of superconductivity in all these compounds. They find that it has the same $E_r = 5.8k_B T_c$ relationship as other cuprates, but that it does not derive from incommensurate ‘hour-glass’ peaks that merge together as in YBCO and LSCO (Arai *et al.*, 1999; Tranquada *et al.*, 2004b). Instead it appears to rise out of the commensurate $(1/2, 1/2, 0)$ features found in the electron-doped systems (Yamada *et al.*, 1999). The inferred resonance energy also scales with the different T_c ’s for different annealing conditions (Li *et al.*, 2008a). It is important to

note that as mentioned above superconducting PLCCO spectra are essentially gapless below T_c (Yamada *et al.*, 2003) and in fact, except for the resonance, show very little temperature dependence at all below 30 K. Supporting evidence for this feature being ‘the resonance’ comes also from Niestemski *et al.* (2007) who have - as mentioned above - found signatures of a bosonic mode coupling to charge in their STM spectra at $10.5 \text{ meV} \pm 2.5 \text{ meV}$ (Fig. 32) and Schachinger *et al.* (2008) who find a feature in the electron-boson coupling function $I^2\chi(\omega)$ extracted from the optical conductivity at 10 meV. Additionally Wilson *et al.* (2007) have shown that a magnetic field suppresses the superconducting condensation energy and this resonance feature in PLCCO in a remarkably similar way.

In continuing work Zhao *et al.* (2007) have claimed that optimally doped NCCO has a resonance at 9.5 meV, which also obeys the $E_r = 5.8k_B T_c$ relation. However, their assignment of this intensity enhancement has been disputed by Yu *et al.* (2008), who claim that their full ω scans show the spectra are better described by an inhomogeneity broadened spin gap at ≈ 6.4 meV and a sub gap resonance at the much smaller energy of ≈ 4.5 meV as shown in Fig. 43. This scenario has a number of appealing features. Both energy positions show sudden onsets below T_c . Moreover, the spin gap they assign is to within error bars equal to the full electronic gap maximum 2Δ (as measured by techniques like Raman scattering (Qazilbash *et al.*, 2005)), suggesting that - unlike the hole-doped cuprates - the commensurate response allows electronic features to be directly imaged in the magnetic scattering as (π, π) bridges these portions of the FS. Like the hole-doped cuprates the resonance they find is at energies less than the full superconducting gap, which is a reasonable condition for the stability of spin-exciton-like excitations. This interpretation is at odds with the original observation of the spin gap in NCCO by Yamada *et al.* (2003) and as the authors point out necessitates a reinterpretation of that data as well as some of their own previous work. These authors are careful to state that their result does not necessarily invalidate the claim of a resonance peak at the larger energy of 11 meV in PLCCO as the superconducting gap may be much larger in PLCCO (Niestemski *et al.*, 2007) and may allow a stable coherent excitation at this energy. Irrespective of whether it is a ‘resonance’ or not, the below T_c gain in intensity in NCCO at energies above the spin gap is remarkably similar to the behavior found in optimally doped LSCO at incommensurate wavevectors (Christensen *et al.*, 2004; Tranquada *et al.*, 2004b), and suggests that these pile ups of spectral weight in such compounds may have the same microscopic origins.

3. Magnetic field dependence

Recently, the dependence of the ordered spin structure on magnetic field of superconducting samples and the

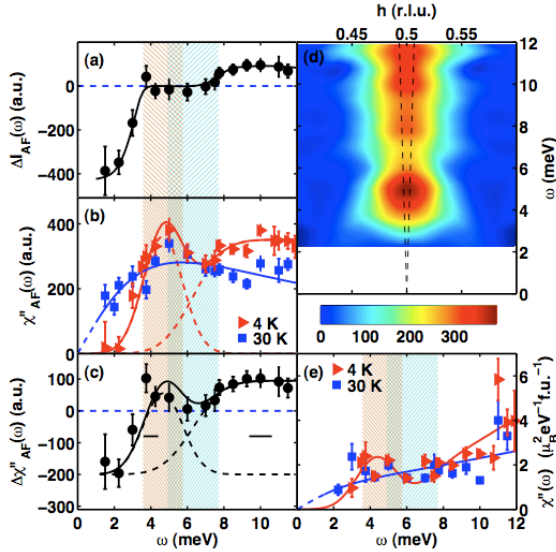


FIG. 43 (a) Change in scattering intensity between 4 K and 30 K at the antiferromagnetic wavevector $(1/2, 1/2, 0)$. (b) Dynamic susceptibility $\chi''(Q, \omega)$ which shows two peaks after correcting the measured intensity for the thermal factor. (c) Relative change from 30 K to 4 K in susceptibility at the AF wavevector. (d) Contour plot of $\chi''(Q, \omega)$ at 4K, made by interpolation of symmetrized momentum scans through the AF zone center with a constant background removed. (e) Local susceptibility in absolute units from the momentum-integral of the dynamic susceptibility by comparing with the measured intensity of acoustic phonons. The shaded vertical bands in (a) - (c) indicates the range of values of $2\Delta_{el}$ from Raman scattering (Qazilbash *et al.*, 2005) corresponding to the author's estimation of the distribution of gap sizes from chemical inhomogeneity. From Yu *et al.* (2008).

possibility of field induced antiferromagnetism has become of intense interest. These studies parallel those on underdoped LSCO, where neutron scattering has shown that a c -axis-aligned magnetic field not only can suppress superconductivity but also creates a static incommensurate spin density wave order, thus implying that such an order directly competes with the superconducting state (Katano *et al.*, 2000; Khaykovich *et al.*, 2002; Lake *et al.*, 2001, 2002). The effect of field on n -type superconducting and reduced samples is a matter of some controversy. While experiments by Matsuda *et al.* (2002) found that a 10-T c -axis-aligned field has no effect on the AF signal in their superconducting NCCO $x=0.14$ samples, Kang *et al.* (2003a) demonstrated in similar $x=0.15$ samples that upon application of a magnetic field antiferromagnetic related Bragg reflections such as $(1/2, 1/2, 0)$ grew in intensity until a field close to the critical field B_{c2} and then decreased. The experiments were interpreted as demonstrating that a quantum phase transition from the superconducting state to an antiferromagnetic state is induced at B_{c2} .

Although their raw data are similar to Kang *et al.* (2003a), this interpretation was disputed by Mang *et al.*

(2003) who found that additional magnetic intensity comes from a secondary phase of $(Nd, Ce)_2O_3$. As noted above, a severe oxygen reduction procedure always has to be applied to as-grown crystals to induce superconductivity. Mang *et al.* (2003) discovered that the reduction process decomposes a small amount of NCCO (0.1 - 1.0 % by volume fraction). The resultant $(Nd, Ce)_2O_3$ secondary phase has a complex cubic bixbyite structure, with a lattice constant approximately $2\sqrt{2}$ times the planar lattice constant of tetragonal NCCO. The $(Nd, Ce)_2O_3$ impurity phase grows in epitaxial register with the host lattice in sheets on average five unit cells thick. Because of the simple $2\sqrt{2}$ relationship between the lattice constants of NCCO and $(Nd, Ce)_2O_3$ the structural reflections of the impurity phase - for instance the cubic $(2, 0, 0)_c$ - can be observed at the commensurate NCCO positions $(1/2, 1/2, 0)$. However the c axis is different and there is approximately a 10% mismatch between $(Nd, Ce)_2O_3$'s lattice constant and a_c of NCCO, and therefore the impurity phase's $(0, 0, 2)_c$ can be indexed as $(0, 0, 2.2)$. Moreover, as shown in Fig. 44 Mang *et al.* (2004a) found that the field effects reported by Kang *et al.* (2003a) are observable in non-superconducting, but still oxygen-reduced, $x=0.10$ samples, both at the previously reported lattice positions and at positions unrelated to NCCO but equivalent in the cubic lattice of $(Nd, Ce)_2O_3$. The incommensurate positions $(0, 0, 2.2)$ and $(1/4, 1/4, 1.1)$ are unrelated to the proposed NCCO magnetic order, and the physical situation of the magnetic field applied parallel (in the cases of the $(0, 0, 2.2)$ and $(1/4, 1/4, 1.1)$) or perpendicular (in the other cases) to the CuO_2 planes should be fundamentally different within the original interpretation in that the upper critical fields for the two directions is significantly different. Mang *et al.* (2004a) interpreted the non-monotonic field dependence of the scattering amplitude as a consequence of the two inequivalent crystalline sites of the Nd atoms in Nd_2O_3 and in accordance with such a model, showed that the intensity scales as a function of B/T as shown in Fig. 44. They concluded that the maximum being found in a field region near B_{c2} was a coincidence.

Dai and coworkers subsequently confirmed the presence of a cubic impurity phase, but feel additional results support their original scenario. Kang *et al.* (2003b); Matsuura *et al.* (2003) pointed out, that while one would expect the field induced intensity of the impurity phase to be the same along all axis directions due to its cubic symmetry, the effect at $(1/2, 1/2, 0)$ is much larger when B is parallel to the c -axis. This is consistent with the much smaller upper critical field along the c -axis. Moreover the $(1/2, 1/2, 3)$ peak has a z index which cannot be contaminated by the impurity phase and yet shows an induced antiferromagnetic component when the field is along the c -axis and hence superconductivity is strongly suppressed, but not when in-plane and superconductivity is only weakly affected. (Matsuura *et al.*, 2003).

Fujita *et al.* (2004) studied similar effects in $Pr_{1-x}LaCe_xCuO_4$ (PLCCO) with $x = 0.11$ ($T_c = 25$

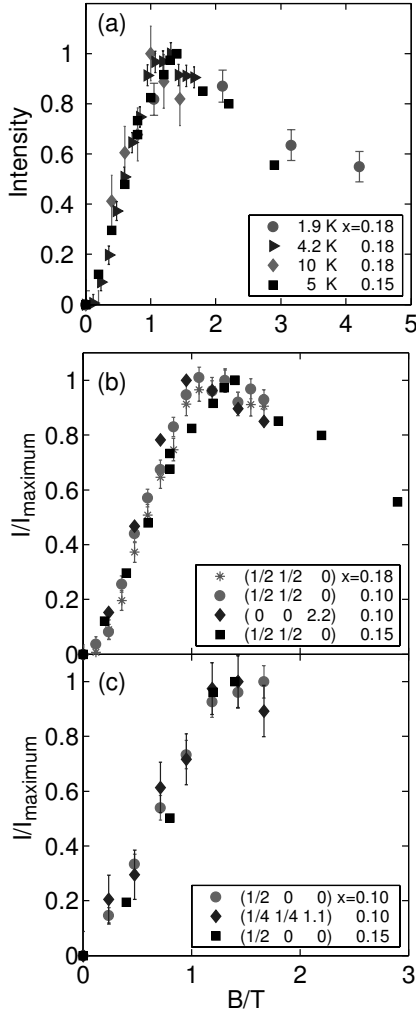


FIG. 44 (a) Scaled scattering intensity at $(1/2, 1/2, 0)$ for a superconducting sample of NCCO ($x = 0.18$; $T_c = 20$ K), plotted as a function of B/T . Field direction is $[0, 0, 1]$. Data is compared with the results at $T = 5$ K of Kang *et al.* (2003a) ($x = 0.15$; $T_c = 25$ K). (b,c) Comparison of Kang *et al.* (2003a)'s data at $T = 4$ K for a superconducting sample ($x = 0.18$) and a non-superconducting sample ($x = 0.10$). The magnetic field direction is in the $[1, 1, 0]$ direction for $(0, 0, 2.2)$ and $(1/4, 1/4, 1.1)$ and along $[0, 0, 1]$ in the other cases. From Mang *et al.* (2004a).

K) and $x = 0.15$ ($T_c = 16$ K). Interestingly, near the AF/SC phase boundary at $x = 0.11$ a commensurate magnetic order develops below approximately T_c at zero field. With application of a c -axis magnetic field the magnetic intensity and the onset temperature of the order increase with the maximum effect observed at 5 T. The effect was much smaller than similar ones in NCCO. In contrast, to both the $x = 0.11$ sample and the measurements on NCCO, in the overdoped $x = 0.15$ sample static AF order is not observed or induced at fields up to 8.5 T.

Kang *et al.* (2005) has confirmed the lack of magnetic order in optimally doped PLCCO (their measurements

at $x = 0.12$), but found different behavior in the ‘underdoped’ regime reached by more aggressive annealing for the $T_c = 21$ K and 16 K PLCCO samples. They find that the $(1/2, 3/2, 0)$ peak that is associated with the unusual non-collinear 3D AF order has no observable field dependence. In contrast to Fujita *et al.* (2004) they found a field dependence only in the $(1/2, 1/2, 0)$ (and related) peaks, that are forbidden in the non-collinear 3D AF order (Sachidanandam *et al.*, 1997; Sumarlin *et al.*, 1995). This was interpreted as a coexistence of 3D AF and quasi-2D SDW orders. Moreover, it was argued that the presence of a field-induced effect at the $(1/2, 1/2, 0)$ SDW position but not at the AF $(1/2, 3/2, 0)$ Bragg position was evidence for phase separation in that the Cu spins contributing to the SDW cannot arise from the same Cu spins which give the 3D (non-collinear) AF moments. Due to much smaller RE moments in PLCCO Kang *et al.* (2005) also argued there is no field effect in the PLCCO impurity phase and therefore there was no possibility of signal contamination from a cubic impurity phase. These observations in PLCCO seem to argue for intrinsic such effects in the n -type cuprates that are associated with the suppression of superconductivity.

The fact that optimally doped SC PLCCO has no static SDW or residual AF order is similar to hole-doped LSCO (Kastner *et al.*, 1998). Still, it is difficult to draw generalized conclusions about the field dependence of the neutron scattering response in the electron-doped cuprates as important differences exist between the measurements of NCCO and PLCCO. Optimally doped PLCCO has no residual AF order while a 3D AF order has been inferred to coexist with superconductivity in NCCO even for optimally doped samples²⁶. Additionally, the magnetic field of its maximum induced intensity is independent of temperature, in contrast to the peak position scaled by H/T in NCCO and in opposition to the impurity model proposed by Mang *et al.* (2003). A c -axis magnetic field enhances not only the scattering signal in optimally doped NCCO at $(1/2, 1/2, 0)$ but also at the 3D AF Bragg positions such as $(1/2, 3/2, 0)$ and $(1/2, 1/2, 3)$, whereas for underdoped PLCCO, there is no observable effect on $(1/2, 3/2, 0)$ (and related) 3D peaks up to 14 T. At this point the effect of magnetic field on the AF state has to be regarded as an open question.

G. Local magnetic probes: μ SR and NMR

Nuclear Magnetic Resonance (NMR) (Asayama *et al.*, 1996) and muon spin resonance and rotation (μ SR) (Luke *et al.*, 1990; Sonier *et al.*, 2000) measurements are sensitive probes of *local* magnetic structure and have been

²⁶ As noted above and discussed more detail below, Motoyama *et al.* (2007) have concluded that true long-range order in NCCO terminates at $x = 0.13$ and that the Bragg peaks seen near optimal doping are due to insufficiently reduced portions of the sample.

used widely in the cuprate superconductors. As mentioned above, using μ SR on polycrystalline samples, Luke *et al.* (1990) first showed that the Mott insulating parent compound Nd_2CuO_4 has a Néel temperature (T_N) of approximately 250K, which decreases gradually upon substitution of Nd by Ce to reach a zero value close to optimal doping ($x \sim 0.15$). Fujita *et al.* (2003) performed a comprehensive μ SR study, which established the phase diagram of PLCCO. They found bulk superconductivity from $x = 0.09$ to 0.2 and only a weak dependence of T_c on x for much of that range. The antiferromagnetic state was found to terminate right at the edge of the superconducting region, which was interpreted as a competitive relationship between the two phases. Only a very narrow coexistence regime was observed (≈ 0.01 wide). Although changes in the form of the muon relaxation were observed below a temperature T_{N1} where elastic neutron Bragg peaks have been observed (Fujita *et al.*, 2003), there was no evidence for a static internal field until a lower temperature T_{N2} . At the lowest temperatures, it was found that the magnitude of the internal field decreased upon electron doping, showing a continuous and apparently spatially uniform degradation of magnetism. This is in contrast to the hole-doped system where in the Néel state ($x < 0.02$) the internal field was constant (Borsa *et al.*, 1995; Harshman *et al.*, 1988), which has been taken as evidence for phase separation (Chou *et al.*, 1993; Matsuda *et al.*, 2002).

A homogeneous state was also consistent with the measurements of Williams *et al.* (2005) who found no indication of the Cu NMR “wipe out” effect in $x=0.15$ PCCO that has been taken to be a sign of spatial inhomogeneity in $\text{La}_{2-x}\text{Sr}_x\text{CuO}_4$ (Singer *et al.*, 1999). However, in $\text{Pr}_{1.85}\text{Ce}_{0.15}\text{CuO}_4$ Zamborszky *et al.* (2004) found that the spin-echo decay rate ($1/T_2$) of their Cu NMR signal showed a substantial dependence on the radio frequency pulse parameters below 25 K. This was interpreted as being consistent with static inhomogeneous electronic structure that couples to the rf field of the pulse. Similarly, Bakharev *et al.* (2004) found via Cu NMR evidence for an inhomogeneous “blob-phase” in carefully reoxygenated superconducting $\text{Nd}_{1.85}\text{Ce}_{0.15}\text{CuO}_4$. They found that for a narrow region of oxygen levels just above the suppression of superconductivity there was evidence for an inhomogeneous charge distribution. It was also suggested that superconductivity competes with the antiferromagnetic state.

Zheng *et al.* (2003) showed that when the superconducting state was suppressed in $x = 0.11$ PLCCO with a large out-of-plane magnetic field the NMR spin relaxation rate obeyed the Fermi-liquid Korringa law $1/T_1 \propto T$ over 2 decades in temperature. This result is at odds with the inferred non-Fermi liquid nature of PCCO’s field induced normal state from a violation of the Wiedemann-Franz law (Hill *et al.*, 2001). We discuss this result in more detail below (Sec. IV.F). Zheng *et al.* (2003) also found no sign of a spin pseudogap opening up at temperatures much larger than T_c , which is a hallmark of NMR

in the underdoped p -type cuprates. Here they found that above the superconducting T_c $1/T_1T$ showed only a weak increase, consistent with the development of antiferromagnetic correlation.

Related to the neutron scattering studies in field detailed above, under a weak perpendicular field Sonier *et al.* (2003) observed via μ SR the onset of a substantial magnetic order signal (Knight shift) which was static on the μ SR time scales in the superconducting state of optimally doped PCCO single crystals. The data was consistent with moments as large as 0.4μ being induced by fields as small as 90 Oe. There was evidence that the antiferromagnetism was not confined to the vortex cores, since nearly all the muons saw an increase in the internal field and the vortex density was so low and so again the magnetism looked uniform. It has been argued however that this study overestimated the induced Cu moments by not explicitly taking into account the superexchange coupling between Pr and Cu ions as well as an unconventional hyperfine interaction between the Pr ions and the muons (Kadono *et al.*, 2004b, 2005). Kadono *et al.* (2004b, 2005) have interpreted their measurements as then consistent with only a weak field induced Cu magnetism in $x = 0.11$ PLCCO (near the AF boundary of $x \approx 0.10$) which becomes even smaller at $x = 0.15$. Overall μ SR results in the field applied state of the electron-doped cuprates appear to show substantial differences from the p -type compounds. At the onset of superconductivity, there is a well-defined Knight shift whereas in the hole-doped materials, superconductivity under applied field only evinces from an enhancement in the spin relaxation rate (Kakuyanagi *et al.*, 2002; Mitrovic *et al.*, 2001; Savici *et al.*, 2005) or changes in the field profile of the vortex cores (Kadono *et al.*, 2004a; Miller *et al.*, 2002). This again indicates that the induced polarization of Cu ions in the electron-doped compounds appears to be relatively uniform over the sample volume, whereas it appears to be more localized to the vortex cores in the hole-doped materials.

IV. DISCUSSION

A. Symmetry of the superconducting order parameter

There is a consensus picture emerging of the order parameter symmetry for the n -type cuprates. The original generation of measurements on polycrystals, single crystals and thin films seemed to favor s-wave symmetry of the order parameter, but experiments on improved samples including tricrystal measurements (Tsuei and Kirtley, 2000b), penetration depth (Côté *et al.*, 2008; Kokales *et al.*, 2000; Prozorov *et al.*, 2000), ARPES (Armitage *et al.*, 2001a; Matsui *et al.*, 2005a; Sato *et al.*, 2001), and others favor a d-wave symmetry over most of the phase diagram. However, several experimental results can be interpreted as a sign for a possible crossover from a pure d-wave symmetry at low doping to a superimposed sub-

dominant order parameter at higher doping levels (Biswas *et al.*, 2002; Skinta *et al.*, 2002). This is a subject that deserves a comprehensive review, which sorts through the multitude of experiments to present the current picture. We give only a comparatively brief overview here.

In order to identify the mechanism of superconductivity in cuprates and other correlated superconductors, many experimental techniques have been designed to probe the Cooper pair wave-function symmetry (i.e. the order parameter $\psi(\vec{k})$ or the gap function $\Delta(\vec{k})$). In the case of the hole-doped cuprates, most of the convincing experiments demonstrate that the pairing symmetry is of dominant $d_{x^2-y^2}$ - wave character (Campuzano *et al.*, 2004; Damascelli *et al.*, 2003; Deutscher, 2005; van Harlingen, 1995; Tsuei and Kirtley, 2000a). In general, experiments are sensitive either to the presence of a zero gap value for some specific \vec{k} directions, to the related issue of the magnitude of the superconducting gap $|\Delta(\vec{k})|$, or to the phase of the pair wave-function. In the first case, the experiments probe the low energy density of states, which goes linearly in energy for a d -wave superconductor. Such experiments demonstrate the presence of zeros (lines or points of nodes) in $\Delta(\vec{k})$. In the last case, the experiments are sensitive to changes in sign in momentum space of the phase of the order parameter $\Delta(\vec{k})$ (Sigrist and Rice, 1995).

As mentioned, most experiments now seem to indicate an order parameter of a $d_{x^2-y^2}$ form in the electron-doped cuprates, albeit with an interesting non-monotonic functional form. Below, we give an overview of the main results of their order parameter and discuss similarities and differences with respect to the hole-doped cuprates

1. Penetration depth

In the mid 90's, penetration depth λ measurements on high quality $\text{YBa}_2\text{Cu}_3\text{O}_7$ single crystals gave some of the first clear signatures for an anomalous order parameter in the cuprates. The linear temperature dependence of $\Delta\lambda(T)$ (related to the superfluid density) was a clear demonstration that the density of states of this material was linear for sub-gap energies ($E < 20$ meV), in agreement with the behavior expected from a d -wave symmetry of the order parameter with line nodes (Hardy *et al.*, 1993).

Early $\Delta\lambda(T)$ data obtained on single crystals and thin films of optimally doped NCCO showed no such temperature dependence (Andreone *et al.*, 1994; Anlage *et al.*, 1994; Schneider *et al.*, 1994; Wu *et al.*, 1993), not even the expected dirty d -wave behavior characterized by a $\Delta\lambda \propto T^2$ dependence at low temperature (Hirschfeld and Goldenfeld, 1993) seen for example in thin films of $\text{YBa}_2\text{Cu}_3\text{O}_7$ (Ma *et al.*, 1993). The NCCO data was best fit to a BCS s -wave-like temperature dependence down to $T/T_c \sim 0.1$ with unusually small values of $2\Delta_o/k_B T_c \sim 1.5 - 2.5$ (Andreone *et al.*, 1994; Anlage *et al.*, 1994; Schneider *et al.*, 1994; Wu *et al.*, 1993).

Later, Cooper proposed that the intrinsic temperature dependence of the superfluid density measured with these particular techniques had been masked by the strong Nd magnetic response (see Section II.F) at low T (Cooper, 1996). Using the data of Wu *et al.* (1993) and correcting for the contribution of the low temperature magnetic permeability $\mu_{DC}(T)$ in NCCO (Dalichaouch *et al.*, 1993), he reached the conclusion that the real temperature dependence of $\Delta\lambda(T)$ could be close to T^2 at low temperature.

To circumvent the inherent magnetism of Nd ions in NCCO, slightly different experimental probes were used by Kokales *et al.* (2000) and Prozorov *et al.* (2000) to evaluate $\Delta\lambda(T)$ in $\text{Pr}_{1.85}\text{Ce}_{0.15}\text{CuO}_4$ single crystals which has a much weaker RE magnetism. As shown in Fig. 45, both experiments showed for the first time that $\Delta\lambda(T)$ follows a $\sim T^2$ behavior at low temperatures in PCCO, in agreement with the dirty d -wave scenario. Moreover, by extending the temperature range of the measurements for NCCO, they showed the presence of an upturn in the magnetic response due to Nd residual magnetism, confirming Cooper's interpretation.

More recent reports targeting in particular the doping dependence of the normalized superfluid density give a still controversial picture on thin films. Skinta *et al.* (2002) observed that the exact temperature dependence of $\Delta\lambda(T)$ evolves with increasing cerium doping. Using PCCO and LCCO thin films grown by Molecular Beam Epitaxy (MBE) (Naito *et al.*, 2002), the low temperature data present the gradual development of a gapped-like behavior for increasing doping (Skinta *et al.*, 2002) observed as a flattening of $\Delta\lambda(T)$ at low temperature. The growth of this T-independent s -wave-like behavior was interpreted as a possible signature of a transition from a pure d -wave symmetry on the underdoped regime to a d - and s -wave admixture on the overdoped regime. A similar trend was also deduced by Pronin *et al.* (2003) from a quasioptical transmission measurement of $\Delta\lambda(T)$ at millimeter wavelengths (far-infrared). Another report (Kim *et al.*, 2003) on MBE-grown buffered PCCO thin films from under- to overdoping range claimed that $\lambda(T)$ can only be explained with a fully gapped density of states with a $d + is$ -wave admixture for all doping. In contrast, Snezhko *et al.* (2004) showed that the T^2 behavior of thin films grown by pulsed-laser ablation deposition (PLD) is preserved even in the overdoped regime. These very conflicting results have yet to be explained, but the answers may lie partly in the different growth techniques, the quality of films, the presence of parasitic phases (Section II.E) and the differences in the experimental probes. It has been proposed that the presence of electron and hole Fermi surface pockets, as observed by ARPES (Section III.C) and confirmed by electrical transport (Section III.A.1), could result in an s -wave-like contribution despite that the dominant pairing channel has a $d_{x^2-y^2}$ symmetry (Luo and Xiang, 2005). The variability between different kinds of samples may reflect the influence of different oxygen content on the presence and

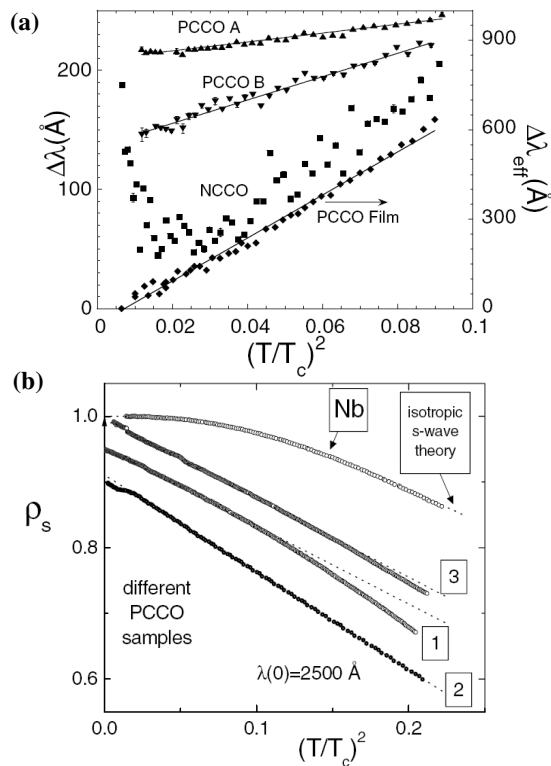


FIG. 45 Penetration depth measurements $\Delta\lambda$ as a function of $(T/T_c)^2$ using different techniques for optimally doped $\text{Pr}_{2-x}\text{Ce}_x\text{CuO}_4$ and $\text{Nd}_{2-x}\text{Ce}_x\text{CuO}_4$ single crystals and thin films presenting a broad range of behavior. (a) Microwave cavity data showing a power-law dependence for PCCO and an upturn for NCCO. From Kokales *et al.* (2000). (b) Tunnel-diode driven LC resonator data for three different PCCO single crystals showing power law behavior. From Prozorov *et al.* (2000).

the contribution of these pockets (arcs) as shown recently by ARPES (Richard *et al.*, 2007).

As a possible demonstration of material-related issues, Côté *et al.* (2008) recently compared the penetration depth measurements by the microwave perturbation technique of optimally doped PCCO thin films grown by PLD with very similar T_c 's but with different quality as characterized by their different normal-state resistivity close to T_c . They found that lower quality films shows a flat $\lambda_1(T)$ at low temperature, showing that oxygen reduction and the presence of defects may be of crucial importance in determining the actual symmetry using penetration depth measurements.

Another avenue for the estimation of the temperature dependence of the penetration depth relies on the properties of grain boundary junctions (GBJ) made on SrTiO_3 bicrystal substrates (Hilgenkamp and Mannhart, 2002). Using the maximum critical current density J_c of small Josephson junctions, Alff *et al.* (1999) estimated $\Delta\lambda_{ab}/\lambda_{ab}$ as a function of temperature for both NCCO

and PCCO GBJ's using thin films made by MBE. This scheme assumes that $J_c \propto n_s$, thus $\lambda_{ab} \propto 1/\sqrt{n_s} \propto 1/\sqrt{J_c}$. The striking aspect of this data is the upturn of the estimated effective λ_{ab} for NCCO due to Nd magnetism. Using the same correction scheme as that proposed by Cooper (1996), the NCCO data could be superimposed on top of the PCCO GBJ data (Alff *et al.*, 1999). However, it was concluded that the penetration depth followed an s-wave-like exponential temperature dependence with $2\Delta_o/k_B T_c \sim 3$, in agreement with the initial penetration depth measurements and indicating a nodeless gap. This result together with the unresolved doping dependence controversy mentioned above may result from the different sample preparations leading to many superimposed extrinsic contributions.

2. Tunnelling spectroscopy

There are two main signatures in tunnelling spectroscopy that can reveal the presence of d-wave symmetry. The first is related to their 'V-shaped' density of states. Unlike the conductance characteristic observed for tunnelling between a metal and a conventional s-wave superconductor at $T = 0$, which shows zero conductance until a threshold voltage $V = \Delta_o/e$ is reached (Tinkham, 1996), tunnelling into d-wave superconductors reveals substantial conductance at sub-gap energies even at $T \rightarrow 0$. The second signature, a zero-bias conductance peak (ZBCP), reveals the presence of an Andreev quasiparticle bound state (ABS) at the interface of a d-wave superconductor arising from the phase change of the order parameter as a function of angle in \vec{k} -space (Deutscher, 2005; Hu, 1994; Kashiwaya *et al.*, 1995; Lofwander *et al.*, 2001). This bound state occurs for all interface orientations with projection on the (110) direction. The ZBCP can also split under an increasing magnetic field (Beck *et al.*, 2004; Deutscher, 2005) and, in some instances, it is reported to even show splitting at zero magnetic field in the holed doped cuprates (Covington *et al.*, 1997; Deutscher, 2005; Fogelström *et al.*, 1997).

As discussed above, tunnelling experiments on n-doped cuprates have been particularly difficult, which is presumably related to difficulties in preparing high quality tunnel junctions. See Sec. III.B for more details. Typical quasi-particle conductance $G(V) = dI/dV$ spectra on optimal-doped NCCO (Shan *et al.*, 2005) are shown in Figure 31. Similar spectra are found for Pb/I/PCCO (where I is a natural barrier) (Dagan *et al.*, 2005b), and GB junctions (Alff *et al.*, 1998a; Chesca *et al.*, 2005). The main features of the n-doped tunnel spectra are: prominent coherence peaks which reveal an energy gap of order 4 meV at 1.8K for optimal doping, an asymmetric linear background $G(V)$ for voltage well above the energy gap, a characteristic 'V' shape, coherence peaks which disappear completely by $T \approx T_c$ at $H=0$ (and by $H \approx H_{c2}$ for $T=1.8\text{K}$), and typically the absence of a zero bias

conductance peak (ZBCP) at $V=0$.

Tunneling has given conflicting views of the pairing symmetry in n-doped cuprates. The characteristic 'V' shape of $G(V)$ cannot be fit by an isotropic s-wave BCS behavior and closely resembles that of d-wave hole-doped cuprates (Fischer *et al.*, 2007). On the other hand the ZBCP has been observed only sporadically (Biswas *et al.*, 2002; Chesca *et al.*, 2005; Qazilbash *et al.*, 2003; Wagenknecht *et al.*, 2008). Its absence in most spectra of tunnel junctions with large barriers may be the consequence of the coherence length ($\sim 50\text{\AA}$) being comparable to the mean free path (Biswas *et al.*, 2002) similar to the effect observed in YBCO (Aprili *et al.*, 1998). Its absence has also been attributed to the coexistence of AFM and SC orders (Liu and Wu, 2007).

Point contact spectroscopy data have shown a ZBCP in underdoped ($x = 0.13$) PCCO films, while it is absent for optimal and overdoped compositions (Biswas *et al.*, 2002; Qazilbash *et al.*, 2003). Combined with an analysis of the $G(V)$ data based on Blonder-Tinkham-Klapwijk theory (Blonder *et al.*, 1982; Tanaka and Kashiwaya, 1995), this result has been interpreted as a signature of a d- to s-wave symmetry transition with increasing doping. However, there has been a more recent claim that all such tunneling spectra are better fit with a non-monotonic d-wave functional form (Dagan and Greene, 2007) over the entire doping range of superconductivity. This may explain in part the many reports claiming that the tunnelling spectra from several experimental configurations can not be fit with either pure d-wave or s-wave gaps [see for example Alff *et al.* (1998b); Kashiwaya *et al.* (1998); Shan *et al.* (2005)]. The SIS planar tunnelling work of Dagan and Greene (2007) and a detailed point contact tunnelling study as a function of doping of Shan *et al.* (2008a) also provide strong evidence that the n-doped cuprates are weak coupling, d-wave BCS superconductor over the whole phase diagram. This is in agreement with other techniques including Raman scattering (Qazilbash *et al.*, 2005).

As discussed above (Sec. III.B) Niestemski *et al.* (2007) recently reported the first reproducible high resolution STM measurements of PLCCO ($T_c = 24$ K) (Fig. 32). Previous STM measurements on NCCO revealed gaps on the order 3.5 to 5 meV, but no obvious coherence peaks (Kashiwaya *et al.*, 1998). The linecut (Fig. 32a) shows spectra that vary from ones with sharp coherence peaks to a few with more pseudogap-like features and no coherence peaks. However almost all spectra show the very notable 'V' shaped higher energy background, which is consistent with d-wave symmetry.

Chesca *et al.* (2005) used a bicrystal GBJ with optimal doped LCCO films (a SIS junction) and measured both Josephson tunnelling and quasiparticle tunnelling below $T_c \sim 29$ K. A ZBCP was clearly seen in their quasiparticle tunnelling spectrum and it has the magnetic field and temperature dependence expected for a d-wave symmetry, ABS-induced, zero energy peak. These authors argue that it requires extremely high-quality GB junctions— to

reduce disorder at the barrier and to have a large enough critical current— in order to observe the ZBCP. Given the sporadic observations of a ZBCP in n-doped cuprates [Shan *et al.* (2005) and references therein], the authors suggest that perhaps the observation of a ZBCP rather than its absence should be regarded as a true test of the pairing symmetry. There has also been the recent claim that residual antiferromagnetic order can destroy the ZBCP in even pure d-wave superconductors (Liu and Wu, 2007).

Finally, similar GB junctions of LCCO have also revealed an intriguing behavior with the observation of a ZBCP for magnetic field much larger than the usual upper critical field measured on the same film using in-plane resistivity (Wagenknecht *et al.*, 2008). With increasing temperature T , they find that the ZBCP vanishes at the critical temperature $T_c = 29$ K if $B = 0$, and at $T = 12$ K for $B = 16$ T. These observations may suggest that the real upper critical field is larger than the one inferred from transport. They estimate $H_{c2} \approx 25$ T. However, this is in complete disagreement with the bulk upper critical field that has been estimated to remain below 10T at 2K for all doping using specific heat (Balci and Greene, 2004) and the Nernst effect (Balci *et al.*, 2003; Li and Greene, 2007).

3. Low-energy spectroscopy using Raman scattering

Raman scattering is sensitive to the symmetry of the superconducting gap, as particular polarization configurations probe specific regions of momentum space. It is possible to isolate signatures related to the superconducting gap, and in particular demonstrate anisotropy and zeros in the gap function (Devereaux *et al.*, 1994; Devereaux and Hackl, 2007). As observed in hole-doped cuprates (Stadlober *et al.*, 1995), peaks related to the magnitude of the gap are extracted in two specific polarization configurations, B_{1g} and B_{2g} . With a d-wave gap anisotropy, these peaks are expected to be found at different frequencies in different polarizations. Moreover, the presence of low-energy excitations below the maximum gap value (down to zero energy in the case of lines of nodes for d-wave symmetry) implies that the Raman response follows very specific power law frequency dependencies for these various polarizations (Devereaux *et al.*, 1994; Devereaux and Hackl, 2007). In the original Raman work on NCCO's order parameter, Stadlober *et al.* (1995) showed that the peaks in the B_{1g} and B_{2g} channels (Fig. 46) were positioned at close to the same energy, much like older works on s-wave classical superconductors like Nb_3Sn (Dierker *et al.*, 1983).

However, more recent experiments on single crystals and thin films reveal a more complicated picture. The low-frequency behavior of the B_{1g} and B_{2g} channels approach power laws consistent with the presence of lines of nodes in the gap function (Kendziora *et al.*, 2001). These power laws, although not perfect, indicate the presence

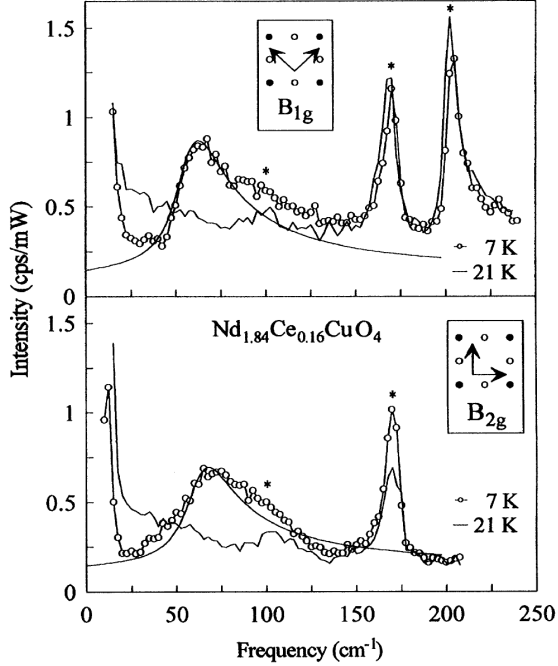


FIG. 46 Electronic Raman scattering results comparing the response above (21K) and below (7K) the critical temperature in the B_{1g} (top panel) and the B_{2g} (bottom panel) configurations. The additional lines are fits using a slightly anisotropic s-wave gap. From Stadlober *et al.* (1995).

of low energy excitations. Moreover, in some instances, the peak energy values in the B_{1g} and B_{2g} channels can be different (Kendziora *et al.*, 2001), and in some others, they are virtually identical (Blumberg *et al.*, 2002; Qazilbash *et al.*, 2005). In all these recent data however, the low energy spectrum continues to follow the expected power laws for lines of nodes. To reconcile the fact that these power laws are always observed and that some samples present peaks at identical energies in both channels, Blumberg *et al.* (2002) first proposed that a non-monotonic d-wave gap function could explain this anomalous response (Blumberg *et al.*, 2002; Qazilbash *et al.*, 2005). In Fig. 47, we show a representative dataset in the B_{1g} , B_{2g} and A_{1g} channels, together with the non-monotonic gap function proposed by Blumberg *et al.* (2002). In this picture, the maximum value of the gap function ($\Delta_{max} \sim 4$ meV) coincides with the ‘hot spots’ on the Fermi surface (HS in Fig. 47), namely the position in \vec{k} -space where the Fermi surface crosses the antiferromagnetic Brillouin zone (AFBZ) as found by Armitage *et al.* (2001b). At the zone boundary (ZB in Fig. 47), the gap value drops to ~ 3 meV²⁷.

²⁷ It has been argued recently that the non-monotonic gap pro-

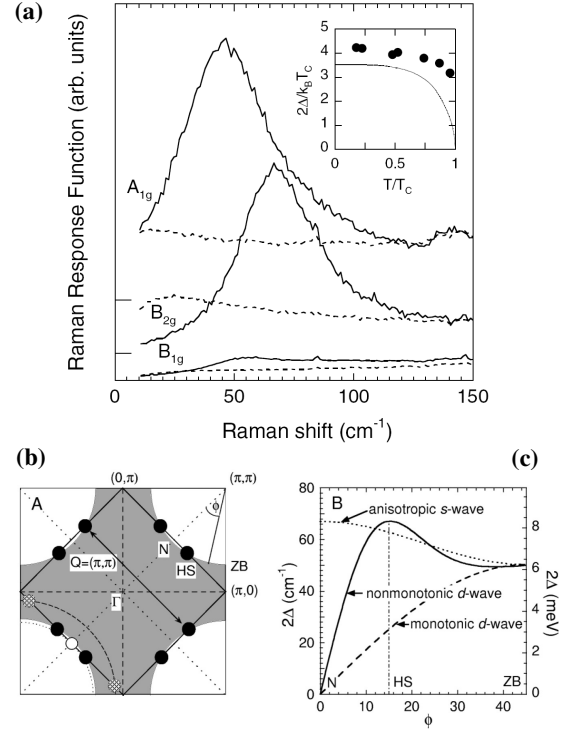


FIG. 47 (a) Electronic Raman scattering results comparing the response above (35K - dashed line) and below (11K - solid line) the critical temperature in the B_{1g} , the B_{2g} and the A_{1g} configurations; (b) a sketch of the position of the hot spots (HS) on the Fermi surface where the gap maximum also occurs; (c) a comparison of the angular dependence of the non-monotonic d-wave gap (solid line) with monotonic d-wave (dashed line) and anisotropic s-wave gap (dotted line). From Blumberg *et al.* (2002).

However, Venturini *et al.* (2003) countered that the basis for the conclusion of Blumberg *et al.* (2002) was insufficient and so an s-wave form can still not be ruled out. They argued that since the Raman scattering amplitudes are finite at the maximum of the proposed gap function for all symmetries, the spectra in all these symmetries should exhibit multiple structures at the same energies in the limit of low damping as opposed to simply different size gaps in the different geometries (i.e. peaks should appear for energies corresponding to $\partial\Delta/\partial\phi = 0$). They also claim that if the damping rate is increased high enough to wash out this fine structure then the low frequency power laws which have been taken to be evidence for d-wave nodes are also suppressed. Blumberg *et al.* (2003) stand by their original interpretation and replied that no sharp threshold gap structures had ever been observed in any electron-doped cuprates even at the lowest

posed by Blumberg *et al.* (2002) and others is not purely the superconducting one, but in fact reflects a coexistence of antiferromagnetic and superconducting orders (Yuan *et al.*, 2006a)

temperature and frequencies and therefore irrespective of any other arguments an s wave symmetry can be definitively ruled out. Moreover, they claim that the damping functions used by Venturini *et al.* (2003) are unphysical and detailed agreement with measured spectra and calculation is only expected if realistic Fermi surface topologies, energy and momentum-dependent relaxational behavior, possible impurity scattering rates and inhomogeneous broadening are included.

A very detailed study on single crystals and thin films has been reported recently by Qazilbash *et al.* (2005) who followed the doping dependence of PCCO and NCCO's Raman response. The authors extracted the magnitude of the gap as a function of doping and concluded that the smooth continuous decrease of the Raman response below the gap signatures (coherence peaks) is a sign that the superconducting gap preserves its lines of nodes throughout the whole doping range from under- to overdoping. Obviously, this non-monotonic d-wave gap function should have a definite impact on properties sensitive to the low energy spectrum.

4. ARPES

ARPES provided some of the first dramatic evidence for an anisotropic superconducting gap in the hole-doped cuprates (Shen *et al.*, 1993). Comparing the photoemission response close to the Fermi energy on the same sample for temperatures above and below T_c , one can clearly distinguish a shift of the intensity in the spectral function for momentum regions near $(\pi, 0)$. This "leading-edge" shift gets its origin from the opening of the superconducting gap and one can then map it as a function of \vec{k} on the Fermi surface in the Brillouin zone (BZ). In the case of hole-doped cuprates, the first $\Delta(\vec{k})$ mapping was obtained with $\text{Bi}_2\text{Sr}_2\text{CaCu}_2\text{O}_{8+\delta}$ (Shen *et al.*, 1993), which is easily cleaved due to its weakly coupled Bi-O planes. Gap values consistent with zero were observed along the diagonal directions in the BZ, i.e. along the $(0,0)$ to (π,π) line (Ding *et al.*, 1996). Away from the zone diagonal, the magnitude of the gap tracks the \vec{k} -dependence of the monotonic d-wave functional form.

Until modern advances in the technology, the smaller energy gap of the electron-doped cuprates, on the order of 5 meV for optimal doping, was at the limit of ARPES resolution. The first reports of a measured superconducting gap in NCCO were presented by Armitage *et al.* (2001a) and reported independently by Sato *et al.* (2001) and are shown in Fig. 48. They found an gap anisotropy with a negligible gap value along the zone diagonal directions and a leading-edge shift of ~ 2 -3 meV along the Cu-O bond directions (Armitage *et al.*, 2001a; Sato *et al.*, 2001). Such behavior was consistent with an order parameter of d-wave symmetry. Using a model taking into account thermal broadening and the finite energy resolution, Sato *et al.* estimated the maximum gap value to be on the order of 4 to 5 meV, in close agreement with the

values observed by tunnelling (see Section IV.A.2) and Raman Sec. IV.A.3.

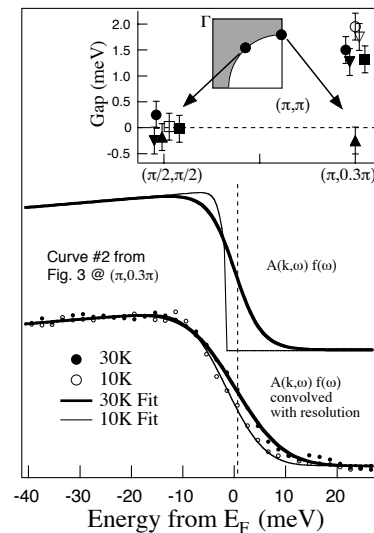


FIG. 48 Bottom curves are near E_F ARPES EDCs of optimally doped NCCO from \vec{k}_F close to $(\pi, 0.3\pi)$. Open and solid circles are the experimental data at 10 and 30K respectively, while solid lines are fits. Upper curves are the experimental fits without resolution convolution. "Curve #2 from Fig. 3" refers to figures in Armitage *et al.* (2001a). Upper panel: Gap values extracted from fits at the two \vec{k} -space positions using the difference between the 10 and 30K data. Different symbols are for different samples. From Armitage *et al.* (2001a).

In these early studies, the limited number of momentum space positions measured could not give the explicit shape of the gap function. Matsui *et al.* followed a few years later with more comprehensive results on $\text{Pr}_{0.89}\text{LaCe}_{0.11}\text{CuO}_4$ (PLCCO) that mapped out the explicit momentum dependence of the superconducting gap. Their data shown in Fig. 49 confirm the presence of a very anisotropic gap function with zeros along the diagonal directions (Matsui *et al.*, 2005b) as in BSCCO. They also concluded that the gap function is non-monotonic as found by Blumberg *et al.* (2002) *via* Raman, with the maximum gap value coinciding with the position of the hot spots in the BZ. Matsui *et al.* fit their data with the function: $\Delta = \Delta_o[1.43 \cos 2\phi - 0.43 \cos 6\phi]$, with $\Delta_o = 1.9$ meV. Intriguingly, the maximum value of the gap extracted from the ARPES data ($\Delta_{max} \sim 2.5$ meV) seems to fall short from the values obtained from other experiments, in particular in comparison to the data of Blumberg *et al.* in Fig. 47, but also tunnelling data giving a maximum gap value of 4 meV for optimal doping (see Section IV.A.2). Perhaps the different materials used for the separate experiments (namely NCCO vs PLCCO) present slightly different properties. In fact, it remains unclear to which extent the reduction process giving superconductivity really leads to similar materials (taking into account their different cerium content), and to some

extent, if band filling (controlled by doping) is actually the same. These issues will have to be addressed seriously to get a clear picture of the origin of the non-monotonic gap and its link to the hot spots on the Fermi surface. Again, the possibility exists that the non-monotonic gap reflects a superposition of superconducting and antiferromagnetic order parameter gaps (Yuan *et al.*, 2006a).

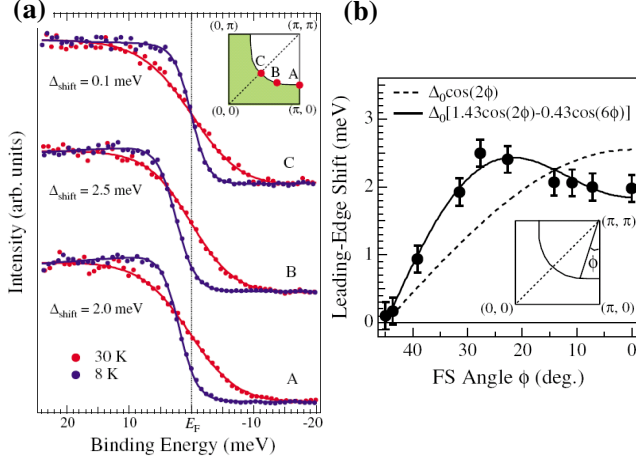


FIG. 49 (a) EDCs from ARPES measurements for temperatures above (30K : red) and below (8K : blue) the transition temperature for $\text{Pr}_{0.89}\text{LaCe}_{0.11}\text{CuO}_4$ single crystals at three distinct points in k-space on the Fermi surface; (b) Leading-edge shift determined as a function of position (angle) on the Fermi surface showing that it fits a non-monotonic d-wave symmetry. From Matsui *et al.* (2005b).

5. Specific Heat

Specific heat measurements probe the low energy excitations of the bulk and are not sensitive to surface quality. Its temperature and field dependencies away from T_c and H_{c2} in hole-doped cuprates are sensitive to the energy dependence of the density of states below the gap energy. The specific heat for a pure d-wave superconductor with line nodes and a linear density of states should have an electronic contribution given by $c_{el}(T) = \gamma_n T^2 / T_c$ where $\gamma_n T$ is the expected normal state electronic contribution to the specific heat (Scalapino, 1995; Volovik, 1993). In the presence of a magnetic field at fixed temperature, this electronic contribution should grow as $c_{el}(H) \propto \sqrt{H}$. This is the so-called ‘Volovik effect’ (Volovik, 1993) for a clean d-wave superconductor. Moler *et al.* showed that the electronic specific heat of YBCO, has the expected square root dependence on magnetic field, although the temperature dependence exhibited a non-zero *linear* (not T^2) term down to zero temperature (Moler94a, Moler97a). This is consistent with various ‘dirty d-wave’ scenarios however.

For the electron-doped cuprates, extracting similar information about the electronic contribution to the specific heat is challenging because of its relatively small magnitude with respect to the phonon contribution (Marcenat *et al.*, 1993, 1994), the magnitude of T_c and the relatively small value for $H_{c2} \sim 10T$ [see Refs. (Balci *et al.*, 2003; Fournier and Greene, 2003; Qazilbash *et al.*, 2005) and references therein]. Moreover, rare-earth magnetism gives rise to additional anomalies at low temperature that makes it difficult to extract the electronic contribution. For example, superconducting SCCO specific heat data is completely dominated by the Néel transition of the Sm moment sublattice (Dalichaouch *et al.*, 1993; Hundley *et al.*, 1989) at low T. To a lesser extent, a similar situation occurs in NCCO (Dalichaouch *et al.*, 1993). For this reason, most recent studies of the electronic specific heat to unravel the symmetry of the gap have been performed with PCCO single crystals (Balci and Greene, 2004; Balci *et al.*, 2002; Yu *et al.*, 2005) with its weaker RE magnetism (Sect. II.F). The most recent results demonstrate that the field dependence follows very closely the expected $\gamma(H) \propto \sqrt{H}$ for all superconducting dopant concentrations (Balci and Greene, 2004; Balci *et al.*, 2002; Yu *et al.*, 2005).

The initial measurements on optimally doped PCCO ($x = 0.15$) showed a large non-zero linear in temperature electronic contribution down to the lowest temperature ($T/T_c \sim 0.1$) very similar to YBCO (Moler *et al.*, 1994, 1997). Furthermore, it presented a magnetic field dependence approaching \sqrt{H} over a 2 - 7K temperature range as long as the field was well below H_{c2} (Balci *et al.*, 2002). Similar to hole-doped cuprates, these features were interpreted as evidence for lines of nodes in the gap function. However, a subsequent study from the same group seemed to reveal that the temperature range over which $c_{el}(H) \propto \sqrt{H}$ is limited to high temperatures, and that a possible transition (from d- to s-wave) is observed as the temperature is lowered (Balci and Greene, 2004). This behavior was believed to be consistent with recent trends observed in tunnelling (see Section IV.A.2) and penetration depth (see Section IV.A.1). It was also interpreted as a possible sign that the FS pocket around $(\pi/2, \pi/2)$ has not yet formed leading to a finite quasiparticle excitation gap (Yuan *et al.*, 2006a) over the full FS.

However, a different measurement scheme that removes the vortex pinning contribution through field cooling reveals (Fig. 50) that the anomalies interpreted as a possible d- to s-wave transition are actually resulting from the thermomagnetic history of the samples (Yu *et al.*, 2005). Thus, the $c_{el}(H) \propto \sqrt{H}$ behavior is preserved down to the lowest temperatures for all dopant concentrations. It extends over a limited field region followed by a saturation at approximately $\mu_0 H \sim 6T$ interpreted as a value close to the bulk upper critical field. From a quantitative point of view, the analysis of the field dependence using a clean d-wave scenario according to $c_{el}/T \equiv \gamma(H) = \gamma_0 + A\sqrt{H}$ yields $A \sim 1.92$ mJ/mol $K^2 T^{1/2}$. In the clean limit, this A param-

ter can be related to the normal state electronic specific heat measured at high magnetic fields leading to $A = \gamma_n (8a^2/\pi H_{c2})^{1/2}$ (Wang *et al.*, 2001) where a is a constant approaching 0.7. With $H_{c2} \sim 6\text{T}$, one gets $\gamma_n \sim 4.1 \text{ mJ/mol K}^2$ and $\gamma_o + \gamma_n \sim 5.7 \text{ mJ/mol K}^2$ approaching the normal state Sommerfeld constant measured at 6T. These recent results confirm that the bulk of the electron-doped cuprates presents specific heat behaviors in full agreement with a dominant d-wave symmetry over the whole range of doping at all temperatures explored.

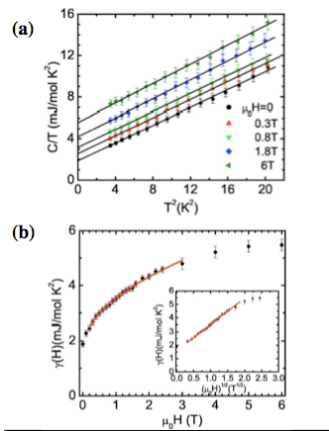


FIG. 50 Specific heat data from Yu *et al.* (2005) on a single crystal of $\text{Pr}_{1.85}\text{Ce}_{0.15}\text{CuO}_4$. In (a), the temperature dependence at various magnetic fields is used to extract the linear-T electronic contribution. (b) Field dependence of the linear in T coefficient that shows close to \sqrt{H} dependence in a magnetic field range considerably below H_{c2} . The red line is a fit to $\gamma(H) = \gamma_o + A\sqrt{H}$. These data show also the saturation of the electronic specific heat at roughly 6T interpreted as the bulk upper critical field.

6. Thermal conductivity

Thermal conductivity at very low temperatures is a sensitive probe of the very lowest energy excitations of a system (Durst and Lee, 2000). The electronic contribution to the thermal conductivity given usually by $\kappa_{el} = \frac{1}{3}c_{el}v_F l$ (where c_{el} is the electronic specific heat, v_F is the Fermi velocity and l is the mean-free path of the carriers) becomes a very sensitive test of the presence of zeroes in the gap function. In the case of conventional BCS s-wave superconductor, the fully gapped Fermi surface leads to an exponentially suppressed number of electronic thermal excitations as $T \rightarrow 0$. On the contrary, a non-zero electronic contribution is expected down to the lowest temperatures in a d-wave superconductor with line nodes. To extract this part from the total thermal conductivity that includes also a phonon contribution, a plot of κ/T as a function of T^2 yields a non-zero intercept at $T = 0$ (Taillefer *et al.*, 1997). Assuming that $\kappa = \kappa_{el} + \kappa_{ph} = AT + CT^3$, one can

compare the measured value of A to the theoretical predictions that relates it to the slope of the gap function at the nodes [$S \equiv \left(\frac{d\Delta}{d\phi}\right)_{node}$], i.e. its angular dependence along the Fermi surface. Durst and Lee (2000) showed that the electronic part is given by :

$$\kappa_{el}/T = \frac{k_B^2}{3\hbar} \frac{n}{d} \left(\frac{v_F}{v_2} + \frac{v_2}{v_F} \right) \quad (2)$$

where $\frac{d}{n}$ is the average distance between CuO_2 planes. The first term of Eq. 2 is expected to give the primary contribution (for example, $\frac{v_F}{v_2} \sim 14$ in YBCO (Chiao *et al.*, 2000)), such that $\kappa_{el}/T \approx \frac{k_B^2}{3\hbar} \frac{n}{d} \left(\frac{v_F}{v_2} \right)$ where $v_2 = S/\hbar k_F$. For a monotonic d-wave gap function, $\Delta = \Delta_o \cos(2\phi)$ such that $\kappa_{el}/T \propto 1/S \propto 1/\Delta_o$. This linear temperature dependence and its link to v_F/v_2 (which is sample-dependent) were confirmed in hole-doped cuprates by Chiao *et al.* (2000) for example. Similar to the specific heat, the Volovik effect should give rise also to $\kappa_{el}(H) \propto \sqrt{H}$ as was observed in YBCO (Chiao *et al.*, 1999).

In the case of the electron-doped cuprates, the low temperature data obtained by Hill *et al.* (2001) show a significant phonon contribution at low temperature as observed in a plot of κ/T as a function of T^2 as evinced by the straight lines in Figure 51. Moreover, a substantial increase of thermal conductivity with the magnetic field confirms the presence of a large electronic contribution growing towards saturation at large fields (roughly 8T), in agreement with the above mentioned specific heat data. At high fields, one recovers the full normal-state density of states, which pinpoints the approximate value of the upper critical field of $\sim 8\text{T}$. However, as demonstrated by the lack of a y -intercept the observed electronic contribution does not extend down to the lowest temperatures as in YBCO (Chiao *et al.*, 1999). Instead a clear downturn is observed below 200mK that has recently been attributed to thermal decoupling of the charge carriers and the phonons (Smith *et al.*, 2005). The electrons and the phonons that carry heat are not reaching thermal equilibrium at low temperature because of a poor electron-phonon coupling. This decoupling is obviously a major drawback for a direct extraction of the electronic contribution without the use of a theory (Smith *et al.*, 2005) and makes it difficult to confirm the presence of a non-zero value at zero field in the electron-doped cuprates.

One can make a crude estimate of the expected linear coefficient of the specific heat A parameter (discussed above in Sec. IV.A.5) using $v_F \sim 270 \text{ km/s}$ (Park *et al.*, 2008; Schmitt *et al.*, 2008) for nodal quasiparticle excitations and $v_2 = 2\Delta_o/\hbar k_F$ assuming a monotonic d-wave gap with the tunnelling maximum value of $\Delta_o \sim 4 \text{ meV}$ for optimal doping (Biswas *et al.*, 2002). This gives $v_F/v_2 \sim 96$ and a $\kappa_{el}/T \approx 0.96 \text{ mW/K}^2\text{-cm}$, which is shown as a blue circle in Fig. 51. Assuming instead a non-monotonic d-wave gap with $\Delta =$

$\Delta_o[1.43 \cos 2\phi - 0.43 \cos 6\phi]$ (Matsui *et al.*, 2005a), with $\Delta_o = 3$ meV (Blumberg *et al.*, 2002; Qazilbash *et al.*, 2005) leads to $v_F/v_2 \sim 47$, and $\kappa_{el}/T \approx 0.47$ mW/K²-cm, which is shown as the red circle in Fig. 51²⁸. This analysis gives indication that the linear coefficient of specific heat is of the right order. In Figure 52, an unpublished analysis of the thermal conductivity (courtesy of L. Taillefer) of an optimally doped PCCO samples allows one to isolate the linear term at low temperature as $\kappa_{el}/T \approx 0.60$ mW/K²-cm by taking into account the thermal decoupling of the charge carriers and the phonons mentioned above (Smith *et al.*, 2005). This value is intermediate to the estimates given above for monotonic and non-monotonic d-wave superconductors (red and blue dots of Fig. 51). In Fig. 52 one can see the clear downturn from electron-phonon decoupling around 300 mK, which prevents the explicit measurement of κ/T .

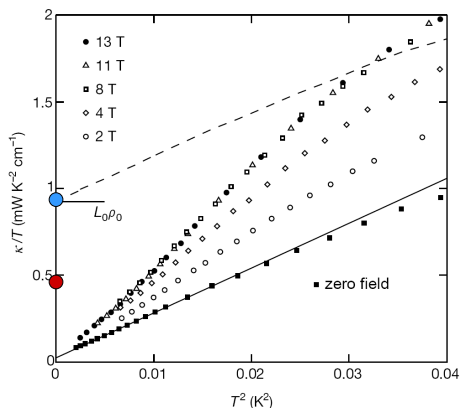


FIG. 51 Thermal conductivity of PCCO for a heat current in the basal plane, plotted as κ/T versus T^2 , at different values of the magnetic field applied normal to the plane. The solid line is a linear fit to the zero-field data below 130 mK. The dashed line shows the behaviour of a Fermi liquid consisting of the expected electronic part extracted from the Wiedemann-Franz law using the residual resistivity ρ_o for this sample obtained at high magnetic and a phonon contribution given by the solid line (zero-field data). From Hill *et al.* (2001). The blue (near (0,1)) and red (near (0,0.5)) dots are estimates for the coefficient of the electronic contribution for monotonic and non-monotonic gap functions as given in the text. The experimental data show a zero y -intercept because of electron-phonon decoupling at low temperature.

²⁸ Note that we have used the non-monotonic gap function from Matsui *et al.* (2005a) but the maximum gap values obtained by Blumberg *et al.* (2002); Qazilbash *et al.* (2005) to evaluate v_F/v_2 . This takes into account the inconsistency between the absolute values of the gap maximum measured by various probes as discussed in section IV.A.3.

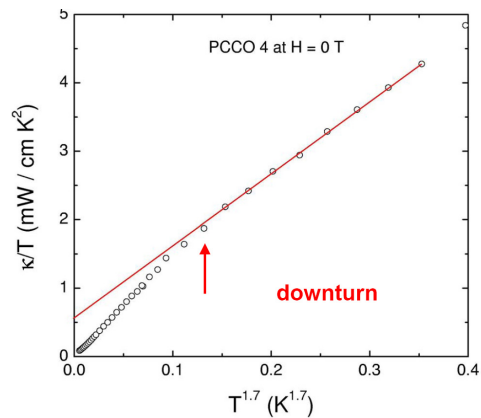


FIG. 52 Thermal conductivity of an optimal PCCO single crystal for a heat current in the basal plane, plotted as κ/T versus $T^{1.7}$. These data show the downturn to the decoupling of the electron and phonons. The data above the electron-phonon decoupling temperature of $T_D \sim 300$ mK extrapolate to $\kappa/T \sim 0.60$ mW/K²-cm. Note that the data above the downturn goes as a power of 1.7 and not 2. Courtesy of L. Taillefer.

7. Nuclear Magnetic Resonance

Measuring the nuclear magnetic resonance (NMR) response of electron-doped cuprates is also a difficult task because of the large magnetic contribution of the rare earth ion. It leads to dipolar and quadrupolar local field that makes interpretation difficult. For this reason, only measurements with Pr and La (and eventually Eu) as the rare earth atoms have been of real interest to extract the symmetry of the order parameter. Zheng *et al.* (2003) have shown explicitly that the spin relaxation rate $1/T_1$ of ⁶³Cu in $x=0.11$ PLCCO falls dramatically in the superconducting state over some temperature range following a power law close to T^3 as shown in Figure 53. This temperature dependence is consistent with the existence of line nodes and a d-wave superconducting order parameter as was observed in hole-doped cuprates (Asayama *et al.*, 1996). At the lowest temperatures the relaxation rate deviates from T^3 behavior which was interpreted by Zheng *et al.* (2003) as a consequence of disorder scattering. Also consistent with d-wave, there was no sign of a Hebel-Schlichter peak just below T_c (see also Fig. 53) which is a signature of class II coherence factors and s-wave superconductivity. A comparison of the data with calculation using a $d_{x^2-y^2}$ order parameter reveals a superconducting gap $2\Delta_0 = 3.8 k_B T_c$, which is consistent with many other probes.

8. Phase sensitive measurements

Some of the most convincing and definitive experiments to demonstrate the d-wave pairing symmetry in the hole-doped cuprates measure the phase of the order

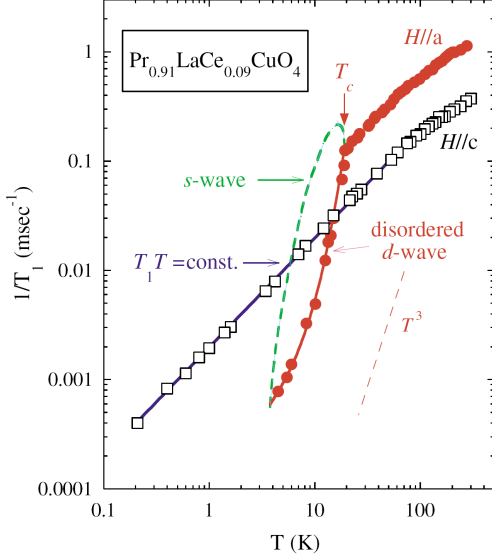


FIG. 53 ^{63}Cu spin relaxation rate $1/T_1$ as a function of temperature in the superconducting and the normal states of a $\text{Pr}_{0.91}\text{LaCe}_{0.09}\text{CuO}_{4-y}$ single crystal. Red solid circles: data in the superconducting state measured with a magnetic field of 6.2T parallel to the CuO_2 planes. Open black circles: data in the normal state measured with an out-of-plane magnetic field of 15.3T. The red solid line is a fit using a $d_{x^2-y^2}$ order parameter leading with $2\Delta_0 = 3.8 k_B T_c$. The solid line is a fit to the Korringa law, which is consistent with Fermi liquid behavior. From Zheng *et al.* (2003).

parameter directly instead of its magnitude. Such techniques are sensitive to changes in the sign of the pair wave-function in momentum space. Most are based on the fact that the current flowing through a Josephson junction is sensitive to the phase difference between superconducting electrodes (Tinkham, 1996). By designing very special geometries of junctions and SQUIDs (Superconducting Quantum Interference Devices) that incorporate high- T_c and possibly conventional superconductors, one can demonstrate the presence of the sign change in the order parameter (van Harlingen, 1995; Tsuei and Kirtley, 2000a). Quasiparticle tunnelling can also be sensitive to the sign change. The presence of the so-called Andreev bound states at the interface of normal-insulator-superconductor (N-I-S) tunnel junctions is a direct consequence of the particular symmetry of the high- T_c cuprates.

The most convincing phase sensitive measurement for the electron-doped cuprates has been reported by Tsuei and Kirtley (2000b) who observed a spontaneous half flux quantum ($\phi_0/2$) trapped at the intersection of a tri-crystal thin film. This epitaxial thin-film-based experiment has been used extensively by the same authors to demonstrate the universality of the d-wave order param-

eter for hole-doped cuprates (Tsuei and Kirtley, 2000a). It relies on the measurement of the magnetic flux threading a thin film using a scanning SQUID microscope. When the epitaxial thin film is deposited on a tri-crystal substrate with carefully chosen geometry as in Figure 54(a), Josephson junctions are formed in the films at the grain boundaries of the substrates (Hilgenkamp and Mannhart, 2002). The presence of spontaneous currents induced by phase frustration at the tri-crystal junction point is a definitive test of a sign change in the order parameter.

In the case of the electron-doped cuprates, Tsuei and Kirtley (2000b) showed using a fit of the magnetic field (Kirtley *et al.*, 1996) as a function of position in Fig. 54(c) that the magnetic flux at the tri-crystal junction in Fig. 54(b) corresponds to half a flux quantum (Tsuei and Kirtley, 2000b). This observation was made despite very small critical current densities for the junctions along the grain boundaries, implying very weak coupling and very long penetration depth of the field along the grain boundary junctions. Similar to hole-doped cuprates (van Harlingen, 1995; Tsuei and Kirtley, 2000a), this observation is consistent with pure d-wave pairing symmetry.

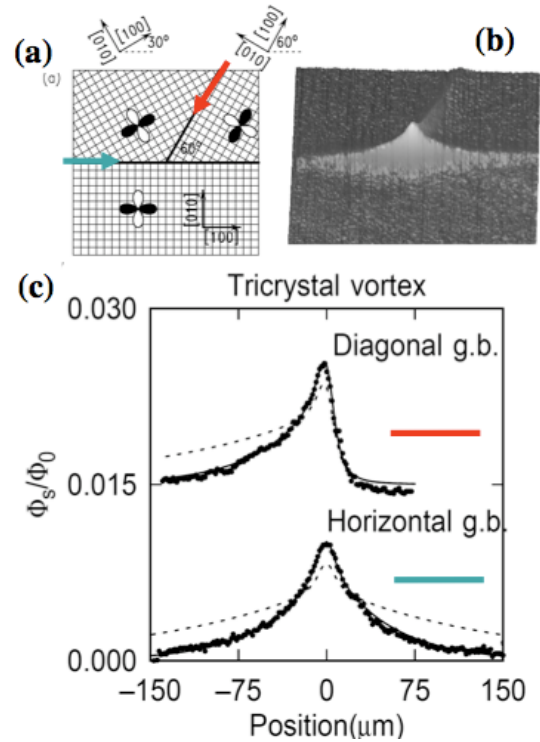


FIG. 54 (a) Tri-crystal geometry used to force phase frustration and spontaneous generation of a half-flux quantum at the tri-crystal junction point. The red and the blue arrows indicate the diagonal and horizontal grain boundaries respectively; (b) 3D image of the flux threading the film; (c) Fit to the field profile along the corresponding grain boundaries. The solid and the dashed lines are fits assuming $\phi = \phi_0/2$ and $\phi = \phi_0$ respectively trapped at the tri-crystal point. From Ref. (Tsuei and Kirtley, 2000b).

In the hole-doped cuprates, a related method has

been employed using Josephson junctions between high- T_c cuprates (d-wave superconductors) and conventional s-wave superconductors to also demonstrate the high- T_c 's d-wave nature (van Harlingen, 1995). This set-up is inspired by proposals by A.J. Leggett, Geshkenbein *et al.* (1987) Sigrist and Rice (1995) that a d-wave/s-wave ‘corner’ SQUID would carry a self-induced current resulting also in the presence of a half-flux quantum trapped in the SQUID loop (van Harlingen, 1995). In the case of the electron-doped cuprates, there has been very little success in fabricating similar well-controlled and reproducible Josephson junctions that incorporate conventional superconductors, which makes the fabrication of full SQUID geometries even more complicated. To the best of our knowledge, no electron-doped/s-wave SQUIDS have been reported in the literature. Up to now, only one study with successful HTSC / s-wave junctions was reported by Ariando *et al.* (2005). These authors fabricated ramp-edge junctions between NCCO ($x = 0.15$ and 0.165) and Nb in a special zigzag geometry as shown in Figure 55. Since the critical current density of the NCCO/Au/Nb ramp-edge junctions is very small ($J_c \sim 30$ A/cm²), the zigzag geometry presented by Ariando *et al.* is in the small junction limit and one expects an anomalous magnetic field dependence in the d-wave case. For instance, one can note that the critical current density of this zigzag junction is suppressed at zero field. As one applies a small magnetic field to this junction, the critical current grows and then oscillates as the first quanta of flux penetrate the zigzag junction.

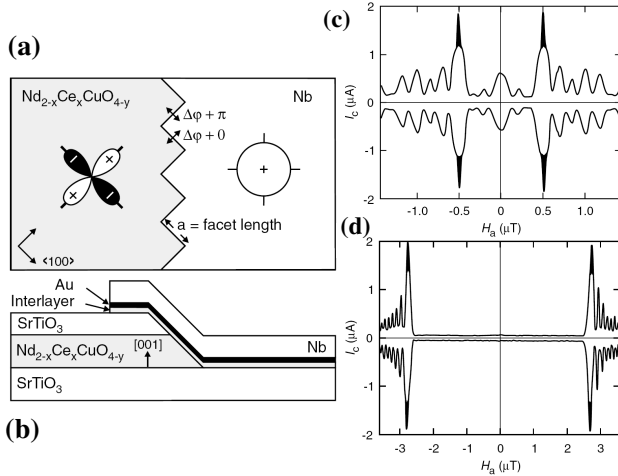


FIG. 55 Zigzag ramp-edge Josephson junctions made of $\text{Nd}_{2-x}\text{Ce}_x\text{CuO}_{4-y}$ and conventional s-wave Nb. (a) Top view of the zigzag design; (b) Cross-section view of a ramp-edge junction including a thin interlayer of NCCO. Examples of anomalous field modulations of the critical current arising from the d-wave symmetry for devices made of (c) 8 facets of $25\mu\text{m}$ width and (d) 80 facets of $5\mu\text{m}$ width. From Ariando *et al.* (2005).

One important conclusion of Ariando *et al.* is the fact that their zigzag junctions for $x = 0.15$ and 0.165 do not

show any trend for modification of the pairing symmetry from d-wave with decreasing temperature (and/or cerium doping) as initially proposed by Balci and Greene (2004) from specific heat data (see Section IV.A.5). This is consistent with the most recent specific heat data obtained by Yu *et al.* (2005) on similar single crystals.

Chesca *et al.* (2003) patterned a $500\mu\text{m}$ thick LCCO film made by MBE on a tetracystal substrate to create a π -SQUID at the junction point as shown in Figure 56. The minimum in critical current at zero field for the π -design is consistent with d-wave pairing symmetry (Chesca *et al.*, 2003). We should stress however that, similar to the above-mentioned experiments performed by Tsuei *et al.* and Ariando *et al.*, these devices are characterized by low critical current densities, which are many orders of magnitude smaller than those used for the hole-doped cuprates (van Harlingen, 1995; Hilgenkamp and Mannhart, 2002; Tafuri and Kirtley, 2005; Tsuei and Kirtley, 2000a). To this day, there has been little progress on the improvement of these junctions, probably an indication that the difficult material issues mentioned in section II.E may be playing an important role.

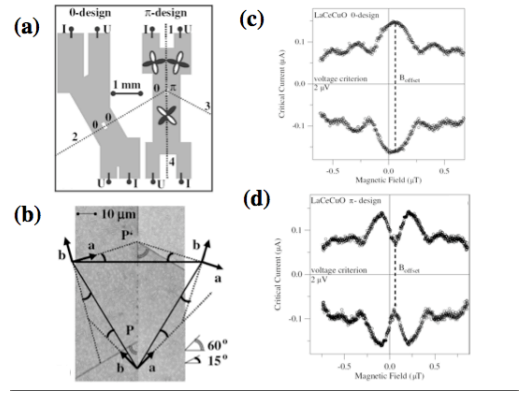


FIG. 56 (a) Schematic layout of the LCCO SQUID on a tetracystal SrTiO_3 substrate. The hole of the right hand SQUID contains the ‘‘tetracystal point’’ which consists actually of two tricrystal points P and P’, $56\mu\text{m}$ apart as shown in (b). In (c) and (d), the critical current as a function of magnetic field is presented for the 0-design and the π designs respectively. The minimum in the critical current at zero field in (d) is a common signature of π -SQUID (van Harlingen, 1995). From Chesca *et al.* (2003).

9. Order parameter of the infinite layer compounds

As mentioned previously, although measurements of the normal state properties of the infinite layer compound SLCO are rare, there have been a few experiments of their pairing symmetry. In general, measurements on the infinite layer compounds have been hampered by a lack of single crystals or thin films and give conflicting conclusions. The spatial independence of the STM spectra

observed when performing a line scan across many randomly oriented grains on a polycrystalline sample has, along with the lack of ZBCP, been interpreted as being consistent with an s-wave symmetry (Chen *et al.*, 2002). Low temperature specific heat (Liu *et al.*, 2005) also suggests a conventional s-wave pairing symmetry while NMR suggests an unconventional, non s-wave, symmetry (Imai *et al.*, 1995). Stronger suppression of T_c by the magnetic impurity Ni than the non-magnetic impurity Zn is indirect supporting evidence for s-wave (Jung *et al.*, 2002). Chen *et al.* (2002) also concluded in their STM study that the suppression of their tunneling coherence peaks with Ni doping, in contrast to the much smaller effect with Zn doping, was consistent with an s-wave symmetry. This is a system that certainly needs further investigation, both on the materials side as well as high quality experimentation. Measurements like μ SR have not been able to measure the T dependence of the penetration depth to determine the pairing symmetry as they require single crystal (Shengelaya *et al.*, 2005).

B. Position of the chemical potential and midgap states

One long outstanding issue in the cuprates is the position of the chemical potential μ upon doping. In the case that the cuprates are in fact described by some Mott-Hubbard-like model, the simplest scenario is that from the insulator the chemical potential shifts into the lower Hubbard band (or CTB) upon hole doping and into the upper Hubbard band upon electron doping (see Fig. 3). This is the exact result for the one dimensional Hubbard model (Woynarovich, 1982). In contrast, dynamic mean field theory (DMFT) calculations show that, at least for infinitely coordinated Mott-Hubbard system, for doped systems μ lies in coherent mid-gap states (Fisher *et al.*, 1995). Similarly, systems which have a tendency towards phase separation and inhomogeneity will generically generate mid-gap states in which the chemical potential will reside (Emery and Kivelson, 1992). The position of the chemical potential and its movement upon doping is an absolutely central issue, as its resolution will shed light on the local character of the states involved in superconductivity, the issue of whether or not the physics of these materials can in fact be captured by Mott-Hubbard like models, and the fundamental problem of how the electronic structure evolves from that of a Mott insulator to a metal with a large Luttinger theorem (Luttinger, 1960) respecting Fermi surface.

In the first detailed photoemission measurements of the n-type cuprates, Allen *et al.* (1990) claimed that μ did not cross the insulator's gap upon going from hole to electron doping and lies in states that fill the gap. This inference was based on a comparison of the angle integrated valence band resonant photoemission spectra of $\text{Nd}_{2-x}\text{Ce}_x\text{CuO}_4$ at $x=0$ and 0.15 with $\text{La}_{2-x}\text{Sr}_x\text{CuO}_4$ which showed that the Fermi level lies at nearly the same energy in both cases as compared to the valence band

maximum. Similar conclusions based on x-ray photoemission have been reached by other authors (Matsuyama *et al.*, 1989; Namatame *et al.*, 1990). However, these results have been called into question by Steeneken *et al.* (2003) who showed that due to the large 4f electron occupation of $\text{Nd}_{2-x}\text{Ce}_x\text{CuO}_{4-y}$ (not to mention the crystal structure differences) the valence band maximum in NCCO is dominated by 4f electrons, making it a poor energy reference for the chemical potential. They proposed instead that the appropriate reference for the internal energies of the copper oxygen plane across material classes was the peak at the $3d^8$ final states of the photoemission process, which represents configurations where the hole left from electron removal has its majority weight on the copper site instead of an oxygen (a $3d^9\bar{L}$ configuration).

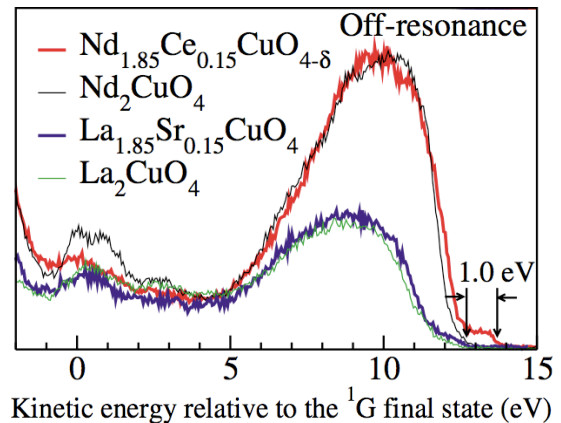


FIG. 57 (color) Photoemission valence band spectra of $\text{Nd}_{1.85}\text{Ce}_{0.15}\text{CuO}_{4-\delta}$, Nd_2CuO_4 , La_2CuO_4 , and $\text{La}_{1.85}\text{Sr}_{0.15}\text{CuO}_4$ taken 5eV below the Cu L_3 edge. Energies of the spectra are aligned with respect to the Cu $3d^8\ ^1G$ final states. From Steeneken *et al.* (2003).

These $3d^9 \rightarrow 3d^8$ electron removal states are expected to be found at an energy approximately U (the microscopic onsite Hubbard interaction energy) below the $3d^{10} \rightarrow 3d^9$ states and so give a good energy reference that refers directly to the electronic structure of the CuO_2 plane. $3d^{10}$ initial states are assumed to be the primary result of electron doping, as electrons are believed to mostly be doped to Cu orbitals. Lining up valence band spectra to the $3d^8$ states (see Fig. 57), Steeneken *et al.* (2003) found that both Nd_2CuO_4 , La_2CuO_4 , and $\text{La}_{1.85}\text{Sr}_{0.15}\text{CuO}_4$ showed a spectral weight onset at the same energy (approximately 13 eV above the $3d^8$ reference), which was presumably the CTB. However, $\text{Nd}_{1.85}\text{Ce}_{0.15}\text{CuO}_{4-\delta}$ showed an onset approximately 1eV higher and so it was concluded that the chemical potential shifts by this amount (across the charge transfer gap) going from lightly hole- to electron-doped materials. As the onset in the optical charge transfer gap is of this order (1 -1.5 eV (Tokura *et al.*, 1990)), it was concluded that μ lies near the bottom of the conduction band (presumably the upper Hubbard band) of the Ce doped system and

1990; Ishii *et al.*, 1989; Nücker *et al.*, 1989). Note that in general, most of these kind of spectroscopies suffer from a strong sensitivity to surface quality. These studies undoubtedly had problems from surface contamination due to surface preparation methods. In many of these measurements surfaces were prepared by scraping poly-crystalline ceramics (resulting in significant residual contamination signal as judged by the appearance of a shoulder on the high energy side of the main O 1s peak) or by high-temperature annealing which undoubtedly changes the surface charge densities (Cummins and Egdell, 1993). In contrast, in most of the measurements emphasized here, surfaces were prepared by breaking single crystals open in vacuum or the technique was inherently bulk sensitive (EELS or XAS in transmission or fluorescence yield mode for example).

Via Ce core level photoemission Cummins and Egdell (1993) demonstrated that Ce substitutes as Ce^{+4} rather than Ce^{+3} across the full doping range showing that effects of Ce substitution is electron donation. With EELS Alexander *et al.* (1991) observed that Th doping into $\text{Nd}_{1.85}\text{Th}_{0.15}\text{CuO}_4$ caused a 14% reduction in the relative intensity of the Cu $2p_{3/2}$ excitonic feature and only minor changes to the O $2p$ states, which is consistent with doping the Cu sites. Similarly, Liang *et al.* (1995) found that across the family of $\text{RE}_{2-x}\text{Th}_x\text{CuO}_4$ (RE = Pr, Nd, Sm, Eu, and Gd) that Cu $3d^{10}$ features in the XAS Cu K edge spectra increases linearly with Ce doping as shown in Fig 59. A similar picture was arrived at by Pellegrin *et al.* (1993). In x-ray core level photoemission Steeneken *et al.* (2003) observed that the $2p3d^9$ “satellites” decreased in intensity with increasing Ce content, while new structures like $2p3d^{10}$ appear (where $2p$ denotes a photoemission final state with a Cu core hole). Additionally they found that the Cu L_3 x-ray absorption spectra intensity decreases with Ce doping. As this absorption is dominated by the transition $3d^9 + h\nu \rightarrow 2p3d^{10}$, these results also imply that Ce doping results in a decrease of the Cu^{+2} and increase in Cu^{+1} content. All these studies provide strong support for the expected increase in the mean $3d^{10}$ electron count with Ce doping²⁹.

As discussed above, in neutron scattering, Mang *et al.* (2004b) found that the *instantaneous* AF correlation length of doped unreduced NCCO can be described by a quantum Monte Carlo calculations for the randomly site-diluted nearest-neighbor spin 1/2 square-lattice Heisenberg antiferromagnet. Setting the number of non-magnetic sites to within $\Delta x \approx 0.02$ of the nominal Ce concentration gave quantitative agreement with their calculation. This also shows that every Ce atom donates

approximately one electron to the CuO_2 planes.

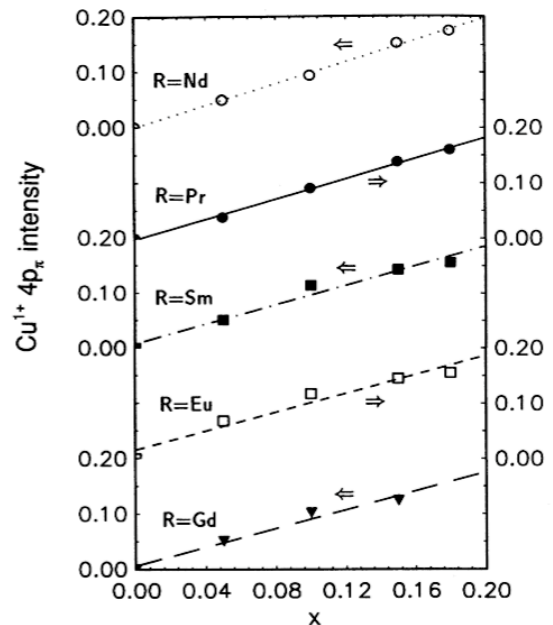


FIG. 59 Peak height of the Cu^{+1} $4p_\pi$ spectral feature in the Cu K-edge XAS spectra as a function of Ce concentration for a large number of (RE)CCO compounds. Its intensity is approximately proportional to the $3d^{10}$ occupation. From Liang *et al.* (1995).

Does the enclosed volume of the FS as measured from ARPES reflect a metallic band that is greater than half-filled? - This is an equivalent question to the one immediately above if one agrees that there is a single metallic band that crosses E_F which is formed out of Cu $d_{x^2-y^2}$ and O $2p_{x,y}$ states. However, this specific issue can be addressed in a different, but very direct fashion from the area of the FS as measured by ARPES. If one neglects the issue of ‘hot-spots’ and speaks only of the underlying FS the Luttinger sum rule appears to be approximately obeyed (King *et al.*, 1993). Armitage *et al.* (2001b) found that in NCCO the enclosed volume is 1.09 for a nominally $x = 0.15$ NCCO sample. Others have found FS volumes closer to that expected (Park *et al.*, 2007; Santander-Syro *et al.*, 2009), but in all cases the Luttinger sum rule is consistent with a band greater than half-filling (approximately $1+x$). As hole-doped systems seem to have a Luttinger volume which closely reflects the number of doped holes $1-x$ (Kordyuk *et al.*, 2002), in this sense also (RE)CCO systems can be regarded as electron-doped.

What is the nature of charge carriers from transport? - It was pointed out early on that there are both hole and electron contributions to transport (Fournier *et al.*, 1997; Gollnik and Naito, 1998; Wang *et al.*, 1991). At low concentrations an electron contribution is naively expected within a model of electrons being doped into a semiconductor. At higher dopings these observations were at odds with the shape of the experimentally determined

²⁹ Similar studies on the hole-doped compounds in contrast give no evidence for $3d^{10}$ occupation and instead signatures of O 2p holes are found, which is consistent with the picture presented above in which doped holes reside primarily on the in-plane oxygens atoms. See for instance, Alp *et al.* (1987); Kuiper *et al.* (1988) and reference therein

FS, which King *et al.* (1993) had found to be a large hole pocket centered at (π, π) . Later, it was found by Armitage *et al.* (2001b, 2002) that at low dopings the FS was a small electron pocket around the $(\pi, 0)$ position. At higher dopings there is a rearrangement of the electronic structure and a large Fermi surface is developed, which derives from electron- and hole-like sections of the FS and may retain remnant signatures of them. Therefore the hole-like experimental signatures may result from electron doping itself. These issues are discussed in more detail above in Sec. III.A.1 and III.C.

Do doped electrons occupy electronic states analogous to those occupied by holes in the p-type compounds? - As discussed in a number of places in this review (see Section II.C), although the local orbital character of doped electrons is undoubtedly different than doped holes within certain models, it appears that one can map the hole and electron addition states to an effective Hubbard model with an approximate electron-hole symmetry. Although mid-gap states are undoubtedly also created upon doping, it appears (Sec. IV.B) that the chemical potential crosses the effective Hubbard gap (formally the CT gap) upon moving from hole to electron doping. Additional evidence for the existence of an effective upper Hubbard band in NCO comes from Alexander *et al.* (1991) who found the same prepeak in undoped (RE)CO and doped (RE)CCO $O\ 1s \rightarrow 2p$ EELS absorption spectra as found in LCO. To first approximation this absorption probes the local unoccupied O density of states. Here however this prepeak is not interpreted as holes in a nominally filled $2p^6$ local configuration and instead has been interpreted as excitations into a Hubbard band of predominantly Cu $3d$ character with a small O $2p$ admixture as expected. In this way Ce doping may be described as the addition of electrons to an effective upper Hubbard band, just as hole doping is the addition of holes to an effective lower Hubbard band. In this sense also these systems may be considered as electron-doped.

D. Electron-phonon interaction

There has been increasing discussion on the subject of strong electron-phonon coupling in the cuprate high temperature superconductors. This has been inferred from both possible phonon signatures in the charge spectra (Lanzara *et al.*, 2001; Lee *et al.*, 2006a), as well as directly in the doping induced softening of a number of high-frequency oxygen bond-stretching modes in many p-doped cuprates as observed by neutron and x-ray scattering (Fukuda *et al.*, 2005; McQueeney *et al.*, 1999, 2001; Pintschovius and Braden, 1999; Pintschovius *et al.*, 2006; Uchiyama *et al.*, 2004). These phonon anomalies have been associated with a tendency towards charge ordering. Recently, similar signatures of phononic anomalies have also been found in the electron-doped compounds (Braden *et al.*, 2005; d’Astuto *et al.*, 2002; Kang *et al.*, 2002). For instance, in NCCO Kang *et al.* (2002) found

changes with doping in the generalized phonon density of states around ≈ 70 meV by neutron scattering. d’Astuto *et al.* (2002) measured NCCO’s phonon dispersions via inelastic x-ray scattering. They assigned the softening in the 55 - 75 meV energy range to the same oxygen half-breathing mode in which anomalies are found in the p-type materials. They found that the frequency of these modes with bond-stretching character suffered a drop near $\sim (0.2\ 0\ 0)$. These studies give evidence for phononic effects in the electron-doped materials that are somewhat similar to those of the hole-doped compounds.

Although, these findings support the generic nature of phonon anomalies in the cuprates, there are a number of differences from the p-type that could in principle exist. On general grounds, since the purported soft phonon is the oxygen half-breathing mode, one may naively expect a weaker coupling for these modes with electron doping, as Madelung potential considerations (Torrance and Metzger, 1989) indicate that doped electrons will preferentially sit on the Cu site, whereas doped holes have primarily oxygen character. Additionally since the biggest changes in the phonon density of states probed by Kang *et al.* (2002) happen at similar doping levels in $\text{La}_{2-x}\text{Sr}_x\text{CuO}_4$ and $\text{Nd}_{2-x}\text{Ce}_x\text{CuO}_4$ ($x \approx 0.04$), the doping levels are at very different relative positions in the phase diagram, with $x = 0.04$ being still well into the antiferromagnetic and more insulating phase for the electron-doped compound. As such modifications in the phonon spectrum may be associated generally with screening changes (and hence electron-phonon coupling) with the onset of metallicity, this demonstrates the possibility that the changes in the NCCO phonon spectrum, although superficially similar in the electron and hole-doped materials, may have some differences.

As mentioned above, although initial measurements of the electron-phonon coupling in the ARPES spectra seemed to give little sign of the ‘kink’ in the angle-resolved photoemission spectra (Armitage *et al.*, 2003) that has been taken to be indicative of strong electron-phonon coupling on the hole-doped side of the phase diagram, more recent measurements show evidence for such a kink (Liu *et al.*, 2008; Park *et al.*, 2008; Schmitt *et al.*, 2008). This work gives additional evidence that electron-phonon interaction may be not so different on the two sides of the phase diagram. Pseudogap features and renormalizations in the optical conductivity have also been interpreted (Cappelluti *et al.*, 2008) in terms of electron-phonon coupling and lattice polaron formation within the Holstein- $t-J$ model in the context of DMFT. Cappelluti *et al.* (2008) point that the moderately large electron-phonon coupling of $\lambda \approx 0.7$ they extract is still not large enough to induce lattice polaron effects in the absence of exchange coupling. This means that if lattice polaronic features exist in these compounds, they can be found only in the presence of (short-range) AF correlations. The disappearance of pseudogap features near the termination of the AF phase is then consistent with this interpretation.

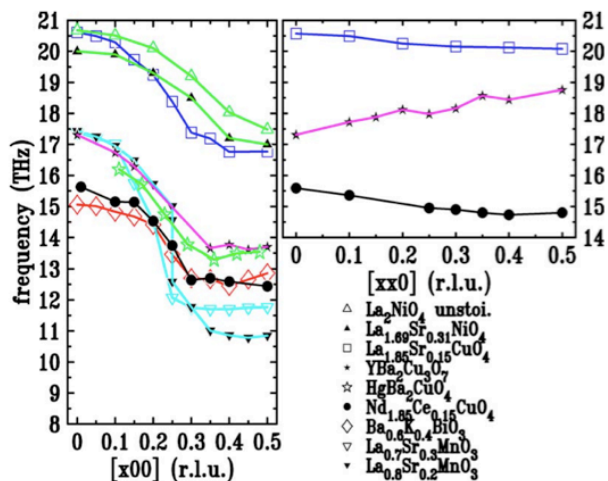


FIG. 60 (Color) Comparison of the phonon anomaly in the bond-stretching branches observed *via* neutron scattering in a number of metallic oxide perovskites. (left) [100] direction. (right) [110] direction. From Braden *et al.* (2005).

d’Astuto *et al.* (2002) claimed that the frequencies of the modes with Cu-O bond-stretching character drop near $q \approx (0.2 \ 0 \ 0)$, however it was difficult to follow the mode much beyond $(0.15 \ 0 \ 0)$ in the $(1 \ 0 \ 0)$ direction with inelastic x-ray scattering due to a complex anti-crossing behavior of several phonon branches in this energy range in NCCO. Braden *et al.* (2005) showed that with the higher accuracy of neutron scattering measurements (which present similar oxygen and heavy-ion dynamic structure factors) all cuprates including NCCO are found to have exceedingly similar phonon anomalies along the [100] direction, showing a drop of ≈ 3 THz (12.4 meV) as shown in Fig. 60. The differences between compounds are larger along the [110] direction (Fig. 60), but still small overall. NCCO shows a slight downward dispersion, whereas the corresponding branch in LSCO is nearly flat and the one in Y123 exhibits only a weak increase. NCCO shows the least anisotropy between the frequency renormalization along the [100] and the [110] directions of all optimally doped cuprates studied so far. NCCO then has the least one-dimensional character of all the measured cuprates, with YBCO having the most anisotropy. It is unknown whether this is related to the very different local character of the charge carriers (see for instance Bauer and Falter (2008)) in these materials. Irrespective of the differences it was emphasized by Braden *et al.* (2005) that the anomalous bond-stretching phonon dispersion in all superconducting cuprates “is astonishingly similar.” This indicates that all these systems (as well as many other perovskites (Fig. 60)) may have similar character of electron-phonon coupling and be close to similar charge-ordering instabilities. However, the close similarity in the electron-phonon coupling between material classes and their very different scales of T_c shows that there is clearly physics beyond electron-

phonon coupling playing a role in superconductivity.

E. Inhomogeneous charge distributions

As discussed above, it is not necessarily the case that doping a Mott insulator results in a spatially homogeneous state (Emery and Kivelson, 1993; Lee and Kivelson, 2003). A number of competing effects can lead to scenarios in which charges phase separate into various structures including charge puddles, stripes (Mook *et al.*, 1998, 2002; Tranquada *et al.*, 1995), or checkerboard patterns (Hanaguri *et al.*, 2004; Seo *et al.*, 2007). There is extensive evidence for such correlations in the hole-doped cuprates (Kivelson *et al.*, 2003).

The situation is much less clear in the *n*-type compounds. As some of the strongest evidence for ‘stripe’ correlations in the hole-doped materials has come from the preponderance of incommensurate spin and charge correlations, the commensurate magnetic response in the *n*-type materials has been taken to be evidence for a lack of such forms of phase separation in these materials. However, Yamada *et al.* (2003) has pointed out that the commensurate short range spin correlations detected by neutron scattering in the SC phase of the *n*-type cuprates can reflect an inhomogeneous distribution of doped electrons in the form of droplets/bubbles in the CuO_2 planes. The commensurate magnetic signatures may also arise from ‘in-phase’ stripe domains as contrasted to the ‘antiphase’ domains of stripes in the *p*-type compounds (Sun *et al.*, 2004). One can then consider the possibility of phase separation and inhomogeneity an open issue.

There has been a number of studies that have argued for an inhomogeneous state in the electron-doped cuprates. Sun *et al.* (2004) found in $\text{Pr}_{1.3-x}\text{La}_{0.7}\text{Ce}_x\text{CuO}_4$ the same unusual transport features that have been argued to be evidence for stripe formation in LSCO (Ando *et al.*, 2001). They measured the *ab*-plane and *c*-axis thermal conductivity and found an anomalous damping of the *c*-axis phonons, which has been associated with scattering off of lattice distortions induced by stripes which are relatively well ordered in the plane, but disordered along the *c* axis. Additionally, in the AF state the *ab*-plane resistivity is consistent with “high mobility” metallic transport, consistent with motion along “rivers of charge.” They interpret these peculiar transport features as evidence for stripe formation in the underdoped *n*-type cuprates. In $\text{Pr}_{1.85}\text{Ce}_{0.15}\text{CuO}_4$ Zamborszky *et al.* (2004) found signatures in the NMR spin-echo decay rate ($1/T_2$) for static inhomogeneous electronic structure. Similarly, Bakharev *et al.* (2004) found via Cu NMR evidence for an inhomogeneous “blob-phase” (bubble) in reoxygenated superconducting $\text{Nd}_{1.85}\text{Sr}_{0.15}\text{CuO}_4$. They found that for a narrow region of oxygen levels just above the suppression of superconductivity there was evidence for an inhomogeneous charge distribution. Moreover, Granath (2004) has shown that some unusual aspects of the doping evolution of the FS found by ARPES

(Armitage *et al.*, 2002) could be explained by an inhomogeneous in-phase stripes or ‘bubble’ phases. ‘Bubble’ phases, where the doped charge is confined to small zero-dimensional droplets instead of the one-dimensional stripes, arise naturally instead of stripes in $t - J$ type models with long-range Coulomb repulsion in the limit of $t \ll J$, because of the lower magnetic energy (Granath, 2004). They may be favored in the electron-doped materials, which have more robust antiferromagnetism than the hole-doped materials. From their neutron scattering Dai *et al.* (2005) argue that $x = 0.12$ PLCCO is electronically phase separated and has a superconducting state, which coexists with both a 3D AF state and a 2D commensurate magnetic order that is consistent with in-phase stripes. Onose *et al.* (1999) found infrared and Raman Cu-O phonon modes that grew in intensity with decreasing temperature in unreduced crystals. This was interpreted as being due to a charge ordering instability promoted by a small amount of apical oxygen. Additionally as mentioned above (Sec. IV.D) there is ample evidence for phononic anomalies in the n -type compounds of which corresponding ones have been associated with charge order and stripe formation in the hole-doped materials.

In contrast to these measurements, Williams *et al.* (2005) found no sign of the Cu NMR “wipe out” effect in $x=0.15$ PCCO which has been interpreted to be consistent with spatial inhomogeneity in $\text{La}_{2-x}\text{Sr}_x\text{CuO}_4$ (Singer *et al.*, 1999). Similarly, in the first spatially resolved STM measurements Niestemski *et al.* (2007) showed that $T_c = 12\text{K}$ PLCCO had a relatively narrow gap distribution of 6.5 - 7.0 meV (Fig. 32), with no signs of the gross inhomogeneity of some p -type compounds (Howald *et al.*, 2001; Lang *et al.*, 2002). In neutron scattering Motoyama *et al.* (2006) found that the field induced response at low temperature is momentum resolution limited, which implies that the dynamic magnetic correlations are long-range ($> 200\text{\AA}$) with correlation lengths that span vortex-core and SC regions. This provides further evidence that NCCO forms a uniform state. Circumstantial evidence for a homogeneous doped state also comes from other neutron measurements, where it has been found that the spin pseudogap closes with increasing temperature and field, in contrast to the hole-doped material where it is better described as “filling in” (Motoyama *et al.*, 2007; Yamada *et al.*, 2003). This ‘filling-in’ behavior has been associated with phase separation and so argues against such phenomena in the n -type cuprates. Likewise, quantities like the inelastic scattering spectral weight (ω integration of $\chi''(\omega)$) appear not to show much doping dependence (Fujita *et al.*, 2008a). This is also unlike the p -type systems and was associated by these authors with a lack of phase separation in the n -type compounds.

Finally there is the very interesting result of Harima *et al.* (2001) (Fig. 61) who demonstrated that chemical potential shifts very differently with hole and electron doping, which argues against phase separation in the

n -type compounds. Harima *et al.* (2001) compared the chemical potential shifts in NCCO and LSCO *via* measurements of core-level photoemission spectra. Although the relative shift between LCO and NCO was uncertain in such measurements due to different crystal structures, they found that the chemical potential monotonously increases with electron doping, in contrast to the case of hole doping, where the shift is suppressed in the underdoped region (Fig. 61 (top)). The differences were ascribed to a tendency towards phase separation and mid-gap states in LSCO as compared to NCCO in this doping region (Fig. 61 (middle)). We should note however that this suppression of the chemical potential shift in the hole-doped compounds does not seem to be universal as Bi2212 shows a much smaller suppression (Harima *et al.*, 2003) and Na doped CCOC (Yagi *et al.*, 2006) apparently none at all. Interestingly however, they found that the previously discussed electron-hole asymmetry of the NCCO/LSCO joint phase diagram with respect to the extent of antiferromagnetism and superconductivity is actually symmetric if plotted in terms of chemical potential (Fig. 61 (bottom)). This is a fascinating result that deserves further investigation.

F. Nature of normal state near optimal doping

A central subject of debate in the field of cuprate superconductivity is the nature of the ‘normal’ state. Is the metal above T_c well described by Fermi liquid theory or are interactions such as to drive the system into a non-Fermi liquid state of some variety? One of the problems with the resolution of this question experimentally is the “unfortunate” intervention of superconductivity at relatively high temperatures and energy scales. The matter of whether a material is or is not a Fermi liquid can only be resolved definitively at low energy scales as the criteria to have well-defined quasiparticles will always break down at sufficiently high temperatures or energies. The advantage of trying to answer these question for the electron-doped cuprates as opposed to the p -type materials is that superconductivity can apparently be completely suppressed by modest magnetic fields ($\approx 10\text{ T}$) allowing access to the low temperature behavior of the normal state.

This issue has been discussed frequently in the context of the electron-doped cuprates due to the approximately quadratic dependence of the resistivity above T_c (Fournier *et al.*, 1998a; Hidaka and Suzuki, 1989; Tsuei *et al.*, 1989). For further discussion see Sec. III.A.1. The conventional wisdom is that this is evidence of a “more Fermi liquid-like” normal state (T^2 being the nominal functional form for electron-electron scattering in a conventional metal). It is not. While it is certainly true that the quadratic temperature dependence is very different than the remarkable linear dependence found in the hole-doped materials, it is not likely evidence for a Fermi liquid state. The temperature range over which T^2

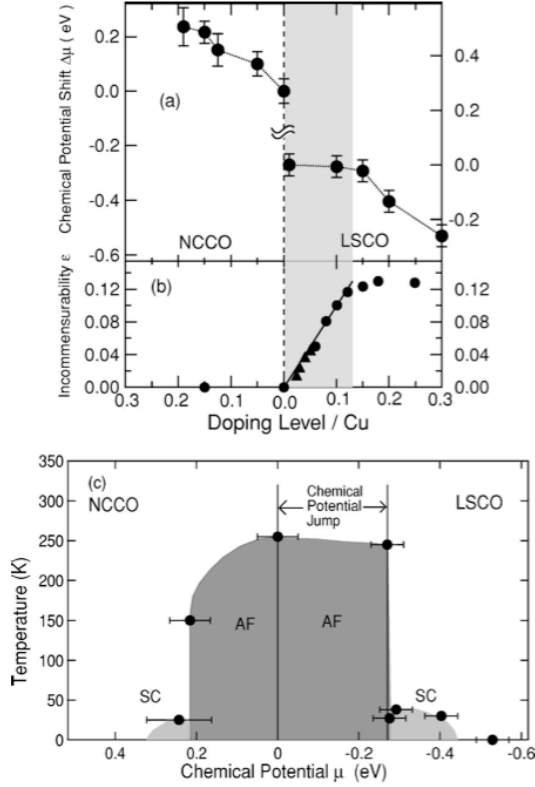


FIG. 61 (top) Chemical potential shift μ in NCCO and LSCO. (middle) Incommensurability measured by inelastic neutron scattering experiments as given in Refs. (Yamada *et al.*, 1998) and (Yamada *et al.*, 2003). In the hatched region, the incommensurability varies linearly and $\Delta\mu$ is constant as functions of doping level. (bottom) μ -T phase diagram of NCCO and LSCO. Note that there is an uncertainty in the absolute value of the chemical potential jump between NCO and LCO. From Harima *et al.* (2001).

is found (from T_c to room temperature) is much larger than that ever expected for purely electron-electron scattering to manifest. Within conventional transport theory, one will almost invariably have a phonon contribution that in certain limits will give a linear dependence to the resistivity and destroy the T^2 form except at the lowest temperatures. As mentioned above, in fact the linear temperature dependence of many hole-doped cuprates can be well fit by reasonable phonon parameters by the Bloch-Grüneisen equations up to at least room temperature (Allen, 2001)³⁰. Moreover, realistic treatments for electron-electron scattering give functional forms for various temperature ranges that depend on such factors as the Fermi surface geometry (Hodges *et al.*, 1971) and it

³⁰ It is unphysical however to fit the temperature dependence up to the highest temperatures to Bloch-Grüneisen. At mean free paths on order of the lattice spacing one should expect a resistivity saturation that is not observed

is seldom that a pure T^2 functional form is observed even in conventional metals. Whatever is causing the T^2 functional form almost certainly cannot be electron-electron scattering of a conventional variety and is therefore not evidence of a Fermi liquid ground state. In a similar fashion the quadratic frequency dependence of the effective scattering rate that is found by Wang *et al.* (2006a) up to the high frequency scale of 6000 cm^{-1} (0.74 eV) in overdoped NCCO is also unlikely to be evidence for a Fermi-liquid.

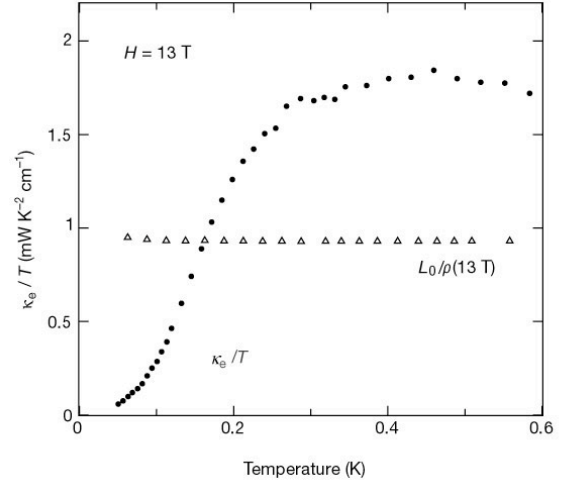


FIG. 62 A comparison of charge conductivity $\sigma(T) = 1/\rho(T)$, plotted as $L_0/\rho(T)$ (triangles) (i.e. given by the Wiedemann-Franz expectation), and electronic contribution to the heat conductivity κ_e , plotted as κ_e/T (circles), as a function of temperature in the normal state at $H = 13 \text{ T}$. A clear violation of the Wiedemann-Franz law is found (Hill *et al.*, 2001). The downturn below 300 mK is an artifact of thermal decoupling of the electronic and phononic degrees of freedom (Smith *et al.*, 2005), but an approximately factor of two discrepancy remains in the magnitude of the thermal conductivity and the value inferred from the charge conductivity at low temperature.

Recently however this issue of the Fermi liquid nature of the electron-doped cuprates has been put on more rigorous ground with sensitive measurements of the thermal conductivity of $x=0.15$ PCCO. Taking advantage of the low critical magnetic fields of these compounds, Hill *et al.* (2001) measured both the thermal and electric conductivity of the resulting normal state and discovered a clear violation of the “Wiedemann-Franz law” (Fig. 62). The Wiedemann-Franz law is one of the defining experimental signatures of Fermi liquids and states that the ratio $\kappa/\sigma T$ where κ is the thermal conductivity and σ is the electrical conductivity should be universally close to Sommerfeld’s value for the Lorenz ratio $L_0 = \pi^2/3(k_B/e)^2 = 2.45 \times 10^{-8} \text{ W}\Omega\text{K}^{-2}$. This relation reflects the fact that at low temperature the particles that carry charge are the same as those that carry heat. No known material has thus far been found to be in violation

of it ³¹. However, Hill *et al.* (2001) demonstrated that there was no correspondence between thermal and electrical conductivities in PCCO at low temperature. For much of the temperature range, the heat conductivity was found to be greater than expected³². Because the Wiedemann-Franz law is a natural property of Fermi liquids, this violation had immediate consequences for understanding the ground state and elementary excitations of these materials and implies that charge and heat are not carried by the same electronic excitations. A similar violation of the WF law has now been reported in underdoped $\text{Bi}_{2+x}\text{Sr}_{2-x}\text{CuO}_{6-\delta}$ (Proust *et al.*, 2005). On the other hand, agreement with the WF law is found in some overdoped cuprates (Nakamae *et al.*, 2003; Proust *et al.*, 2002). These measurements suggest that underdoped cuprates (both n and p) have non-FL ground states.

However, in NMR Zheng *et al.* (2003) have measured a similar ratio that should also show universal behavior in a Fermi liquid. They demonstrated that when the superconducting state was suppressed by magnetic field in $x=0.11$ PLCCO the spin relaxation rate measured obeyed the Fermi-liquid Korringa law $1/T_1 \propto T$ down to the lowest measured temperature (0.2K). With the measured value for the Knight shift K_s , it was found that the even stronger condition $T_1TK_s^2 = \text{constant}$ was obeyed below 55K albeit with a small $T_1TK_s^2$ value of 7.5×10^{-8} sec K, which is 50 times less than the non-interacting value. This points to the significance of strong correlations, but gives indication that the ground state revealed by application of a strong magnetic field is actually a Fermi liquid. These measurements are at odds with those of Hill *et al.* (2001).

Clearly, this is a subject that deserves much more in-depth investigation. It would be worthwhile to search for both Wiedemann-Franz and Korringa law violations over the larger phase diagram of electron-doped cuprates to see for what doping ranges - if any - violations exist.

G. Extent of antiferromagnetism and existence of a quantum critical point

While it has long been known that antiferromagnetism extends to much higher doping levels in the n -type as compared to the p -type compounds, reports differ on what doping level the AF phase actually terminates and whether it coexists or not with superconductivity (Fujita *et al.*, 2003; Kang *et al.*, 2005; Motoyama *et al.*, 2007). There are at least two important questions here:

³¹ Subsequent to the measurements described herein, violations of the Wiedemann-Franz law has been found near heavy-electron quantum critical points (Tanatar *et al.*, 2007).

³² The sudden drop around 300mK of the excess heat shown in Fig. 62 has been shown subsequently to be an artifact of thermal decoupling of the electronic and phononic degrees of freedom (Smith *et al.*, 2005).

Do the intrinsic regimes of superconductivity and AF coincide? And does the AF regime at higher dopings terminate in a second order transition and a T=0 QCP that manifests itself in the ‘scaling forms’ of response functions and in physical observables like transport and susceptibility? These are issues of utmost importance with regards to data interpretation in both n - and p -type compounds. Their resolution impinges on issues of the impact of quantum criticality (Sachdev, 2003), coupling of electrons to antiferromagnetism (Abanov *et al.*, 2001; B. Kyung, 2009; Carbotte *et al.*, 1999; Maier *et al.*, 2008; Schachinger *et al.*, 2003), and $SO(5)$ symmetry (Chen *et al.*, 2004; Zhang, 1997) - yet a complete understanding of it requires weighing the competing claims of different neutron scattering groups, the information provided by μSR , as well as materials growth and oxygen reduction issues.

It has long been known that samples at superconducting stoichiometries show a substantial AF magnetic response, as in for instance the existence of commensurate Bragg peaks (Yamada *et al.*, 1999, 2003). Whether this is because phases truly coexist, or because samples are (chemically or intrinsically) spatially inhomogeneous has been unclear ³³. Motoyama *et al.* (2007) have concluded however that they can distinguish these scenarios *via* inelastic scattering by following the spin stiffness ρ_s that sets the instantaneous correlation length. They find it falls to zero at a doping level of $x \approx 0.134$ (Fig. 40a) in NCCO at the onset of superconductivity ³⁴ and hence there is no intrinsic AF/SC coexistence regime. They found that the instantaneous spin-spin correlation length at low temperature remains at some small, but non-negligible value well into the superconducting regime showing the AF correlations are finite but not long range ordered in the superconductor (Fig. 40a). As other inelastic neutron scattering experiments have clearly shown the presence of a superconducting magnetic gap (Yamada *et al.*, 2003), (despite the presence of Bragg peaks in the elastic response) Motoyama *et al.* (2007) concluded that the actual antiferromagnetic phase boundary terminates at $x \approx 0.134$, and that magnetic Bragg peaks observed at higher Ce concentrations originate from rare portions of the sample which were insufficiently oxygen reduced (Fig. 40b) ³⁵. This group had previously shown that the

³³ In this regard see also Sec. IV.E that addresses the question of intrinsic charge inhomogeneity

³⁴ Note that the definitions for the spin stiffness of Fujita *et al.* (2008a) and Motoyama *et al.* (2007) differ, which accounts for their differences on where ρ_s extrapolates to zero. Motoyama *et al.* (2007) derived it from the T dependence of the linewidth of the *instantaneous* spin correlations over a wide range of temperatures, while as noted below Fujita *et al.* (2008a) get it from the ω dependence of the peak width at a particular T .

³⁵ In a related, but ultimately different interpretation, Yamada *et al.* (2003) interpreted their narrow coexistence regime as evidence that the AF/SC phase boundary is first order and therefore these systems lack a QCP and the associated critical fluctuations

inner core of large TSFZ annealed crystals have a different oxygen concentration than the outer shell (Mang *et al.*, 2004b). They speculate that the antiferromagnetism of an ideally reduced NCCO sample would terminate in a 1st order transition [possibly rendered 2nd order by quenched randomness (Aizenman and Wehr, 1990; Hui and Berker, 1989; Imry and Wortis, 1979)].

A similar inference about the termination of AF state near the superconducting phase boundary can be reached from the neutron and μ SR PLCCO data of Fujita *et al.* (2003, 2008a). Fujita *et al.* (2008a) found only a narrow coexistence regime near the SC phase boundary ($\Delta x \approx 0.01$ near $x \approx 0.1$) which could also be a consequence of rare slightly less reduced regions. They also find a dramatic decrease in AF signatures near this doping level. However, Li *et al.* (2008a) caution that since both the superconducting coherence length and spin-spin correlation length are both strongly affected by the oxygen annealing process, this issue of the true extent of AF and its coexistence with SC in the n -type cuprates may not be completely solved and there may be some oxygen reduction conditions where superconductivity and antiferromagnetism can genuinely coexist. It is undoubtedly true that the annealing conditions depend on Ce concentration and in this regard it may be challenging to settle the question definitively about whether or not AF and superconductivity compete in all regions of phase space. But in support of a scenario of a AF QCP somewhere nearby in PLCCO, Wilson *et al.* (2006b) showed that at higher temperatures and frequencies, the dynamical spin susceptibility $\chi(\omega, T)$ of an $x = 0.12$ sample can be scaled as a function of $\frac{\omega}{T}$ at AF ordering wavevectors. The low energy cut-off of the scaling regime is connected to the onset of AF order, which comes down as the antiferromagnetic phase is suppressed by oxygen reduction.

In contrast to these magnetic measurements, based on their transport data Dagan *et al.* (2004) proposed that a quantum phase transition (QPT) exists at dopings near optimal in PCCO. Their evidence for a quantum critical point (QCP) at $x \approx 0.165$ were: 1) the kink in R_H at 350mK (see Fig 25), 2) the doping dependence of the resistivity's temperature dependent exponent β in the temperature range 0.35 - 20K, 3) the reduced temperature region near $x=0.165$ over which a T^2 dependence is observed, and 4) the disappearance of the low T resistivity upturn. More recent very high-field (up to 60T) Hall effect and resistivity results support this scenario (Li *et al.*, 2007a).

The 'funnel-like' dependence of the threshold T_0 below which T^2 resistivity is observed shown in Fig 63 (top), is precisely the behavior expected near a quantum phase transition (Dagan *et al.*, 2004). This is particularly striking in the n -type cuprates where the resistivity has a T^2 dependence for all dopings at temperatures above 30K (or the resistivity minimum). The phase diagram looks qualitatively similar to quantum phase transition diagrams found in the heavy fermions (see for instance Custers *et al.* (2003)). One may also take as evidence

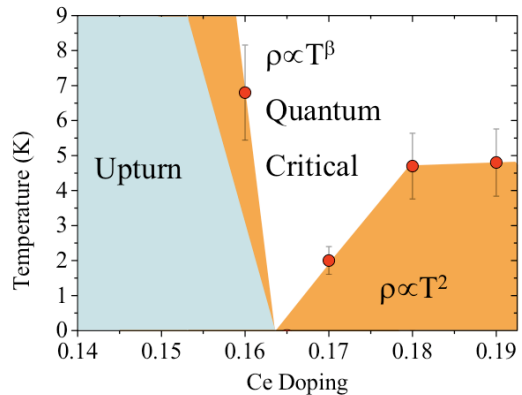


FIG. 63 (top) Schematic illustration of the phase diagram of $\text{Pr}_{2-x}\text{Ce}_x\text{CuO}_4$ from resistivity measurements in high field. Plotted as red dots is T_0 , the temperature below which the T^2 behavior is observed (in orange). At dopings lower than that of the nominal QCP the resistivity shows a low temperature upturn (Dagan and Greene, 2004).

the striking linear in T resistivity found from 35mK to 10 K for $x=0.17$ PCCO (Fournier *et al.*, 1998b) as evidence for a QCP near this doping. A recent study of the doping dependence of the low-temperature normal state thermoelectric power has also been interpreted as evidence for a quantum phase transition (QPT) that occurs near $x=0.16$ doping (Li *et al.*, 2007c). As discussed elsewhere, a number of other experiments such as optical conductivity (Onose *et al.*, 2004; Zimmers *et al.*, 2005), ARPES (Matsui *et al.*, 2007) and angular magnetoresistance (Yu *et al.*, 2007b) experiments have also suggested that there is a phase transition at a higher doping.

Clearly, the inference of a QCP in PCCO and NCCO at $x \approx 0.165$ dopings is in disagreement with the conclusion of Motoyama *et al.* (2007) who have found that the AF phase terminates at $x \approx 0.134$, before the occurrence of SC. There are a number of possible different explanations for this. It may be that the QCP of Dagan *et al.* (2004) and others is due not to the disappearance of the magnetic phase *per se*, but instead due to the occurrence of something like a Fermi surface topological transition. For instance, it could be associated with the emergence of the full Fermi surface around the (π, π) position from the pockets around $(\pi, 0)$ at low dopings. Such behavior, is consistent with the kink-like behavior in the Hall coefficient (Fig 25). It is also consistent with recent magnetic quantum oscillation experiments, which show a change in FS topology between $x = 0.16$ and $x = 0.17$ doping (Helm *et al.*, 2009). Such a transition could occur just as a result of the natural evolution of the FS with doping, or it may be that this 2nd transition signifies the termination of an additional order parameter hidden within the superconducting dome (Alff *et al.*, 2003), such as for instance DDW (Chakravarty *et al.*, 2001) or other orbital current states (Varma, 1999). However a transition involving only charge degrees of freedom is superficially at odds with experiments that show a relationship

of this transition to magnetism such as the sharp change in angular magnetoresistance at $x \approx 0.165$ (Dagan *et al.*, 2005b; Yu *et al.*, 2007b).

Another possibility is that the upper and lower transitions are one and the same and that there are large differences in effective doping between different groups' samples due to differing oxygen reduction procedures or other effects. This might be more expected in this case as the transport results of Dagan *et al.* (2004) and others have been mostly performed on films (in which the annealing process is more controllable), vs. the scattering measurements which have entirely been performed on single crystals. However, it is difficult to believe that differences in oxygen annealing could be causing such a large shift in the effective transition, as the crystal chemistry is not that imperfectly understood.

An alternative, but particularly plausible scenario is that the magnetic field used to suppress superconductivity to reveal the low temperature normal state actually stabilizes the SDW state at higher dopings. A similar situation is believed to be the case in the hole-doped materials (Demler *et al.*, 2001; Khaykovich *et al.*, 2002; Lake *et al.*, 2001, 2002; Moon and Sachdev, 2009). The situation in the electron-doped materials is inconclusive (see the discussion in Sec. III.F.3), but it has been argued that magnetic field enhances the magnetic ordered state in a somewhat similar fashion (Kang *et al.*, 2003b, 2005; Matsuura *et al.*, 2003). However, this scenario does not explain measurements like the optical or ARPES ones, which have been done in zero field.

It is also possible that what some of these latter measurements are actually sensitive to is the development of short range order or fluctuations. Measurements such as ARPES and optics have inferred the existence of a QCP by the extrapolated doping level where a magnetic pseudogap closes. However, as pointed out by Wang *et al.* (2006a) optical data clearly show the existence of a large pseudogap in underdoped samples at temperatures well above the Néel temperature. (Jenkins *et al.*, 2009b; Zimmers *et al.*, 2007b) showed that gap-like features still appear in their infrared Hall angle measurements even above those of the nominal QCP. As this implies that only short-range order is necessary for the existence of relatively well defined magnetic pseudogap in the charge spectra, it calls into question the utility of inferring the critical concentration of a magnetic QCP from such data. For instance, in Hubbard model calculations Kyung *et al.* (2004) have shown that a pseudogap can develop in the photoemission spectra when the AF correlation length exceeds the thermal de Broglie wavelength (see Sec. IV.I below) i.e. long range order in the ground state is not necessary to develop a PG at finite temperatures. However, it seems difficult to imagine however that calculations which only incorporate short range order and fluctuations can reproduce the sharp anomalies in transport (Hall effect etc.) found near $x = 0.165$. For this, it seems likely that some sort of long-range order must be involved. More work on this issue is clearly needed; For

instance we are not aware of any measurements that show QPT-like anomalies in transport near $x = 0.13$ and so even more detailed studies should be done.

H. Spin-density wave description of the normal state

As originally noticed by Armitage *et al.* (2001a), electron-doped samples near optimal doping present a FS, that while very close to that predicted by band structure calculations, have near- E_F ARPES spectral weight that is strongly suppressed (pseudogapped) at the momentum space positions where the underlying Fermi surface (FS) contour crosses the AF Brillouin zone boundary. This suggests the existence of a (π, π) scattering channel and a strong importance of this wavevector to the underlying physics. This should not be surprising when considering the close proximity of AF.

As discussed by Armitage (2001); Armitage *et al.* (2001a), one possible way to view the results - at least qualitatively - for samples near optimal doping is as a manifestation of a $\sqrt{2} \times \sqrt{2}$ band reconstruction from a static (or slowly fluctuating) spin density wave (SDW) or similar order with characteristic wavevector (π, π) . This distortion or symmetry reduction is such that if the order is long-range and static the BZ decreases in volume by 1/2 and rotates by 45° . The AFBZ boundary becomes the new BZ boundary and gaps form at the BZ edge in the usual way. Although an SDW is the natural choice based on the close proximity of the antiferromagnetic phase, the data are consistent with any ordering of characteristic wave vector (π, π) such as DDW (Chakravarty *et al.*, 2001). The $\sqrt{2} \times \sqrt{2}$ reconstructed band structure can be obtained *via* simple degenerate perturbation theory Armitage (2001); Matsui *et al.* (2005b); Park *et al.* (2007). This treatment gives

$$E_k = E_0 + 4t'(\cos k_x \cos k_y) + 2t''(\cos 2k_x + \cos 2k_y) \pm \sqrt{4t^2(\cos k_x + \cos k_y)^2 + |V_{\pi\pi}|^2} \quad (3)$$

where $V_{\pi\pi}$ is the strength of the effective (π, π) scattering, and t , t' and t'' are nearest, next nearest, and next next nearest hopping amplitudes. The even and odd solutions correspond to new band sheets that appear due to the additional Bragg scattering potential. With realistic hopping parameters for the cuprates (as discussed in Sec. II.C) a small hole pocket centered around $(\pi/2, \pi/2)$ and a small electron pocket around $(\pi, 0)$ appears at optimal doping as shown in Fig. 64b. All measured n -type cuprates near optimal doping show a phenomenology roughly consistent with this band structure (Armitage, 2001; Armitage *et al.*, 2001b; Matsui *et al.*, 2007; Zimmers *et al.*, 2005)³⁶. For instance, the $2V_{\pi, \pi}$ splitting

³⁶ Small differences between material classes do exist (Fig. 36). See

between the two band sheets in Fig 64b can be seen directly in a measurement of the ARPES spectral function along the AFBZ boundary as shown for SCCO in Fig. 64a.

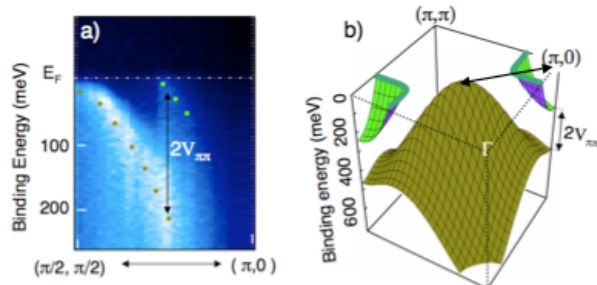


FIG. 64 (a) Measured ARPES spectral function along the AFBZ as given by the arrow in (b). The SDW gap $2V_{\pi\pi}$ is readily visible in the raw spectra. (b) Schematic of the band structure from a $\sqrt{2} \times \sqrt{2}$ reconstruction. Adapted from Park *et al.* (2007).

This derivation is for a potential with long-range order, which according to the Motoyama *et al.* (2007) does not exist above $x \approx 0.134$. Due to the ambiguity associated with the exact position of the phase boundary, possibly more relevant to the typical experimental case may be a situation where true long range order of the $\sqrt{2} \times \sqrt{2}$ phase does not exist, but where the material still has strong (but slow) fluctuations of this order. In this case more complicated treatments are necessary for quantitative treatments as discussed below. An analysis in the spirit of the above is then much harder, but as long as the fluctuations are slow, then some aspects of the above zone folding picture should remain. For instance depending on their particular time scales, some experiments may be sensitive to the proto-electron pocket around $(\pi, 0)$.

An interpretation based on such a zone folding scheme enables one to understand - at least qualitatively - issues such as the sign change in the Hall coefficient (Dagan *et al.*, 2007, 2004; Fournier *et al.*, 1997; Gollnik and Naito, 1998; Wang *et al.*, 1991). It had been a long standing mystery how a simply connected hole-like FS centered around (π, π) (originally thought to be the case from the first ARPES experiments of Anderson *et al.* (1993); King *et al.* (1993)) could give both positive and negative contribution to the Hall coefficient and thermopower. A mean field calculation of the Hall conductance based on the band structure in Eq. 3 shows that the data are qualitatively consistent with the reconstruction of the Fermi surface expected upon density wave ordering (Lin and Millis, 2005), although the calculation has difficulty reproducing the R_H values precisely^{37 38}.

the discussion in Sec. III.C.

³⁷ Again, in these calculations long range order has been assumed. It is difficult to reconcile the reasonable agreement of the data

Zimmers *et al.* (2005) showed that the notable pseudogaps in the optical conductivity as well as its overall shape can be reasonably modeled by a calculation based on the band structure in Eq. 3 and Fig. 64. As seen in Fig. 65 the overall temperature and frequency dependence matches well to the experimental data seen in the $x=0.10$ curves in Fig. 37 for instance.

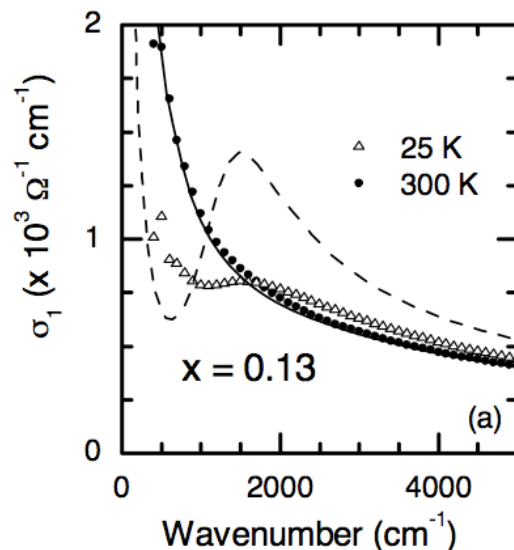


FIG. 65 Calculation of the optical conductivity based on the SDW band structure in Fig. 64. Spectra were calculated for a $x=0.13$ doping with a value of $2V_{\pi\pi} = 0.25$ eV and a gap opening temperature of 170K. The symbols are the measured optical conductivity for $x=0.13$ and the lines the spin density wave model calculation. Compare also to the $x = 0.10$ data in Fig. 37. From Zimmers *et al.* (2005).

Although it works best for samples near optimal doping, the SDW picture can be used to understand the doping dependence of the FS for a limited range near optimal doping. As materials are progressively underdoped and the antiferromagnetic phase is approached, antiferromagnetic correlations become stronger and the “hot spot” regions may spread so that the zone-diagonal spectral weight is gapped by the approximate (π, π) nesting of the $(\pi/2, \pi/2)$ section of FS with the $(-\pi/2, -\pi/2)$ section of FS. However a scheme based on nesting obviously breaks down as one approaches the Mott state, where the

and the mean-field model with the termination of the AF phase at $x \approx 0.134$ as inferred by Motoyama *et al.* (2007). More theoretical work and the explicit calculation of transport coefficients for systems with short range order and AF fluctuations are needed.

³⁸ More recent calculations by Jenkins *et al.* (2009a) using a band structure that takes into account the very anisotropic Fermi velocities observed experimentally in ARPES results has even worse quantitative agreement with the experimental R_H . They claim that with the inclusion of vertex corrections within the FLEX approximation (Kontani, 2008) can one describe the spectra.

zone diagonal spectral weight is not only gapped, but also vanishes. Experimentally, the near- E_F spectral weight near $(\pi/2, \pi/2)$ becomes progressively gapped with underdoping and by $x = 0.04$ in NCCO only an electron FS pocket exists around the $(\pi, 0)$ point (Fig. 33) (Armitage *et al.*, 2002). On the overdoped side, Matsui *et al.* (2007) have shown that this hot spot effect at E_F goes away in the ARPES spectra by $x = 0.17$ as expected by the virtual disappearance of antiferromagnetism and $V_{\pi, \pi}$ at that doping. In SCCO, Park *et al.* (2007) clearly resolved the $V_{\pi, \pi}$ splitting between SDW bands in underdoped ($x=0.14$ $T_c = 13$ K) in a cut along the AFBZ (See Fig. 64), while in essentially the same measurement Santander-Syro *et al.* (2009) showed that this splitting goes away by $x=0.15$ $T_c = 19$ K³⁹. That the FS is no longer reconstructed for overdoped samples, can also be seen in the quantum oscillations experiments of Helm *et al.* (2009).

However, interestingly, while infrared Hall angle measurements find that the low temperature response of underdoped and optimally doped samples' response is consistent with the SDW model, overdoped samples *cannot* be understood within a simple Drude or extended Drude model analysis at dopings beyond the nominal closing of the SDW gap at $x=0.17$ (Zimmers *et al.*, 2007b). Some signatures of the SDW remain. This shows the strong role of fluctuations even out of the ordered state. Jenkins *et al.* (2009b) claim these signatures in their overdoped lower energy far infrared data can be well described by a model incorporating vertex corrections due to AF fluctuations. Similarly even for underdoped samples the signatures of the gap remain in infrared Hall angle even above the gap closing temperature in σ_{xx} . These observations show the obvious limits of such a simple picture to understand all aspects of the data. As discussed elsewhere, the observation of AF-like spectral gap in parts of the phase diagram, which don't exhibit long-range AF might be understandable within models that propose that a PG evinces in the charge spectra when the AF correlation length exceeds the thermal de Broglie wavelength (Kyung *et al.*, 2004).

I. Existence of a pseudogap in the electron-doped cuprates?

As discussed above (Sec. II.A), the pseudogap of the p -type cuprates is one of the most enigmatic aspects of the high- T_c problem. Below a temperature scale T^* , underdoped cuprates are dominated by a suppression in various low-energy excitation spectra (Randeria, 2007; Timusk and Statt, 1999). It has been a matter of much

long standing debate whether this pseudogap is a manifestation of precursor superconductivity at temperatures well above T_c , or rather is indicative of some competing ordered phase.

An answer to the question of whether or not 'the Pseudogap' in the n -type cuprates exists is difficult to address conclusively because of a large ambiguity in its definition in the p -type materials. Moreover, its precise boundary depends on the material system and the experimental probe. Additionally, there has frequently been the distinction made between a 'high-energy' PG, which is associated with physics on the scale of the magnetic exchange J and a 'low-energy' PG, which is of the same order of the superconducting gap (Again see Sec. II.A above). What is clear is that there are undoubtedly a number of competing effects in underdoped cuprates. These have all frequently been confusingly conflated under the rubric of pseudogap phenomena. Here we concentrate on a number of manifestations of the phenomenology which can be directly compared to the p -type side. A number of similarities and differences are found.

At the outset of our discussion, it is interesting to point out that much of the pseudogap phenomena in the electron-doped cuprates seems to be related to antiferromagnetism and this phase's relative robustness in these materials. The issue of whether the PG exists is of course then intimately related to the issues presented above in Secs. IV.G and IV.H on the extent of antiferromagnetism and the SDW description of the normal state. It is interesting to note that the doping dependence of the Néel temperature T_N on the n -type side seems to have an approximate mirror symmetry with the dependence of the pseudogap onset T^* on the hole-doped side. Whether this is indicative of the fact that the pseudogap of the hole-doped side is a consequence of a very strong fluctuations of antiferromagnetism, but no long range order is an open issue.

As mentioned above, the optical conductivity of underdoped single crystals ($x = 0$ to 0.125) shows the opening of a high energy gap-like structure at temperatures well above the Néel temperature (Onose *et al.*, 2004). It can be viewed directly in the optical conductivity, which is in contrast to the hole-doped side, where gap-like features do not appear in the ab -plane optical conductivity itself and a 'pseudogap' is only exhibited in the frequency dependent scattering rate (Puchkov *et al.*, 1996). The gap closes gradually with doping and vanishes by superconducting concentrations of approximately $x = 0.15$ (Onose *et al.*, 2004) to $x = 0.17$ (Zimmers *et al.*, 2005). Onose *et al.* (2004) found that both its magnitude (Δ_{PG}) and its onset temperature (T^*) obeys the approximate relation $\Delta_{PG} = 10k_B T^*$ (Fig. 66). The magnitude of Δ_{PG} is comparable in magnitude to the pseudogap near $(\pi/2, \pi/2)$ in the photoemission spectra reported by (Armitage *et al.*, 2002) (also Fig. 66), which indicates that the pseudogap appearing in the optical spectra is the same as that found in photoemission. Note that this is the same gap-like feature, of which a remarkable number

³⁹ It is likely that these samples had different O levels due to different annealing procedures. This could account for the relative strength of AF

of aspects can be modeled at low T by the SDW band structure as given in Sec. IV.H. Onose *et al.* (2004) identify the pseudogap with the buildup of antiferromagnetic correlations because: (a) In the underdoped region long range AF order develops at a temperature T_N approximately half of T^* . (b) The intrinsic scale of the AF exchange interaction J is on the scale of the pseudogap magnitude (c) The gap anisotropy found in photoemission is consistent with that expected for 2D AF correlations with characteristic wavevector (π, π) as pointed out by Armitage *et al.* (2002).

These PG phenomena may be analogous to the ‘high-energy’ PG found in the hole-doped, although there are a number of differences as emphasized by Onose *et al.* (2004). (a) The large pseudogap of the hole-doped system is maximal near $(\pi, 0)$ in contrast with one more centered around $(\pi/2, \pi/2)$ of the n -type cuprate. (b) As mentioned, the pseudogap feature is not discernible in the ab -plane optical conductivity itself in the hole-doped cuprate, which may be because it is weaker than that in the electron-doped compound. (c) The ground state in the underdoped n -type system, where the pseudogap formation is observed strongest, is antiferromagnetic, while the superconducting phase is present even for underdoped samples in the hole-doped cuprate.

As pointed out above, it is also interesting that for a PG related to AF, it forms at a temperature well above T_N . This is presumably related to the fact that the spin correlation length ξ is found to be quite large at temperatures even 100 K above T_N , which follows from the quasi-2D nature of the magnetism. In this regard Motoyama *et al.* (2007) found that at the PG temperature T^* (as defined from the optical spectra) their spin correlation length ξ becomes of order the estimated thermal de Broglie wavelength $\xi_{th} = \hbar v_F / \pi k_B T$. This is a condition for the onset of the PG consistent with a number of theoretical calculations based on $t - t' - t'' - U$ models (Kyung *et al.*, 2004) that emphasize the build-up of AF correlations. In these models, it is proposed that the weaker coupling regime (smaller U/W) of the electron-doped cuprates allows the identification of the pseudogap with long AF correlation lengths. These theories make quantitative predictions of the momentum dependence of the PG in the ARPES spectra, the pseudogap onset temperature T^* , and the temperature and doping dependence of the AF correlation length, which are in accord with experiment. The hole-doped compounds appear to have stronger coupling and similar treatments give a pseudogap which is tied to the stronger local repulsive interaction and has different attributes (Kyung *et al.*, 2004, 2003). Although aspects (such as the PG’s momentum space location) are in qualitative agreement with experiment, quantities like the AF correlation length are in strong quantitative disagreement with neutron scattering results.

At lower energy scales, there have also been a number of tunneling experiments that have found evidence for a small normal state energy gap (NSG) (~ 5 meV)

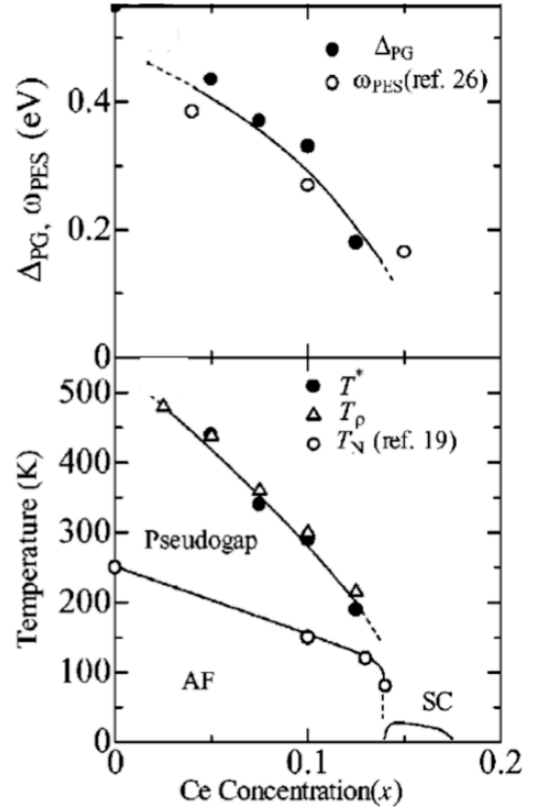


FIG. 66 (top) The x variation of the pseudogap magnitude Δ_{PG} as defined by the higher-lying isosbetic (equal-absorption) point in the temperature-dependent conductivity spectra and the magnitude of the pseudogap (ω_{PES}) in the photoemission spectra (Armitage *et al.*, 2002) (Ref. 26 in the figure). The ω_{PES} is defined as the maximum energy of the quasiparticle peak on the putative large Fermi surface in the ARPES spectra shown in the Figs. 2(c) - (e) of Armitage *et al.* (2002). (bottom) The obtained phase diagram. The onset temperature of pseudogap formation T^* and the crossover temperature of out-of-plane resistivity T_ρ (as given by the arrows in Fig. 28) are plotted against x together with the Néel temperature T_N reported previously by Luke *et al.* (1990) (Ref. 19 in the figure).

that seems somewhat analogous to the low-energy pseudogap found in the p -type materials. This normal state gap (NSG) is probed in the ab -plane by applying a c -axis magnetic field greater than H_{c2} (Alff *et al.*, 2003; Biswas *et al.*, 2001; Dagan *et al.*, 2005a; Kleefisch *et al.*, 2001). Dagan *et al.* (2005a) find that it is present at all doping from 0.11 to 0.19 and the temperature at which it disappears correlates with T_c , at least on the overdoped side of the SC dome. However, the NSG survives to very large magnetic fields and this is not obviously explained by the preformed Cooper pair scenario (Biswas *et al.*, 2001; Kleefisch *et al.*, 2001). Recently, Shan *et al.* (2008b) conclude that the NSG and the SC gap are different across the phase diagram, which is consistent with various ‘two-gap’ scenario in the underdoped p -type cuprates.

In contrast to these measurements, in PLCCO NMR

Zheng *et al.* (2003) found no sign of a *spin* pseudogap opening up at temperatures much larger than T_c , which is a hallmark of underdoped *p*-type cuprates and has been interpreted as singlet formation at high temperatures. Likewise the spin pseudogap observed in neutron scattering appears to close at T_c (Yamada *et al.*, 2003) and not at some higher temperature. This is consistent with a more mean field-like superconducting transition in these compounds, which may be tied to their apparently larger relative superfluid stiffness (4-15 times as compared to hole-doped compounds of similar T_c (Emery and Kivelson, 1995; Shengelaya *et al.*, 2005; Wu *et al.*, 1993)).⁴⁰

V. CONCLUDING REMARKS

Our understanding of the electron-doped cuprates has advanced tremendously in recent years. Still, some important issues remain unresolved and more research will be needed to gain a full understanding. In this review, we have tried show what aspects of the problem in the electron-doped cuprates are understood and which aspects are still unresolved. For instance, the role of oxygen and Ce doping is an important unresolved issue. There is no universal empirical relation for T_c vs in-plane carrier concentration in the *n*-type compounds, which is a reflection of the uncertainty in the true in-plane carrier concentration. However, it is clear that the oxygen reduction process does more than change the carrier concentration and results for instance in the formation of Cu-free epitaxial layers.

In the superconducting state, the evidence is now very strong that the pairing symmetry in both *n*- and *p*-type cuprates is predominately *d*-wave, although of a non-monotonic form in the *n*-type compounds. In both *n*- and *p*-type cuprates, AFM gives way to SC upon doping and eventually the systems turn to a metallic, non-SC Fermi liquid-like state. For both dopings, the normal state at the SC compositions is anomalous (non-FL) and is not yet well understood, although it is obvious that there is significant and important coupling to antiferromagnetism on at least the electron-doped side. Clearly an understanding of the metallic state on both sides is crucial to an understanding of the mechanism of the high- T_c SC.

Similarly, there is convincing evidence for a pseudogap which derives from AFM in the *n*-type compounds. This is in contrast to the pseudogap in the hole doped compounds, which is as of yet of unknown origin. An understanding of this difference between material classes is an important goal for future study. The issue of whether an additional competing order parameter co-exists with

SC and ends at a critical point just before or within the SC dome is still unresolved for both hole and electron doping, although there is strong evidence for such a scenario from transport measurements in the *n*-type cuprates. However, exactly what this competing order may be, and whether it is the same for both signs of charge carrier, is unclear at present. Interaction effects play a central role in both classes of cuprates, although they may be weaker on the *n*-doped side. For instance, numerical cluster calculations have been able to explain the gross features of the *n*-type phase diagram, pseudogap, and the evolution of the Fermi surface, in a manner not possible on the hole doped side.

A detailed comparison between the properties of *n*- and *p*-type cuprates will continue to be an important area of future investigation. Such studies should also prove themselves useful for understanding new classes of superconducting materials, such as the recently discovered iron-pnictides, which also show electron and hole doped varieties. With regards to the high- T_c problem, our hope is that systematic comparisons between the two sides of the cuprate phase diagram will give unique insight into what aspects of these compounds are universal, what aspects are not universal, and what aspects are crucial for the existence of high temperature superconductivity.

Acknowledgments

We would like to thank our various close collaborators on this subject including, S.M. Anlage, P. Bach, F. F. Balakirev, H. Balci, K. Behnia, J. Beauvais, A. Biswas, G. Blumberg, N. Bontemps, R. Budhani, S. Charlebois, S. Charpentier, G. Côté, Y. Dagan, A. Damascelli, H.D. Drew, D.L. Feng, J. Gauthier, R.G. Gianneta, S. G.-Proulx, M.È. Gosselin, M. Greven, I. Hetel, J. Higgins, R. Hill, C.C. Homes, S. Jandl, C. Kim, C.A. Kendziora, X. B.-Laganière, P. Li, B. Liang, C. Lobb, R.P.S.M. Lobo, D.H. Lu, E. Maiser, P.K. Mang, A. Millis, Y. Onose, M. Poirier, R. Prozorov, M. Qazilbash, P. Rauwel, J. Renaud, P. Richard, G. Riou, G. Roberge, F. Ronning, A.F. Santander-Syro, K.M. Shen, Z.-X. Shen, J. Sonier, L. Taillefer, F. Tafuri, I. Takeuchi, Y. Tokura, K.D. Truong, W. Yu, T. Venkatesan, and A. Zimmers.

We would also like to thank M.F. Armitage, D. Basov, C. Bourbonnais, C. Broholm, S. Brown, A. Chubukov, Y. Dagan, P. Dai, M. d' Astuto, T. Deveraux, H.D. Drew, N. Drichko, T. Giamarchi, M. Greven, G.S. Jenkins, H. Jung, C. Kim, F. Kruger, H.-G. Luo, J. Lynn, F. Marsiglio, E. Motoyama, J.P. Paglione, P. Richard, S. Sachdev, T. Sato, D. Sénéchal, K.M. Shen, M.P. Singh, T. Takahashi, Z. Tesanovic, A.-M. Tremblay, C. Varma, S. Wilson, W. Yu, J. Zaanen, J. Zhao, and A. Zimmers for various helpful conversations on these topics and/or their careful reading of this manuscript. NPA is also thankful for the hospitality of the Université de Genève, Département de Physique de la Matière Condensée where work on this manuscript began. Our work

⁴⁰ However, signs of superconducting fluctuations in the resistance have recently been found up to 32 K in a 26 K sample (Yu *et al.*, 2006).

has been supported by the Sloan Foundation, DOE DE-FG02-08ER46544, NSF DMR-0847652 [NPA], NSERC (Canada), CIFAR, CFI and FQRNT [PF], and NSF DMR-0653535 [RG].

References

- Abanov, A., A. V. Chubukov, and J. Schmalian, 2001, Phys. Rev. B **63**(18), 180510.
- Abbamonte, P., A. Rusydi, S. Smadici, G. D. Gu, G. A. Sawatzky, , and D. L. Feng, 2005, Nature Physics **1**, 155 .
- Abrahams, E., and C. M. Varma, 2003, Phys. Rev. B **68**(9), 094502.
- Aharony, A., R. J. Birgeneau, A. Coniglio, M. A. Kastner, and H. E. Stanley, 1988, Physical Review Letters **60**(13), 1330.
- Aichhorn, M., E. Arrigoni, M. Potthoff, and W. Hanke, 2006, Physical Review B (Condensed Matter and Materials Physics) **74**(23), 235117 (pages 6).
- Aizenman, M., and J. Wehr, 1990, Communications in Mathematical Physics **130**(3), 489.
- Akimitsu, J., S. Suzuki, M. Watanabe, and H. Sawa, 1988, Jpn. J. Appl. Phys. **27**(19), L1859.
- Alexander, M., H. Romberg, N. Nücker, P. Adelmann, J. Fink, J. T. Markert, M. B. Maple, S. Uchida, H. Takagi, Y. Tokura, A. C. W. P. James, and D. W. Murphy, 1991, Phys. Rev. B **43**(1), 333.
- Alexandrov, A. S., and N. F. Mott, 1996.
- Alff, L., A. Beck, R. Gross, A. Marx, S. Kleefisch, T. Bauch, H. Sato, M. Naito, and G. Koren, 1998a, Phys. Rev. B **58**(17), 11197.
- Alff, L., S. Kleefisch, U. Schoop, M. Zittartz, T. Kemen, T. Bauch, A. Marx, and R. Gross, 1998b, The European Physical Journal B - Condensed Matter and Complex Systems **5**(3), 423.
- Alff, L., Y. Krockenberger, B. Welter, M. Schonecke, R. Gross, D. Manske, and M. Naito, 2003, Nature **422**, 698.
- Alff, L., S. Meyer, S. Kleefisch, U. Schoop, A. Marx, H. Sato, M. Naito, and R. Gross, 1999, Phys. Rev. Lett. **83**(13), 2644.
- Allen, J. W., C. G. Olson, M. B. Maple, J.-S. Kang, L. Z. Liu, J.-H. Park, R. O. Anderson, W. P. Ellis, J. T. Markert, Y. Dalichaouch, and R. Liu, 1990, Phys. Rev. Lett. **64**(5), 595.
- Allen, P. B., 2001, Nature **412**, 494.
- Alloul, H., J. Bobroff, M. Gabay, and P. J. Hirschfeld, 2009, Reviews of Modern Physics **81**(1), 45 (pages 64).
- Alloul, H., T. Ohno, and P. Mendels, 1989, Phys. Rev. Lett. **63**(16), 1700.
- Alp, E. E., G. K. Shenoy, D. G. Hinks, D. W. C. II, L. Soderholm, H.-B. Schuttler, J. Guo, D. E. Ellis, P. A. Montano, and M. Ramanathan, 1987, Phys. Rev. B **35**(13), 7199.
- Alvarenga, A. D., D. Rao, J. A. Sanjurjo, E. Granado, I. Torriani, C. Rettori, S. Oseroff, J. Sarrao, and Z. Fisk, 1996, Phys. Rev. B **53**(2), 837.
- Andersen, O. K., A. I. Liechtenstein, O. Jepsen, and F. Paulsen, 1995, Journal of Physics and Chemistry of Solids **56**(12), 1573 (pages 19).
- Anderson, P., 1997, Advances in Physics **46**, 3.
- Anderson, P., 2006, arXiv:cond-mat/0609040 .
- Anderson, P. W., 1987, Science **235**(4793), 1196.
- Anderson, R. O., R. Claessen, J. W. Allen, C. G. Olson, C. Janowitz, L. Z. Liu, J.-H. Park, M. B. Maple, Y. Dalichaouch, M. C. de Andrade, R. F. Jardim, E. A. Early, *et al.*, 1993, Physical Review Letters **70**(20), 3163.
- Ando, Y., A. N. Lavrov, S. Komiyama, K. Segawa, and X. F. Sun, 2001, Phys. Rev. Lett. **87**(1), 017001.
- Andreone, A., A. Cassinese, A. Di Chiara, R. Vaglio, A. Gupta, and E. Sarnelli, 1994, Phys. Rev. B **49**(9), 6392.
- Anlage, S. M., D.-H. Wu, J. Mao, S. N. Mao, X. X. Xi, T. Venkatesan, J. L. Peng, and R. L. Greene, 1994, Phys. Rev. B **50**(1), 523.
- Aprili, M., M. Covington, E. Paraoanu, B. Niedermeier, and L. H. Greene, 1998, Phys. Rev. B **57**(14), R8139.
- Arai, M., T. Nishijima, Y. Endoh, T. Egami, S. Tajima, K. Tomimoto, Y. Shiohara, M. Takahashi, A. Garrett, and S. M. Bennington, 1999, Phys. Rev. Lett. **83**(3), 608.
- Ariando, D. Darminto, H. J. H. Smilde, V. Leca, D. H. A. Blank, H. Rogalla, and H. Hilgenkamp, 2005, Phys. Rev. Lett. **94**(16), 167001 (pages 4).
- Arima, T., Y. Tokura, and S. Uchida, 1993, Phys. Rev. B **48**(9), 6597.
- Armitage, N., and J. Hu, 2004, Phil. Mag. Lett. **84**, 105.
- Armitage, N. P., 2001, Stanford University thesis .
- Armitage, N. P., D. H. Lu, D. L. Feng, C. Kim, A. Damascelli, K. M. Shen, F. Ronning, Z.-X. Shen, Y. Onose, Y. Taguchi, and Y. Tokura, 2001a, Phys. Rev. Lett. **86**(6), 1126.
- Armitage, N. P., D. H. Lu, C. Kim, A. Damascelli, K. M. Shen, F. Ronning, D. L. Feng, P. Bogdanov, Z.-X. Shen, Y. Onose, Y. Taguchi, Y. Tokura, *et al.*, 2001b, Phys. Rev. Lett. **87**(14), 147003 (pages 4).
- Armitage, N. P., D. H. Lu, C. Kim, A. Damascelli, K. M. Shen, F. Ronning, D. L. Feng, P. Bogdanov, X. J. Zhou, W. L. Yang, Z. Hussain, P. K. Mang, *et al.*, 2003, Phys. Rev. B **68**(6), 064517 (pages 7).
- Armitage, N. P., F. Ronning, D. H. Lu, C. Kim, A. Damascelli, K. M. Shen, D. L. Feng, H. Eisaki, Z.-X. Shen, P. K. Mang, N. Kaneko, M. Greven, *et al.*, 2002, Phys. Rev. Lett. **88**(25), 257001 (pages 4).
- Asaf, U., I. Felner, and U. Yaron, 1993, Physica C **211**, 45 .
- Asayama, K., Y. Kitaoka, G. qing Zheng, and K. Ishida, 1996, Progress in Nuclear Magnetic Resonance Spectroscopy **28**(3-4), 221 , ISSN 0079-6565.
- B. Kyung, A.-M. T., D. Sénéchal, 2009, arXiv:0812.1228 .
- Bacci, S. B., E. R. Gagliano, R. M. Martin, and J. F. Annett, 1991, Phys. Rev. B **44**(14), 7504.
- Bakharev, O. N., I. M. Abu-Shiekh, H. B. Brom, A. A. Nugroho, I. P. McCulloch, and J. Zaanen, 2004, Physical Review Letters **93**(3), 037002 (pages 4).
- Balci, H., and R. L. Greene, 2004, Phys. Rev. Lett. **93**(6), 067001 (pages 4).
- Balci, H., C. P. Hill, M. M. Qazilbash, and R. L. Greene, 2003, Phys. Rev. B **68**(5), 054520 (pages 7).
- Balci, H., V. N. Smolyaninova, P. Fournier, A. Biswas, and R. L. Greene, 2002, Phys. Rev. B **66**, 174510.
- Basov, D. N., R. Liang, B. Dabrowski, D. A. Bonn, W. N. Hardy, and T. Timusk, 1996, Phys. Rev. Lett. **77**(19), 4090.
- Basov, D. N., and T. Timusk, 2005, Reviews of Modern Physics **77**(2), 721 (pages 59).
- Bauer, T., and C. Falter, 2008, Physical Review B (Condensed Matter and Materials Physics) **77**(14), 144503 (pages 21).
- Beal-Monod, M., C. Bourbonnais, and V. Emery, 1986, Phys. Rev. B **34**, 7716 .
- Beck, R., Y. Dagan, A. Milner, A. Gerber, and G. Deutscher, 2004, Phys. Rev. B **69**(14), 144506.

- Bednorz, J., and K. A. Müller, 1986, *Z. Phys. B* **64**, 189 (pages 4).
- Beesabathina, D. P., L. Salamanca-Riba, S. N. Mao, X. X. Xi, and T. Venkatesan, 1993, *Applied Physics Letters* **62**(23), 3022.
- Billinge, S. J. L., and T. Egami, 1993, *Phys. Rev. B* **47**(21), 14386.
- Biswas, A., P. Fournier, M. M. Qazilbash, V. N. Smolyaninova, H. Balmi, and R. L. Greene, 2002, *Phys. Rev. Lett.* **88**(20), 207004.
- Biswas, A., P. Fournier, V. N. Smolyaninova, R. C. Budhani, J. S. Higgins, and R. L. Greene, 2001, *Phys. Rev. B* **64**, 104519.
- Blonder, G. E., M. Tinkham, and T. M. Klapwijk, 1982, *Phys. Rev. B* **25**(7), 4515.
- Blumberg, G., P. Abbamonte, M. V. Klein, W. C. Lee, D. M. Ginsberg, L. L. Miller, and A. Zibold, 1996, *Phys. Rev. B* **53**(18), R11930.
- Blumberg, G., M. Kang, and M. V. Klein, 1997, *Phys. Rev. Lett.* **78**(12), 2461.
- Blumberg, G., A. Koitzsch, A. Gozar, B. S. Dennis, C. A. Kendziora, P. Fournier, and R. L. Greene, 2002, *Phys. Rev. Lett.* **88**, 107002.
- Blumberg, G., A. Koitzsch, A. Gozar, B. S. Dennis, C. A. Kendziora, P. Fournier, and R. L. Greene, 2003, *Phys. Rev. Lett.* **90**(14), 149702.
- Boeinger, G. S., Y. Ando, A. Passner, T. Kimura, M. Okuya, J. Shimoyama, K. Kishio, K. Tamasaku, N. Ichikawa, and S. Uchida, 1996, *Phys. Rev. Lett.* **77**(27), 5417.
- Bogdanov, P. V., A. Lanzara, S. A. Kellar, X. J. Zhou, E. D. Lu, W. J. Zheng, G. Gu, J.-I. Shimoyama, K. Kishio, H. Ikeda, R. Yoshizaki, Z. Hussain, *et al.*, 2000, *Phys. Rev. Lett.* **85**(12), 2581.
- Bonn, D., and W. Hardy, 1996, in *Physical Properties of High Temperature Superconductors V*, edited by D. Ginsberg (World Scientific, Singapore), p. 7.
- Bonn, D. A., P. Dosanjh, R. Liang, and W. N. Hardy, 1992, *Phys. Rev. Lett.* **68**(15), 2390.
- Borisenko, S. V., A. A. Kordyuk, A. Koitzsch, M. Knupfer, J. Fink, H. Berger, and C. T. Lin, 2004, *Nature B*, 431.
- Borsa, F., P. Carreta, J. H. Cho, F. C. Chou, Q. Hu, D. C. Johnston, A. Lascialfari, D. R. Torgeson, R. J. Gooding, N. M. Salem, and K. J. E. Vos, 1995, *Phys. Rev. B* **52**(10), 7334.
- Bourges, P., 1999, in *The gap Symmetry and Fluctuations in High Temperature Superconductors: Proceedings of NATO ASI summer school held September 1-13, 1997 in Carg'ese, France*, edited by D. P. J. Bok, G. Deutscher and S. Wolf (Plenum Press, 1998), pp. 349-371.
- Bourges, P., L. Boudarene, D. Petitgrand, and P. Galez, 1992, *Physica B* **180**, 447.
- Bourges, P., H. Casalta, A. S. Ivanov, and D. Petitgrand, 1997, *Physical Review Letters* **79**(24), 4906.
- Boyer, M. C., W. D. Wise, K. Chatterjee, M. Yi, T. Kondo, T. Takeuchi, H. Ikuta, and E. W. Hudson, 2007, *Nature Physics* **3**, 802.
- Braden, M., W. Paulius, A. Cousson, P. Vigoureux, G. Heger, A. Goukassov, P. Bourges, and D. Petitgrand, 1994, *Europhys. Lett.* **25**, 625.
- Braden, M., L. Pintschovius, T. Uefuji, and K. Yamada, 2005, *Physical Review B (Condensed Matter and Materials Physics)* **72**(18), 184517 (pages 10).
- Brinkmann, M., T. Rex, H. Bach, and K. Westerholt, 1996a, *Journal of Crystal Growth* **163**(4), 369, ISSN 0022-0248.
- Brinkmann, M., T. Rex, M. Stief, H. Bach, and K. Westerholt, 1996b, *Physica C* **269**(1-2), 76.
- Brookes, N. B., G. Ghiringhelli, O. Tjernberg, L. H. Tjeng, T. Mizokawa, T. W. Li, and A. A. Menovsky, 2001, *Phys. Rev. Lett.* **87**(23), 237003.
- Broun, D. M., W. A. Huttema, P. J. Turner, S. Özcan, B. Morgan, R. Liang, W. N. Hardy, and D. A. Bonn, 2007, *Physical Review Letters* **99**(23), 237003 (pages 4).
- Budhani, R. C., M. C. Sullivan, C. J. Lobb, and R. L. Greene, 2002, *Phys. Rev. B* **65**(10), 100517 (pages 4).
- Byczuk, K., M. Kollar, K. Held, Y.-F. Yang, I. A. Nekrasov, T. Pruschke, and D. Vollhardt, 2007, *Nature Physics* **3**, 168.
- Campuzano, J. C., M. R. Norman, and M. Randeria, 2004, in *Physics of Conventional and Unconventional Superconductors*, edited by K. H. Bennemann and J. B. Ketterson (Springer-Verlag, Berlin), volume II, pp. 167-273.
- Cappelluti, E., S. Ciuchi, and S. Fratini, 2008, arXiv:0801.4691v1.
- Carbotte, J., D. N. Basov, and E. Schachinger, 1999, *Nature* **401**, 354.
- Carlson, E. W., V. J. Emery, S. A. Kivelson, and D. Orgad, 2003, *The Physics of Conventional and Unconventional Superconductors*, edited by K. H. Bennemann, and J. B. Ketterson.
- Cassanho, A., D. R. Gabbe, and H. P. Jenssen, 1989, *Journal of Crystal Growth* **96**(4), 999.
- Chakravarty, S., R. B. Laughlin, D. K. Morr, and C. Nayak, 2001, *Phys. Rev. B* **63**(9), 094503.
- Chakravarty, S., A. Sudbo, P. W. Anderson, and S. Strong, 1993, *SCIENCE* **261**, 337 (pages 4).
- Chakravarty, B., 1981, *J. Phys. (Paris)* **42**, 1351.
- Chattopadhyay, T., J. W. Lynn, N. Rosov, T. E. Grigereit, S. N. Barilo, and D. I. Zhigunov, 1994, *Physical Review B (Condensed Matter)* **49**(14), 9944.
- Chen, C.-T., P. Seneor, N.-C. Yeh, R. P. Vasquez, L. D. Bell, C. U. Jung, J. Y. Kim, M.-S. Park, H.-J. Kim, and S.-I. Lee, 2002, *Phys. Rev. Lett.* **88**(22), 227002.
- Chen, H.-D., O. Vafek, A. Yazdani, and S.-C. Zhang, 2004, *Physical Review Letters* **93**(18), 187002 (pages 4).
- Chen, X. H., C. H. Wang, G. Y. Wang, X. G. Luo, J. L. Luo, G. T. Liu, and N. L. Wang, 2005, *Physical Review B (Condensed Matter and Materials Physics)* **72**(6), 064517 (pages 5).
- Cheong, S.-W., G. Aeppli, T. E. Mason, H. Mook, S. M. Hayden, P. C. Canfield, Z. Fisk, K. N. Clausen, and J. L. Martinez, 1991, *Phys. Rev. Lett.* **67**(13), 1791.
- Cherny, A. S., E. N. Khats'ko, G. Chouteau, J. M. Louis, A. A. Stepanov, P. Wyder, S. N. Barilo, and D. I. Zhigunov, 1992, *Phys. Rev. B* **45**(21), 12600.
- Chesca, B., K. Ehrhardt, M. Mossle, R. Straub, D. Koelle, R. Kleiner, and A. Tsukada, 2003, *Phys. Rev. Lett.* **90**(5), 057004 (pages 4).
- Chesca, B., M. Seifried, T. Dahm, N. Schopohl, D. Koelle, R. Kleiner, and A. Tsukada, 2005, *Phys. Rev. B* **71**(10), 104504 (pages 7).
- Chiao, M., R. W. Hill, C. Lupien, B. Popić, R. Gagnon, and L. Taillefer, 1999, *Phys. Rev. Lett.* **82**(14), 2943.
- Chiao, M., R. W. Hill, C. Lupien, L. Taillefer, P. Lambert, R. Gagnon, and P. Fournier, 2000, *Phys. Rev. B* **62**(5), 3554.
- Cho, B. K., J. H. Kim, Y. J. Kim, B.-h. O, J. S. Kim, and G. R. Stewart, 2001, *Phys. Rev. B* **63**(21), 214504.

- Chou, F. C., F. Borsa, J. H. Cho, D. C. Johnston, A. Lascialfari, D. R. Torgeson, and J. Ziolo, 1993, *Phys. Rev. Lett.* **71**(14), 2323.
- Christensen, N. B., D. F. McMorro, H. M. Rønnow, B. Lake, S. M. Hayden, G. Aeppli, T. G. Perring, M. Mangkorntong, M. Nohara, and H. Takagi, 2004, *Phys. Rev. Lett.* **93**(14), 147002.
- Claesson, T., M. Mnsson, C. Dallera, F. Venturini, C. D. Nadai, N. B. Brookes, and O. Tjernberg, 2004, *Physical Review Letters* **93**(13), 136402 (pages 4).
- Coldea, R., S. M. Hayden, G. Aeppli, T. G. Perring, C. D. Frost, T. E. Mason, S.-W. Cheong, and Z. Fisk, 2001, *Phys. Rev. Lett.* **86**(23), 5377.
- Coleman, P., 2007, in *Handbook of Magnetism and Advanced Magnetic Materials*, edited by H. Kronmüller and S. Parkin (J. Wiley and Sons), volume 1, pp. 95–148.
- Cooper, J. R., 1996, *Phys. Rev. B* **54**(6), R3753.
- Cooper, S. L., G. A. Thomas, J. Orenstein, D. H. Rapkin, M. Capizzi, T. Timusk, A. J. Millis, L. F. Schneemeyer, and J. V. Waszczak, 1989, *Phys. Rev. B* **40**(16), 11358.
- Corson, J., R. Mallozzi, J. Orenstein, J. Eckstein, and I. Bozovic, 1999, *Nature* **398**, 221.
- Côté, G., M. Poirier, and P. Fournier, 2008, *Journal of Applied Physics* **104**(12), 123914 (pages 7).
- Covington, M., M. Aprili, E. Paraoanu, L. H. Greene, F. Xu, J. Zhu, and C. A. Mirkin, 1997, *Phys. Rev. Lett.* **79**(2), 277.
- Covington, M., R. Scheuerer, K. Bloom, and L. H. Greene, 1996, *Applied Physics Letters* **68**(12), 1717.
- Cox, D. E., A. I. Goldman, M. A. Subramanian, J. Gopalakrishnan, and A. W. Sleight, 1989, *Phys. Rev. B* **40**(10), 6998.
- Cummins, T. R., and R. G. Egdell, 1993, *Phys. Rev. B* **48**(9), 6556.
- Curro, N. J., T. Imai, C. P. Slichter, and B. Dabrowski, 1997, *Phys. Rev. B* **56**(2), 877.
- Custers, J., P. Gegenwart, H. Wilhelm, K. Neumaier, Y. Tokiwa, O. Trovarelli, C. Geibel, F. Steglich, C. Ppin, and P. Coleman, 2003, *Nature* **424**, 524.
- Cyr-Choiniere, O., R. Daou, F. Laliberte, D. LeBoeuf, N. Doiron-Leyraud, J. Chang, J.-Q. Yan, J.-G. Cheng, J.-S. Zhou, J. B. Goodenough, S. Pyon, T. Takayama, *et al.*, 2009, *Nature* **458**(7239), 743, ISSN 0028-0836.
- Dagan, Y., M. C. Barr, W. M. Fisher, R. Beck, T. Dhakal, A. Biswas, and R. L. Greene, 2005a, *Physical Review Letters* **94**(5), 057005 (pages 4).
- Dagan, Y., R. Beck, and R. L. Greene, 2007, *Physical Review Letters* **99**(14), 147004 (pages 4).
- Dagan, Y., and R. L. Greene, 2004, unpublished .
- Dagan, Y., and R. L. Greene, 2007, *Physical Review B (Condensed Matter and Materials Physics)* **76**(2), 024506 (pages 4).
- Dagan, Y., M. M. Qazilbash, and R. L. Greene, 2005b, *Phys. Rev. Lett.* **94**(18), 187003.
- Dagan, Y., M. M. Qazilbash, C. P. Hill, V. N. Kulkarni, and R. L. Greene, 2004, *Phys. Rev. Lett.* **92**(16), 167001 (pages 4).
- Dagotto, E., 1994, *Rev. Mod. Phys.* **66**(3), 763.
- Dai, P., H. J. Kang, H. A. Mook, M. Matsuura, J. W. Lynn, Y. Kurita, S. Komiyama, and Y. Ando, 2005, *Phys. Rev. B* **71**(10), 100502 (pages 4).
- Dalichaouch, Y., M. de Andrade, and M. Maple, 1993, *Physica C: Superconductivity* **218**(1-2), 309, ISSN 0921-4534.
- Damascelli, A., Z. Hussain, and Z.-X. Shen, 2003, *Rev. Mod. Phys.* **75**(2), 473 (pages 69).
- Das, T., R. S. Markiewicz, and A. Bansil, 2007, *Physical Review Letters* **98**(19), 197004 (pages 4).
- d'Astuto, M., P. K. Mang, P. Giura, A. Shukla, P. Ghigna, A. Mirone, M. Braden, M. Greven, M. Krisch, and F. Sette, 2002, *Phys. Rev. Lett.* **88**(16), 167002.
- Demler, E., S. Sachdev, and Y. Zhang, 2001, *Phys. Rev. Lett.* **87**(6), 067202.
- Deutscher, G., 1999, *Nature* **397**, 410.
- Deutscher, G., 2005, *Rev. Mod. Phys.* **77**(1), 109 (pages 27).
- Devereaux, T. P., D. Einzel, B. Stadlober, R. Hackl, D. H. Leach, and J. J. Neumeier, 1994, *Phys. Rev. Lett.* **72**(3), 396.
- Devereaux, T. P., and R. Hackl, 2007, *Reviews of Modern Physics* **79**(1), 175 (pages 59).
- Dierker, S. B., M. V. Klein, G. W. Webb, and Z. Fisk, 1983, *Phys. Rev. Lett.* **50**(11), 853.
- Ding, H., M. R. Norman, J. C. Campuzano, M. Randeria, A. F. Bellman, T. Yokoya, T. Takahashi, T. Mochiku, and K. Kadowaki, 1996, *Phys. Rev. B* **54**(14), R9678.
- Ding, H., M. R. Norman, T. Yokoya, T. Takeuchi, M. Randeria, J. C. Campuzano, T. Takahashi, T. Mochiku, and K. Kadowaki, 1997, *Phys. Rev. Lett.* **78**(13), 2628.
- Doiron-Leyraud, N., C. Proust, D. LeBoeuf, J. Levallois, J.-B. Bonnemaison, R. Liang, D. Bonn, W. Hardy, and L. Taillefer, 2007, *Nature* **447**, 565.
- Durst, A. C., and P. A. Lee, 2000, *Phys. Rev. B* **62**(2), 1270.
- Emery, V. J., and S. A. Kivelson, 1992, *Journal of Physics and Chemistry of Solids* **53**(12), 1499.
- Emery, V. J., and S. A. Kivelson, 1993, *Physica C* **209**, 597.
- Emery, V. J., and S. A. Kivelson, 1995, *Nature* **374**, 434 (pages 4).
- Emery, V. J., and G. Reiter, 1988, *Phys. Rev. B* **38**(16), 11938.
- Endoh, Y., M. Matsuda, K. Yamada, K. Kakurai, Y. Hidaka, G. Shirane, and R. J. Birgeneau, 1989, *Phys. Rev. B* **40**(10), 7023.
- Eskes, H., G. Sawatzky, and L. Feiner, 1989, *Physica C* **160**, 424.
- Fauqué, B., Y. Sidis, V. Hinkov, S. Pailhès, C. T. Lin, X. Chaud, and P. Bourges, 2006, *Physical Review Letters* **96**(19), 197001 (pages 4).
- Fischer, O., M. Kugler, I. Maggio-Aprile, C. Berthod, and C. Renner, 2007, *Reviews of Modern Physics* **79**(1), 353 (pages 67).
- Fisher, D. S., G. Kotliar, and G. Moeller, 1995, *Phys. Rev. B* **52**(24), 17112.
- Fogelström, M., D. Rainer, and J. A. Sauls, 1997, *Phys. Rev. Lett.* **79**(2), 281.
- Fontcuberta, J. T., and L. Fabrega, 1996, in *Studies of High Temperature Superconductors*, edited by A. V. Narlikar (Nova Science Publishers, Commack, NY), volume 16, p. 185.
- Fournier, P., M.-E. Gosselin, S. Savard, J. Renaud, I. Hetel, P. Richard, and G. Riou, 2004, *Phys. Rev. B* **69**, 220501.
- Fournier, P., and R. L. Greene, 2003, *Phys. Rev. B* **68**, 094507.
- Fournier, P., J. Higgins, H. Balci, E. Maiser, C. J. Lobb, and R. L. Greene, 2000, *Phys. Rev. B* **62**, 11 993.
- Fournier, P., X. Jiang, W. Jiang, S. N. Mao, T. Venkatesan, C. J. Lobb, and R. L. Greene, 1997, *Phys. Rev. B* **56**, 14149.
- Fournier, P., E. Maiser, and R. L. Greene, 1998a, in *The Gap Symmetry and Fluctuations in High-T_c Superconductors*,

- edited by J. Bok, G. Deutscher, D. Pavuna, and S. Wolf (NATO ASI Series B), volume 371, p. 145.
- Fournier, P., P. Mohanty, E. Maiser, S. Darzens, T. Venkatesan, C. J. Lobb, G. Czjzek, R. A. Webb, and R. L. Greene, 1998b, *Phys. Rev. Lett.* **81**, 4720.
- Fujimori, A., Y. Tokura, H. Eisaki, H. Takagi, S. Uchida, and E. Takayama-Muromachi, 1990, *Phys. Rev. B* **42**(1), 325.
- Fujita, M., H. Goka, K. Yamada, and M. Matsuda, 2002, *Phys. Rev. Lett.* **88**(16), 167008.
- Fujita, M., T. Kubo, S. Kuroshima, T. Uefuji, K. Kawashima, K. Yamada, I. Watanabe, and K. Nagamine, 2003, *Phys. Rev. B* **67**(1), 014514 (pages 5).
- Fujita, M., M. Matsuda, B. Fak, C. D. Frost, and K. Yamada, 2006, *J. Phys. Soc. Jpn.* **75**, 093704.
- Fujita, M., M. Matsuda, S. Katano, and K. Yamada, 2004, *Physical Review Letters* **93**(14), 147003 (pages 4).
- Fujita, M., M. Matsuda, S.-H. Lee, M. Nakagawa, and K. Yamada, 2008a, *Physical Review Letters* **101**(10), 107003 (pages 4).
- Fujita, M., M. Nakagawa, C. D. Frost, and K. Yamada, 2008b, *Journal of Physics: Conference Series* **108**, 012006 (4pp).
- Fukuda, M., M. K. Zalalutdinov, V. Kovacik, T. Minoguchi, T. Obata, M. Kubota, and E. B. Sonin, 2005, *Phys. Rev. B* **71**(21), 212502 (pages 4).
- Gamayunov, K., I. Tanaka, and H. Kojima, 1994, *Physica C: Superconductivity* **228**(1-2), 58.
- Gantmakher, V. F., S. N. Ermolov, G. E. Tsydynzhapov, A. A. Zhukov, and T. I. Baturina, 2003, *JETP Letters* **77**(8), 424.
- Gauthier, J., S. Gagné, J. Renaud, M.-E. Gosselin, P. Fournier, and P. Richard, 2007, *Physical Review B (Condensed Matter and Materials Physics)* **75**(2), 024424 (pages 6).
- Georges, A., G. Kotliar, W. Krauth, and M. Rozenberg, 1996, *Rev. Mod. Phys.* **68**, 13 .
- Geshkenbein, V. B., A. I. Larkin, and A. Barone, 1987, *Phys. Rev. B* **36**(1), 235.
- Ghamaty, S., B. Lee, J. Markert, E. Early, T. Bjrnholm, C. Seaman, and M. Maple, 1989, *Physica C: Superconductivity* **160**(2), 217 , ISSN 0921-4534.
- Gilardi, R., A. Hiess, N. Momono, M. Oda, M. Ido, and J. Mesot, 2004, *Europhys. Lett.* **66**(6), 840 (pages 7).
- Goldman, A. M., and N. Markovic, 1998, *Physics Today* **51**(11), 39.
- Gollnik, F., and M. Naito, 1998, *Phys. Rev. B* **58**(17), 11734.
- Gomes, K., A. Pasupathy, A. Pushp, S. Ono, Y. Ando, and A. Yazdani, 2007, *Nature* **447**, 569.
- Gooding, R. J., K. J. E. Vos, and P. W. Leung, 1994, *Phys. Rev. B* **50**(17), 12866.
- Graf, J., G.-H. Gweon, K. McElroy, S. Y. Zhou, C. Jozwiak, E. Rotenberg, A. Bill, T. Sasagawa, H. Eisaki, S. Uchida, H. Takagi, D.-H. Lee, *et al.*, 2007, *Physical Review Letters* **98**(6), 067004 (pages 4).
- Granath, M., 2004, *Phys. Rev. B* **69**(21), 214433.
- Granath, M., V. Oganessian, S. A. Kivelson, E. Fradkin, and V. J. Emery, 2001, *Phys. Rev. Lett.* **87**(16), 167011.
- Gromko, A. D., A. V. Fedorov, Y.-D. Chuang, J. D. Koralek, Y. Aiura, Y. Yamaguchi, K. Oka, Y. Ando, and D. S. Dessau, 2003, *Phys. Rev. B* **68**(17), 174520.
- Gupta, A., G. Koren, C. C. Tsuei, A. Segmüller, and T. R. McGuire, 1989, *Applied Physics Letters* **55**(17), 1795.
- Gurvitch, M., and A. T. Fiory, 1987, *Phys. Rev. Lett.* **59**(12), 1337.
- Hackl, A., and S. Sachdev, 2009, arXiv:0901.2348 .
- Hagen, S. J., J. L. Peng, Z. Y. Li, and R. L. Greene, 1991, *Physical Review B (Condensed Matter)* **43**(16), 13606.
- Hanaguri, T., C. Lupien, Y. Kohsaka, D. H. Lee, M. Azuma, M. Takano, H. Takagi, and J. C. Davis, 2004, *Nature* **430**, 1001.
- Hardy, W. N., D. A. Bonn, D. C. Morgan, R. Liang, and K. Zhang, 1993, *Phys. Rev. Lett.* **70**(25), 3999.
- Harima, N., A. Fujimori, T. Sugaya, and I. Terasaki, 2003, *Phys. Rev. B* **67**(17), 172501.
- Harima, N., J. Matsuno, A. Fujimori, Y. Onose, Y. Taguchi, and Y. Tokura, 2001, *Phys. Rev. B* **64**(22), 220507.
- van Harlingen, D. J., 1995, *Rev. Mod. Phys.* **67**(2), 515.
- Harshman, D. R., G. Aeppli, G. P. Espinosa, A. S. Cooper, J. P. Remeika, E. J. Ansaldo, T. M. Riseman, D. L. Williams, D. R. Noakes, B. Ellman, and T. F. Rosenbaum, 1988, *Phys. Rev. B* **38**(1), 852.
- Haule, K., and G. Kotliar, 2007, *Physical Review B (Condensed Matter and Materials Physics)* **76**(10), 104509 (pages 37).
- Helm, T., M. V. Kartsovnik, M. Bartkowiak, N. Bittner, M. Lambacher, A. Erb, J. Wosnitza, and R. Gross, 2009, arXiv:0906.1431v1 .
- Heyen, E. T., R. Liu, M. Cardona, S. Piol, R. J. Melville, D. M. Paul, E. Morán, and M. A. Alario-Franco, 1991, *Phys. Rev. B* **43**(4), 2857.
- Hidaka, Y., and M. Suzuki, 1989, *Nature* **338**, 635 .
- Higgins, J. S., Y. Dagan, M. C. Barr, B. D. Weaver, and R. L. Greene, 2006, *Phys. Rev. B* **73**(10), 104510 (pages 5).
- Hilgenkamp, H., and J. Mannhart, 2002, *Reviews of Modern Physics* **74**(2), 485 (pages 65).
- Hill, R. W., C. Proust, L. Taillefer, P. Fournier, and R. L. Greene, 2001, *Nature* **414**, 711.
- Hirsch, J. E., 1995, *Physica C* **243**, 319.
- Hirschfeld, P. J., and N. Goldenfeld, 1993, *Phys. Rev. B* **48**(6), 4219.
- Hlubina, R., and T. M. Rice, 1995, *Physical Review B (Condensed Matter)* **51**(14), 9253.
- Hodges, C., H. Smith, and J. W. Wilkins, 1971, *Phys. Rev. B* **4**(2), 302.
- Hoffman, J. E., E. W. Hudson, K. M. Lang, V. Madhavan, H. Eisaki, S. Uchida, and J. C. Davis, 2002a, *Science* **295**(5554), 466.
- Hoffman, J. E., K. McElroy, D.-H. Lee, K. M. Lang, H. Eisaki, S. Uchida, and J. C. Davis, 2002b, *Science* **297**(5584), 1148.
- Homes, C. C., B. P. Clayman, J. L. Peng, and R. L. Greene, 1997, *Physical Review B (Condensed Matter)* **56**(9), 5525.
- Homes, C. C., R. P. S. M. Lobo, P. Fournier, A. Zimmers, and R. L. Greene, 2006, *Physical Review B (Condensed Matter and Materials Physics)* **74**(21), 214515 (pages 8).
- Homes, C. C., T. Timusk, R. Liang, D. A. Bonn, and W. N. Hardy, 1993, *Phys. Rev. Lett.* **71**(10), 1645.
- Howald, C., H. Eisaki, N. Kaneko, M. Greven, and A. Kapitulnik, 2003a, *Phys. Rev. B* **67**(1), 014533.
- Howald, C., H. Eisaki, N. Kaneko, and A. Kapitulnik, 2003b, *PNAS* **100**, 9705.
- Howald, C., P. Fournier, and A. Kapitulnik, 2001, *Phys. Rev. B* **64**(10), 100504.
- Hu, C.-R., 1994, *Phys. Rev. Lett.* **72**(10), 1526.
- Hui, K., and A. N. Berker, 1989, *Phys. Rev. Lett.* **62**(21), 2507.
- Hundley, M. F., J. D. Thompson, S.-W. Cheong, Z. Fisk, and B. Oseroff, 1989, *Physica C* **158**, 102.
- Hybertsen, M. S., E. B. Stechel, M. Schluter, and D. R. Jennison, 1990, *Phys. Rev. B* **41**(16), 11068.

- Ignatov, A. Y., A. A. Ivanov, A. P. Menushenkov, S. Iacobucci, and P. Lagarde, 1998, *Phys. Rev. B* **57**(14), 8671.
- Ikeda, M., T. Yoshida, A. Fujimori, M. Kubota, K. Ono, H. Das, T. Saha-Dasgupta, K. Unozawa, Y. Kaga, T. Sasagawa, and H. Takagi, 2008, arXiv:0803.4059 .
- Ikeda, M., T. Yoshida, A. Fujimori, M. Kubota, K. Ono, Y. Kaga, T. Sasagawa, and H. Takagi, 2009, arXiv:0902.4280v1 .
- Ikeda, M., T. Yoshida, A. Fujimori, M. Kubota, K. Ono, K. Unozawa, T. Sasagawa, and H. Takagi, 2007, *J. Supercond. Nov. Mag.* **20**, 563.
- Ikeda, N., Z. Hiroi, M. Azuma, M. Takano, Y. Bando, and Y. Takeda, 1993, *Physica C: Superconductivity* **210**(3-4), 367 .
- Imai, T., C. P. Slichter, J. L. Cobb, and J. T. Markert, 1995, *J. Phys. Chem. Solids* **56**, 1921.
- Imry, Y., and M. Wortis, 1979, *Phys. Rev. B* **19**(7), 3580.
- Ino, A., C. Kim, M. Nakamura, T. Yoshida, T. Mizokawa, Z.-X. Shen, A. Fujimori, T. Kakeshita, H. Eisaki, and S. Uchida, 2000, *Phys. Rev. B* **62**(6), 4137.
- Ioffe, A. F., and A. R. Regel, 1960, *Prog. Semicond.* **4**, 237.
- Ishii, H., T. Koshizawa, H. Kataura, T. Hanyu, H. Takai, K. Mizoguchi, K. Kume, I. Shiozaki, and S. Yamaguchi, 1989, *Jpn. J. Appl. Phys.* **28**, L1952.
- Ismer, J.-P., I. Eremin, E. Rossi, and D. K. Morr, 2007, *Physical Review Letters* **99**(4), 047005 (pages 4).
- James, A. C. W. P., S. M. Zahurak, and D. W. Murphy, 1989, *Nature* **338**, 240.
- Jandl, S., P. Dufour, T. Strach, T. Ruf, M. Cardona, V. Nekvasil, C. Chen, B. M. Wanklyn, and S. Piñol, 1996, *Phys. Rev. B* **53**(13), 8632.
- Jandl, S., M. Iliev, C. Thomsen, T. Ruf, M. Cardona, B. M. Wanklyn, and C. Chen, 1993, *Solid State Communications* **87**(7), 609.
- Jandl, S., P. Richard, V. Nekvasil, D. I. Zhigunov, S. N. Barilo, and S. V. Shiryayev, 1999, *Physica C* **314**, 189.
- Jenkins, G. S., D. C. Schmadel, P. L. Bach, R. L. Greene, X. Bechamp-Laganiere, G. Roberge, P. Fournier, , and H. D. Drew, 2009a, arXiv:0902.1455v1 .
- Jenkins, G. S., D. C. Schmadel, P. L. Bach, R. L. Greene, X. B.-L. G. Roberge, P. Fournier, H. Kontani, , and H. D. Drew, 2009b, arXiv:0901.1701v1 .
- Jiang, W., S. N. Mao, X. X. Xi, X. Jiang, J. L. Peng, T. Venkatesan, C. J. Lobb, and R. L. Greene, 1994, *Phys. Rev. Lett.* **73**(9), 1291.
- Johnson, P. D., T. Valla, A. V. Fedorov, Z. Yusof, B. O. Wells, Q. Li, A. R. Moodenbaugh, G. D. Gu, N. Koshizuka, C. Kendziora, S. Jian, and D. G. Hinks, 2001, *Phys. Rev. Lett.* **87**(17), 177007.
- Jorgensen, J. D., P. G. Radaelli, D. G. Hinks, J. L. Wagner, S. Kikkawa, G. Er, and F. Kanamaru, 1993, *Phys. Rev. B* **47**(21), 14654.
- Joynt, R., and L. Taillefer, 2002, *Rev. Mod. Phys.* **74**(1), 235 (pages 60).
- Jung, C. U., J. Y. Kim, M.-S. Park, M.-S. Kim, H.-J. Kim, S. Y. Lee, and S.-I. Lee, 2002, *Phys. Rev. B* **65**(17), 172501.
- Kadono, R., W. Higemoto, A. Koda, M. I. Larkin, G. M. Luke, A. T. Savici, Y. J. Uemura, K. M. Kojima, T. Okamoto, T. Kakeshita, S. Uchida, T. Ito, *et al.*, 2004a, *Physical Review B (Condensed Matter and Materials Physics)* **69**(10), 104523 (pages 5).
- Kadono, R., K. Ohishi, A. Koda, , W. Higemoto, K. M. Kojima, S. ichi Kuroshima, M. Fujita, and K. Yamada, 2004b, *Journal of the Physical Society of Japan* **73**(11), 2944.
- Kadono, R., K. Ohishi, A. Koda, S. R. Saha, W. Higemoto, M. Fujita, and K. Yamada, 2005, *Journal of the Physical Society of Japan* **74**(10), 2806.
- Kakuyanagi, K., K.-i. Kumagai, and Y. Matsuda, 2002, *Phys. Rev. B* **65**(6), 060503.
- Kaminski, A., J. Mesot, H. Fretwell, J. C. Campuzano, M. R. Norman, M. Randeria, H. Ding, T. Sato, T. Takahashi, T. Mochiku, K. Kadowaki, and H. Hoehchst, 2000, *Phys. Rev. Lett.* **84**(8), 1788.
- Kaminski, A., M. Randeria, J. C. Campuzano, M. R. Norman, H. Fretwell, J. Mesot, T. Sato, T. Takahashi, and K. Kadowaki, 2001, *Phys. Rev. Lett.* **86**(6), 1070.
- Kaminski, A., S. Rosenkranz, H. M. Fretwell, J. C. Campuzano, Z. Li, H. Raffy, W. G. Cullen, H. You, C. G. Olson, C. M. Varma, , and H. Hochst, 2002, *Nature* **416**, 610.
- Kampf, A. P., and J. R. Schrieffer, 1990, *Phys. Rev. B* **42**(13), 7967.
- Kancharla, S. S., B. Kyung, D. Senechal, M. Civelli, M. Capone, G. Kotliar, and A.-M. S. Tremblay, 2008, *Physical Review B (Condensed Matter and Materials Physics)* **77**(18), 184516 (pages 12).
- Kaneko, N., Y. Hidaka, S. Hosoya, K. Yamada, Y. Endoh, S. Takekawa, and K. Kitamura, 1999, *Journal of Crystal Growth* **197**(4), 818 , ISSN 0022-0248.
- Kang, H. J., P. Dai, B. J. Campbell, P. J. Chupas, S. Rosenkranz, P. L. Lee, Q. Huang, S. Li, S. Komiya, and Y. Ando, 2007, *Nat Mater* **6**(3), 224, ISSN 1476-1122.
- Kang, H. J., P. Dai, J. W. Lynn, M. Matsuura, J. R. Thompson, S.-C. Zhang, D. N. Argyriou, Y. Onose, and Y. Tokura, 2003a, *Nature* **423**(6939), 522, ISSN 0028-0836.
- Kang, H. J., P. Dai, J. W. Lynn, M. Matsuura, J. R. Thompson, S.-C. Zhang, D. N. Argyriou, Y. Onose, and Y. Tokura, 2003b, *Nature* **429**, 140 (pages 1).
- Kang, H. J., P. Dai, D. Mandrus, R. Jin, H. A. Mook, D. T. Adroja, S. M. Bennington, S.-H. Lee, and J. W. Lynn, 2002, *Phys. Rev. B* **66**(6), 064506.
- Kang, H. J., P. Dai, H. A. Mook, D. N. Argyriou, V. Sikolenko, J. W. Lynn, Y. Kurita, S. Komiya, and Y. Ando, 2005, *Phys. Rev. B* **71**(21), 214512 (pages 17).
- ichi Karimoto, S., and M. Naito, 2004, *Applied Physics Letters* **84**(12), 2136.
- Kashiwaya, S., T. Ito, K. Oka, S. Ueno, H. Takashima, M. Koyanagi, Y. Tanaka, and K. Kajimura, 1998, *Phys. Rev. B* **57**(14), 8680.
- Kashiwaya, S., Y. Tanaka, M. Koyanagi, H. Takashima, and K. Kajimura, 1995, *Phys. Rev. B* **51**(2), 1350.
- Kastner, M. A., R. J. Birgeneau, G. Shirane, and Y. Endoh, 1998, *Rev. Mod. Phys.* **70**(3), 897.
- Katano, S., M. Sato, K. Yamada, T. Suzuki, and T. Fukase, 2000, *Physical Review B (Condensed Matter and Materials Physics)* **62**(22), R14677.
- Kawakami, T., T. Shibauchi, Y. Terao, and M. Suzuki, 2006, *Physical Review B (Condensed Matter and Materials Physics)* **74**(14), 144520 (pages 7).
- Kawakami, T., T. Shibauchi, Y. Terao, M. Suzuki, and L. Krusin-Elbaum, 2005, *Physical Review Letters* **95**(1), 017001 (pages 4).
- Keimer, B., A. Aharony, A. Auerbach, R. J. Birgeneau, A. Cassanho, Y. Endoh, R. W. Erwin, M. A. Kastner, and G. Shirane, 1992, *Physical Review B (Condensed Matter)* **45**(13), 7430.
- Kendziora, C., B. Nachumi, P. Fournier, Z. Y. Li, R. L. Greene, and D. G. Hinks, 2001, *Physica C* **364-365**, 541.
- Khasanov, R., A. Shengelaya, A. Maisuradze, D. D. Castro,

- I. M. Savić, S. Weyeneth, M. S. Park, D. J. Jang, S.-I. Lee, and H. Keller, 2008, *Physical Review B (Condensed Matter and Materials Physics)* **77**(18), 184512.
- Khaykovich, B., Y. S. Lee, R. W. Erwin, S.-H. Lee, S. Wakimoto, K. J. Thomas, M. A. Kastner, and R. J. Birgeneau, 2002, *Physical Review B (Condensed Matter and Materials Physics)* **66**(1), 014528 (pages 8).
- Khurana, A., 1989, *Physics Today* **42**(April), 17.
- Kikkawa, G., F. Kanamaru, Y. Miyamoto, S. Tanaka, M. Sera, M. Sato, Z. Hiroi, M. Takano, and Y. Bando, 1992, *Physica C: Superconductivity* **196**(3-4), 271 .
- Kim, J. S., and D. R. Gaskell, 1993, *Physica C* **209**(4), 381.
- Kim, M.-S., T. R. Lemberger, C. U. Jung, J.-H. Choi, J. Y. Kim, H.-J. Kim, and S.-I. Lee, 2002, *Phys. Rev. B* **66**(21), 214509.
- Kim, M.-S., J. A. Skinta, T. R. Lemberger, A. Tsukada, and M. Naito, 2003, *Phys. Rev. Lett.* **91**(8), 087001 (pages 4).
- King, D. M., Z.-X. Shen, D. S. Dessau, B. O. Wells, W. E. Spicer, A. J. Arko, D. S. Marshall, J. DiCarlo, A. G. Loeser, C. H. Park, E. R. Ratner, J. L. Peng, *et al.*, 1993, *Physical Review Letters* **70**(20), 3159.
- Kirtley, J. R., C. C. Tsuei, M. Rupp, J. Z. Sun, L. S. Yu-Jahnes, A. Gupta, M. B. Ketchen, K. A. Moler, and M. Bhusan, 1996, *Phys. Rev. Lett.* **76**(8), 1336.
- Kivelson, S. A., I. P. Bindloss, E. Fradkin, V. Oganesyan, J. M. Tranquada, A. Kapitulnik, and C. Howald, 2003, *Rev. Mod. Phys.* **75**(4), 1201.
- Klamut, P., A. Sikora, Z. Bukowski, B. Dabrowski, and J. Klamut, 1997, *Physica C* **282-287**, 541.
- Kleefisch, S., B. Welter, A. Marx, L. Alff, R. Gross, and M. Naito, 2001, *Phys. Rev. B* **63**(10), 100507.
- Koike, Y., A. Kakimoto, M. Mochida, H. Sato, T. Noji, M. Kato, and Y. Saito, 1992, *Jpn. J. Appl. Phys* **31**, 2721.
- Koitzsch, A., G. Blumberg, A. Gozar, B. Dennis, P. Fournier, and R. Greene, 2003, *Phys. Rev. B* **67**, 184522.
- Kokales, J. D., P. Fournier, L. V. Mercaldo, V. V. Talanov, R. L. Greene, and S. M. Anlage, 2000, *Phys. Rev. Lett.* **85**, 3696.
- Kontani, H., 2008, *Rep. Prog. Phys.* **71**, 026501.
- Kordyuk, A. A., S. V. Borisenko, M. S. Golden, S. Legner, K. A. Nenkov, M. Knupfer, J. Fink, H. Berger, L. Forró, and R. Follath, 2002, *Phys. Rev. B* **66**(1), 014502.
- Kramers, H., 1930, *Proc. Amsterdam Acad.* **33**, 959.
- Krishana, K., J. M. Harris, and N. P. Ong, 1995, *Phys. Rev. Lett.* **75**(19), 3529.
- Krol, A., Y. L. Soo, Z. H. Ming, S. Huang, Y. H. Kao, G. C. Smith, K. Lee, A. C. W. P. James, and D. W. Murphy, 1992, *Phys. Rev. B* **46**(1), 443.
- Krüger, F., S. D. Wilson, L. Shan, S. Li, Y. Huang, H.-H. Wen, S.-C. Zhang, P. Dai, and J. Zaanen, 2007, *Physical Review B (Condensed Matter and Materials Physics)* **76**(9), 094506 (pages 9).
- Kuiper, P., G. Kruizinga, J. Ghijsen, M. Gioni, P. J. W. Weijs, F. M. F. de Groot, G. A. Sawatzky, H. Verweij, L. F. Feiner, and H. Petersen, 1988, *Phys. Rev. B* **38**(10), 6483.
- Kurahashi, K., H. Matsushita, M. Fujita, and K. Yamada, 2002, *Journal of the Physical Society of Japan* **71**(3), 910.
- Kuroshima, S., M. Fujita, T. Uefuji, M. Matsuda, and K. Yamada, 2003, *Physica C* **392-396**, 216.
- Kusko, C., R. S. Markiewicz, M. Lindroos, and A. Bansil, 2002, *Phys. Rev. B* **66**(14), 140513 (pages 4).
- Kwei, G. H., S.-W. Cheong, Z. Fisk, F. H. Garzon, J. A. Goldstone, and J. D. Thompson, 1989, *Phys. Rev. B* **40**(13), 9370.
- Kyung, B., V. Hankevych, A.-M. Dare, and A.-M. S. Tremblay, 2004, *Phys. Rev. Lett.* **93**(14), 147004 (pages 4).
- Kyung, B., J.-S. Landry, and A.-M. S. Tremblay, 2003, *Phys. Rev. B* **68**(17), 174502 (pages 5).
- Lake, B., G. Aeppli, K. N. Clausen, D. F. McMorrow, K. Lefmann, N. E. Hussey, N. Mangkorntong, M. Nohara, H. Takagi, T. E. Mason, and A. Schrder, 2001, *Science* **291**(5509), 1759 .
- Lake, B., H. M. Rønnow, N. B. Christensen, G. Aeppli, K. Lefmann, D. F. McMorrow, P. Vorderwisch, P. Smeibidl, N. Mangkorntong, T. Sasagawa, M. Nohara, H. Takagi, *et al.*, 2002, *Nature* **415**, 219.
- Laufredi, A., S. Sergeenkov, and F. Araujo-Moreira, 2006, *Physica C: Superconductivity* **450**(1-2), 40.
- Lang, K., V. Madhavan, J. Hoffman, E. Hudson, H. Eisaki, S. Uchida, and J. Davis, 2002, *Nature* **415**, 412.
- Lanzara, A., P. V. Bogdanov, S. A. K. X. J. Zhou and, D. L. Feng, E. D. Lu, T. Yoshida, H. Eisaki, A. Fujimori, K. Kishio, J.-I. Shimoyama, T. Noda, S. Uchida, *et al.*, 2001, *Nature* **412**, 510.
- Lavrov, A. N., H. J. Kang, Y. Kurita, T. Suzuki, S. Komiya, J. W. Lynn, S.-H. Lee, P. Dai, and Y. Ando, 2004, *Phys. Rev. Lett.* **92**(22), 227003 (pages 4).
- LeBoeuf, D., N. Doiron-Leyraud, J. Levallois, R. Daou, J.-B. Bonnemaison, N. Hussey, L. B. and B.J. Ramshaw, R. Liang, D. Bonn, W. Hardy, C. Proust, and L. Taillefer, 2007, *Nature* **450**, 533.
- Leca, V., D. H. A. Blank, G. Rijnders, S. Bals, and G. van Tendeloo, 2006, *Applied Physics Letters* **89**(9), 092504.
- Lee, D.-H., and S. A. Kivelson, 2003, *Phys. Rev. B* **67**(2), 024506.
- Lee, J., K. Fujita, K. McElroy, J. A. Slezak, M. Wang, Y. Aiura, H. Bando, M. Ishikado, T. Masui, J. X. Zhu, A. V. Balatsky, H. Eisaki, *et al.*, 2006a, *Nature* **442**(7102), 546.
- Lee, P. A., N. Nagaosa, and X.-G. Wen, 2006b, *Reviews of Modern Physics* **78**(1), 17 (pages 69).
- Lee, P. A., and N. Read, 1987, *Phys. Rev. Lett.* **58**(25), 2691.
- Lee, W. S., I. M. Vishik, K. Tanaka, D. H. Lu, T. Sasagawa, N. Nagaosa, T. P. Devereaux, Z. Hussain, and Z.-X. Shen, 2007, *Nature* **450**, 81.
- Lefebvre, S., P. Wzietek, S. Brown, C. Bourbonnais, D. Jérôme, C. Mézière, M. Fourmigué, and P. Batail, 2000, *Phys. Rev. Lett.* **85**(25), 5420.
- Li, P., F. F. Balakirev, and R. L. Greene, 2007a, *Physical Review Letters* **99**(4), 047003 (pages 4).
- Li, P., F. F. Balakirev, and R. L. Greene, 2007b, *Physical Review B (Condensed Matter and Materials Physics)* **75**(17), 172508 (pages 4).
- Li, P., K. Behnia, and R. L. Greene, 2007c, *Physical Review B (Condensed Matter and Materials Physics)* **75**(2), 020506 (pages 4).
- Li, P., and R. L. Greene, 2007, *Physical Review B (Condensed Matter and Materials Physics)* **76**(17), 174512 (pages 9).
- Li, S., S. Chi, J. Zhao, H.-H. Wen, M. B. Stone, J. W. Lynn, and P. Dai, 2008a, *Physical Review B (Condensed Matter and Materials Physics)* **78**(1), 014520 (pages 5).
- Li, S., S. D. Wilson, D. Mandrus, B. Zhao, Y. Onose, Y. Tokura, and P. Dai, 2005a, *Phys. Rev. B* **71**(5), 054505 (pages 10).
- Li, S. Y., L. Taillefer, C. H. Wang, and X. H. Chen, 2005b, *Physical Review Letters* **95**(15), 156603 (pages 4).
- Li, Y., V. Balédent, N. Barisic, Y. Cho, B. Fauqué, Y. Sidis,

- G. Yu, X. Zhao, P. Bourges, and M. Greven, 2008b, *Nature* **455**, 372.
- Li, Z., V. Jovanovic, H. Raffy, and S. Megtert, 2008c, *Physica C: Superconductivity*, In Press, Accepted Manuscript.
- Liang, G., Y. Guo, D. Badresingh, W. Xu, Y. Tang, M. Croft, J. Chen, A. Sahiner, B.-h. O, and J. T. Markert, 1995, *Phys. Rev. B* **51**(2), 1258.
- Lin, J., and A. J. Millis, 2005, *Phys. Rev. B* **72**(21), 214506 (pages 9).
- Liu, C. S., and W. C. Wu, 2007, *Physical Review B (Condensed Matter and Materials Physics)* **76**(22), 220504 (pages 4).
- Liu, R., J. Chen, P. Nachimuthu, R. Gundakaram, C. Jung, J. Kim, and S. Lee, 2001, *Solid State Comm.* **118**, 367.
- Liu, R., L. Zhao, H. Yang, and X. Chen, 2008, *Physica C: Superconductivity* **468**(21), 2197, ISSN 0921-4534.
- Liu, Z. Y., H. H. Wen, L. Shan, H. P. Yang, X. F. Lu, H. Gao, M.-S. Park, C. U. Jung, and S.-I. Lee, 2005, *Europhys. Lett.* **69**(2), 263.
- Loeser, A. G., Z.-X. Shen, D. S. Dessau, D. S. Marshall, C. H. Park, P. Fournier, and A. Kapitulnik, 1996, *Science* **273**(5273), 325.
- Lofwander, T., V. S. Shumeiko, and G. Wendin, 2001, *Superconductor Science and Technology* **14**(5), R53.
- Loram, J. W., K. A. Mirza, J. R. Cooper, and W. Y. Liang, 1993, *Phys. Rev. Lett.* **71**(11), 1740.
- Luke, G. M., L. P. Le, B. J. Sternlieb, Y. J. Uemura, J. H. Brewer, R. Kadono, R. F. Kiefl, S. R. Kreitzman, T. M. Riseman, C. E. Stronach, M. R. Davis, S. Uchida, *et al.*, 1990, *Phys. Rev. B* **42**(13), 7981.
- Luo, H. G., and T. Xiang, 2005, *Physical Review Letters* **94**(2), 027001 (pages 4).
- Lupi, S., P. Maselli, M. Capizzi, P. Calvani, P. Giura, and P. Roy, 1999, *Physical Review Letters* **83**(23), 4852.
- Luttinger, J. M., 1960, *Phys. Rev.* **119**(4), 1153.
- Lynn, J., and S. Skanthakumar, 2001, in *Handbook on the Physics and Chemistry of Rare Earths*, edited by L. E. K.A. Gschneidner, Jr. and M. Maple (Elsevier Science B.V), volume 31, p. 313.
- Lynn, J. W., I. W. Sumarlin, S. Skanthakumar, W.-H. Li, R. N. Shelton, J. L. Peng, Z. Fisk, and S.-W. Cheong, 1990, *Phys. Rev. B* **41**(4), 2569.
- Lyons, K. B., P. A. Fleury, J. P. Remeika, A. S. Cooper, and T. J. Negran, 1988, *Phys. Rev. B* **37**(4), 2353.
- Ma, Z., R. C. Taber, L. W. Lombardo, A. Kapitulnik, M. R. Beasley, P. Merchant, C. B. Eom, S. Y. Hou, and J. M. Phillips, 1993, *Phys. Rev. Lett.* **71**(5), 781.
- Macridin, A., M. Jarrell, T. Maier, P. R. C. Kent, and E. D'Azevedo, 2006, *Physical Review Letters* **97**(3), 036401 (pages 4).
- Maier, T., M. Jarrell, T. Pruschke, and M. H. Hettler, 2005a, *Reviews of Modern Physics* **77**, 1027.
- Maier, T. A., M. Jarrell, T. C. Schulthess, P. R. C. Kent, and J. B. White, 2005b, *Physical Review Letters* **95**(23), 237001 (pages 4).
- Maier, T. A., D. Poilblanc, and D. J. Scalapino, 2008, *Physical Review Letters* **100**(23), 237001 (pages 4).
- Maiser, E., P. Fournier, J.-L. Peng, F. M. Araujo-Moreira, T. Venkatesan, R. Greene, and G. Czjzek, 1998, *Physica C* **297**, 15.
- Maljuk, A. N., G. A. Emel'chenko, and A. V. Kosenko, 1996, *Journal of Alloys and Compounds* **234**(1), 52.
- Maljuk, A. N., A. A. Jokhov, I. G. Naumenko, I. K. Bdikin, S. A. Zver'kov, and G. A. Emel'chenko, 2000, *Physica C: Superconductivity* **329**(1), 51.
- Mang, P. K., S. Larochele, A. Mehta, O. P. Vajk, A. S. Erickson, L. Lu, W. J. L. Buyers, A. F. Marshall, K. Prokes, and M. Greven, 2004a, *Phys. Rev. B* **70**(9), 094507 (pages 15).
- Mang, P. K., S. Larochele, and M. Greven, 2003, *Nature* **429**, 139 (pages 2).
- Mang, P. K., O. P. Vajk, A. Arvanitaki, J. W. Lynn, and M. Greven, 2004b, *Phys. Rev. Lett.* **93**(2), 027002 (pages 4).
- Mao, S. N., X. X. Xi, S. Bhattacharya, Q. Li, T. Venkatesan, J. L. Peng, R. L. Greene, J. Mao, D. H. Wu, and S. M. Anlage, 1992, *Applied Physics Letters* **61**(19), 2356.
- Mao, S. N., X. X. Xi, Q. Li, T. Venkatesan, D. P. Beesabathina, L. Salamanca-Riba, and X. D. Wu, 1994, *Journal of Applied Physics* **75**(4), 2119.
- Maple, M. B., 1990, *Mater. Res. Bull.* **15**, 60.
- Marcenat, C., R. Calemczuk, A. F. Khoder, E. Bonjour, C. Marin, and J. Y. Henry, 1993, *Physica C: Superconductivity* **216**(3-4), 443.
- Marcenat, C., J. Y. Henry, and R. Calemczuk, 1994, *Physica C: Superconductivity* **235-240**(Part 3), 1747.
- Marin, C., J. Y. Henry, and J. X. Boucherle, 1993, *Solid State Comm.* **86**(7), 425.
- Markert, J. T., J. Beille, J. J. Neumeier, E. A. Early, C. L. Seaman, T. Moran, and M. B. Maple, 1990, *Phys. Rev. Lett.* **64**(1), 80.
- Marshall, D. S., D. S. Dessau, A. G. Loeser, C.-H. Park, A. Y. Matsuura, J. N. Eckstein, I. Bozovic, P. Fournier, A. Kapitulnik, W. E. Spicer, and Z.-X. Shen, 1996, *Phys. Rev. Lett.* **76**(25), 4841.
- Martin, S., A. T. Fiory, R. M. Fleming, L. F. Schneemeyer, and J. V. Waszczak, 1990, *Phys. Rev. B* **41**(1), 846.
- Martindale, J. A., S. E. Barrett, K. E. O'Hara, C. P. Slichter, W. C. Lee, and D. M. Ginsberg, 1993, *Phys. Rev. B* **47**(14), 9155.
- Massidda, S., N. Hamada, J. Yu, and A. J. Freeman, 1989, *Physica C Superconductivity* **157**, 571.
- Matsuda, M., Y. Endoh, and Y. Hidaka, 1991, *Physica C: Superconductivity* **179**(4-6), 347.
- Matsuda, M., Y. Endoh, K. Yamada, H. Kojima, I. Tanaka, R. J. Birgeneau, M. A. Kastner, and G. Shirane, 1992, *Phys. Rev. B* **45**(21), 12548.
- Matsuda, M., M. Fujita, K. Yamada, R. J. Birgeneau, Y. Endoh, and G. Shirane, 2002, *Phys. Rev. B* **65**(13), 134515.
- Matsuda, M., K. Yamada, K. Kakurai, H. Kadowaki, T. R. Thurston, Y. Endoh, Y. Hidaka, R. J. Birgeneau, M. A. Kastner, P. M. Gehring, A. H. Moudden, and G. Shirane, 1990, *Phys. Rev. B* **42**(16), 10098.
- Matsui, H., T. Takahashi, T. Sato, K. Terashima, H. Ding, T. Uefuji, and K. Yamada, 2007, *Physical Review B (Condensed Matter and Materials Physics)* **75**(22), 224514 (pages 4).
- Matsui, H., K. Terashima, T. Sato, T. Takahashi, M. Fujita, and K. Yamada, 2005a, *Phys. Rev. Lett.* **95**(1), 017003 (pages 4).
- Matsui, H., K. Terashima, T. Sato, T. Takahashi, S.-C. Wang, H.-B. Yang, H. Ding, T. Uefuji, and K. Yamada, 2005b, *Phys. Rev. Lett.* **94**(4), 047005 (pages 4).
- Matsumoto, O., A. Utsuki, A. Tsukada, H. Yamamoto, T. Manabe, and M. Naito, 2009, *Phys. Rev. B* **79**(10), 100508 (pages 4).
- Matsuura, M., P. Dai, H. J. Kang, J. W. Lynn, D. N. Argyriou, K. Prokes, Y. Onose, and Y. Tokura, 2003, *Phys. Rev. B* **68**(14), 144503 (pages 13).

- Matsuyama, H., T. Takahashi, H. Katayama-Yoshida, T. Kashiwakura, Y. Okabe, S. Sato, N. Kosugi, A. Yagishita, K. Tanaka, H. Fujimoto, and H. Inokuchi, 1989, *Physica C: Superconductivity* **160**(5-6), 567, ISSN 0921-4534.
- McElroy, K., J. Lee, J. A. Slezak, D.-H. Lee, H. Eisaki, S. Uchida, and J. C. Davis, 2005, *Science* **309**(5737), 1048.
- McKenzie, R. H., 1997, *Science* **278**(5339), 820.
- McQueeney, R. J., Y. Petrov, T. Egami, M. Yethiraj, G. Shirane, and Y. Endoh, 1999, *Phys. Rev. Lett.* **82**(3), 628.
- McQueeney, R. J., J. L. Sarrao, P. G. Pagliuso, P. W. Stephens, and R. Osborn, 2001, *Phys. Rev. Lett.* **87**(7), 077001.
- Meevasana, W., X. J. Zhou, S. Sahrakorpi, W. S. Lee, W. L. Yang, K. Tanaka, N. Mannella, T. Yoshida, D. H. Lu, Y. L. Chen, R. H. He, H. Lin, *et al.*, 2007, *Physical Review B (Condensed Matter and Materials Physics)* **75**(17), 174506 (pages 7).
- Meinders, M. B. J., H. Eskes, and G. A. Sawatzky, 1993, *Phys. Rev. B* **48**(6), 3916.
- Micnas, R., J. Ramlinger, and S. Robaszkiewicz, 1990, *Rev. Mod. Phys.* **62**(1), 113.
- Miller, R. I., R. F. Kiefl, J. H. Brewer, J. E. Sonier, J. Chakhalian, S. Dunsiger, G. D. Morris, A. N. Price, D. A. Bonn, W. H. Hardy, and R. Liang, 2002, *Phys. Rev. Lett.* **88**(13), 137002.
- Mira, J., J. Rivas, D. Fiorani, R. Caciuffo, D. Rinaldi, C. Vázquez-Vázquez, J. Mahía, M. A. López-Quintela, and S. B. Oseroff, 1995, *Phys. Rev. B* **52**(22), 16020.
- Mitrovic, V. F., E. E. Sigmund, M. Eschrig, H. N. Bachman, W. P. Halperin, A. P. Reyes, P. Kuhns, and W. G. Moulton, 2001, *Nature* **413**, 501.
- Miyake, K., S. Schmitt-Rink, and C. Varma, 1986, *Phys. Rev. B* **34**, 6554.
- Molegraaf, H. J. A., C. Presura, D. van der Marel, P. H. Kes, and M. Li, 2002, *Science* **295**(5563), 2239.
- Moler, K. A., D. J. Baar, J. S. Urbach, R. Liang, W. N. Hardy, and A. Kapitulnik, 1994, *Phys. Rev. Lett.* **73**(20), 2744.
- Moler, K. A., D. L. Sisson, J. S. Urbach, M. R. Beasley, A. Kapitulnik, D. J. Baar, R. Liang, and W. N. Hardy, 1997, *Phys. Rev. B* **55**(6), 3954.
- Mook, H. A., P. Dai, S. M. Hayden, G. Aeppli, T. G. Perring, and F. Dogan, 1998, *Nature* **395**, 580.
- Mook, H. A., P. Dai, and F. Doğan, 2002, *Phys. Rev. Lett.* **88**(9), 097004.
- Mook, H. A., M. Yethiraj, G. Aeppli, T. E. Mason, and T. Armstrong, 1993, *Phys. Rev. Lett.* **70**(22), 3490.
- Moon, E. G., and S. Sachdev, 2009, arXiv:0905.2608.
- Moran, E., A. I. Nazzal, T. C. Huang, and J. B. Torrance, 1989, *Physica C* **160**, 30.
- Moritz, B., F. Schmitt, W. Meevasana, S. Johnston, E. M. Motoyama, M. Greven, D. H. Lu, C. Kim, R. T. Scalettar, Z.-X. Shen, and T. P. Devereaux, 2008, arXiv:0807.3359v1.
- Motoyama, E. M., P. K. Mang, D. Petitgrand, G. Yu, O. P. Vajk, I. M. Vishik, and M. Greven, 2006, *Physical Review Letters* **96**(13), 137002 (pages 4).
- Motoyama, E. M., G. Yu, I. M. Vishik, O. P. Vajk, P. K. Mang, and M. Greven, 2007, *Nature* **445**(7124), 186, ISSN 0028-0836.
- Muller-Buschbaum, X., and X. Wollschlager, 1975, *Z. Anorg. Allg. Chem.* **414**, 76.
- Naito, M., and M. Hepp, 2000, *Japanese Journal of Applied Physics* **39**(Part 2, No. 6A), L485.
- Naito, M., S. Karimoto, and A. Tsukada, 2002, *Supercond. Sci. Technol.* **15**, 1663.
- Naito, M., H. Sato, and H. Yamamoto, 1997, *Physica C: Superconductivity* **293**(1-4), 36, ISSN 0921-4534, intrinsic Josephson Effects and THz Plasma Oscillations in High-Tc Superconductors.
- Nakamae, S., K. Behnia, N. Mangkorntong, M. Nohara, H. Takagi, S. J. C. Yates, and N. E. Hussey, 2003, *Phys. Rev. B* **68**(10), 100502.
- Namatame, H., A. Fujimori, Y. Tokura, M. Nakamura, K. Yamaguchi, A. Misu, H. Matsubara, S. Suga, H. Eisaki, T. Ito, H. Takagi, and S. Uchida, 1990, *Phys. Rev. B* **41**(10), 7205.
- Navarro, E., D. Jaque, J. Villegas, J. Martyn, A. Serquis, F. Prado, A. Caneiro, and J. Vicent, 2001, *J. of Alloys and Compounds* **323-324**, 580.
- Nedil'ko, A., 1982, *Russian J. Inorg. Chem.* **27**, 634.
- Nekvasil, V., and M. Divis, 2001, in *Encyclopedia of Materials: Science and Technology*, edited by K. H. J. Buschow, R. W. Cahn, M. C. Flemings, B. I. (print), E. J. Kramer, S. Mahajan, and P. V. (updates) (Elsevier, Oxford), pp. 4613 – 4627.
- Nie, J. C., P. Badica, M. Hirai, A. Sundaresan, A. Crisan, H. Kito, N. Terada, Y. Kodama, A. Iyo, Y. Tanaka, and H. Ihara, 2003, *Superconductor Science and Technology* **16**(1), L1.
- Niستمski, F. C., S. Kunwar, S. Zhou, S. Li, H. Ding, Z. Wang, P. Dai, and V. Madhavan, 2007, *Nature* **450**(7172), 1058, ISSN 0028-0836.
- Norman, M., H. Ding, M. Randeria, J. Campuzano, T. Yokoya, T. Takeuchi, T. Takahashi, T. Mochiku, K. Kadowaki, P. Guptasarma, and D. Hinks, 1998, *Nature* **392**, 157.
- Nücker, N., P. Adelman, M. Alexander, H. Romberg, S. Nakai, J. Fink, H. Rietschel, G. Roth, H. Schmidt, and H. Spille, 1989, *Z. Phys. B* **75**, 421.
- Oka, K., H. Shibata, S. Kashiwaya, and H. Eisaki, 2003, *Physica C* **388**, 389.
- Oka, K., and H. Unoki, 1990, *Jap. J. Appl. Phys.* **29**, L909.
- Okada, K., Y. Seino, and A. Kotani, 1990, *Journal of the Physical Society of Japan* **59**(8), 2639.
- Onose, Y., Y. Taguchi, T. Ishikawa, S. Shinomori, K. Ishizaka, and Y. Tokura, 1999, *Phys. Rev. Lett.* **82**(25), 5120.
- Onose, Y., Y. Taguchi, K. Ishizaka, and Y. Tokura, 2001, *Phys. Rev. Lett.* **87**(21), 217001 (pages 4).
- Onose, Y., Y. Taguchi, K. Ishizaka, and Y. Tokura, 2004, *Phys. Rev. B* **69**(2), 024504 (pages 13).
- Orenstein, J., and A. J. Millis, 2000, *Science* **288**(5465), 468.
- Oseroff, S. B., D. Rao, F. Wright, D. C. Vier, S. Schultz, J. D. Thompson, Z. Fisk, S.-W. Cheong, M. F. Hundley, and M. Tovar, 1990, *Phys. Rev. B* **41**(4), 1934.
- Pan, Z.-H., P. Richard, A. V. Fedrov, T. Kondo, T. Takeuchi, S. L. Li, P. Dai, G. Gu, W. Ku, Z. Wang, and H. Ding, 2006, arXiv:cond-mat/0610442 xxx(xxx).
- Park, S. R., Y. S. Roh, Y. K. Yoon, C. S. Leem, J. H. Kim, B. J. Kim, H. Koh, H. Eisaki, N. P. Armitage, and C. Kim, 2007, *Physical Review B (Condensed Matter and Materials Physics)* **75**(6), 060501 (pages 4).
- Park, S. R., D. J. Song, C. S. Leem, C. Kim, C. Kim, B. J. Kim, and H. Eisaki, 2008, *Physical Review Letters* **101**(11), 117006 (pages 4).
- Pathak, S., V. B. Shenoy, M. Randeria, and N. Trivedi, 2009, *Physical Review Letters* **102**(2), 027002 (pages 4).
- Pellegrin, E., N. Nücker, J. Fink, S. L. Molodtsov, A. Gutiérrez, E. Navas, O. Strelbel, Z. Hu, M. Domke,

- G. Kaindl, S. Uchida, Y. Nakamura, *et al.*, 1993, Phys. Rev. B **47**(6), 3354.
- Peng, J. L., Z. Y. Li, and R. L. Greene, 1991, Physica C: Superconductivity **177**(1-3), 79.
- Peters, C. J., R. J. Birgeneau, M. A. Kastner, H. Yoshizawa, Y. Endoh, J. Tranquada, G. Shirane, Y. Hidaka, M. Oda, M. Suzuki, and T. Murakami, 1988, Phys. Rev. B **37**(16), 9761.
- Petitgrand, D., S. V. Maleyev, P. Bourges, and A. S. Ivanov, 1999, Phys. Rev. B **59**(2), 1079.
- Phillips, P., and C. Chamon, 2005, Physical Review Letters **95**(10), 107002 (pages 4).
- Pimenov, A., A. V. Pronin, A. Loidl, U. Michelucci, A. P. Kampf, S. I. Krasnosvobodtsev, V. S. Nozdrin, and D. Rainer, 2000, Physical Review B (Condensed Matter and Materials Physics) **62**(14), 9822.
- Pinol, S., J. Fontcuberta, C. Miravittles, and D. M. Paul, 1990, Physica C: Superconductivity **165**(3-4), 265.
- Pintschovius, L., and M. Braden, 1999, Phys. Rev. B **60**(22), R15039.
- Pintschovius, L., D. Reznik, and K. Yamada, 2006, Physical Review B (Condensed Matter and Materials Physics) **74**(17), 174514 (pages 5).
- Plakhty, V. P., S. V. Maleyev, S. V. Gavrilov, E. Bourdarot, S. Pouget, and S. N. Barilo, 2003, Europhys. Lett. **61**, 534.
- Podolsky, D., E. Demler, K. Damle, and B. I. Halperin, 2003, Phys. Rev. B **67**(9), 094514.
- Podolsky, D., S. Raghu, and A. Vishwanath, 2007, Physical Review Letters **99**(11), 117004 (pages 4).
- Ponomarev, A. I., T. B. Charikova, A. N. Ignatenkov, A. O. Tashlykov, and A. A. Ivanov, 2004, Low Temp. Phys. **30**(11), 885.
- Prijamboedi, B., and S. Kashiwaya, 2006, Journal of Materials Science: Materials in Electronics **17**(7), 483.
- Pronin, A. V., A. Pimenov, A. Loidl, A. Tsukada, and M. Naito, 2003, Phys. Rev. B **68**(5), 054511.
- Proust, C., K. Behnia, R. Bel, D. Maude, and S. I. Vedenev, 2005, Physical Review B (Condensed Matter and Materials Physics) **72**(21), 214511 (pages 9).
- Proust, C., E. Boaknin, R. W. Hill, L. Taillefer, and A. P. Mackenzie, 2002, Phys. Rev. Lett. **89**(14), 147003.
- Prozorov, R., R. Giannetta, P. Fournier, and R. L. Greene, 2000, Phys. Rev. Lett. **85**, 3700.
- Puchkov, A., D. B. DN, and T. Timusk, 1996, J. Phys. Condens. Matter **8**(10), 10049.
- Qazilbash, M. M., A. Biswas, Y. Dagan, R. A. Ott, and R. L. Greene, 2003, Phys. Rev. B **68**(2), 024502 (pages 9).
- Qazilbash, M. M., A. Koitzsch, B. S. Dennis, A. Gozar, H. Balci, C. A. Kendziora, R. L. Greene, and G. Blumberg, 2005, Physical Review B (Condensed Matter and Materials Physics) **72**(21), 214510 (pages 12).
- Radaelli, P. G., J. D. Jorgensen, A. J. Schultz, J. L. Peng, and R. L. Greene, 1994, Phys. Rev. B **49**(21), 15322.
- Randeria, M., 2007, in *Models and Phenomenology for Conventional and High-temperature Superconductivity*, edited by G. Iadonisi, J. R. Schrieffer, and M. Chiofalo (Ios Pr Inc), pp. 53–75.
- Renner, C., and O. Fischer, 1995, Phys. Rev. B **51**(14), 9208.
- Richard, P., S. Jandl, M. Poirier, P. Fournier, V. Nekvasil, and M. L. Sadowski, 2005a, Physical Review B (Condensed Matter and Materials Physics) **72**(1), 014506 (pages 10).
- Richard, P., M. Neupane, Y.-M. Xu, P. Fournier, S. Li, P. Dai, Z. Wang, and H. Ding, 2007, Physical Review Letters **99**(15), 157002 (pages 4).
- Richard, P., M. Poirier, and S. Jandl, 2005b, Phys. Rev. B **71**(14), 144425 (pages 7).
- Richard, P., G. Riou, I. Hetel, S. Jandl, M. Poirier, and P. Fournier, 2004, Phys. Rev. B **70**(6), 064513.
- Riou, G., S. Jandl, M. Poirier, V. Nekvasil, M. Divis, P. Fournier, R. Greene, D. Zhigunov, and S. Barilo, 2001, Eur. Phys. J. B **23**, 179.
- Riou, G., P. Richard, S. Jandl, M. Poirier, P. Fournier, V. Nekvasil, S. N. Barilo, and L. A. Kurnevich, 2004, Phys. Rev. B **69**(2), 024511.
- Roberge, G., S. Charpentier, S. Godin-Proulx, P. Rauwel, K. Truong, and P. Fournier, 2009, J. Crystal Growth **311**(5), 1340.
- Ronning, F., C. Kim, D. L. Feng, D. S. Marshall, A. G. Loeser, L. L. Miller, J. N. Eckstein, I. Bozovic, and Z.-X. Shen, 1998, Science **282**(5396), 2067.
- Ronning, F., T. Sasagawa, Y. Kohsaka, K. M. Shen, A. Damascelli, C. Kim, T. Yoshida, N. P. Armitage, D. H. Lu, D. L. Feng, L. L. Miller, H. Takagi, *et al.*, 2003, Phys. Rev. B **67**(16), 165101.
- Ronning, F., K. M. Shen, N. P. Armitage, A. Damascelli, D. H. Lu, Z.-X. Shen, L. L. Miller, and C. Kim, 2005, Physical Review B (Condensed Matter and Materials Physics) **71**(9), 094518 (pages 5).
- Rossat-Mignod, J. M., L. P. Regnault, C. Vettier, P. Bourges, P. Bulet, J. Bossy, J. Y. Henry, and G. Lapertot, 1991, Physica C **185**, 86 (pages 7).
- Rotter, L. D., Z. Schlesinger, R. T. Collins, F. Holtzberg, C. Field, U. W. Welp, G. W. Crabtree, J. Z. Liu, Y. Fang, K. G. Vandervoort, and S. Fleshler, 1991, Phys. Rev. Lett. **67**(19), 2741.
- Rullier-Albenque, F., H. Alloul, F. Balakirev, and C. Proust, 2008, EPL (Europhysics Letters) **81**(3), 37008 (6pp).
- Rullier-Albenque, F., H. Alloul, and R. Tourbot, 2003, Physical Review Letters **91**(4), 047001 (pages 4).
- Sachdev, S., 2003, Rev. Mod. Phys. **75**(3), 913.
- Sachidanandam, R., T. Yildirim, A. B. Harris, A. Aharony, and O. Entin-Wohlman, 1997, Phys. Rev. B **56**(1), 260.
- Sadowski, W., H. Hagemann, M. Franois, H. Bill, M. Peter, E. Walker, and K. Yvon, 1990, Physica C: Superconductivity **170**(1-2), 103, ISSN 0921-4534.
- Sakisaka, Y., T. Maruyama, Y. Morikawa, H. Kato, K. Edamoto, M. Okusawa, Y. Aiura, H. Yanashima, T. Terashima, Y. Bando, K. Iijima, K. Yamamoto, *et al.*, 1990, Phys. Rev. B **42**(7), 4189.
- Santander-Syro, A. F., T. Kondo, J. Chang, A. Kaminski, S. Pailhes, M. Shi, L. Patthey, A. Zimmers, B. Liang, P. Li, and R. L. Greene, 2009, arXiv:0903.3413v1.
- Sato, T., T. Kamiyama, T. Takahashi, K. Kurahashi, and K. Yamada, 2001, Science **291**(5508), 1517.
- Savici, A. T., A. Fukaya, I. M. Gat-Malureanu, T. Ito, P. L. Russo, Y. J. Uemura, C. R. Wiebe, P. P. Kyriakou, G. J. MacDougall, M. T. Rovers, G. M. Luke, K. M. Kojima, *et al.*, 2005, Physical Review Letters **95**(15), 157001 (pages 4).
- Sawa, A., M. Kawasaki, H. Takagi, and Y. Tokura, 2002, Phys. Rev. B **66**(1), 014531.
- Scalapino, D. J., 1995, Physics Reports **250**, 329.
- Scalapino, D. J., E. Loh, and J. E. Hirsch, 1986, Phys. Rev. B **34**(11), 8190.
- Schachinger, E., C. C. Homes, R. P. S. M. Lobo, and J. P. Carbotte, 2008, Physical Review B (Condensed Matter and Materials Physics) **78**(13), 134522 (pages 10).
- Schachinger, E., J. J. Tu, and J. P. Carbotte, 2003, Phys.

- Rev. B **67**(21), 214508.
- Schmitt, F., W. S. Lee, D.-H. Lu, W. Meevasana, E. Motoyama, M. Greven, and Z.-X. Shen, 2008, Physical Review B (Condensed Matter and Materials Physics) **78**(10), 100505 (pages 4).
- Schneider, C. W., Z. H. Barber, J. E. Evetts, S. N. Mao, X. X. Xi, and T. Venkatesan, 1994, Physica C **233**, 77.
- Schultz, A. J., J. D. Jorgensen, J. L. Peng, and R. L. Greene, 1996, Phys. Rev. B **53**(9), 5157.
- Sekitani, T., M. Naito, and N. Miura, 2003, Phys. Rev. B **67**(17), 174503 (pages 5).
- Senechal, D., P.-L. Lavertu, M.-A. Marois, and A.-M. S. Tremblay, 2005, Phys. Rev. Lett. **94**(15), 156404 (pages 4).
- Senechal, D., and A.-M. S. Tremblay, 2004, Phys. Rev. Lett. **92**(12), 126401 (pages 4).
- Seo, K., H.-D. Chen, and J. Hu, 2007, Physical Review B (Condensed Matter and Materials Physics) **76**(2), 020511 (pages 4).
- Shan, L., Y. Huang, H. Gao, Y. Wang, S. L. Li, P. C. Dai, F. Zhou, J. W. Xiong, W. X. Ti, and H. H. Wen, 2005, Phys. Rev. B **72**(14), 144506 (pages 9).
- Shan, L., Y. Huang, Y. L. Wang, S. Li, J. Zhao, P. Dai, Y. Zhang, C. Ren, and H. H. Wen, 2008a, <http://arxiv.org/abs/cond-mat/0703256> xx, xxx.
- Shan, L., Y. L. Wang, Y. Huang, S. L. Li, J. Zhao, P. Dai, and H. H. Wen, 2008b, Physical Review B (Condensed Matter and Materials Physics) **78**(1), 014505 (pages 5).
- Shen, K. M., F. Ronning, D. H. Lu, W. S. Lee, N. J. C. Ingle, W. Meevasana, F. Baumberger, A. Damascelli, N. P. Armitage, L. L. Miller, Y. Kohsaka, M. Azuma, *et al.*, 2004, Physical Review Letters **93**(26), 267002 (pages 4).
- Shen, Z.-X., D. S. Dessau, B. O. Wells, D. M. King, W. E. Spicer, A. J. Arko, D. Marshall, L. W. Lombardo, A. Kapitulnik, P. Dickinson, S. Doniach, J. DiCarlo, *et al.*, 1993, Phys. Rev. Lett. **70**(10), 1553.
- Shengelaya, A., R. Khasanov, D. G. Eshchenko, D. D. Castro, I. M. Savic, M. S. Park, K. H. Kim, S.-I. Lee, K. A. Muller, and H. Keller, 2005, Physical Review Letters **94**(12), 127001 (pages 4).
- Shibauchi, T., L. Krusin-Elbaum, M. Li, M. P. Maley, and P. H. Kes, 2001, Phys. Rev. Lett. **86**(25), 5763.
- Shiladitya Chakraborty, P. P., Dimitrios Galanakis, 2007, arXiv:0712.2838v1.
- Siegrist, T., S. M. Zahurak, D. Murphy, , and R. S. Roth, 1988, Nature **334**, 231 (pages 2).
- Sigrist, M., and T. M. Rice, 1995, Rev. Mod. Phys. **67**(2), 503.
- Singer, P. M., A. W. Hunt, A. F. Cederström, and T. Imai, 1999, Phys. Rev. B **60**(22), 15345.
- Singh, A., and H. Ghosh, 2002, Phys. Rev. B **65**(13), 134414.
- Singh, R. R. P., P. A. Fleury, K. B. Lyons, and P. E. Sulewski, 1989, Phys. Rev. Lett. **62**(23), 2736.
- Singley, E. J., D. N. Basov, K. Kurahashi, T. Uefuji, and K. Yamada, 2001, Phys. Rev. B **64**(22), 224503 (pages 12).
- Skanthakumar, S., J. W. Lynn, J. L. Peng, and Z. Y. Li, 1991, 35th annual conference on magnetism and magnetic materials **69**(8), 4866.
- Skanthakumar, S., J. W. Lynn, J. L. Peng, and Z. Y. Li, 1993, Physical Review B (Condensed Matter) **47**(10), 6173.
- Skelton, E. F., A. R. Drews, M. S. Osofsky, S. B. Qadi, J. Z. Hu, T. A. Vanderah, J. L. Peng, and R. L. Greene, 1994, Science **263**, 1416.
- Skinta, J. A., M.-S. Kim, T. R. Lemberger, T. Greibe, and M. Naito, 2002, Phys. Rev. Lett. **88**(20), 207005 (pages 4).
- Smith, M. F., J. Paglione, M. B. Walker, and L. Taillefer, 2005, Physical Review B (Condensed Matter and Materials Physics) **71**(1), 014506 (pages 8).
- Smith, M. G., A. Manthiram, J. Zhou, J. B. Goodenough, and J. T. Markert, 1991, Nature **351**(6327), 549.
- Snezhko, A., R. Prozorov, D. D. Lawrie, R. Giannetta, J. Gauthier, J. Renaud, and P. Fournier, 2004, Phys. Rev. Lett. **92**, 157005.
- Sondheimer, E. H., 1948, Royal Society of London Proceedings Series A **193**, 484.
- Sonier, J. E., J. H. Brewer, and R. F. Kiefl, 2000, Rev. Mod. Phys. **72**(3), 769.
- Sonier, J. E., K. F. Poon, G. M. Luke, P. Kyriakou, R. I. Miller, R. Liang, C. R. Wiebe, P. Fournier, and R. L. Greene, 2003, Phys. Rev. Lett. **91**(14), 147002.
- Sooryakumar, R., and M. V. Klein, 1980, Phys. Rev. Lett. **45**(8), 660.
- Sooryakumar, R., and M. V. Klein, 1981, Phys. Rev. B **23**(7), 3213.
- Stadlober, B., G. Krug, R. Nemetschek, R. Hackl, J. L. Cobb, and J. T. Markert, 1995, Phys. Rev. Lett. **74**(24), 4911.
- Steeneken, P. G., L. H. Tjeng, G. A. Sawatzky, A. Tanaka, O. Tjernberg, G. Ghiringhelli, N. B. Brookes, A. A. Nugroho, and A. A. Menovsky, 2003, Phys. Rev. Lett. **90**(24), 247005.
- Stepanov, A. A., P. Wyder, T. Chattopadhyay, P. J. Brown, G. Fillion, I. M. Vitebsky, A. Deville, B. Gaillard, S. N. Barilo, and D. I. Zhigunov, 1993, Phys. Rev. B **48**(17), 12979.
- Sugai, S., T. Kobayashi, and J. Akimitsu, 1989, Phys. Rev. B **40**(4), 2686.
- Sugiyama, J., K. Matsuura, M. Kosuge, H. Yamauchi, and S. Tanaka, 1992, Phys. Rev. B **45**(17), 9951.
- Sulewski, P. E., P. A. Fleury, K. B. Lyons, S.-W. Cheong, and Z. Fisk, 1990, Phys. Rev. B **41**(1), 225.
- Sumarlin, I. W., J. W. Lynn, T. Chattopadhyay, S. N. Barilo, D. I. Zhigunov, and J. L. Peng, 1995, Phys. Rev. B **51**(9), 5824.
- Sumarlin, I. W., S. Skanthakumar, J. W. Lynn, J. L. Peng, Z. Y. Li, W. Jiang, and R. L. Greene, 1992, Phys. Rev. Lett. **68**(14), 2228.
- Sun, X. F., Y. Kurita, T. Suzuki, S. Komiyama, and Y. Ando, 2004, Phys. Rev. Lett. **92**(4), 047001 (pages 4).
- Suzuki, K., K. Kishio, T. Hasegawa, and K. Kitazawa, 1990, Physica C **166**, 357.
- Tafari, F., and J. R. Kirtley, 2005, Reports on Progress in Physics **68**(11), 2573.
- Taguchi, M., A. Chainani, K. Horiba, Y. Takata, M. Yabashi, K. Tamasaku, Y. Nishino, D. Miwa, T. Ishikawa, T. Takeuchi, K. Yamamoto, M. Matsunami, *et al.*, 2005, Physical Review Letters **95**(17), 177002 (pages 4).
- Taillefer, L., B. Lussier, R. Gagnon, K. Behnia, and H. Aubin, 1997, Phys. Rev. Lett. **79**(3), 483.
- Takagi, H., S. Uchida, and Y. Tokura, 1989, Phys. Rev. Lett. **62**, 1197.
- Takayama-Muromachi, E., F. Izumi, Y. Uchida, K. Kato, and H. Asano, 1989, Physica C **159**, 634.
- Tagigawa, M., P. C. Hammel, R. H. Heffner, and Z. Fisk, 1989, Phys. Rev. B **39**(10), 7371.
- Tallon, J. L., J. W. Loram, G. V. M. Williams, J. R. Cooper, I. R. Fisher, J. D. Johnson, M. P. Staines, and C. Bernhard, 1999, Phys. Stat. Sol. (b) **215**(25), 531.
- Tan, Z., J. I. Budnick, C. E. Bouldin, J. C. Woicik, S.-W. Cheong, A. S. Cooper, G. P. Espinosa, and Z. Fisk, 1990,

- Phys. Rev. B **42**(1), 1037.
- Tanaka, I., T. Watanabe, N. Komai, and H. Kojima, 1991, *Physica C: Superconductivity* **185-189**(Part 1), 437.
- Tanaka, Y., and S. Kashiwaya, 1995, *Phys. Rev. Lett.* **74**(17), 3451.
- Tanatar, M. A., J. Paglione, C. Petrovic, and L. Taillefer, 2007, *Science* **316**(5829), 1320.
- Tanda, S., S. Ohzeki, and T. Nakayama, 1992, *Phys. Rev. Lett.* **69**(3), 530.
- Tarascon, J.-M., E. Wang, L. H. Greene, B. G. Bagley, G. W. Hull, S. M. D'Egidio, P. F. Miceli, Z. Z. Wang, T. W. Jing, J. Clayhold, D. Brawner, and N. P. Ong, 1989, *Phys. Rev. B* **40**(7), 4494.
- Tešanović, Z., 2004, *Physical Review Letters* **93**(21), 217004 (pages 4).
- Thompson, J. D., S.-W. Cheong, S. E. Brown, Z. Fisk, S. B. Oseroff, M. Tovar, D. C. Vier, and S. Schultz, 1989, *Phys. Rev. B* **39**(10), 6660.
- Thurston, T. R., M. Matsuda, K. Kakurai, K. Yamada, Y. Endoh, R. J. Birgeneau, P. M. Gehring, Y. Hidaka, M. A. Kastner, T. Murakami, and G. Shirane, 1990, *Physical Review Letters* **65**(2), 263.
- Timusk, T., and B. Statt, 1999, *Reports on Progress in Physics* **62**(1), 61.
- Tinkham, M., 1996, *Introduction to superconductivity* (McGraw-Hill), second edition edition.
- Tjeng, L. H., B. Sinkovic, N. B. Brookes, J. B. Goedkoop, R. Hesper, E. Pellegrin, F. M. F. de Groot, S. Altieri, S. L. Hulbert, E. Shekel, and G. A. Sawatzky, 1997, *Phys. Rev. Lett.* **78**(6), 1126.
- Tohyama, T., 2004, *Phys. Rev. B* **70**(17), 174517.
- Tohyama, T., and S. Maekawa, 1990, *J. Phys. Soc. Jpn.* **59**, 1760.
- Tohyama, T., and S. Maekawa, 1994, *Physical Review B (Condensed Matter)* **49**(5), 3596.
- Tohyama, T., and S. Maekawa, 2001, *Phys. Rev. B* **64**(21), 212505.
- Tokura, Y., A. Fujimori, H. Matsubara, H. Watabe, H. Takagi, S. Uchida, M. Sakai, H. Ikeda, S. Okuda, and S. Tanaka, 1989a, *Phys. Rev. B* **39**(13), 9704.
- Tokura, Y., S. Koshihara, T. Arima, H. Takagi, S. Ishibashi, T. Ido, and S. Uchida, 1990, *Physical Review B (Condensed Matter)* **41**(16), 11657.
- Tokura, Y., H. Takagi, and S. Uchida, 1989b, *Nature* **337**, 345.
- Torrance, J. B., and R. M. Metzger, 1989, *Physical Review Letters* **63**(14), 1515.
- Tranquada, J., Y. N. B.J. Sternlieb J.D. Axe, and S. Uchida, 1995, *Nature* **375**, 561.
- Tranquada, J., S. Heald, A. Moodenbaugh, G. Liang, and M. Croft, 1989, *Nature* **337**, 720.
- Tranquada, J. M., C. H. Lee, K. Yamada, Y. S. Lee, L. P. Regnault, and H. M. Ronnow, 2004a, *Physical Review B (Condensed Matter and Materials Physics)* **69**(17), 174507 (pages 7).
- Tranquada, J. M., H. Woo, T. G. Perring, H. Goka, G. D. Gu, G. Xu, M. Fujita, and K. Yamada, 2004b, *Nature* **429**(6991), 534.
- Tremblay, A. M. S., B. Kyung, and D. Senechal, 2006, *Low Temp. Phys.* **32**(4-5), 424.
- Tsuei, C. C., A. Gupta, and G. Koren, 1989, *Physica C* **161**, 415.
- Tsuei, C. C., and J. R. Kirtley, 2000a, *Rev. Mod. Phys.* **72**(4), 969.
- Tsuei, C. C., and J. R. Kirtley, 2000b, *Phys. Rev. Lett.* **85**(1), 182.
- Tsukada, A., Y. Krockenberger, M. Noda, H. Yamamoto, D. Manske, L. Alff, and M. Naito, 2005, *Solid State Comm.* **133**, 427.
- Tsukada, A., M. Naito, and H. Yamamoto, 2007, *Physica C: Superconductivity* **463-465**, 64, ISSN 0921-4534, proceedings of the 19th International Symposium on Superconductivity (ISS 2006).
- Tsunekawa, M., A. Sekiyama, S. Kasai, S. Imada, H. Fujiwara, T. Muro, Y. Onose, Y. Tokura, , and S. Suga, 2008, *New Journal of Physics* **10**, 073005.
- Uchiyama, H., A. Q. R. Baron, S. Tsutsui, Y. Tanaka, W.-Z. Hu, A. Yamamoto, S. Tajima, and Y. Endoh, 2004, *Physical Review Letters* **92**(19), 197005 (pages 4).
- Uefuji, T., T. Kubo, K. Yamada, M. Fujita, K. Kurahashi, I. Watanabe, and K. Nagamine, 2001, *Physica C: Superconductivity* **357-360**(Part 1), 208.
- Uemura, Y. J., V. J. Emery, A. R. Moodenbaugh, M. Suenaga, D. C. Johnston, A. J. Jacobson, J. T. Lewandowski, J. H. Brewer, R. F. Kiefl, S. R. Kreitzman, G. M. Luke, T. Riseman, *et al.*, 1988, *Phys. Rev. B* **38**(1), 909.
- Uemura, Y. J., L. P. Le, G. M. Luke, B. J. Sternlieb, W. D. Wu, J. H. Brewer, T. M. Riseman, C. L. Seaman, M. B. Maple, M. Ishikawa, D. G. Hinks, J. D. Jorgensen, *et al.*, 1991, *Phys. Rev. Lett.* **66**(20), 2665.
- Uemura, Y. J., G. M. Luke, B. J. Sternlieb, J. H. Brewer, J. F. Carolan, W. N. Hardy, R. Kadono, J. R. Kempton, R. F. Kiefl, S. R. Kreitzman, P. Mulhern, T. M. Riseman, *et al.*, 1989, *Phys. Rev. Lett.* **62**(19), 2317.
- Uzumaki, X., X. Kamehura, and X. Niwa, 1991, *Jap. J. Appl. Phys.* **30**, 981.
- Vaknin, D., S. K. Sinha, D. E. Moncton, D. C. Johnston, J. M. Newsam, C. R. Safinya, and H. E. King, 1987, *Phys. Rev. Lett.* **58**(26), 2802.
- Varma, C. M., 1997, *Phys. Rev. B* **55**(21), 14554.
- Varma, C. M., 1999, *Phys. Rev. Lett.* **83**(17), 3538.
- Varma, C. M., P. B. Littlewood, S. Schmitt-Rink, E. Abrahams, and A. E. Ruckenstein, 1989, *Phys. Rev. Lett.* **63**(18), 1996.
- Varma, C. M., S. Schmitt-Rink, and E. Abrahams, 1987, *Solid State Communications* **62**, 681.
- Venturini, F., R. Hackl, and U. Michelucci, 2003, *Physical Review Letters* **90**(14), 149701 (pages 1).
- Vigoureux, P., 1995, *Études structurales des composés supraconducteurs de type n : R_{2-x}Ce_xCuO_{4d} (R = Gd, Eu, Sm, Nd, Pr); influences des traitements chimiques sur les propriétés physiques, thèse de doctorat, Université Paris XI, Orsay, France (1995).*, Ph.D. thesis, Université Paris XI, Orsay, France.
- Vigoureux, P., M. Braden, A. Gukasov, W. Paulus, P. Bourges, A. Cousson, D. Petitgrand, J.-P. Lauriat, M. Meven, S. N. Barilo, D. Zhigunov, P. Adelman, *et al.*, 1997, *Physica C* **273**, 239 .
- Volovik, G. E., 1993, *JETP Lett.* **58**, 469.
- Wagenknecht, M., D. Koelle, R. Kleiner, S. Graser, N. Schopohl, B. Chesca, A. Tsukada, S. T. B. Goennenwein, and R. Gross, 2008, *Physical Review Letters* **100**(22), 227001 (pages 4).
- Wakimoto, S., G. Shirane, Y. Endoh, K. Hirota, S. Ueki, K. Yamada, R. J. Birgeneau, M. A. Kastner, Y. S. Lee, P. M. Gehring, and S. H. Lee, 1999, *Phys. Rev. B* **60**(2), R769.

- Walstedt, R. E., and J. Warren, W. W., 1990, *Science* **248**(4959), 1082.
- Wang, C. H., G. Y. Wang, T. Wu, Z. Feng, X. G. Luo, and X. H. Chen, 2005a, *Physical Review B (Condensed Matter and Materials Physics)* **72**(13), 132506 (pages 4).
- Wang, C. H., G. Y. Wang, T. Wu, Z. Feng, X. G. Luo, and X. H. Chen, 2005b, *Physical Review B (Condensed Matter and Materials Physics)* **72**(13), 132506 (pages 4).
- Wang, N. L., G. Li, D. Wu, X. H. Chen, C. H. Wang, and H. Ding, 2006a, *Physical Review B (Condensed Matter and Materials Physics)* **73**(18), 184502 (pages 6).
- Wang, Y., L. Li, and N. P. Ong, 2006b, *Physical Review B (Condensed Matter and Materials Physics)* **73**(2), 024510 (pages 20).
- Wang, Y., B. Revaz, A. Erb, and A. Junod, 2001, *Phys. Rev. B* **63**(9), 094508.
- Wang, Z. Z., T. R. Chien, N. P. Ong, J. M. Tarascon, and E. Wang, 1991, *Phys. Rev. B* **43**(4), 3020.
- Warren, W. W., R. E. Walstedt, G. F. Brennert, R. J. Cava, R. Tycko, R. F. Bell, and G. Dabbagh, 1989, *Phys. Rev. Lett.* **62**(10), 1193.
- Weber, C., A. Läuchli, F. Mila, and T. Giamarchi, 2009, *Physical Review Letters* **102**(1), 017005 (pages 4).
- Wells, B. O., Z.-X. Shen, A. Matsuura, D. M. King, M. A. Kastner, M. Greven, and R. J. Birgeneau, 1995, *Physical Review Letters* **74**(6), 964.
- Williams, G. V. M., J. Haase, M.-S. Park, K. H. Kim, and S.-I. Lee, 2005, *Phys. Rev. B* **72**(21), 212511.
- Wilson, S. D., P. Dai, S. Li, S. Chi, H. J. Kang, and J. W. Lynn, 2006a, *Nature* **442**, 59 .
- Wilson, S. D., S. Li, P. Dai, W. Bao, J.-H. Chung, H. J. Kang, S.-H. Lee, S. Komiya, Y. Ando, and Q. Si, 2006b, *Physical Review B (Condensed Matter and Materials Physics)* **74**(14), 144514 (pages 11).
- Wilson, S. D., S. Li, H. Woo, P. Dai, H. A. Mook, C. D. Frost, S. Komiya, and Y. Ando, 2006c, *Phys. Rev. Lett.* **96**(15), 157001 (pages 4).
- Wilson, S. D., S. Li, J. Zhao, G. Mu, H.-H. Wen, J. W. Lynn, P. G. Freeman, L.-P. Regnault, K. Habicht, and P. Dai, 2007, *Proceedings of the National Academy of Sciences* **104**(39), 15259.
- Woods, S. I., A. S. Katz, M. C. de Andrade, J. Herrmann, M. B. Maple, and R. C. Dynes, 1998, *Phys. Rev. B* **58**(13), 8800.
- Woods, S. I., A. S. Katz, S. I. Applebaum, M. C. de Andrade, M. B. Maple, and R. C. Dynes, 2002, *Phys. Rev. B* **66**(1), 014538.
- Wojnarovich, F., 1982, *Journal of Physics C: Solid State Physics* **15**(1), 97.
- Wu, D. H., J. Mao, S. N. Mao, J. L. Peng, X. X. Xi, T. Venkatesan, R. L. Greene, and S. M. Anlage, 1993, *Phys. Rev. Lett.* **70**(1), 85.
- Wu, H., L. Zhao, J. Yuan, L. X. Cao, J. P. Zhong, L. J. Gao, B. Xu, P. C. Dai, B. Y. Zhu, X. G. Qiu, and B. R. Zhao, 2006, *Phys. Rev. B* **73**(10), 104512 (pages 6).
- Wu, T., C. H. Wang, G. Wu, D. F. Fang, J. L. Luo, G. T. Liu, and X. H. Chen, 2008, *Journal of Physics: Condensed Matter* **20**(27), 275226 (8pp).
- Xia, J., E. Schemm, G. Deutscher, S. A. Kivelson, D. A. Bonn, W. N. Hardy, R. Liang, W. Siemons, G. Koster, M. M. Fejer, and A. Kapitulnik, 2008, *Physical Review Letters* **100**(12), 127002 (pages 4).
- Xiang, T., H. G. Luo, D. H. Lu, K. M. Shen, and Z. X. Shen, 2008, arXiv:0807.2498 .
- Xu, X. Q., S. N. Mao, W. Jiang, J. L. Peng, and R. L. Greene, 1996, *Physical Review B (Condensed Matter)* **53**(2), 871.
- Xu, Z., N. Ong, Y. Wang, T. Kakeshita, and S. Uchida, 2000, *Nature* **406**, 486.
- Yagi, H., T. Yoshida, A. Fujimori, Y. Kohsaka, M. Misawa, T. Sasagawa, H. Takagi, M. Azuma, and M. Takano, 2006, *Physical Review B (Condensed Matter and Materials Physics)* **73**(17), 172503 (pages 4).
- Yamada, K., K. Kurahashi, Y. Endoh, R. J. Birgeneau, and G. Shirane, 1999, *Journal of Physics and Chemistry of Solids* **8-9**(10), 1025.
- Yamada, K., K. Kurahashi, T. Uefuji, M. Fujita, S. Park, S.-H. Lee, and Y. Endoh, 2003, *Phys. Rev. Lett.* **90**(13), 137004 (pages 4).
- Yamada, K., C. H. Lee, K. Kurahashi, J. Wada, S. Wakimoto, S. Ueki, H. Kimura, Y. Endoh, S. Hosoya, G. Shirane, R. J. Birgeneau, M. Greven, *et al.*, 1998, *Phys. Rev. B* **57**(10), 6165.
- Yamada, K., S. Wakimoto, G. Shirane, C. H. Lee, M. A. Kastner, S. Hosoya, M. Greven, Y. Endoh, and R. J. Birgeneau, 1995, *Phys. Rev. Lett.* **75**(8), 1626.
- Yamada, T., K. Kinoshita, and H. Shibata, 1994, *Japanese Journal of Applied Physics* **33**(Part 2, No. 2A), L168.
- Yamamoto, H., M. Naito, and H. Sato, 1997, *Phys. Rev. B* **56**(5), 2852.
- Yu, G., M. Greven, E. Yamamoto, *et al.*, 2008, arXiv:0803.3250 , xxx.
- Yu, R. C., M. B. Salamon, J. P. Lu, and W. C. Lee, 1992, *Phys. Rev. Lett.* **69**(9), 1431.
- Yu, W., J. S. Higgins, P. Bach, and R. L. Greene, 2007a, *Physical Review B (Condensed Matter and Materials Physics)* **76**(2), 020503 (pages 4).
- Yu, W., J. S. Higgins, P. Bach, and R. L. Greene, 2007b, *Physical Review B (Condensed Matter and Materials Physics)* **76**(2), 020503 (pages 4).
- Yu, W., B. Liang, and R. L. Greene, 2005, *Phys. Rev. B* **72**(21), 212512 (pages 3).
- Yu, W., B. Liang, and R. L. Greene, 2006, *Physical Review B (Condensed Matter and Materials Physics)* **74**(21), 212504 (pages 4).
- Yuan, Q., X.-Z. Yan, and C. S. Ting, 2006a, *Physical Review B (Condensed Matter and Materials Physics)* **74**(21), 214503 (pages 9).
- Yuan, Q., F. Yuan, and C. S. Ting, 2005, *Physical Review B (Condensed Matter and Materials Physics)* **72**(5), 054504 (pages 5).
- Yuan, Q., F. Yuan, and C. S. Ting, 2006b, *Physical Review B (Condensed Matter and Materials Physics)* **73**(5), 054501 (pages 5).
- Zaanen, J., and O. Gunnarsson, 1989, *Phys. Rev. B* **40**(10), 7391.
- Zaanen, J., G. A. Sawatzky, and J. W. Allen, 1985, *Phys. Rev. Lett.* **55**(4), 418.
- Zamborszky, F., G. Wu, J. Shinagawa, W. Yu, H. Balci, R. L. Greene, W. G. Clark, and S. E. Brown, 2004, *Phys. Rev. Lett.* **92**(4), 047003 (pages 4).
- Zhang, F. C., and T. M. Rice, 1988, *Phys. Rev. B* **37**(7), 3759.
- Zhang, S.-C., 1997, *Science* **275**(5303), 1089.
- Zhao, J., P. Dai, S. Li, P. G. Freeman, Y. Onose, and Y. Tokura, 2007, *Physical Review Letters* **99**(1), 017001.
- Zhao, L., H. Wu, J. Miao, H. Yang, F. C. Zhang, X. G. Qiu, and B. R. Zhao, 2004, *Superconductor Science and Technology* **17**(11), 1361.
- Zheng, G.-q., T. Sato, Y. Kitaoka, M. Fujita, and K. Yamada,

- 2003, Phys. Rev. Lett. **90**(19), 197005.
- Zimmers, A., R. P. S. M. Lobo, N. Bontemps, C. C. Homes, M. C. Barr, Y. Dagan, and R. L. Greene, 2004, Phys. Rev. B **70**(13), 132502 (pages 4).
- Zimmers, A., Y. Noat, T. Cren, W. Sacks, D. Roditchev, B. Liang, and R. L. Greene, 2007a, Physical Review B (Condensed Matter and Materials Physics) **76**(13), 132505 (pages 4).
- Zimmers, A., L. Shi, D. C. Schmadel, W. M. Fisher, R. L. Greene, H. D. Drew, M. Houseknecht, G. Acbas, M.-H. Kim, M.-H. Yang, J. Cerne, J. Lin, *et al.*, 2007b, Physical Review B (Condensed Matter and Materials Physics) **76**(6), 064515 (pages 6).
- Zimmers, A., J. M. Tomczak, R. P. S. M. Lobo, N. Bontemps, C. P. Hill, M. C. Barr, Y. Dagan, R. L. Greene, A. J. Millis, and C. C. Homes, 2005, EPL (Europhysics Letters) **70**(2), 225.